Resource Allocation for Energy Harvesting Communications

Zhe Wang

Submitted in partial fulfillment of the
requirements for the degree
of Doctor of Philosophy
in the Graduate School of Arts and Sciences

COLUMBIA UNIVERSITY

2015

ABSTRACT

Resource Allocation for Energy Harvesting Communications

Zhe Wang

With the rapid development of energy harvesting technologies, a new paradigm of wireless communications that employs energy harvesting transmitters has become a reality. The renewable energy source enables the flexible deployment of the transmitters and prolongs their lifetimes. To make the best use of the harvested energy, many challenging research issues arise from the new paradigm of communications. In particular, optimal resource (energy, bandwidth, etc.) allocation is key to the design of an efficient wireless system powered by renewable energy sources.

In this thesis, we focus on several resource allocation problems for energy harvesting communications, including the energy allocation for a single energy harvesting transmitter, and the joint energy and spectral resource allocation for energy harvesting networks. More specifically, the resource allocation problems discussed in this thesis are summarized as follows.

- We solve the problem of designing an affordable optimal energy allocation strategy for the system of energy harvesting active networked tags (EnHANTs), that is adapted to the identification request and the energy harvesting dynamic. We formulate a Markov decision process (MDP) problem to optimize the overall system performance which takes into consideration of both the system activity-time and the communication reliability. To solve the problem, both a static exhaustive search method and a modified policy iteration algorithm are employed to obtain the optimal energy allocation policy.

- We develop an energy allocation algorithm to maximize the achievable rate for an access-controlled energy harvesting transmitter based on causal observations of the channel fading states. We formulate the stochastic optimization problem as a Markov decision process (MDP) with continuous states and define an approximate value function based on a piecewise linear

fit in terms of the battery state. We show that with the approximate value function, the update in each iteration consists of a group of convex problems with a continuous parameter and we derive the optimal solution to these convex problems in closed-form. Specifically, the computational complexity of the proposed algorithm is significantly lower than that of the standard discrete MDP method.

- We propose an efficient iterative algorithm to obtain the optimal energy-bandwidth allocation for multiple flat-fading point-to-point channels, maximizing the weighted sum-rate given the predictions of the energy and channel state. For the special case that each transmitter only communicates with one receiver and the objective is to maximize the total throughput, we develop efficient algorithms for optimally solving the subproblems involved in the iterative algorithm. Moreover, a heuristic algorithm is also proposed for energy-bandwidth allocation based on the causal energy and channel observations.

- We consider the energy-bandwidth allocation problem in multiple orthogonal and non-orthogonal flat-fading broadcast channels to maximize the weighted sum-rate given the predictions of energy and channel states. To efficiently obtain the optimal allocation, we extend the iterative algorithm originally proposed for multiple flat-fading point-to-point channels and further develop the optimal algorithms to solve the corresponding subproblems. For the orthogonal broadcast channel, the proportionally-fair (PF) throughput maximization problem is formulated and we derive the equivalence conditions such that the optimal solution can be obtained by solving a weighted throughput maximization problem. The algorithm to obtain the proper weights is also proposed.

- We consider the energy-subchannel allocation problem for energy harvesting networks in frequency-selective fading channels. We first assume that the harvested energy and subchannel gains can be predicted and propose an algorithm to efficiently obtain the energy-subchannel allocations for all links over the scheduling period based on controlled water-filling. The proposed algorithm is shown to be asymptotically optimal when the bandwidth of the subchannel goes to zero. A causal algorithm is also proposed based on the Q-learning technique that makes use of the statistics of the energy harvesting and channel fading processes.

Table of Contents

List of Figures

List of Tables

Acknowledgments

First of all, I would like to express my greatest gratitude to my advisor, Prof. Xiaodong Wang, who offered me the opportunity of my Ph.D. training at Columbia University and made this thesis possible. Form the first moment I entered his group to the final stage of my Ph.D. study, his dedication to top quality research is truly inspiring and he guided me with patience and wisdom. In my Ph.D. years, Prof. Wang spent lots of time and efforts on my research, enriching my knowledge and enhancing my problem solving ability in terms of my research and many things beyond studying and working. The years of my challenging and meaningful Ph.D. life will become a treasure in my life.

I would like to extend my thanks to the thesis committee members, Prof. John Wright, Prof. Javad Ghaderi, Prof. Ali Tajer, and Dr. Kai Yang for taking time to read this dissertation and sharing their wisdom with me. Dr. Ali Tajer graduated from Columbia University and now is a professor at Rensselaer Polytechnic Institute. He offered me lots of helps for starting my first Ph.D. research when he was at Columbia University. Dr. Kai Yang is a talent researcher at Huawei U.S. Lab and collaborated with me for my research about the optimization in Smart Grid. His discussion and guide help me quite a lot. Moreover, I would thank Dr. Vaneet Aggarwal, a professor at Purdue University, for collaborating with me for my research on energy harvesting transmitters, which constitutes the core of this dissertation. His insight and experience help me finish my Ph.D. work. I would also like to thank my M.S. advisors Prof. Wenjun Zhang and Prof. Lin Gui at Shanghai Jiao Tong University. They offered me the opportunities and experiences of practical projects, providing me another sight of thinking the theoretical research. Also, they gave me the strong support for my abroad study at Columbia University.

Moreover, I am grateful to my friends and colleagues at Columbia University, who accompanied in my Ph.D. years, especially Prof. Chenhao Qi, Dr. Hua Xiao, Prof. Chen Gong, Prof. Fanggang Wang, Dr. Jinxin Zhang, Prof. Yanzan Sun, Prof. Peter Kinget, Dr. Kun Wang, Dr. Zan Yang,

Dr. Yan Feng, Prof. Lei Deng, Prof. Conghui Zhou, Dr. Hui Li, Dr. Guoxia Zhang, Dr. Liming Wang, Dr. Yasin Yilmaz, Dr. Bin Jia, Prof. Gorge Moustakides, Abdulkadir Elmas, Hao Wu, Dr. Rong Ye, Ju Sun, Shang Li, Xing Su, Yuqian Zhang, Mehdi Ashraphijuo, Han-wen Kuo, Jueran Li, Ziyu Guo, Xiaoyang Liu, Le Zheng, Prof. Irving Kalet, Prof. Zhuwei Wang, Shan Zhong, Qing Qu, Prof. Pengcheng Zhu, Prof. Lan Tang, Prof. Chen Li, Prof. Ying Hao, Prof. Marco Moretti. Their encouragements helped me to overcome obstacles in my Ph.D. life.

Last but not least, my most special thanks are reserved for my parents, Jiankun Wang and Weiying Cui, who always give me the strongest supports unconditionally for my Ph.D. study, including both the moral support and financial support. Also, they took care of me carefully when I was a child, and shared all of my happiness and sadness in the past thirty years - since they brought me to the world. Their supports and encouragements are my backbone for finally completing the Ph.D. study. At the end of the acknowledgments, I would like to say: thank you, my Mom and Dad! I love you!!

TO MY PARENTS

Chapter 1

Introduction

With the rapid development of energy harvesting technologies, information transmission powered by energy harvesting devices has became a new paradigm of communications [1][2]. The renewable energy source enables the flexible deployment of the transmitters and prolongs their lifetimes. With a stochastic energy supply, resource scheduling is key to efficient and reliable energy-harvesting communications. To make the best use of the harvested energy for wireless communications, many challenging research issues arise and the energy scheduling is key to the design of an efficient wireless system powered by renewable energy sources [3]. Moreover, traditionally, with constant power sources, transmitter-end resource allocation for wireless communications involves the allocation of transmission power, MIMO precoders, and frequency bands to different users, to maximize the system rate. With energy harvesting transmitters, scheduling transmission energy together with other resource, e.g., frequency band, over time, becomes an important problem [4][5].

1.1 Background

Motivated by the growing concern on power consumption, green communications is a new concept proposed in recent years, which aims to reduce the consumption of the traditional fossil energy. To convert green communications from concept to reality, green communication techniques have been intensively investigated in the past years, including the research perspectives on energy-efficient devices (e.g., energy-efficient RF module), employment of renewable energy sources, energy-minimizing adaptive transmission, interference management and mitigation, energy-efficient routing

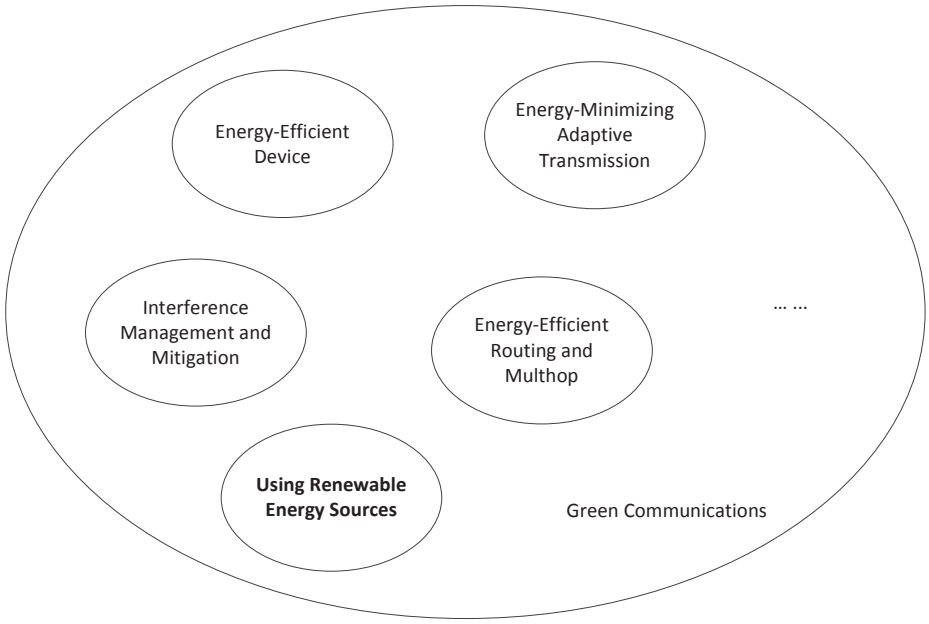

Figure 1.1: Research perspectives on green wireless communications.

and multhop, and so on [3–12], as illustrated in Fig. 1.1. Specifically, the green communication techniques have the common objective of improving the energy efficiency.

In addition to the use of energy-efficient devices, energy-efficient adaptive transmission is an effective technique to improve the energy efficiency for a single transmitter. By adapting the transmitter's parameters (e.g., the constellation signaling, the number of diversity branches, etc.) to the channel condition, the adaptive transmission can trade off between the energy efficiency and spectral efficiency under the performance constraints [6][7][13]. For a network with multiple transmitters, the interference management and mitigation technique can be used to mitigate the interference level at the receivers so that the transmission energy at the transmitters can be reduced accordingly without compromising the SINR of the wireless link [3][7]. Moreover, on network level, using the energy-efficient routing and multhop techniques, information exchanges between two transceivers (e.g., the base station and mobile terminal) can be realized by multiple relays with better channel conditions. Since the information is transmitted over better channels, the same rate can be achieved with lower transmission energy [3][14].

Employing the renewable energy is a novel way to realize green communications, which is motivated by the rapid development of the energy harvesting techniques in recent years. For energy

harvesting communications, the employment of the energy harvesting transmitters can not only avoid the use of the traditional fossil energy but also provide the flexible deployment and perpetual operation [15][16]. Due to the limited capability of the energy harvesting and storage, energy harvesting communications require the best use of the harvested energy, balancing the communication performance and the potential energy outage and overflow caused by the energy harvesting dynamics [8], which is different from some traditional techniques that realize the improvement on energy efficiency by solely reducing the energy consumption.

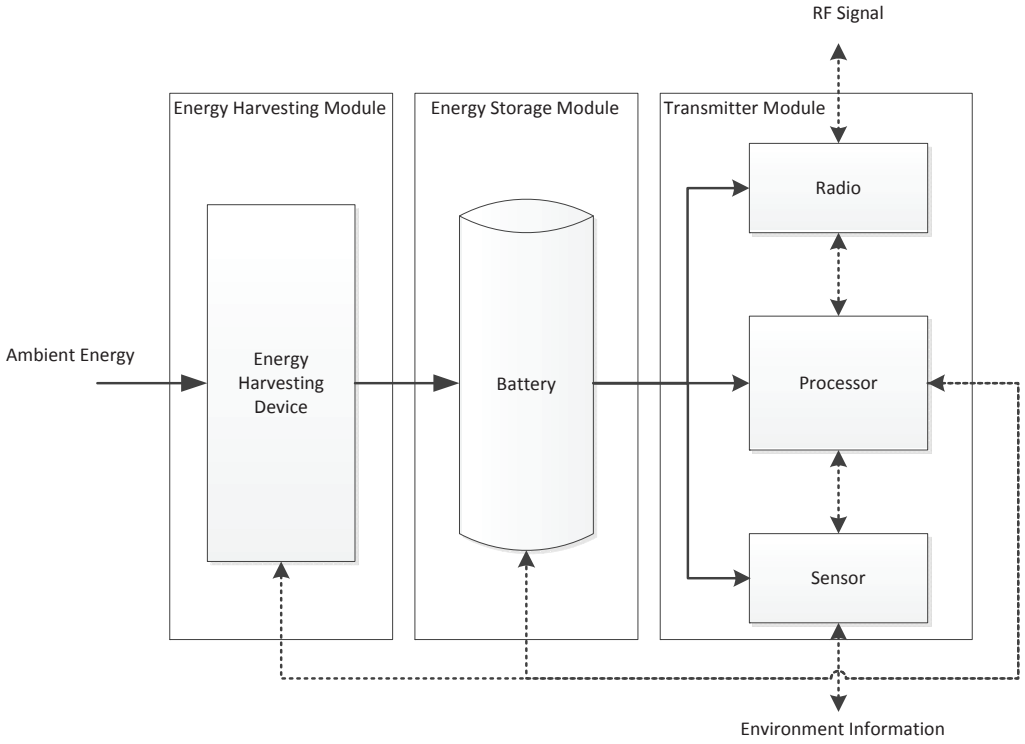

Figure 1.2: The block diagram of a typical energy harvesting transmitter.

Energy harvesting transmitter is the fundamental unit of the energy harvesting communication system, typically consisting of the energy harvesting module, energy storage module, and transmitter module [8][15], as shown in Fig. 1.2. The energy harvesting module harvests ambient energy from the surrounding environment and stores it in the energy storage module, which could be a rechargeable battery or supper capacitor. The storage module powers the transmitter, which contains the processor, sensing and radio blocks. Specifically, the sensing block performs the sensing functionality, e.g., collecting the environment information, depending on the application, and the

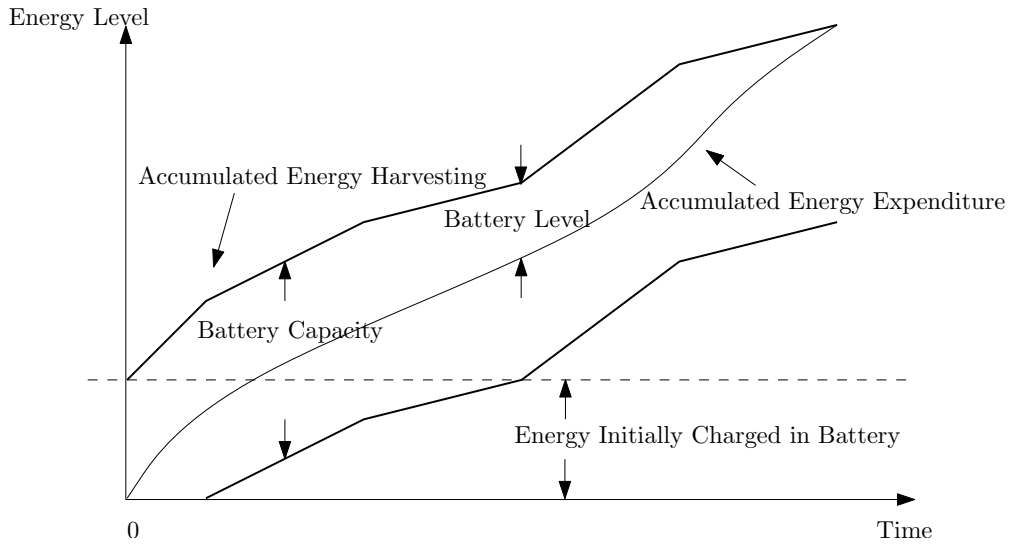

Figure 1.3: The energy expenditure curve and its feasible region.

radio block transmits the information processed by the processor and receives the data from the control center or another transmitters. In particular, in addition to processing the information, the processor is also the control unit of the energy harvesting transmitter, controlling the transmitter's working status, e.g., the transmitting or receiving status, the modulation and code scheme, and the transmission power.

Using the renewable energy is the most important feature of the energy harvesting transmitter and we can characterize the transmitter's operation (e.g., use specific transmission policy) in terms of the energy consumption by the energy expenditure curve (i.e., the integration of the energy expenditure over time) along with its feasible region [17], as shown in Fig. 1.3. Specifically, each energy expenditure curve corresponds to a particular communication performance and must be in the feasible region constrained by the energy harvesting process and the battery capacity. It is easy to understand that the feasible region is upper-bounded by the accumulative energy harvesting curve (i.e., the integration of the harvested energy over time) such that the accumulated energy expenditure cannot exceed the accumulated energy harvesting for all time otherwise the battery level would be negative. Also, the energy expenditure curve cannot be below the curve formed by subtracting the battery capacity from the accumulated energy harvesting (or zero, whichever is larger) since the battery level cannot exceed its capacity [17].

For traditional grid- and battery-powered transmitters, we can also use the similar way to char-

acterize their energy expenditure curves along with the feasible regions; however, we will see that their curves and feasible regions are quite different from those of the energy harvesting transmitter. Specifically, for the grid-powered transmitter subject to the maximum transmission power, its energy expenditure curve is continuous and the derivative (both left- and right-derivatives at the non-differentiable point) cannot exceed the value of the maximum transmission power; for the battery-powered transmitter, since the energy is not replenishable, its energy expenditure curve must stay below a constant horizon line (e.g., the dashed line in Fig. 1.3) that represents the energy initially charged in the battery. Note that, since the different energy expenditure curves represent different operation schemes and correspond to the different communication performances, the energy harvesting transmitters operate significantly differently as compared to the grid- and battery-powered transmitters. Therefore, lots of interesting and changeling research issues arise for the energy harvesting transmitters, including the architecture design of energy harvesting transmitter, channel capacity of energy harvesting communications, resource allocation, routing and relay selection for energy harvesting networks, and so on, as illustrated in Fig. 1.4.

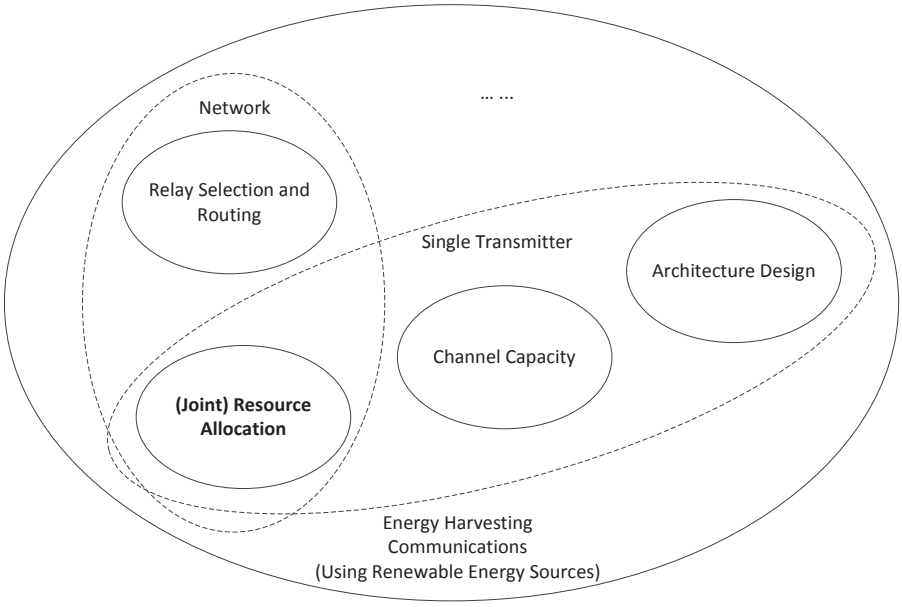

Figure 1.4: Research perspectives on energy harvesting communications.

For energy harvesting transmitters, the architecture design is the most essential issue, i.e., how to design the energy harvesting transmitter based on the specific application. Since the energy

harvesting transmitter is ideally expected to work perpetually, we need to design and adapt the energy harvesting, modulation, and sensing techniques to strike a balance between the communication performance required by the specific application and the system reliability affected by the potential energy outage. The architecture design was addressed by lots of works [1][15][18]. Specifically, the energy-harvesting active networked tags (EnHANTs) were developed in [19] and [20] as small devices that can be attached to small objects that are not traditionally networked.

Channel capacity is an interesting and challenging theoretical topic for energy harvesting communications, which provides the theoretical bounds on the performance. Unlike the traditional battery-powered systems, energy arrival of the energy harvesting transmitter is a random process over the symbol durations and the harvested energy is not necessarily consumed up immediately. On the other hand, when the battery is empty, the transmission has to be interrupted. Thus energy harvesting communications require a major shift in terms of the energy constraint imposed on the channel input compared to those in the existing literature. Specifically, the channel capacities for energy harvesting communications were discussed in [21], [22], [23], and [24] with various energy conditions for various channels.

At the transmitter-end, the resource allocation is key to make the best use of the harvested energy, ensuring the quality, long-term, and uninterrupted communications. With the battery, the harvested energy can be used immediately or stored for future transmission. Therefore, by properly choosing the energy allocation policy, the transmitter may use the energy to receive its maximum marginal utility, e.g., sum-rate. Moreover, in energy harvesting networks, joint resource allocation, e.g., the joint energy and spectral resource allocation, can provide additional degrees of freedom for optimization, thus the harvested energy may be better utilized for achieving an outperformed performance. The resource allocation for energy harvesting communications is widely investigated in the past years, which is also the subject of this thesis. We will provide a detailed literature review for the existing resource allocation techniques in the next section.

On network level, the studies of the relay selection and routing are also interesting for energy harvesting communications, which aim to effectively schedule the data transmissions in the energy harvesting networks. Specifically, in energy harvesting networks, the energy consumed by the transmitter is mostly harvested from the surrounding environment rather than the energy initially charged in the battery. Thus, the traditional relaying and routing policies have to be revised in

order to decide how to deliver packets using the harvested energy efficiently for perpetual operation. This requires a paradigm shift in the design of relaying and routing algorithms. For example, a few works, e.g., [25], [26], [27], [28], and [29], investigate the relaying and routing policies for energy harvesting communications.

Moreover, some new research topics emerged for energy harvesting communications recently. For example, incorporating the energy harvesting transmitter with the cellular network, [30] discussed the availability of the energy harvesting base station in multi-tier heterogeneous cellular networks. The topology planing problem was considered in [31] for the cellular networks enhanced by energy harvesting. Instead of passively harvesting the ambient energy, an interesting and challenging scenario arises when the transmitter performs simultaneous wireless information and power transfer [32][33]. It leads to the open problem for joint power control and user scheduling, energy and information scheduling, and interference management [16].

1.2 Literature Review

The system of energy-harvesting active networked tags (EnHANTs) has been proposed as small devices that can be attached to small objects that are not traditionally networked, e.g., books, clothes, and keys [19][20], representing a futuristic transition from the radio frequency identification (RFID) technology to a novel one with two main features [34]. Traditionally, the problems of activity-time maximization and reliability maximization have been treated independently in the contexts of RFID and WSN, respectively. For example, [35] and [36] considered maximizing the activity-time and coverage range (readability) of the RFID tags, respectively. Specifically, [35] proposed a mechanism for jointly energy harvesting and energy saving and [36] introduced a passive RFID system whose tags are equipped with power amplifiers and energy storage devices. Both systems are designed for typical application of tag identification information reading and do not support state information exchange among the tags. On the other hand, [37], [38], and [39] discussed energy optimization for the WSNs, where the optimal transmission schemes subject to the battery state and delay constraints are developed.

For general energy harvesting transmitters, a number of works addressed energy scheduling for a single transmitter. In particular, when the harvested energy and channel gains can be predicted, a

shortest-path-based algorithm was proposed in [17] for optimal energy scheduling in static channels, and the optimality properties of the energy schedule were studied in [40] based on the energy causality. For fading channels, with infinite battery capacity, [41] proposed a staircase water-filling algorithm for optimal energy scheduling; by analyzing the energy flow behaviors with finite battery capacity, the directional water-filling algorithm was further proposed in [42]. Taking the maximum transmission power into account, [43] proposed a dynamic water-filling algorithm to efficiently obtain the energy schedule to maximize the achievable rate. On the other hand, when the prediction of the harvested energy is not available, an algorithm was proposed in [44] to maximize the average throughput by allocating the discrete transmission power with causal energy arrival information. Moreover, when the statistics of the energy harvesting and channel fading processes are not available, a learning approach was used in [45] to maximize the number of packet transmissions by controlling the binary package sending status in each time slot.

Energy scheduling for multiuser energy harvesting networks has also been investigated. [46] characterized the general capacity region for a static multiple-access channel (MAC) without the constraints on the battery capacity and maximum transmission power. For two-user Gaussian interference channels, the optimal energy scheduling policy was discussed in [47] for the energy harvesting transmitters; and for static broadcast channels, the optimal energy scheduling algorithm was proposed in [48]. A causal algorithm was also proposed in [49] without using the predictions based on the Lyapunov optimization technique to optimize the utility of network. Incorporating the energy cooperation, [50] studied the transmission and energy transfer policies for various relay channels with one-way energy transfer; and with two-way energy transfer, the energy cooperation was studied in [51] for two-hop communication networks where the transmitters harvest their energy in an intermittent fashion.

The study of the joint resource allocation in multiuser energy harvesting networks emerges recently. In [52], heuristic algorithms were proposed to find the joint time-power allocation subject to the proportional fairness with the unbounded battery capacity; and [53] proposed an iterative algorithm for computing the optimal joint energy-bandwidth allocation in flat-fading point-to-point channels. Moreover, without energy harvesting, the resource allocation techniques were intensively investigated in frequency-selective channels. In [54], a low-complexity heuristic algorithm was proposed to allocate the subcarrier and power in an uplink OFDMA system under the constraint

of maximum transmission power in each slot. [55] grouped a number of adjacent subchannels into a chunk and treated the joint chunk, power and bit allocation for OFDMA systems. For the uplink of multi-carrier system with multiple modulation and code schemes, [56] proposed a distributed algorithms based on the message-passing approach to assign the subchannels and modulation/code schemes with the objective of minimizing the power consumption. For uplink DFT-spread-OFDMA systems, in [57], a polynomial-time message-passing-based algorithm was proposed for subcarrier allocation that is asymptotically optimal as the number of subcarriers goes to infinity. Also, [58] showed that the strong duality holds for the nonconvex spectrum optimization in multicarrier systems when the number of subcarriers goes to infinity.

1.3 Outline and Contributions

In this thesis, we will discuss the resource allocation for energy harvesting (EH) communications, consisting of the following two parts: in the first part, we focus on the energy allocation for a single energy harvesting transmitter; and in the other part, the joint energy and spectral resource allocation is discussed for energy harvesting networks.

1.3.1 Energy Allocation for Single EH Transmitter

In the first part, we first consider the problem of designing an affordable optimal energy allocation strategy for the newly emerged system of energy-harvesting active networked tags (EnHANTs), that is adapted to the identification request and the energy harvesting dynamics. Specifically, we propose an energy allocation strategy for EnHANTs that optimizes a *long-term* average of the communication reliability. The reliability part of this objective reflects the impact of energy management on communications and the long-term average implicitly incorporates the activity-time maximization goal. We show that the energy-spending policy associated with the information transmission can be cast as a Markov decision process (MDP), and we use a modified policy iteration algorithm to obtain the optimal energy allocation policy. This problem is addressed in detail in Chapter 2.

Next, we focus on the energy allocation for an access-controlled energy harvesting transmitter based on causal observations of the channel fading state. We assume that the system operates in

a time-slotted fashion and the channel gain in each slot is a random variable which is independent across slots. With the additional access control for the transmitter and the maximum power constraint, we formulate the stochastic optimization problem of maximizing the achievable rate as a Markov decision process (MDP) with continuous state. To efficiently solve the problem, we define an approximate value function based on a piecewise linear fit in terms of the battery state. We show that with the approximate value function, the update in each iteration consists of a group of convex problems with a continuous parameter. Moreover, we derive the optimal solution to these convex problems in closed-form. Further, we propose energy allocation algorithms for both the finite- and infinite-horizon cases, whose computational complexities are significantly lower than that of the standard discrete MDP method but with improved performance. Extension to the case of a general payoff function and imperfect energy prediction is also considered. Finally, simulation results demonstrate that the proposed algorithms closely approach the optimal performance. This problem is addressed in detail in Chapter 3.

1.3.2 Joint Energy-Bandwidth Allocation for EH Networks

In the second part, we focus on the energy harvesting networks and first consider the joint energy-bandwidth allocation in various flat-fading channels. We assume that the side information of both the channel states and the energy harvesting states is known for K time slots *a priori*. Then an optimal energy-bandwidth allocation algorithm is developed for multiple energy harvesting transmitters, each may communicate with multiple receivers via orthogonal point-to-point channels with the finite battery capacity and the maximum transmission energy in each time slot. We aim to maximize the weighted sum-rate of all transmitters over the K time slots by assigning the transmission energy and bandwidth for each transmitter in each slot and the problem is formulated as a convex optimization problem with $\mathcal{O}(MK)$ constraints, where M is the number of the receivers, making it hard to solve with a generic convex solver. An iterative algorithm is proposed that alternatively solves the energy allocation and bandwidth allocation subproblems in each iteration. The convergence and the optimality of this algorithm are also shown. We then consider the special case that each transmitter only communicates with one receiver and the objective is to maximize the total throughput. For this case, we develop the efficient algorithms to solve the two energy allocation and bandwidth allocation subproblems involved in the iterative algorithm optimally. A

heuristic algorithm is also proposed for energy-bandwidth allocation based on causal information of channel and energy harvesting states in multiple point-to-point channels with equal weights. This problem is addressed in detail in Chapter 4.

We next consider the energy-bandwidth allocation in multiple flat-fading orthogonal and non-orthogonal broadcast channels. To efficiently solve this problem, we extend the iterative algorithm in Chapter 4 and develop algorithms for solving the corresponding two subproblems in flat-fading orthogonal and non-orthogonal broadcast channels, respectively. For the orthogonal broadcast channel, we further formulate a proportionally-fair (PF) throughput maximization problem and derive the equivalence conditions such that the optimal solution can be obtained by solving a weighted throughput maximization problem. Further, the algorithm to obtain the proper weights is proposed. Simulation results show that the proposed algorithm can make efficient use of the harvested energy and the available bandwidth, and achieve significantly better performance than some heuristic policies for energy and bandwidth allocation. Moreover, it is seen that with energy-harvesting transmitters, non-orthogonal broadcast offers limited gain over orthogonal broadcast. This extension is made in Chapter 5.

In frequency-selective fading channels, we split the frequency band into multiple flat fading sub-channels with equal bandwidth and consider the energy-subchannel allocation problem for energy harvesting networks. Specifically, we first assume that the harvested energy and subchannel gains can be predicted and propose an algorithm to obtain the energy-subchannel allocation based on controlled water-filling, with the objective of maximizing the sum-rate in a scheduling period. The proposed algorithm is shown to be asymptotically optimal when the bandwidth of the subchannel goes to zero. A causal algorithm is also proposed based on the Q-learning method without using the predictions of the harvested energy and channel gain. This problem is addressed in detail in Chapter 6.

In summary, this thesis is organized as follows. In Chapter 2, we focus on the optimal energy allocation for the enhanced energy harvesting tags to improve the service reliability and quality. In Chapter 3, we consider the energy allocation problem for energy harvesting transmitters to maximize the achievable rate based on the observation of the channel gains and harvested energy. The optimal energy-bandwidth allocations in various flat-fading channels are discussed in Chapters 4 and 5, where Chapter 4 focuses on the optimal iterative algorithm and the efficient algorithms

for multiple point-to-point channels, and Chapter 5 focuses on the multiple orthogonal and non-orthogonal broadcast channels and the proportional fairness issue. In frequency-selective fading channels, the energy-subchannel allocation problem is considered in Chapter 6. Finally, Chapter 7 concludes the thesis.

Chapter 2

Energy Allocation for Enhanced Energy Harvesting Communication Tags

The system of energy-harvesting active networked tags (EnHANTs) has been recently proposed as small devices that can be attached to small objects that are not traditionally networked, e.g., books, clothes, and keys [19][20]. The EnHANTs system represents a futuristic transition from the radio frequency identification (RFID) technology [34] to a novel one with two main features. First, it enables communications among tag-equipped objects and secondly, the objects are autonomous and self-sufficient from an energy consumption perspective as they harvest and store energy from ambient light, motion, and temperature gradients.

The EnHANTs system mainly facilitates object tracking applications that are not viable through the existing technologies that either lack networking capability (e.g., RFID) or do not satisfy the size or energy autonomy constraints (e.g., Bluetooth). Examples of such tracking applications by energy autonomous networked objects include disaster recovery, emergency alert, and collecting temporal and spatial proximity information. This system enjoys the main features of both the RFID and wireless sensor network (WSN) technologies. In particular, the tags are designed to provide a timely response to any request for their identification information, as done by RFIDs, and also to report their functioning states and surrounding environment information, as done in a

WSN.

The major challenge in designing the communication protocols for EnHANTs pertains to managing the energy resources. For such energy management, there exists a tension between maximizing the activity-time[1] of the tags on one hand, which necessitates a conservative consumption of the energy resources, and increasing the communication reliability on the other hand, which suggests consuming more energy. The optimal consumption of the energy resources, therefore, requires striking a balance between maximizing the activity-time and communication reliability. Maintaining such a balance becomes more complicated due to the fact that the tags harvest energy on an ad-hoc basis, depending on the physical conditions of the environment (e.g., light, temperature, or motion). Therefore, an object might not have adequate energy for responding to any communication request it receives, and more importantly, even if it does, it might not be necessarily optimal to respond to such a request as preserving the energy for subsequent communications might bring about more overall communication reliability and activity-time.

In this chapter, we propose an energy allocation for EnHANTs that optimizes a *long-term* average of the communication reliability. The reliability part of this objective reflects the impact of energy management on communications and the long-term average implicitly incorporates the activity-time maximization goal. We show that the energy-spending policy associated with the information transmission can be cast as a Markov decision process (MDP), and we provide an efficient algorithm for computing the optimal policy.

2.1 System Descriptions

2.1.1 Communication Model

Consider a network of objects equipped with EnHANTs that communicate with a tag reader. Upon the request of the reader, the objects provide it with their identity and state information about their surrounding conditions. The communications occur in a time-slotted fashion with slots of

[1]The meaning of lifetime for energy-harvesting tags is slightly different from that of more conventional tags. For this reason we have adopted the term "activity-time", which similar to the traditional definitions of lifetime, refers to the time spans during which the tag has enough energy to respond to the inquiries. Its difference, nevertheless, is that activity-time is not of finite-horizon and can potentially extend for a long duration given that the tag is capable of harvesting adequate energy.

equal durations. The beginning of a time slot is reserved for the reader to broadcast its inquiries for collecting identification and information. Upon receiving the inquiries, the objects promptly respond to the reader, where they are allowed to use the remaining portion of the time slot for transmitting their information to the reader. A communication error occurs when either the objects fail to respond to the reader's inquires, or the reader fails to correctly decode the data from the objects.

To ensure low energy consumption, we assume that the ultra wideband (UWB)-based the pulse-position modulation (PPM) [59] is employed at each tag for sending information to the reader. Specifically, the information is encoded to the different positions of a single pulse (or a group of pulses) within a given time interval T. Given an encoded PPM symbol

$$\boldsymbol{s} = [s_1, s_2, \ldots, s_J],\ s_i \in \{0, 1\}\ ,$$

and a pulse $p(t)$ of duration T_p, where $T_p < T/J$, the received signal corresponding to $\boldsymbol{s}$ is given by

$$x(t) = \sum_{i=1}^{J} s_i p(t - iT/J) + v(t), \quad 0 \le t \le T\ , \tag{2.1}$$

where $v(t)$ is the ambient Gaussian noise. We assume that all encoded symbols are mutually orthogonal. Assuming that the pulses in a symbol are all unit pulses, i.e., $\int p^2(t)dt = 1$, then we define the weight w of the symbol as the number of non-zero pulses in the symbol, which is also the energy of the symbol.

In order for the reader to process the received PPM signal from the tagged object, conventionally a front-end A/D converter is employed which requires a very high-sampling rate for the UWB PPM signal. In particular, the sampling rate is the inverse of the pulse width T_p, e.g., $1/T_p = 5$GHz, which is prohibitively high. Alternatively, given the sparsity of the PPM signal, the compressive sensing technique [60] together with the signal detection method with compressive measurements [61] can be employed at the reader to significantly reduce the sampling rate. The basic idea is to project the received UWB PPM signal to some (random) basis waveforms at the analog front-end. The resulting projections constitute the compressive measurements based on which the original transmitted PPM signal can be detected. Mathematically the projection operation is characterized by a (random) projection matrix $\boldsymbol{\Phi} \in \mathbb{R}^{M \times N}$ [60]. After projection, the original received PPM signal $\boldsymbol{x} \in \mathbb{R}^N$, corresponding to the samples of the received PPM waveform $x(t)$ at the $1/T_p$ sampling rate, is

converted to the compressed samples $\tilde{\boldsymbol{x}} = \boldsymbol{\Phi}\boldsymbol{x} \in \mathbb{R}^M$ with a compression ratio of M/N. Note that no sampling at rate $1/T_p$ is needed; instead, we obtain the compressed samples $\tilde{\boldsymbol{x}}$ directly by the analog projection operation.

Assume that there are totally K PPM symbols $\boldsymbol{s}_1, \boldsymbol{s}_2, \ldots, \boldsymbol{s}_K$. Denote their corresponding projections as $\tilde{\boldsymbol{x}}_i = \boldsymbol{\Phi}\boldsymbol{x}_i, i = 1, 2, \ldots, K$. Then the receiver implements the following decision rule on the compressed signal to decide the PPM symbol that was transmitted:

$$\hat{i} = \arg \min_{1 \le i \le K} (\tilde{\boldsymbol{x}} - \tilde{\boldsymbol{x}}_i)^T \boldsymbol{\Psi} (\tilde{\boldsymbol{x}} - \tilde{\boldsymbol{x}}_i) \ , \tag{2.2}$$

where $\boldsymbol{\Psi} = (\boldsymbol{\Phi}\boldsymbol{\Phi}^T)^{-1}$. Under this classification method, the probability of mis-detecting a symbol of weight w, denoted by $P_{\mathrm{md}}(w)$, is well-approximated by [61]

$$P_{\mathrm{md}}(w) = 1 - Q\left(-\sqrt{\frac{M}{N}}\frac{w}{\sigma^2}\right)^{K-1} \ , \tag{2.3}$$

where σ^2 is the variance the additive white Gaussian noise, and $Q(x) = \frac{1}{\sqrt{2\pi}} \int_{-\infty}^{x} e^{-t^2/2} dt$.

A good timer synchronization is necessary for the EnHANTs as they work on a time-slot basis. Designing the appropriate synchronizers follow the same principles as those needed in the more conventional RFID systems. The system architectures provided in [19] and [20] employ a simple schemes in which the tags and readers use an analog circuit to detect the reader's inquiries and the tag's responses. These inquires and responses occur in the forms of a single pulse or a train of pulses. By locating the positions of the pulses, the system can obtain the underlying time reference, which in turn serves as the basis for synchronized communication. More information on implementing these synchronization methods is available in [62] and [63].

2.1.2 Energy Harvesting Model

We assume that the reader has a passive and continuous power source and has no power constraint. For the tags, we assume that they are equipped with rechargeable batteries and light energy harvesting devices. Due to the size constraints, the batteries must be small and consequently, have low capacity. Therefore, a considerable portion of the energy consumed by the tags should be harvested from the environment and the battery essentially functions as an energy buffer.

We consider probabilistic models for inquiries made by the reader as well as the energy harvesting dynamics of the devices. We aim to optimize the energy allocation policy from the perspective of

each object and therefore restrict the analysis to the case of one reader and one EnHANT equipped object. To model the identification request state of the reader at the beginning of the k-th time slot, for $k \in \mathbb{N}$, we define the random variable

$$a_k \sim \text{Bernoulli}(r) \ ,$$

where $a_k = 1$, occurring with probability r, indicates that the reader inquires about the tag's information at the beginning of the k-th time-slot and $a_k = 0$, that occurs with probability $(1-r)$, indicates otherwise. We also define the indicator b_k to reflect whether the tag is harvesting energy in the k-th time slot ($b_k = 1$) or it is not harvesting energy ($b_k = 0$). Moreover, we model the energy harvesting process as a correlated, two-state process [64]. If the tag harvests energy in a time slot, it will continue to harvest energy in the subsequent time slot with probability p and if no energy is harvested in a time slot, the probability of not harvesting any energy in the subsequent time slot either is q.

We denote the energy level that a tag can harvest and consume in the subsequent time slots by E_h. We also denote the capacity of the battery by $B_{\max}$ and denote the energy level restored in the battery of the object at the beginning of the k-th time slot by B_k, with $B_k \leq B_{\max}$. By defining W_k as the weight of the symbol transmitted in the k-th time slots, we get the following recursive relationship between the energy levels at the beginning of two consecutive time slots

$$B_{k+1} = \min\left\{B_k - a_k \cdot W_k \cdot \mathbf{1}_{\{B_k \cdot \geq W_k\}} + b_k \cdot E_h \ , \ B_{\max}\right\} \ , \tag{2.4}$$

where the indicator function $\mathbf{1}_{\{A\}}$ is defined as $\mathbf{1}_{\{A\}} = 1$ if A is true, and 0 otherwise. We remark that W_k, for all $k \in \mathbb{N}$, take discrete values from $\mathcal{W} = \{0, w_1, \ldots, w_m\}$ which are determined by the design of the hardware.

2.2 Problem Statement

2.2.1 Performance Measure

We define $S_k \triangleq (B_k, a_k, b_k)$, as the *state* of the tag in the k-th time slot. Since all components of S_k, i.e., B_k, a_k, and b_k, take discrete values and are all bounded, there are a finite number of possible states. We denote the number of such possible states by $|\mathcal{S}|$ and the set of possible states

by $\mathcal{S} \triangleq \{s_1, \ldots, s_{|\mathcal{S}|}\}$. Due to the structure of PPM that encodes the data in the positions of the non-zero pulses, the data to be transmitted govern the positions of the pulses, and the state of the tag determines the energy of the pulse. As a result, irrespective of the data content to be conveyed to the reader, the energy of the tag in the k-th time interval is uniquely determined by S_k. Therefore, identical states $S_k = S_l$ for $k \neq l$ will give rise to identical symbol weights, consuming identical energy. We denote an energy allocation policy ϕ as a mapping from the set of states $\mathcal{S}$ to the set of weights $\mathcal{W}$, so that $\phi(s_k)$ is the symbol weight corresponding to the state s_k, which is also the energy consumption in time slot k. Our objective is to determine the optimal design of $\phi(\cdot)$ such that a performance measure, that incorporates both the tag activity-time and communication reliability, is optimized.

Erroneous communication has two origins, namely *no-response errors* and *mis-detection errors*. The no-response error in the k-th time slot occurs when the battery cannot afford the energy required for sending a response to the reader, i.e., $B_k < W_k$, or when the tag operates under a certain policy that may voluntarily give up responding to the reader's request. For this reason, in order to allow for the possibility of letting $\phi(s_k) = 0$, we must have $0 \in \mathcal{W}$. For any given energy allocation policy ϕ, these two factors combined give rise to the following long-term average no-response error, where the average is taken over all time-slots,

$$\hat{P}_{\text{nr}}(\phi) = \lim_{N\to\infty} \frac{\sum_{k=1}^{N} \mathbf{1}_{\{W_k=0\}} \cdot a_k}{\sum_{k=1}^{N} a_k} \ , \tag{2.5}$$

where $W_k = \phi(S_k)$. The mis-detection errors take place when the reader cannot successfully decode the data transmitted by the object and its pertinent infinite-horizon average error for the given energy allocation policy ϕ is

$$\hat{P}_{\text{md}}(\phi) = \lim_{N\to\infty} \frac{\sum_{k=1}^{N} P_{\text{md}}(W_k) \cdot \mathbf{1}_{\{W_k>0\}} \cdot a_k}{\sum_{k=1}^{N} a_k} \ , \tag{2.6}$$

where $W_k = \phi(S_k)$. Finally, in order to incorporate the no-response and mis-detection error probabilities under the same performance measure, we define a weighed average of the two error probabilities as

$$P_{\text{err}}(\phi) = \beta \hat{P}_{\text{nr}}(\phi) + (1-\beta)\hat{P}_{\text{md}}(\phi) \ , \tag{2.7}$$

where $\beta \in [0, 1]$ is the weighting factor. By changing β one can adjust the error probability $P_{\text{err}}(\phi)$ based on the application of interest depending on whether the no-response or mis-detection error

is more important. Equations (2.5)-(2.7) provide

$$P_{\text{err}}(\phi) = \lim_{N\to\infty} \frac{\sum_{k=1}^{N} \left(\beta \cdot \mathbf{1}_{\{W_k=0\}} + (1-\beta) \cdot P_{\text{md}}(W_k) \cdot \mathbf{1}_{\{W_k>0\}}\right) \cdot a_k}{\sum_{k=1}^{N} a_k} \ . \tag{2.8}$$

Therefore, the optimization problem that we strive to solve can be formalized as follows:

$$\mathcal{P} = \begin{cases} \min_{\phi} & P_{\text{err}}(\phi) \\ \text{s.t.} & \text{the battery states satisfy (2.4)} \end{cases} \ . \tag{2.9}$$

2.2.2 Markov Decision Process

The optimization problem as formulated in (2.9) designs the optimal policy ϕ, which is valid throughout the activity-time of the tag. In other words, the solution we have is stationary in the sense that it does not change over time. This means that we can solve (2.9) offline and provide the tags with the corresponding look-up tables, without requiring them to spend their energy resources on computations. We next show that the optimization problem that finds a stationary policy, which is the mapping from the states in $\mathcal{S}$ to the weights in $\mathcal{W}$, can be modeled as a standard Markov decision process (MDP) problem.

A standard MDP, which provides a framework for decision-making in situations where outcomes are partly random, can be defined via a quadruplet $\big(\mathcal{S}, \mathcal{W}, p_{w_i}(s_i, s_j), R_{w_i}(s_i, s_j)\big)$, where in our settings $\mathcal{S}$ denotes the set of states S; $\mathcal{W}$ is the set of actions taken based on the states, i.e., the set of weights assigned to the states; $p_{w_i}(s_i, s_j)$ denotes the probability of transition from state s_i to state s_j when action $w_i \in \mathcal{W}$ is taken. Note that the transition probabilities satisfy

$$\forall w_i \in \mathcal{W}, \forall i \in \{1, 2, \ldots, M\} : \sum_{j=1} p_{w_i}(s_i, s_j) = 1 \ .$$

Finally, $R_{w_i}(s_i, s_j)$ denotes the penalty (or reward) associated with the transition from s_i to s_j under action w_i. The objective of an MDP is to choose a policy $\phi : \mathcal{S} \to \mathcal{W}$ that assigns an action to each state such that the average penalty is minimized. Specifically, the policy of interest minimizes the infinite horizon penalty

$$R_{ih}(\phi) \triangleq \lim_{N\to\infty} \frac{1}{N} \sum_{k=1}^{N} R_{W_k}(S_k, S_{k+1}) \ , \tag{2.10}$$

where $W_k = \phi(S_k)$.

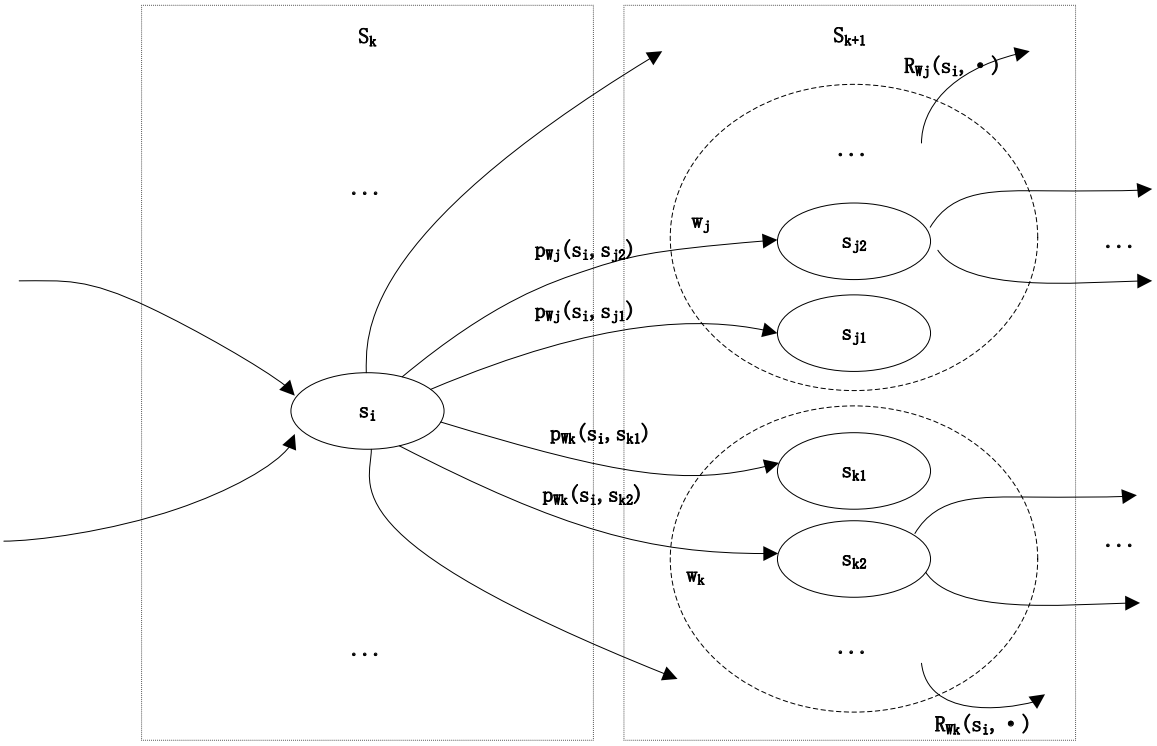

Figure 2.1: The state transition diagram.

2.2.3 The MDP Formulation

As described in Section 2.1, the reader operates in a time-slotted fashion with slots of equal durations. During the k-th time slot, the tag selects the symbol weight $W_k = \phi(S_k)$ for the signal to be sent to the reader. Under the choice of W_k the tag's state changes from S_k to S_{k+1}, as shown in Fig. 2.1. Therefore, the penalty associated with this transition is $R_{W_k}(S_k, S_{k+1})$.

A natural choice for the penalty term $R_{W_k}(S_k, S_{k+1})$ is the probability that such a transition is sensed by the reader erroneously. In particular, we aim to associate $R_{W_k}(S_k, S_{k+1})$ with the communication error probability given by

$$R_{W_k}(S_k, S_{k+1}) = \Big(\beta \cdot \mathbf{1}_{\{W_k=0\}} + (1-\beta) \cdot P_{\mathrm{md}}(W_k) \cdot \mathbf{1}_{\{W_k>0\}}\Big) \cdot a_k \ . \tag{2.11}$$

By invoking (2.10), the infinite-horizon penalty becomes

$$R_{ih}(\phi) = \lim_{N\to\infty} \frac{1}{N} \sum_{k=1}^{N} \Big(\beta \cdot \mathbf{1}_{\{W_k=0\}} + (1-\beta) \cdot P_{\mathrm{md}}(W_k) \cdot \mathbf{1}_{\{W_k>0\}}\Big) \cdot a_k \ . \tag{2.12}$$

By comparing (2.12) and $P_{err}(\phi)$ in (2.8), we find that $R_{ih}(\phi)$ and $P_{err}(\phi)$ are identical up to a scaling factor. This scaling factor is $\lim_{N\to\infty}\sum_{K=1}^{N} a_k/N$, which by considering the distribution of a_i and the law of large numbers is equal to Nr. Therefore, the optimal weight assignment policy ϕ, which is the solution to (2.9) can be equivalently found by solving the following the MDP problem

$$\hat{\mathcal{P}} = \begin{cases} \min_{\phi} & R_{ih}(\phi) \\ \text{s.t.} & \text{the battery states satisfy (2.4)} \end{cases} . \tag{2.13}$$

This statement is formalized in the following proposition.

Proposition 1. *The solution to the optimization problem in* (2.9) *can be obtained by solving the MDP problem in* (2.13)*.*

2.3 Computing the Optimal Energy Allocation Policy

In this section we discuss how to solve (2.9). We denote the set of all possible energy allocation policies as $\Phi = \{\phi : \mathcal{S} \to \mathcal{W}\}$. Then we have $|\Phi| = |\mathcal{W}|^{|\mathcal{S}|}$.

We first consider a naive exhaustive search method. Assuming the MDP process starts form the 0-th time slot and is continuously observed for N time slots, we can simulate the $\{a_0, a_1, \ldots, a_N\}$, which is the sequence of the identification request state of each time slot, and $\{b_0, b_1, \ldots, b_N\}$, which is the sequence of the energy harvesting state of each time slot, based on their respective underlying statistical models. Based on the battery state transition process in (2.4), a finite-horizon state sequence $\mathcal{S}(\phi) = \{S_0, S_1, \ldots, S_N\}$ can then be generated under each possible policy $\phi \in \Phi$.

Using (2.8) for finite N, we can calculate the average penalty associated with the state-sequence $\mathcal{S}(\phi)$, which we denote as $P_{\text{err}}(\phi)$. The optimal policy is then

$$\phi^* = \arg\min_{\phi\in\Phi} P_{\text{err}}(\phi) . \tag{2.14}$$

Obviously if we choose the sequence length N to be large enough, ϕ^* can be considered as a close approximation to the solution to the original problem in (2.9).

2.3.1 Modified Policy Iteration Algorithm

The complexity of the exhaustive search method becomes prohibitive when $|\mathcal{W}|$ or $|\mathcal{S}|$ is large. We next apply the *modified policy iteration* (MPI) algorithm [65] to compute the optimal energy

Table 2.1: State transition probabilities $p_{w_k}(S_k, S_{k+1})$.

	$S_k = (B_k, 0, 0)$	$S_k = (B_k, 0, 1)$	$S_k = (B_k, 1, 0)$	$S_k = (B_k, 1, 1)$
$S_{k+1}^1 = (B_{k+1}, 0, 0)$	$(1-r)q$	$(1-r)(1-p)$	$(1-r)q$	$(1-r)(1-p)$
$S_{k+1}^2 = (B_{k+1}, 0, 1)$	$(1-r)(1-q)$	$(1-r)p$	$(1-r)(1-q)$	$(1-r)p$
$S_{k+1}^3 = (B_{k+1}, 1, 0)$	rq	$r(1-p)$	rq	$r(1-p)$
$S_{k+1}^4 = (B_{k+1}, 1, 1)$	$r(1-q)$	rp	$r(1-q)$	rp

allocation policy. The basic idea is to iterate the policy search process until an iteration variable converges. This variable is calculated in each iteration by another value iteration process.

All iterations in the MPI algorithm are based on the state transition probabilities. According to the state definition and the battery state transition process in (2.4), at any state S_k an action w_k leads to a transition to the following four possible next state S_{k+1}, $S_{k+1}^1 = (B_{k+1}, 0, 0)$, $S_{k+1}^2 = (B_{k+1}, 0, 1)$, $S_{k+1}^3 = (B_{k+1}, 1, 0)$, and $S_{k+1}^4 = (B_{k+1}, 1, 1)$, where

$$B_{k+1} = \min\{B_k + E_h b_k - w_k a_k, B_{\max}\} \ . \tag{2.15}$$

The transition probabilities from S_k to S_{k+1}^j, $j = 1, 2, 3, 4$, depend on the state S_k and the system parameters r, p and q. Assuming that the current state is $S_k = (B_k, a_k, b_k)$ and the next state is $S_{k+1} = (B_{k+1}, a_{k+1}, b_{k+1})$, when the action $w_k = \phi(S_k)$ is taken, we have

$$p_{w_k}(S_k, S_{k+1}) = p(a_{k+1}) p(b_{k+1} \mid b_k) \ . \tag{2.16}$$

The transition probabilities are summarized in Table 2.1.

The MPI algorithm consists of two phases, policy improvement and partial policy evaluation. In the policy improvement phase, the algorithm searches for a policy based on the iteration variable, the current *penalty iteration value*. Specifically, at the n-th iteration, we have the iteration variables $v^{(n-1)}(s_i),\ s_i \in \mathcal{S}$, which are the penalty iteration values corresponding to different states calculated in the previous iteration (We set $v^{(0)}(s_i) = 0,\ s_i \in \mathcal{S}$). Denote

$$\boldsymbol{v}^{(n)} \triangleq \left[v^{(n)}(s_1), v^{(n)}(s_2), \ldots . v^{(n)}(s_{|\mathcal{S}|})\right] \ ,$$

and

$$f(S_k, w, \boldsymbol{v}^{(n-1)}) = \sum_{j=1}^{4} p_w(S_k, S_{k+1}^j)\Big(R_w(S_k, S_{k+1}^j) + v^{(n-1)}(S_{k+1}^j)\Big),\ S_k \in \mathcal{S},\ w \in \mathcal{W} \ . \tag{2.17}$$

Then the policy $\phi^{(n)}$ at this iteration is computed as

$$\phi^{(n)}(s) = \arg\min_{w \in \mathcal{W}} f(s, w, \boldsymbol{v}^{(n-1)}),\ s \in \mathcal{S}\ . \tag{2.18}$$

And the penalty iteration value is updated as

$$v^{(n)}(s) = f(s, \phi^{(n)}(s), \boldsymbol{v}^{(n-1)}),\ s \in \mathcal{S}\ . \tag{2.19}$$

In the partial policy evaluation phase, the algorithm determines whether $\phi^{(n)}$ found in the policy improvement phase is the overall optimal policy. If not, the algorithm starts a sub-iteration process to update the penalty iteration values $v^{(n)}(s_i)$ and then goes back to the policy improvement phase for another iteration. In order to determine whether $\phi^{(n)}$ is the optimal policy, we compute

$$u^{(1)}(s) \triangleq f(s, \phi^{(n)}(s), \boldsymbol{v}^{(n)}),\ s \in S\ . \tag{2.20}$$

Denote $\boldsymbol{u}^{(n)} = [u^{(n)}(s_1), u^{(n)}(s_2), \ldots, u^{(n)}(s_{|\mathcal{S}|})]$. Given a small value ϵ, if

$$\|\boldsymbol{u}^{(1)} - \boldsymbol{v}^{(n)}\| < \epsilon\ , \tag{2.21}$$

then we consider $\phi^{(n)}$ as the overall optimal policy ϕ^*. Otherwise, we perform the following iteration to update the penalty iteration value,

$$u^{(m)}(s) = f(s, \phi^{(n)}(s), \boldsymbol{u}^{(m-1)}),\ s \in \mathcal{S},\ m = 1, 2, \ldots, M\ . \tag{2.22}$$

Finally we set $v^{(n)}(s_i) = u^{(M)}(s_i),\ s_i \in \mathcal{S}$ and go back to the policy improvement phase for another iteration.

The MPI algorithm for solving the MDP problem in (2.13) is summarized as follows.

Algorithm - Modified Policy Iteration Algorithm for Solving (2.13)

1: Initialization

$\boldsymbol{v}^{(0)} = \mathbf{0}$

$n = 1$

2: Policy Improvement

FOR $s \in \mathcal{S}$

$\phi^{(n)}(s) = \arg\min_{w \in \mathcal{W}} f(s, w, \boldsymbol{v}^{(n-1)})$

$v^{(n)}(s) = f(s, \phi^{(n)}(s), \boldsymbol{v}^{(n-1)})$

ENDFOR

3: Partial Policy Evaluation

FOR $s \in \mathcal{S}$

$u^{(1)}(s) = f(S_k, \phi^{(n)}(s), \boldsymbol{v}^{(n)})$

IF $\|(u^{(1)} - v^{(n+1)}\| < \epsilon$, **GOTO STEP 4**

ELSE FOR $m = 1, 2, \ldots, M$

FOR $s \in \mathcal{S}$

$u^{(m)}(s) = f(s, \phi^{(n)}(s), \boldsymbol{u}^{(m-1)})$

ENDFOR

ENDFOR, ENDIF

$\boldsymbol{v}^{(n)} = \boldsymbol{u}^{(M)}$

$n \leftarrow n + 1$, **GOTO STEP 2**

4: Choose Policy

$\phi^* = \phi^{(n)}$

This algorithm combines the features of both policy iteration and value iteration. The most significant feature is its low computational complexity, compared to the exhaustive search. On the other hand, as will be shown in Section 2.4, its performance is similar to that of the exhaustive search.

2.3.2 Convergence of the MPI Algorithm

The MPI algorithm is designed for solving a class of MDP problems that has finite state space, finite decision space, non-discount average reward, and infinite-horizon [65]. Obviously, the MDP problem in (2.13) belongs to this class.

A sufficient condition for the MPI algorithm to converge is given in [65]. In particular, if

$$\min_{\phi_1,\phi_2\in\Phi}\min_{(u,v)\in S\times S}\sum_{j\in S}\min\left\{p^J_{\phi_1}(j\mid u),p^J_{\phi_2}(j\mid v)\right\}>0\ , \tag{2.23}$$

where $p^J_\phi(j\mid u)$ is the transition probability from $u\in\mathcal{S}$ to $j\in\mathcal{S}$ after J state transitions under the policy ϕ, then the optimal policy can be found by the MPI algorithm within a finite number of iterations. For our problem, we make the reasonable assumption that the rates of both energy harvesting and identification request are positive, i.e., $0<p,q<1$ and $0<r<1$, and the tag will be silent if there is no request, i.e., $a_k=0$. Then we have the following convergence result.

Proposition 2. *The ϵ-optimal solution to the MDP problem in* (2.13) *can be obtained by performing the MPI algorithm within a finite number of iterations.*

Proof. According to (2.4) and the system state definition S, if $0<p,q<1$ and $0<r<1$, and the tag consumes no energy when there is no request, for any stationary policy $\forall s\in\mathcal{S}$ can transit to $s'=(B_{\max},0,1)$ within a finite number of transitions, i.e., $p^j_\phi(s'\mid s)>0$. Therefore, (2.23) is satisfied and the MDP problem in (2.13) can be solved by the MPI algorithm. □

2.4 Simulation Results

We assume that each response message from the tag is encoded using 15 bits, transmitted in 3 PPM symbols with the symbol modulation order of $K=32$. Each symbol may contain 1, 2 or 4 non-zero pulses, i.e., $\mathcal{W}=\{0,1,2,4\}$. The durations of the pulse and the symbol are $T_p=5ns$ and $T=6.4\mu s$ respectively. Assuming a compression ratio of $M/N=0.1$, we obtain the compressed signal samples at the affordable rate of 200MHz. The symbol mis-detection probabilities $P_{\rm md}(w)$ corresponding to different symbol weights are calculated using (2.3) and given in Table 2.2, for the pulse SNR $\frac{1}{\sigma^2}=6dB$. Furthermore, we set the battery capacity $B_{\max}=10$ and the error weight parameter $\beta=0.5$.

Table 2.2: Symbol mis-detection probabilities for different symbol weights.

w	0	1	2	4
$P_{\rm md}(w)$	1.0000	0.6874	0.1625	0.0054

For the purpose of performance comparison, we consider two simple energy allocation strategies, a *conservative policy* and a *greedy policy*. The conservative policy always chooses the minimum available energy $w \in \mathcal{W}$ to transmit the response, such that the probability of no-response is minimized. On the other hand, the greedy policy targets for the best detection performance and always chooses the maximum available $w \in \mathcal{W}$ for responding to the reader's inquiry. For each simulation, the number of simulated time slots is $N = 10^6$. The convergence threshold of the MPI algorithm is $\epsilon = 10^{-5}$.

We first consider an energy-balanced scenario where the energy harvesting parameters are $p = q = 0.5$ and $E_h = 3$. Under such a condition, the battery is neither empty nor full in most time slots. The battery acts as an energy buffer and the scheduling algorithm pursues the best trade-off between the mis-detection errors and the no-response errors. The simulation results for this scenario are shown in Fig. 2.2. For the second scenario, we consider an energy-deficient environment, where $p = 0.3$, $q = 0.7$ and $E_h = 3$, corresponding to the case that a tag has a small probability to obtain energy from its environment at any time slot. In this case, the battery is empty in most time slots and the scheduling algorithm is apt to trade the detection performance for the activity-time. The simulation results for this scenario are shown in Fig. 2.3. In the last scenario, we simulate the policies in the energy-overflow environment, where $p = 0.7$, $q = 0.3$ and $E_h = 6$. This environment ensures that the tags are strongly capable of being over-charged in most time slots. So the scheduling algorithm is apt to spend more energy to reduce the mis-detection errors. The simulation results for this scenario are shown in Fig. 2.4. The optimality of the proposed scheme relies on the knowledge about p and q, which in practice might not be known accurately. Further simulations on the sensitivity of the performance on the design values p and q are demonstrated in Fig. 2.5. This figures shows that perturbations the values of p and q by as much as 30% imposes only negligible performance losses.

It is seen from Fig. 2.2–2.4 that the optimal polices based on the MPI algorithm and exhaustive search give the best performance for all three scenarios. And the conservative policy gives the worst performance. Moreover, the greedy policy performs worse than the optimal policy because it fails to balance the mis-detection errors and the no-response errors by simply ignoring the latter. On the other hand, as the identification request rate increases, the performances of both the optimal policy and the greedy policy degrade due to the energy constraints. Another observation is that

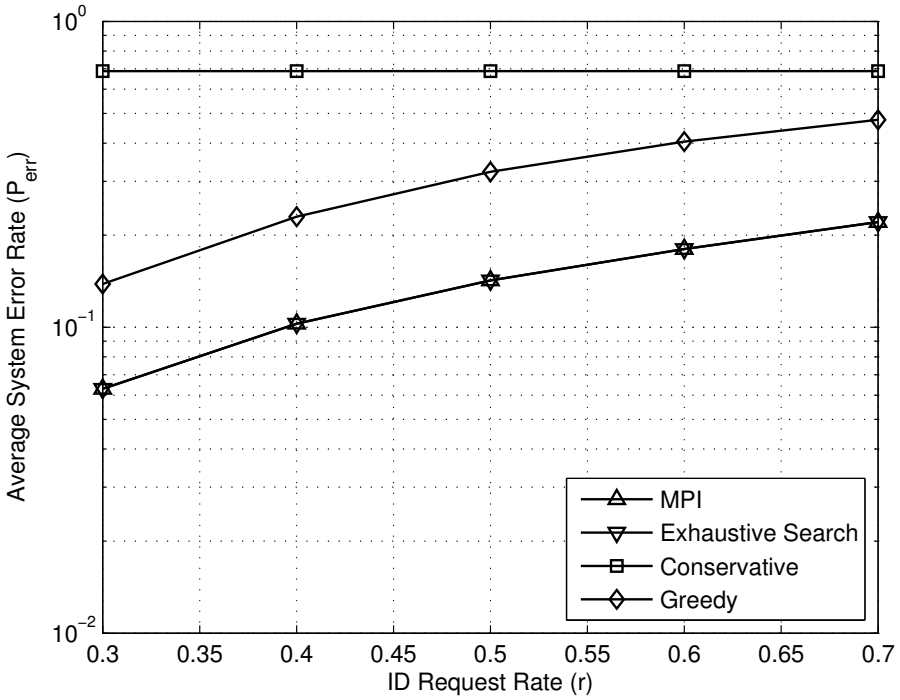

Figure 2.2: Performance comparisons for the energy-balanced scenario.

when the tag's energy harvesting capability becomes stronger, the performances of all these policies improve, since the tag can use more energy to reduce the no-response errors and to improve the detection performance. In addition, by comparing the optimal energy allocation policies found by the MPI algorithm and the exhaustive search method, it is observed that their performance conform precisely in most simulation scenarios and there exist slight discrepancy in rare situations.

Fig. 2.6 shows the MPI algorithm's convergence under the energy-balanced scenario. The number of iterations for the partial policy evaluation phase is $M = 200$. It is seen that the optimal policies are obtained at the 4-th and 5-th policy improvement iterations for $r = 0.7$ and $r = 0.3$, respectively. At each policy improvement iteration, the policy is updated based on the current penalty values, which are converged in the previous evaluation phase. Then, the penalty values are updated for the updated policy. Also, at the last policy improvement iteration, the total error is below the threshold ϵ and the algorithm stops.

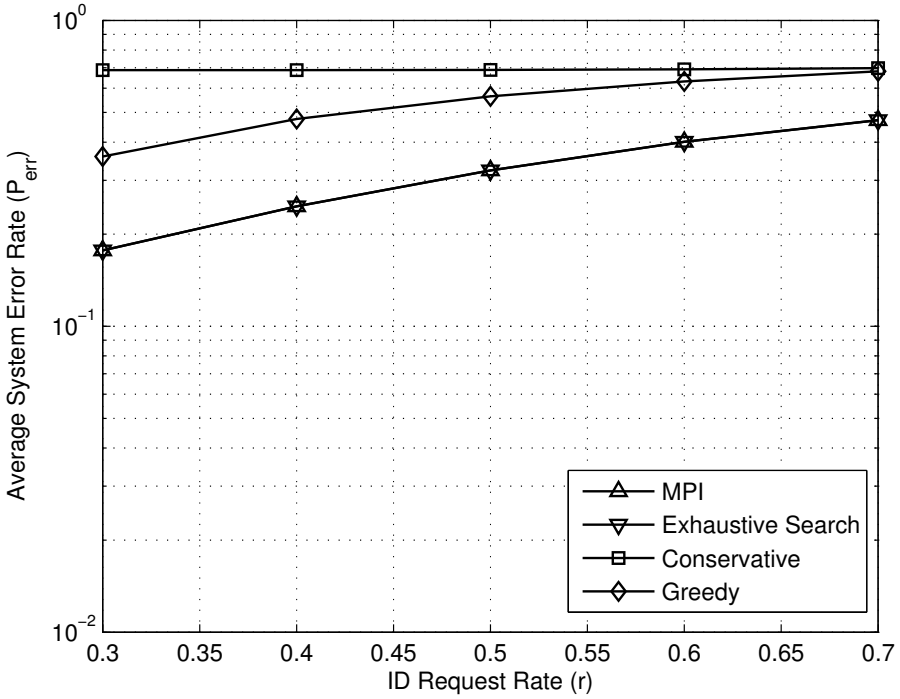

Figure 2.3: Performance comparisons for the energy-deficient scenario.

2.5 Conclusions

We have formed a system model for the system of energy-harvesting active networked tags (EnHANTs), including the communication model and the energy harvesting model, where the events of identification request and energy harvesting are assumed to follow simple Markov processes. A typical application of the EnHANTs system is for the tags to respond to the request by sending some simple information about their own identifications and their surrounding environment. For such an application, we formulate the problem of optimizing the energy allocation policy to maximize both the reliability and activity-time of the system. We have shown that the optimization problem has an inherent MDP structure and therefore can be solved using the modified policy iteration method. Finally simulation studies have demonstrated the effectiveness of the proposed optimal energy allocation policy in terms of making efficient use of the limited energy to improve the system reliability.

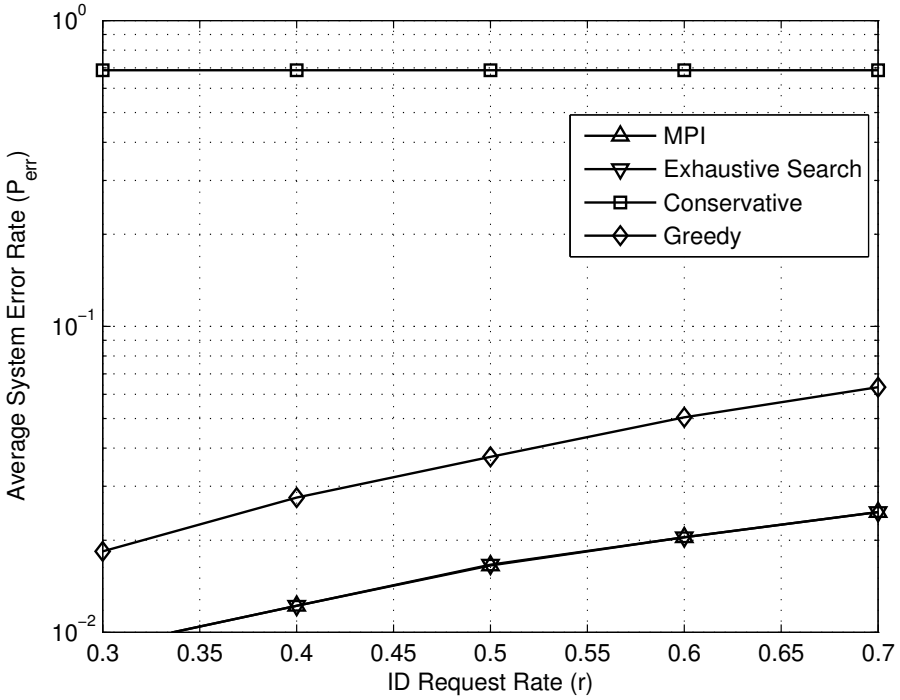

Figure 2.4: Performance comparisons for the energy-overflow scenario.

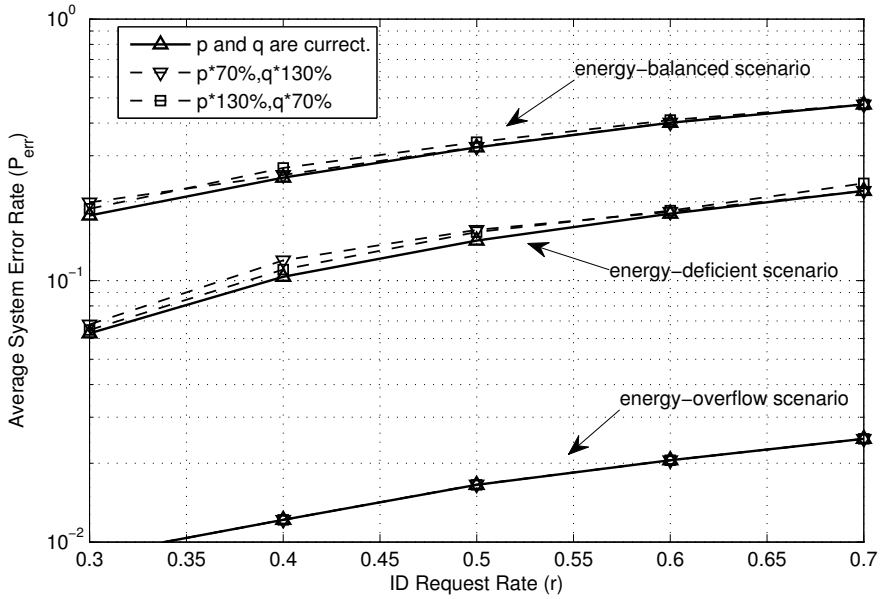

Figure 2.5: Performance comparisons for inaccurate p and q.

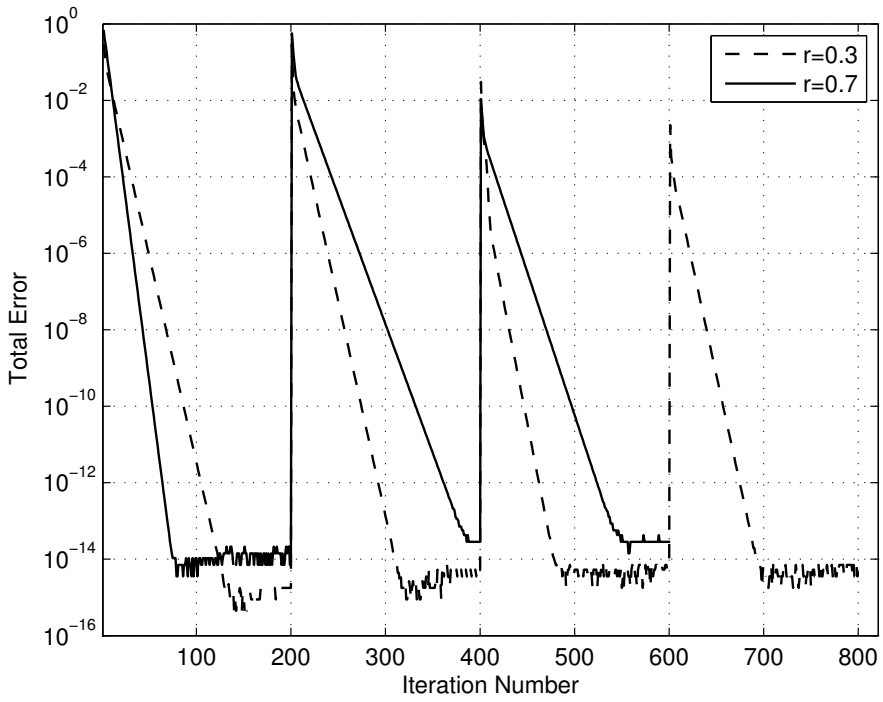

Figure 2.6: The convergence of the MPI algorithm under the energy-balanced scenario.

Chapter 3

Energy Allocation for Energy Harvesting Transmitters

In this chapter, we consider the continuous energy allocation for maximizing the throughput (or network utilities) with causal information on the energy harvesting state and the channel fading state, and under the maximum power constraint. We will formulate it as a continuous MDP problem and develop algorithms to solve it in a computationally efficient manner.

Specifically, we first consider the energy allocation for an access-controlled transmitter, which is powered by a renewable energy source and equipped with a finite-capacity battery and has a maximum power constraint. The channel fading is assumed to be a random variable in a slot and is independent across different slots. For energy harvesting, we first assume that it can be predicted accurately for the scheduling period, which is practically feasible [66][67], and then later introduce the prediction error variables. Furthermore, we assume that a control center can temporarily suspend the transmitter's access due to channel congestion. Such channel access control for the transmitter is modeled as a first-order Markov process. Under the above setting, this chapter finds the approximately optimal energy allocation for both the finite- and infinite-horizon cases.

To obtain the energy allocation, we formulate the stochastic optimization problem as a discrete-time and continuous-state Markov decision process (MDP), with the objective of maximizing the sum of the payoff in the current slot and the discounted expected payoffs in the future slots, where a particular payoff function is the achievable channel rate. Since the state variables including the

battery state and the channel state in the MDP problem are continuous, to avoid the prohibitively high complexity for updating the value function caused by the continuous states, this chapter introduces an approximate value function. We show that the approximate value function is concave and non-decreasing in the variable corresponding to the energy stored in the battery, which further enables the approximate value function to be updated in closed-form. This is then used to find the approximately optimal energy allocation for both the finite- and infinite-horizon cases.

The proposed algorithms provide approximate solutions, whose performances are lower bounded by that of the standard discrete MDP method. Also, to obtain the solution, we solve at most $\mathcal{O}(B_{\max}/\delta \cdot C)$ convex optimization problems where $B_{\max}$ is the battery capacity, δ is the approximation precision, and C is the length of horizon for the finite-horizon case or the maximum number of iterations for the infinite-horizon case. In particular, for the infinite-horizon case, given a convergence tolerance α, the α-converged solution can be obtained within $\mathcal{O}(\log_\gamma \alpha)$ iterations, where γ is the discount factor.

3.1 Problem Formulation

3.1.1 System Model

We consider a point-to-point communication system with one transmitter and one receiver, as shown in Fig. 3.1. We assume a slow fading channel model where the channel gain is constant for a coherence time of T_c (corresponding to a time slot) and changes independently across slots. Assuming that each time slot consists of T time instants, we denote X_{ki} as the symbol sent to the receiver at instant i in time slot k. Then, the corresponding received signal is given by $Y_{ki} = X_{ki}H_k + Z_{ki}$, where H_k represents the complex channel gain in slot k, and $Z_{ki} \sim \mathsf{CN}(0, 1/T)$ is the i.i.d. complex Gaussian noise (i.e., the power spectral density of the noise is $1/T_c$). Therefore, the energy consumption in a slot is the sum of the symbols' energy (in the time slot), which is denoted by $p_k \triangleq \sum_{i=1}^{T} |X_{ki}|^2$.

We assume that the control center performs channel access control and may block the channel access for the transmitter in some slots, e.g., congestion. At the beginning of each slot, the transmitter is informed of the channel access status $A_k \in \{0, 1\}$ for the current slot from the control center, where $A_k = 0$ indicates that the channel access is not permitted for slot k while $A_k = 1$ indi-

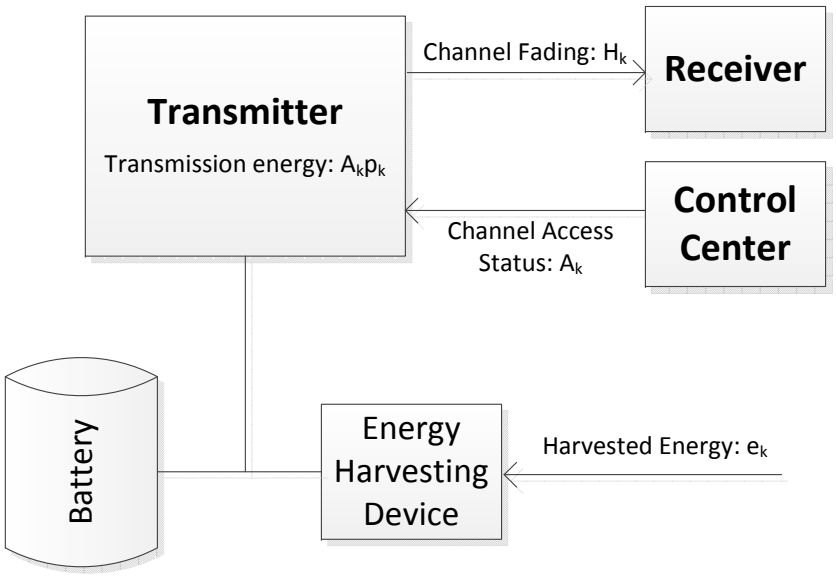

Figure 3.1: The system block diagram.

cates otherwise. To strike the balance between the scheduling complexity and the model accuracy, we assume that A_k follows a stationary first-order Markov process, whose transition probabilities are given as $\Pr(A_{k+1} = 0 \mid A_k = 1) = q_k$ and $\Pr(A_{k+1} = 0 \mid A_k = 0) = \tilde{q}_k$. Note that, if there is no channel access control, we simply have $A_k = 1$ for all k. Moreover, if $A_k = 0$, then the transmission energy in slot k is $p_k = 0$. On the other hand, if $A_k = 1$, then the transmitter needs to decide its transmit energy p_k.

The transmitter is powered by an energy harvesting device, e.g., a solar panel, and a battery. The battery, which buffers the harvested energy, has a finite capacity, denoted by $b_{\max}$. Since the energy harvesting process is steady or can be well predicted, we assume that the energy harvested over the next K slots can be non-causally known, denoted as e_k. We assume $h_k \triangleq |H_k|^2$ is independent across slots (i.i.d. when $K = \infty$).

In slot k, the transmitter transmits at a power level of p_k/T_c ($p_k = 0$ if $A_k = 0$), which is constrained by the maximum transmission power $p_{\max}/T_c$ and the available energy b_k, i.e.,

$$0 \leq p_k \leq \min\left\{p_{\max}, b_k\right\} . \tag{3.1}$$

The battery level at the beginning of slot $k+1$ is given as

$$b_{k+1} = \min\left\{b_{\max}, b_k + e_k - p_k\right\} , \tag{3.2}$$

with the constraint that the battery level is non-negative for all slots, i.e.,

$$b_k \geq 0 \ . \tag{3.3}$$

Further, the transmitter receives a payoff $r(p_k, h_k)$ based on the transmission energy p_k and channel power gain h_k. In Sections 3.2-3.3, we use the upper bound on the achievable rate in each slot as the payoff, i.e., $r(p, h) = \log(1 + ph)$. Then, in Section 3.4, we consider a general payoff function $r(p, h)$ which is continuous, non-decreasing, and concave with respect to p given h.

3.1.2 Problem Formulation

We assume that e_k can be predicted non-causally while all other variables are only known causally to the transmitter. Denote $\boldsymbol{H} \triangleq [h_1, h_2, \ldots, h_K]$, $\boldsymbol{A} \triangleq [A_1, A_2, \ldots, A_K]$ and a discount factor $\gamma \in [0, 1]$. Note that, $\gamma < 1$ discounts the payoff received in the future slots and $\gamma = 1$ means that the payoff received in every slot has the same importance. We assume that all the side information, e.g., the distributions of all random variables and the predictions of the harvested energy, is known before the first slot. Then the energy allocation policy $\mathcal{P} \triangleq \{p_k(\Gamma_k) \mid k = 1, 2, \ldots, K\}$ needs to be calculated to maximize the expected total payoff in the next K slots, where $\Gamma_k \triangleq (b_k, h_k, A_k)$ consists of the observations available at the beginning of slot k. Since b_k and h_k are continuous variables, it is not possible to store $\mathcal{P}$ in a look-up table. Instead, we only store some of the intermediate results, i.e., the approximate value function introduced in Section 3.2, in an efficient way, and then calculate the energy allocation when Γ_k is observed. Specifically, at the beginning of slot k, given Γ_k, if channel access is permitted, i.e., $A_k = 1$, the transmitter calculates the transmission energy p_k. And if the channel access is not permitted, i.e., $A_k = 0$, then $p_k = 0$. To that end, we formulate the following optimization problem for defining the optimal policy

$$\mathcal{P}^* \triangleq \arg\max_{p_k(\cdot)} \left\{ \mathbb{E}_{\boldsymbol{H},\boldsymbol{A}} \Big[\sum_{k=1}^{K} \gamma^{k-1} \log(1 + p_k(\Gamma_k) h_k) \Big] \right\} , \tag{3.4}$$

subject to the constraints in (3.1), (3.2), and (3.3) for $k = 1, 2, \ldots, K$.

Note that by (3.2), the battery level b_k forms a continuous-state first-order Markov chain, whereas the channel access state A_k is a discrete-state Markov chain by assumption. Then, we can convert the problem in (3.4) to its equivalent MDP recursive form [65] in terms of the *value function*, which represents the total payoff received in the current slot and expected to be received in the future slots.

Specifically, in the MDP model we treat the battery level b and the channel access state A, i.e., (b, A), as the state, the channel h as the observation, and the transmission energy p as the decision. Then, the state space becomes $\{0 \leq b \leq b_{\max}\} \times \{0, 1\}$; and the corresponding decision space is $\mathcal{D}_1(b) = \{0 \leq p \leq \min\{b, p_{\max}\}\}$ and $\mathcal{D}_0 = \{0\}$, corresponding to $A = 1$ and $A = 0$, respectively. The value function is then recursively defined as

$$v^k(b_k, A_k) \triangleq \mathbb{E}_{h_k}\Big[\max_{p_k(\Gamma_k)\in\mathcal{D}_{A_k}(b_k)} \big\{\log(1 + p_k(\Gamma_k)h_k) + \gamma u^k(b_k, p_k(\Gamma_k), A_k)\big\}\Big],\ k = 1, 2, \ldots, K\ , \tag{3.5}$$

where

$$u^k(b_k, p_k, A_k) \triangleq \mathbb{E}_{A_{k+1}|A_k}\left[v^{k+1}(\min\{b_{\max}, b_k + e_k - p_k\}, A_{k+1})\right]\ , \tag{3.6}$$

and

$$v^{K+1}(b, A) = 0,\ \text{for all } b \in [0, b_{\max}], A \in \{0, 1\}\ . \tag{3.7}$$

Note that, $v^k(b_k, A_k)$ represents the expected maximum discounted payoff between slots k and K given the side information b_k and A_k. Due to the causality and the backward recursion, the observation Γ_k in slot k does not affect the value function for slot $k + 1$. Also, when $A_k = 1$, given the value function for slot $k + 1$, the optimal energy allocation for slot k can be obtained by

$$p_k^*(\Gamma_k) = \arg\max_{p\in\mathcal{D}_{A_k}(b_k)} \big\{\log(1 + ph_k) + \gamma u^k(b_k, p, 1)\big\}\ , \tag{3.8}$$

where $u^k(b, p, A)$ is calculated using (3.6). Moreover, when $A_k = 0$, we always have

$$p_k^*(\Gamma_k) = 0\ . \tag{3.9}$$

3.2 Approximate Value Function

By recursively computing the value function $v^k(b, A)$ defined in (3.5), in theory we can obtain the optimal solution to (3.8) for each $k \in \{1, 2, \ldots, K\}$. However, a closed-form expression for $v^k(b, A)$ is hard to obtain when K is large, e.g., $K \geq 3$. A typical approach is to quantize the continuous variables (b, p, h) to a finite number of discrete levels, i.e., to convert the original problem to a discrete MDP problem [65]. However, with such discretization, solving the corresponding discrete

MDP problem involves an exhaustive search on $\mathcal{D}_1(b)$ for all discretized h, and we can only obtain discrete transmission energy levels.

In order to efficiently solve the MDP problem and obtain the continuous energy allocation, in this section, we will define an approximate value function by using a piecewise linear approximation based on some discrete samples of $\{v^k(B,A) \mid \ B \in \{0,\delta,2\delta,\ldots,b_{\max}\}, A \in \{0,1\}\}$ where δ is an approximation precision. Note that, the piecewise linear approximation is a standard technique to reconstruct a concave function from a set of the discrete points sampled from another concave function [68]. In this section, we first employ the piecewise linear approximation to obtain an approximate value function, and then show the concavity (and non-decreasing property) of the approximate value function by proving that the set of points used for reconstruction is sampled from a concave (and non-decreasing) function.Finally, we have that the problem in (3.17) a convex optimization problem.

3.2.1 Value Function Approximation

With an approximation precision parameter δ, we define a piecewise linear approximation operator:

$$\mathcal{L}\left[v^k(b,A),\delta\right] \triangleq v^k(\lfloor b/\delta \rfloor \delta, A) + \frac{b-\lfloor b/\delta \rfloor \delta}{\delta}\big(v^k(\lceil b/\delta \rceil \delta, A) - v^k(\lfloor b/\delta \rfloor \delta, A)\big),\ b \in [0, b_{\max}]\ , \quad (3.10)$$

and $\mathcal{L}\left[v^K(b,A),\delta\right] \triangleq v(b_{\max},A)$ for any $b > b_{\max}$, as shown in Fig. 3.3.

Initially, we define

$$W_\delta^K(b,A) \triangleq \mathcal{L}\left[v^K(b,A),\delta\right]\ , \quad (3.11)$$

which is a linear approximation to $v^K(b,A)$. Then, recursively from $k = K-1$ to $k = 1$, we use the approximate value function to replace the original value function in (3.6), i.e., $v^k(b,A) \leftarrow W_\delta^k(b,A)$, and define

$$U^k(b_k,p_k,A_k) \triangleq \mathbb{E}_{A_{k+1}|A_k}\big[W_\delta^{k+1}(\min\{b_{\max}, b_k + e_k - p_k\}, A_{k+1})\big]. \quad (3.12)$$

By setting $u^k(b_k,p_k,A_k) \leftarrow U^k(b_k,p_k,A_k)$ in (3.5), we further define

$$V^k(b_k,A_k) \triangleq \mathbb{E}_{h_k}\Big[\max_{p_k(\Gamma_k)\in\mathcal{D}_{A_k}(b_k)} \big\{\log(1+p_k(\Gamma_k)h_k) + \gamma U^k(b_k,p_k(\Gamma_k),A_k)\big\}\Big]\ . \quad (3.13)$$

Finally, we write the approximate value function as

$$W_\delta^k(b,A) \triangleq \mathcal{L}\left[V^k(b,A),\delta\right]\ . \quad (3.14)$$

Note that, in (3.12)-(3.14), we made the substitutions $v^k(b,A) \leftarrow W_\delta^k(b,A)$ and $u^k(b_k,p_k,A_k) \leftarrow U^k(b_k,p_k,A_k)$ in (3.6) and (3.5), respectively. Thus we can treat the approximate value function $W_\delta^k(b,A) \triangleq \mathcal{L}\left[V^k(b,A),\delta\right]$, which is updated by (3.12)-(3.14), as an approximation to the value function $v^k(b,A)$, which is updated by (3.5)-(3.6).

We consider the approximation error $||W_\delta^k(b,A) - v^k(b,A)||_\infty$ at slot k (or iteration $i = K - k + 1$). In each iteration, the error is produced by the piecewise linear approximation in (3.14) and propagated through solving the problem in (3.13). Then, at the end of each iteration the total error accumulated by the obtained approximate value function is the sum of the newly produced error and the discounted propagated error, growing with the iteration number. Since the update rules for both $v^k(b,A)$ and $W_\delta^k(b,A)$ start from the same initial value function $v^K(b,A)$, then the total error in the i-th iteration (we use the subscript (i) to denote the i-th iteration, which represents slot $K-i+1$) can be bounded by

$$||W_\delta^{(i)}(b,A) - v^{(i)}(b,A)||_\infty \leq \sum_{j=1}^{i} \gamma^{i-j}\epsilon_j(\delta) \tag{3.15}$$

where

$$\epsilon_j(\delta) \triangleq \max_{b\in[0,b_{\max}],A\in\{0,1\}} \{V^{(j)}(b,A) - W_\delta^{(j)}(b,A)\} = ||V^{(j)}(b,A) - W_\delta^{(j)}(b,A)||_\infty \tag{3.16}$$

is the new error produced by (3.14) in the j-th iteration. Moreover, the value of $\epsilon_j(\delta)$ can be further bounded by Proposition 3.4 in Section 3.2.2.

With the approximate value function for each slot k, when $A = 1$, the energy allocation given Γ can be obtained by

$$p_k^*(\Gamma) = \arg\max_{p\in\mathcal{D}_1(b)} \left\{ \log(1+ph) + \gamma U^k(b,p,1) \right\}. \tag{3.17}$$

Define $\mathcal{B}_\delta \triangleq \{0,\delta,2\delta,\ldots,b_{\max}\}$. Note that the approximate value function is linearly recovered from the sample set $\{V^k(b,A) \mid b \in \mathcal{B}_\delta\}$ and $W_\delta^k(b,A) = V^k(b,A)$ for all $b \in \mathcal{B}_\delta$. We can consider the standard dynamic programing with the discretized state space as a special case of the update rules in (3.12)-(3.14). Then, the performance achieved with the approximate value function can be characterized as follows.

Proposition 3.1. *The approximate value function obtained by recursively solving* (3.12)-(3.14) *is no less than the discrete value function obtained by the standard dynamic programming method with the state space* $\mathcal{B}_\delta \times \{0,1\}$ *where* δ *is the approximation precision.*

Proof. Given the discrete state space $\mathcal{B}_\delta \times \{0,1\}$, since $W_\delta^{(i)}(B,A) = V^{(i)}(B,A)$ for any $B \times A \in \mathcal{B}_\delta \times \{0,1\}$, the standard dynamic programming follows the same update rule in (3.12)-(3.14) but with a discrete feasible energy allocation set for the optimization problem in (3.13), which is a subset of $D_1(b)$. □

Moreover, in the standard discrete dynamic programming, we discretize all continuous variables, i.e., b_k, h_k, e_k, p_k, and then perform dynamic programming with an exhaustive search on p_k for all possible combinations of (b_k, h_k); while with the proposed approximate value function, we only discretize the battery state b_k and then obtain the approximate value function for each discretized b_k in closed-form.

3.2.2 Concavity of Approximate Value Function

In (3.12)-(3.14), we note that the approximate value function is based on the solution to an optimization problem (3.13). To facilitate solving (3.13), in this subsection, we will show that the approximate value function $W_\delta^k(b,A)$ given in (3.14) is concave for $0 \le b \le b_{\max}$ given $A \in \{0,1\}$. Then (3.13) is a convex optimization problem given h and b.

First, we introduce the following lemma, which can be easily shown and illustrated in Fig. 3.2.

Lemma 3.1. *If a function $f(x) \in \mathbb{R}$ ($x \in \mathcal{X} \subseteq \mathbb{R}$) is non-decreasing, for any $x' \in \mathcal{X}$, $f(\min\{x, x'\})$ is also non-decreasing. Further, if the non-decreasing function $f(x)$ is concave, then $f(\min\{x, x'\})$ is concave for $x \in \mathcal{X} \cup [x', \infty)$.*

We have the following non-decreasing property of $W_\delta^k(b,A)$.

Proposition 3.2. *For any $k \in \{1, 2, \ldots, K-1\}$, if the approximate value function $W_\delta^{k+1}(b,A)$ is non-decreasing with respect to $b \in [0, b_{\max}]$ given $A \in \{0,1\}$, so is $W_\delta^k(b,A)$.*

Proof. If $W_\delta^{k+1}(b,A)$ is non-decreasing with respect to $b \in [0, b_{\max}]$ for $A \in \{0,1\}$, by Lemma 3.1, we have that $W_\delta^{k+1}(\min\{b_{\max}, b\}, A)$ is also non-decreasing with respect to $b \in [0, +\infty)$. Then, we have that $U^k(b,p,A)$, which is a linear combination of the terms of the form $W_\delta^{k+1}(\min\{b_{\max}, b + e_k - p_k\}, A)$, is also non-decreasing with respect to $b \in [0, b_{\max}]$, given p and A.

Given any battery level $b \in [0, b_{\max})$, channel fading h, the energy p_0 such that $p_0 \in \mathcal{D}_A(b)$, and $\epsilon > 0$ such that $b + \epsilon \le b_{\max}$, we have

$$p_0 \in \mathcal{D}_A(b+\epsilon) \ , \tag{3.18}$$

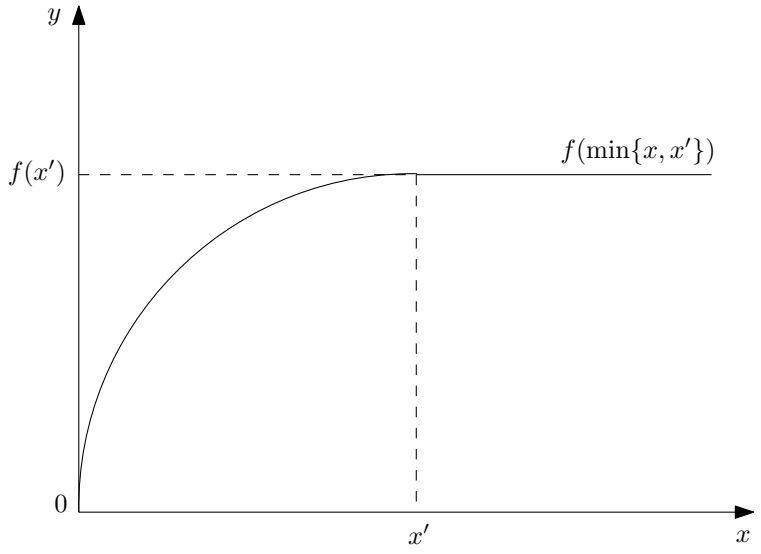

Figure 3.2: Illustration of Lemma 3.1.

and

$$\begin{aligned}\log(1+p_0h)+\gamma U^k(b,p_0,A) &\le \log(1+p_0h)+\gamma U^k(b+\epsilon,p_0,A)\\ &\le \max_{p\in\mathcal{D}_A(b+\epsilon)}\left\{\log(1+ph)+\gamma U^k(b+\epsilon,p,A)\right\}. \qquad (3.19)\end{aligned}$$

Since $V^k(b,A)$ is a non-negative linear combination of the terms of the form $\max_{p\in\mathcal{D}_A(b)}\left\{\log(1+ph)+U^k(b,p,A)\right\}$, $V^k(b,A)$ is non-decreasing with respect to $b\in[0,b_{\max}]$. Then, by (3.14), we have that $W_\delta^k(b,A)$ is also non-decreasing with respect to $b\in[0,b_{\max}]$. □

The next result is on the concavity of $W_\delta^k(b,A)$.

Proposition 3.3. *For any $k\in\{1,2,\ldots,K\}$, if the approximate value function $W_\delta^{k+1}(b,A)$ is non-decreasing and concave with respect to $b\in[0,b_{\max}]$ given $A\in\{0,1\}$, so is $W_\delta^k(b,A)$.*

Proof. Since $W_\delta^{k+1}(b,A)$ is non-decreasing and concave with respect to $b\in[0,b_{\max}]$ given $A\in\{0,1\}$, by Lemma 3.1, we have $W_\delta^{k+1}(\min\{b_{\max},b\},A)$ is non-decreasing and concave with respect to $b\ge 0$ given $A\in\{0,1\}$. Since $b+e-p$ is a linear combination of b and p, then $W_\delta^{k+1}(\min\{b_{\max},b+e-p\},A)$ is jointly concave with respect to b and p. Moreover, it follows that $U^k(b,p,A)$ is also jointly concave with respect to b and p given $A\in\{0,1\}$[68].

Since the feasible domain $\mathcal{D}_A(b)$ is different under $A=0$ and $A=1$. We consider the two cases separately.

When $A = 0$, since $\mathcal{D}_0 = 0$, $v^k(b, 0)$ can be written as

$$V^k(b, 0) = \mathbb{E}_{h_k}\Big[\gamma U^k(b, 0, 0)\Big] . \tag{3.20}$$

Since $U^k(b, p, A)$ is concave with respect to $b \in [0, b_{\max}]$ given p and $A \in \{0, 1\}$, so is $V^k(b, 0)$ [68]. Then, by (3.14), $W^k_\delta(b, 0)$ is non-decreasing with respect to $b \in [0, b_{\max}]$.

When $A = 1$, the feasible domain of the objective function in (3.5) is given by $\mathcal{C} \triangleq \{(b, p) : 0 \le b \le b_{\max}, 0 \le p \le \min\{b, p_{\max}\}\}$. It can be verified that $\mathcal{C}$ is a convex set. Then, for any $(b_1, p_1), (b_2, p_2) \in \mathcal{C}$, their convex combination $(\theta b_1 + \bar{\theta} b_2, \theta p_1 + \bar{\theta} p_2) \in \mathcal{C}$, where $\theta \in [0, 1]$ and $\bar{\theta} \triangleq 1 - \theta$.

Moreover, since $\mathcal{D}_1(b_1), \mathcal{D}_1(b_2)$ are non-empty, we can denote

$$p_1 = \arg \max_{p \in \mathcal{D}_1(b_1)} \Big\{ \log(1 + ph) + \gamma U^k(b_1, p, 1) \Big\} , \tag{3.21}$$

and

$$p_2 = \arg \max_{p \in \mathcal{D}_1(b_2)} \Big\{ \log(1 + ph) + \gamma U^k(b_2, p, 1) \Big\} . \tag{3.22}$$

Then

$$\begin{aligned}
&\max_{p \in \mathcal{D}_1(\theta b_1 + \bar{\theta} b_2)} \Big\{ \log(1 + ph) + \gamma U^{k+1}(\theta b_1 + \bar{\theta} b_2, p, 1) \Big\} \\
&\le \log(1 + (\theta p_1 + \bar{\theta} p_2)h) + \gamma U^{k+1}(\theta b_1 + \bar{\theta} b_2, \theta p_1 + \bar{\theta} p_2, 1) \\
&\le \theta \log(1 + p_1 h) + \bar{\theta} \log(1 + p_2 h) + \theta \gamma U^{k+1}(b_1, p_1, 1) + \bar{\theta} \gamma U^{k+1}(b_2, p_2, 1) \qquad (3.23) \\
&= \theta \big(\log(1 + p_1 h) + \gamma U^{k+1}(b_1, p_1, 1) \big) + \bar{\theta} \big(\log(1 + p_2 h) + \gamma U^{k+1}(b_2, p_2, 1) \big) \\
&= \theta \max_{p \in \mathcal{D}_1(b_1)} \Big\{ \log(1 + ph) + \gamma U^{k+1}(b_1, p, 1) \Big\} + \bar{\theta} \max_{p \in \mathcal{D}_2(b_2)} \Big\{ \log(1 + ph) + \gamma U^{k+1}(b_2, p, 1) \Big\} , \qquad (3.24)
\end{aligned}$$

where (3.23) follows from the joint concavity, and (3.24) follows from the definitions in (3.21) and (3.22).

Therefore, we have that $\max_{p \in \mathcal{D}_1(b)} \big\{ \log(1 + ph) + \gamma U^{k+1}(b, p, 1) \big\}$ is concave with respect to $b \in [0, b_{\max}]$. By (3.13) and (3.14), we further have $W^k_\delta(b, 1)$ is concave with respect to $b \in [0, b_{\max}]$ [68]. □

From Propositions 3.2 and 3.3, we have that if $W^{k+1}_\delta(b, A)$ is non-decreasing and concave so is $W^k_\delta(b, A)$ for any $k \in \{1, 2, \ldots, K - 1\}$. Since $\log(1 + ph)$ is non-decreasing and concave with

respect to $b \in [0, b_{\max}]$, it is easily verified by (3.5) that $W_\delta^K(b, A) = V^K(b, A) = v^K(b, A)$ is also non-decreasing and concave with respect to $b \in [0, b_{\max}]$ given A. By induction, we obtain the following theorem.

Theorem 3.1. *For $k = 1, 2, \ldots, K$, the approximate value function $W_\delta^k(b, A)$ is non-decreasing and concave with respect to $b \in [0, b_{\max}]$ given $A \in \{0, 1\}$. Further, the problem in (3.13) is a convex optimization problem given $b \in [0, b_{\max}]$ and $A \in \{0, 1\}$.*

Therefore, the problem in (3.13) can be solved efficiently by some convex solver and exhaustive search can be avoided.

Since both $V^{(i)}(b, A)$ and $W_\delta^{(i)}(b, A)$ are concave and non-decreasing, where $i = K - k + 1$ is the iteration number, we can further bound the approximation error $\epsilon_i(\delta)$ in (3.16) as follows.

Proposition 3.4. *For any iteration i, we have*

$$0 \leq \epsilon_i(\delta) \leq \max_{A \in \{0,1\}} \left\{ 2V^{(i)}(\delta, A) - V^{(i)}(2\delta, A) - V^{(i)}(0, A) \right\} , \tag{3.25}$$

where $\epsilon_i(\delta) = ||V^{(i)}(b, A) - W_\delta^{(i)}(b, A)||_\infty$.

Proof. By Theorem 3.1, $V^{(i)}(b, A)$ is non-decreasing and concave with respect to b given A. As illustrated in Fig. 3.3, for $b \in [0, \delta]$, the value of $V^{(i)}(b, A)$ is smaller than the value on line (*) but larger than $W_\delta^{(i)}(b, A)$, and therefore the distance between the value on line (*) and $W_\delta^{(i)}(b, A)$ can also be considered as an upper bound on the approximation error, i.e., $V^{(i)}(b, A) - W_\delta^{(i)}(b, A)$ for $b \in [0, \delta]$. According to the second-order derivative property of the concave function, we have that

$$\begin{aligned} &V^{(i)}((n+1)\delta, A) - V^{(i)}(n\delta, A) - (V^{(i)}((n+2)\delta, A) - V^{(i)}((n+1)\delta, A)) \\ \geq &V^{(i)}((n+2)\delta, A) - V^{(i)}((n+1)\delta, A) - (V^{(i)}((n+3)\delta, A) - V^{(i)}((n+2)\delta, A)) \end{aligned} \tag{3.26}$$

for all $n \geq 0$. Then, we further have that $0 \leq \max_b \{V^{(i)}(b, A) - W_\delta^{(i)}(b, A)\} \leq \max\{2V^{(i)}(\delta, A) - V^{(i)}(2\delta, A) - V^{(i)}(0, A), 2V^{(i)}(2\delta, A) - V^{(i)}(3\delta, A) - V^{(i)}(\delta, A), \cdots\} = 2V^{(i)}(\delta, A) - V^{(i)}(2\delta, A) - V^{(i)}(0, A)$. □

Note that, given the specific value of the energy prediction and distribution of the channel gain, the upper bound on $\epsilon_i(\delta)$ can be numerically evaluated. Moreover, using (3.15), an upper bound on the optimal performance (the continuous value function without using the approximation) can be

generated for evaluating the performance of the proposed algorithms. Since $V^{(i)}(b, A)$ is continuous, concave and non-decreasing with respect to $b \in [0, b_{\max}]$ given $A \in \{0, 1\}$, by (3.25), the error bound on $\epsilon_i(\delta) \to 0$ as approximation precision $\delta \to 0$.

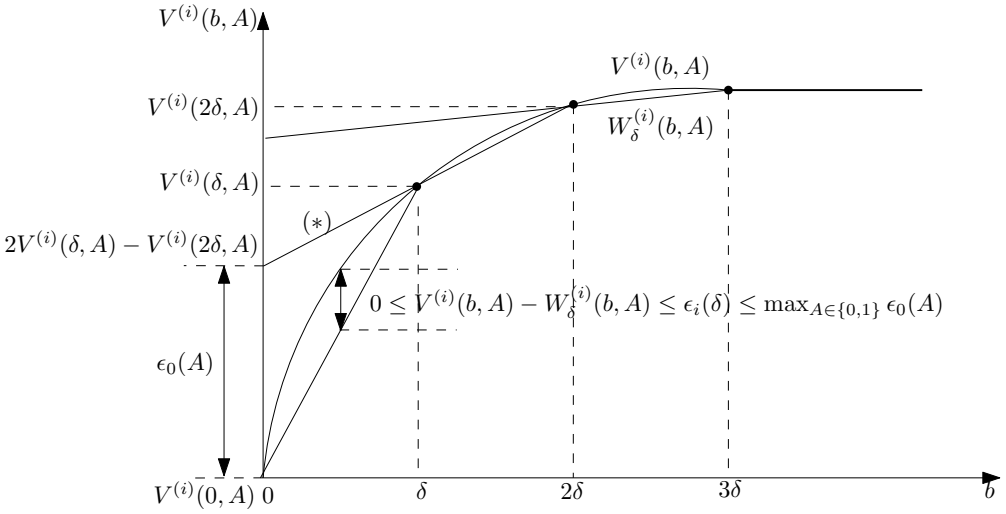

Figure 3.3: The piecewise linear approximation of the value function and the approximation error bound.

Remark 3.1. *In the above discussion, we used a piecewise linear approximation to construct the approximate value function. In fact, any approximation method that preserves the concavity (and non-decreasing property) of the reconstructed function by using samples from a concave (and non-decreasing) function can be used to construct an approximate value function, and our analysis is still valid. In particular, using a higher-order interpolation method can potentially improve the performance. However, in that case it becomes more challenging to ensure the concavity preservation. More importantly, the computational complexity becomes higher when using a high-order interpolation method.*

3.3 energy allocation with Prefect Energy Prediction

Note that in (3.13), we need to solve the following optimization problem for a given $B \in \mathcal{B}_\delta$ and $A \in \{0, 1\}$:

$$p^*(h) = \arg \max_{p(h)\in\mathcal{D}_A(B)} \big\{ \log(1 + p(h)h) + \gamma U^k(B, p(h), A) \big\},\ h \ge 0\ . \tag{3.27}$$

When $A = 0$, $p^*(h) = 0$. On the other hand, when $A = 1$, we will obtain the optimal solution $p^*(h)$ in closed-form.

Since the approximate value function $W_\delta^{k+1}(b, A)$ in (3.14) is a piecewise linear function of b given A, it follows that $U^k(B, p, 1)$ in (3.12) is also a piecewise linear function with respect to p given B, which is differentiable everywhere except at $\mathcal{J} \triangleq \{p \mid p = B + e_k - B_0, B_0 \in \mathcal{B}_\delta\}$. By Theorem 3.1 and Lemma 3.1, $U^k(B, p, 1)$ is also concave and non-decreasing with respect to p.

Since $U^k(B, p, 1)$ is a piecewise linear function, we denote $\mathcal{I} \triangleq \{p_0, p_1, \ldots, p_N\}$ as the set of the non-differentiable points, where $p_0 = 0$, $p_N = \min\{p_{\max}, B\}$, and $p_i, (0 < i < N)$ is the i-th smallest element in $\mathcal{J} \cap \mathcal{D}_1(B) \setminus \{p_0, p_N\}$. Also, we denote $\mathcal{W} = \{w_1, w_2, \ldots, w_N\}$ as the set of the corresponding slopes, where w_i is the slope of the segment $[p_{i-1}, p_i]$, given by

$$w_i \triangleq -\frac{\gamma}{\delta}\mathbb{E}_{A \mid 1}\Big\{V^{k+1}(\lceil \min\{b_{\max}, B + e_k - p_i\}/\delta \rceil\, \delta, A) - V^{k+1}(\lfloor \min\{b_{\max}, B + e_k - p_i\}/\delta \rfloor\, \delta, A)\Big\}\,, \tag{3.28}$$

which is derived from (3.12) and (3.14). Hence, the derivative of $U^k(B, p, 1)$ for $p \in \mathcal{D}_1(B) \setminus \mathcal{I}$ is

$$w(p) = w_i, \text{ if } p \in (p_{i-1}, p_i)\,. \tag{3.29}$$

Since $U^k(b, p, A)$ is concave and non-decreasing with respect to p, we have $0 \geq w_0 > w_1 > \ldots > w_N$. Fig. 3.4 is a sketch of the stair-case function $w(p)$.

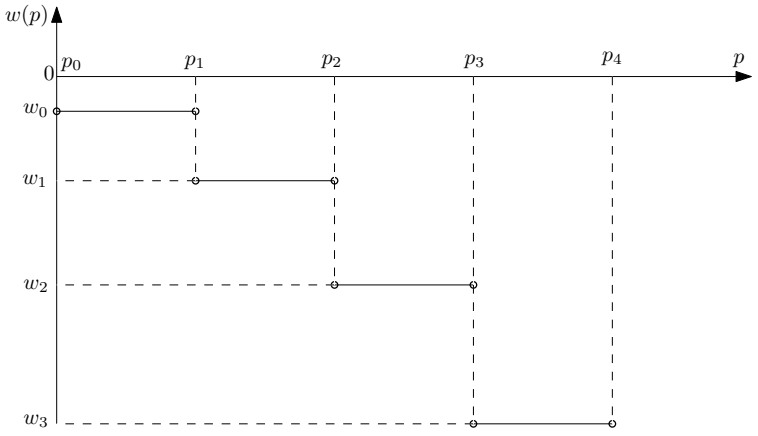

Figure 3.4: The derivative of $U^k(B, p, 1)$ with respect to p.

In this section we first obtain the closed-form solution to (3.27), and then use it to obtain the optimal energy allocation for both finite- and infinite-horizon cases.

3.3.1 The Optimal Solution to (3.27)

In this subsection, for simplicity, we drop the superscript k and denote the objective function in (3.27) as

$$g_h(p) \triangleq \log(1+ph) + \gamma U(B,p,1),\ p \in \mathcal{D}_1(B)\ . \tag{3.30}$$

We note that $g_h(p)$ is differentiable for $p \in \mathcal{D}_1(B) \setminus \mathcal{I}$ with

$$g_h'(p) = \frac{1}{1/h+p} + w(p)\ . \tag{3.31}$$

On the other hand, at the non-differentiable points in $\mathcal{I}$, the right-derivative and the left-derivative of $g_h(p)$ can be written as

$$g_h'(p^+) \triangleq \frac{1}{1/h+p} + w(p^+)\ , \tag{3.32}$$

and

$$g_h'(p^-) \triangleq \frac{1}{1/h+p} + w(p^-)\ , \tag{3.33}$$

respectively.

Theorem 3.2. *The optimal solution to* (3.27) *is given by*

$$p^*(h) = \begin{cases} -\frac{1}{w_i} - \frac{1}{h} & \frac{1}{h} \in [-\frac{1}{w_i} - p_i, -\frac{1}{w_i} - p_{i-1}] \cap [0, +\infty) \\ & \quad i = 1, 2, \ldots, N-1 \\ p_i & \frac{1}{h} \in (-\frac{1}{w_{i+1}} - p_i, -\frac{1}{w_i} - p_i) \cap [0, +\infty) \\ & \quad i = 1, 2, \ldots, N-1 \\ 0 & \frac{1}{h} \in (-\frac{1}{w_1} - p_0, \infty) \\ p_N & \frac{1}{h} \in [0, -\frac{1}{w_N} - p_N) \end{cases}, \tag{3.34}$$

where $p_0 = 0$ *and* $p_N = \min\{p_{\max}, B\}$.

In Fig. 3.5 we give a sketch of $p^*(h)$. To prove Theorem 3.2, we first give the necessary and sufficient conditions for the optimal solution p^* as follows [68].

Lemma 3.2. p^* *is the optimal solution to* (3.27) *given* h*, if and only if,*

1. $g_h'(p^{*+}) \le 0 \le g_h'(p^{*-})$*, when* $g_h'(0^+) > 0$ *and* $g_h'(\min\{B, p_{\max}\}^-) < 0$*;*

2. $p^* = \min\{B, p_{\max}\}$*, when* $g_h'(\min\{B, p_{\max}\}^-) \ge 0$*;*

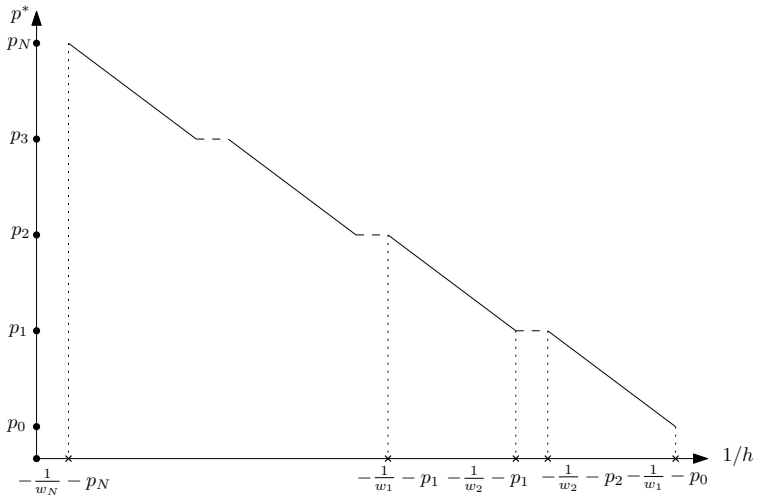

Figure 3.5: The optimal solution $p^*(h)$.

3. $p^* = 0$*, when* $g_h'(0^+) \leq 0$*.*

Note that, Condition 1 corresponds to the case that p^* is in the interior of $\mathcal{D}_1(B)$. In this case, the left-derivative and the right-derivative should have opposite signs or be both zero at p^* so that the increasing and decreasing of p both lead to the decreasing of the objective function. Condition 2 and Condition 3 correspond to the cases that p^* is on each side of the boundary of $\mathcal{D}_1(B)$, where the objective function is non-decreasing and non-increasing for all $p \in \mathcal{D}_1(B)$, respectively.

The following proposition gives a sufficient condition for the optimality of $p^*(h)$ given B.

Proposition 3.5. *Given any* $B \in \mathcal{B}_\delta$*, for* $h \geq 0$*, if the energy schedule* $p^*(h) \in int\mathcal{D}_1(B)$ *satisfies*

$$p^*(h) = \begin{cases} -\frac{1}{w(p^*(h))} - \frac{1}{h}, \\ \qquad \textit{when } p^*(h) \in int\mathcal{D}_1(B) \setminus \mathcal{I}, \\ -\frac{1}{w(p^*(h)^-)} - \frac{1}{h} \ \textit{or} \ -\frac{1}{w(p^*(h)^+)} - \frac{1}{h}, \\ \qquad \textit{when } p^*(h) \in \mathcal{I}, \end{cases} \tag{3.35}$$

then $p^*(h)$ *is the optimal solution to* (3.27)*.*

Proof. Substituting (3.35) into (3.32)-(3.33), we have $g_h'(p^*(h)^+) = 0$ or $g'(p^*(h)^-) = 0$ when $p^*(h) \in \mathcal{I}$, and $g_h'(p^*(h)^+) = g'(p^*(h)^-) = 0$ when $p^*(h) \in int\mathcal{D}_1(B) \setminus \mathcal{I}$. Since $g_h'(p^*(h)^+) \leq g_h'(p^*(h)^-)$, we have $g_h'(p^*(h)^+) \leq 0 \leq g_h'(p^*(h)^-)$. Moreover, since $g_h(p)$ is concave, we have $0 \leq g_h'(p^*(h)^-) < g_h'(0^-)$ and $g_h'(\min\{p_{\max}, B\}^-) < g_h'(p^*(h)^+) \leq 0$. By Lemma 3.2 (Condition 1), we conclude the optimality. □

Then it is easy to verify that for $\frac{1}{h} \in [-\frac{1}{w_i} - p_i, -\frac{1}{w_i} - p_{i-1}] \cap [0, +\infty), i = 1, 2, \ldots, N-1$, the solution given by (3.34) satisfies the optimality condition in Proposition 3.5.

For $\frac{1}{h} \in (-\frac{1}{w_{i+1}} - p_i, -\frac{1}{w_i} - p_i) \cap [0, +\infty), i = 1, 2, \ldots, N-1$, we use the next proposition to prove the optimality of (3.34).

Proposition 3.6. *For any non-differentiable point $p_i \in \mathcal{I} \setminus \{p_0, p_N\}$, p_i is the optimal solution to (3.27) for any $\frac{1}{h} \in (-\frac{1}{w_{i+1}} - p_i, -\frac{1}{w_i} - p_i) \cap [0, +\infty)$.*

Proof. From (3.32)-(3.33), $g'_h(p_i^+)$ and $g'_h(p_i^-)$ are functions of $\frac{1}{h}$ for a given p_i. If $(-\frac{1}{w_{i+1}} - p_i, -\frac{1}{w_i} - p_i) \cap [0, +\infty)$ is not empty, it is easy to verify that $0 = g'_h(p_i{}^-) > g'_h(p_i{}^+)$ when $\frac{1}{h} = -\frac{1}{w_i} - p_i$, and $g'_h(p_i^-) > g'_h(p_i^+)$ and $g'_{h+}(p_i) \leq 0$ when $\frac{1}{h} = -\frac{1}{w_{i+1}} - p_i$. Since given p_i, $g'_h(p_i^-)$ and $g'_h(p_i^+)$ increase as $\frac{1}{h}$ decreases, then decreasing $\frac{1}{h}$ from $-\frac{1}{w_i} - p_i$ to $\max\{0, -\frac{1}{w_{i+1}} - p_i\}$, we have $g'_h(p_i^-) \geq 0 \geq g'_h(p_i^+)$ for all $\frac{1}{h} \in (-\frac{1}{w_{i+1}} - p_i, -\frac{1}{w_i} - p_i) \cap [0, +\infty)$. By Lemma 3.2, the proposition follows. □

Propositions 3.5 and 3.6 obtain the optimal solution for $\frac{1}{h} \in [-\frac{1}{w_N} - p_N, -\frac{1}{w_1}] \cap [0, \infty)$. For other $h \geq 0$, using Conditions 2 and 3 in Lemma 3.2, we can prove the optimality of (3.34) as follows.

Proposition 3.7. *1. For any h such that $\frac{1}{h} \geq -\frac{1}{w_1}$, the optimal solution is $p^*(h) = 0$;*

2. For any h such that $0 \leq \frac{1}{h} \leq -\frac{1}{w_N} - p_N$, the optimal solution $p^*(h) = p_N$.

Proof. Note that, since $U(B, p, 1)$ is non-increasing with respect to p, we have $-\frac{1}{w_1} \geq 0$. When $\frac{1}{h} = -\frac{1}{w_1}$, it is easy to verify that $g'_h(0^+) = 0$. Since $g'_h(0^+)$ is also a function of $\frac{1}{h}$ which decreases as $\frac{1}{h}$ increases, we have for any $\frac{1}{h} \geq -\frac{1}{w_1}$, $g'_h(0^+) \leq 0$. By Condition 3 in Lemma 3.2, we must have $p^*(h) = 0$ for any h such that $\frac{1}{h} \geq -\frac{1}{w_1} \geq 0$. Similarly, we may also verify that for any $\frac{1}{h} \leq -\frac{1}{w_N} - p_N$, $g'_h(p_N^-) \geq 0$. By Condition 2 in Lemma 3.2, we must have $p^*(h) = p_N$ for any h such that $0 \leq \frac{1}{h} \leq -\frac{1}{w_N} - p_N$. □

Note that, given $B \in \mathcal{B}_\delta$, $p^*(h)$ is a piecewise function in closed-form. Then, $V^k(B, A)$ can be efficiently evaluated as

$$V^k(B, 1) = \mathbb{E}_{h_k}\Big\{ \log(1 + p^*(h_k)h_k) + \gamma U^k(B, p^*(h_k), 1)\Big\} , \tag{3.36}$$

and

$$V^k(B, 0) = \mathbb{E}_{h_k}\Big\{ \log(1) + \gamma U^k(B, 0, 0)\Big\} = U^k(B, 0, 0) , \tag{3.37}$$

where

$$U^k(B,p,0)=\sum_{A'=0,1}\Pr(A_{k+1}=A'\mid A_k=0)\big[W_\delta^{k+1}(\min\{b_{\max},B+e_k-p\},A')\big]. \tag{3.38}$$

3.3.2 Calculating the Approximate Value Function

In order to obtain the energy allocation, we need to compute the approximate value function given by (3.12)-(3.14) for $k=1,2,\ldots,K$ ($K=\infty$ for infinite-horizon case). Then, when the observation is available, we solve the problem given in (3.17).

3.3.2.1 Finite K

We first consider the finite-horizon case where K is finite, we assume that the distributions of channel fading are independent across slots but not necessarily identical.

The energy allocation consists of two phases. In the first phase, we recursively compute the approximate value function from $k=K$ to $k=1$, following (3.12)-(3.14). Specifically, in the i-th iteration, we obtain $W_\delta^{(i)}(b,A)$ for slot $k=K-i+1$ as follows. Based on $W_\delta^{(i-1)}(b,A)$ obtained in the previous iteration (or the initial function for the first iteration), for each $B\in\mathcal{B}_\delta$ and $A=\{0,1\}$, we obtain the piecewise linear function $U^{(i)}(B,p,A)$ by specifying the sets $\mathcal{I}$ and $\mathcal{W}$. Then, we use (3.34) to obtain $p^*(h)$ and use (3.36)-(3.37) to update $V^{(i)}(B,A)$ for all $B\in\mathcal{B}_\delta$ and $A=\{0,1\}$. With the set $\{V^{(i)}(B,A)\mid B\in\mathcal{B}_\delta,A=\{0,1\}\}$, the approximate value function $W_\delta^{(i)}(b,A)$ can be obtained using (3.14) and we store the closed-form $W_\delta^{(i)}(b,A)$ in a look-up table. Note that the above first phase should be completed before the first slot.

The second phase is performed at the beginning of each slot, once the observation becomes available. This phase is to solve the problem given in (3.17) using (3.34). Specifically, at the beginning of slot k, the transmitter observes the system state, i.e., the channel access state A, the channel gain h, and the current battery state b. When $A=0$, the transmitter keeps silent. Otherwise, the transmitter retrieves the approximate value function $W_\delta^{k+1}(b,A)$ (i.e., $W_\delta^{(K-i-1)}(b,A)$) from the look-up table and then calculate the energy allocation using (3.34).

The entire computational procedure for the finite-horizon case is summarized in Algorithm 3.1.

Algorithm 3.1 - Finite-Horizon energy allocation

1: Inputs
Distributions of $\boldsymbol{H}$, $\boldsymbol{A}$; value of e_k for $k = 1, 2, \ldots, K$
Approximation precision $\delta > 0$; discount factor $\gamma \in [0, 1]$
2: Phase-I: Compute the approximate value function update
(offline calculation)
FOR $k = K$ **TO** 1
(*) Calculate $V^k(B, h, A)$ for $B \in \mathcal{B}_\delta, A \in \{0, 1\}$
using (3.34) (or general convex solver) and (3.36)-(3.37)
Compute $W_\delta^k(b, A)$ from $V^k(B, A)$ using (3.14) and store it
ENDFOR
3; Phase-II: energy allocation (online calculation)
FOR $k = 1$ **TO** K
Get the observations $\Gamma_k = (b_k, h_k, A_k)$
Retrieve $W_\delta^{k+1}(b, A)$ and calculate $U^k(b_k, p, A_k)$ using (3.12)
Calculate $p^*(h_k)$ using (3.34)
ENDFOR

Remark 3.2. *If the observations can be predicted in a scheduling period K, i.e., $\boldsymbol{H}$, $\boldsymbol{E}$, and $\boldsymbol{A}$ are known in advance, we can rewrite* (3.4) *as follows*

$$\mathcal{P}^* = \arg \max_{p_k, k=1,2,\ldots,K} \left\{ \sum_{k=1}^{K} A_k \log(1 + p_k h_k) \right\}, \tag{3.39}$$

subject to the constraints in (3.1), (3.49), *and* (3.3) *for $k = 1, 2, \ldots, K$.*

We note that in the above case all the observations are non-causally known in advance and the problem in (3.39) *is a convex optimization problem. An efficient dynamic water-filling algorithm was proposed in [69] for solving* (3.39) *optimally. Moreover, since* (3.39) *is a special case of the stochastic case, Algorithm 3.1 is also applicable and would approach the optimal performance as the dynamic water-filling algorithm when $\delta \to 0$. Specifically, the use of Algorithm 3.1 or the dynamic water-filling algorithm strikes a balance between the performance and the computational complexity.*

3.3.2.2 Infinite K

In the infinite-horizon case, although K is infinite, the number of the iterations in the first phase is not infinite since the approximate value function will converge. Moreover, since we have assumed that e_k is static and h_k is i.i.d., the converged approximate value function can be directly used in (3.17) to obtain the energy allocation with the observations in the second phase, for all slots.

We denote

$$\mathcal{T}_\delta \ : \ W_\delta(b, A) \to W_\delta(b, A) \tag{3.40}$$

as the value function update operator in (3.12)-(3.14): based on a given value function $W_\delta^{(i)}(b, A)$, it solves (3.13) to obtain $V^{(i)}(B, p, A)$ for $B \in \mathcal{B}_\delta$, and then generates the new approximate value function $W_\delta^{(i+1)}(b, A)$ by (3.14). Then we can write

$$W_\delta^{(i+1)}(b, A) \triangleq \mathcal{T}_\delta\Big[W_\delta^{(i)}(b, A)\Big], \ b \in [0, b_{\max}] \ . \tag{3.41}$$

Note that $\mathcal{T}_0$ is the standard Bellman operator corresponding to (3.5)-(3.6) without the value function approximation, i.e., $\delta = 0$ [65].

Then the computational procedure for the infinite-horizon case is summarized in Algorithm 3.2.

Algorithm 3.2 - Infinite-Horizon energy allocation

1: Inputs

Distributions of h, A; value of e; discount factor $\gamma \in (0,1)$

Approximation precision $\delta > 0$; termination condition α

2: Phase-I Approximate value function update

(offline calculation)

$i \leftarrow 0$

REPEAT

(*) $W_\delta^{(i+1)}(b,A) = \mathcal{T}_\delta\Big[W_\delta^{(i)}(b,A)\Big]$

$i \leftarrow i+1$

UNTIL $||W_\delta^{(i)}(b,A) - W_\delta^{(i-1)}(b,A)||_\infty \leq \alpha$

$W_\delta^*(b,A) \leftarrow W_\delta^{(i)}(b,A)$

3: Phase-II energy allocation (online calculation)

AT THE BEGINNING OF EACH SLOT

Get the observations $\Gamma = (b,h,A)$

Retrieve $W_\delta^*(b,A)$ and calculate $U^*(b,p,A)$ using (3.12)

Calculate $p^*(h)$ using (3.34)

To show the convergence of the approximate value function update, we first note that, by repeatedly performing $\mathcal{T}_0$ on any initial value function, a converged value function can be obtained as follows [65]:

$$v^*(b,A) \triangleq \mathcal{T}_0 \cdot \mathcal{T}_0 \cdot \ldots \Big[v^{(1)}(b,A)\Big] = \mathcal{T}_0^\infty \Big[v^{(1)}(b,A)\Big]. \tag{3.42}$$

Extending the convergence of $\mathcal{T}_0$ to $\mathcal{T}_\delta$, we introduce the following lemma. The proof is given in Appendix 3.7.1.

Lemma 3.3. *The operator $\mathcal{T}_\delta$ has the γ-contraction property, i.e., for any two functions $V_1(b,A)$ and $V_2(b,A)$, we have*

$$||\mathcal{T}_\delta\Big[V_1(b,A)\Big] - \mathcal{T}_\delta\Big[V_2(b,A)\Big]||_\infty \leq \gamma||V_1(b,A) - V_2(b,A)||_\infty \ . \tag{3.43}$$

It then follows that

$$||T_\delta^{i+1}\Big[W_\delta^{(1)}(b,A)\Big] - \mathcal{T}_\delta^i\Big[W_\delta^{(1)}(b,A)\Big]||_\infty \leq \gamma^i||\mathcal{T}_\delta\Big[W_\delta^{(1)}(b,A)\Big] - W_\delta^{(1)}(b,A)||_\infty \ , \tag{3.44}$$

i.e., $\mathcal{T}_\delta^i\Big[W^{(1)}(b,A)\Big]$ converges as i increases. Then, the converged approximate value function can be denoted as

$$W_\delta^*(b,A) \triangleq \mathcal{T}_\delta^\infty\Big[W_\delta^{(1)}(b,A)\Big] \tag{3.45}$$

and we have

$$W_\delta^*(b,A) = \mathcal{T}_\delta\Big[W_\delta^*(b,A)\Big] \ . \tag{3.46}$$

Using the γ-contraction property in Lemma 3.3, the convergence behavior of Algorithm 3.2 can be further characterized as

$$\begin{aligned} ||W_\delta^{(i+1)}(b,A) - W_\delta^*(b,A)|| =& ||T_\delta^i\Big[W_\delta^{(1)}(b,A)\Big] - \mathcal{T}_\delta^i\Big[W_\delta^*(b,A)\Big]||_\infty \\ \leq& \gamma^{i-j+1}||W_\delta^{(j)}(b,A) - W_\delta^*(b,A)||_\infty \ , \end{aligned} \tag{3.47}$$

for $j \in \{1,2,\ldots,i\}$. Note that, the convergence speed is mainly controlled by the value of the discount factor γ. Moreover, the error between the converged approximate value function and $v^*(b,A)$ is bounded as follows.

Theorem 3.3. *If* $||\mathcal{T}_\delta^i[W_\delta^{(1)}(b,A)] - \mathcal{T}_\delta^{i-1}[W_\delta^{(1)}(b,A)]||_\infty \leq \alpha$*, then the error between* $v^*(b,A)$ *and* $W_\delta^{(i)}(b,A)$ *is bounded by*

$$||W_\delta^{(i)}(b,A) - v^*(b,A)||_\infty \leq \frac{\gamma\alpha + ||2v^*(\delta,A) - v(0,A) - v^*(2\delta,A)||_\infty}{1-\gamma} \ . \tag{3.48}$$

Proof. The proof is provided in Appendix 3.7.2. □

Theorem 3.3 characterizes the performance of Algorithm 3.2 by giving an error bound after it converges with a tolerance α. Specifically, in (3.48), the two terms in the numerator of the right-hand side represent the error introduced by the convergence tolerance α and by the value function approximation δ, respectively. Obviously, as α and δ both go to zero, the error bound in (3.48) goes to zero. Moreover, a smaller discount factor γ leads to a smaller error bound.

Note that, Algorithms 1 and 2 have both the offline calculation part and the online calculation part. During offline calculation, we evaluate $V^k(B,A)$ for each $B \in \mathcal{B}_\delta$ in each iteration, i.e., solve $\mathcal{O}(B_{\max}/\delta)$ convex optimization problems in each iteration. Specifically, rather than using an exhaustive search for each combination of the discretized (B,H) (H is the discretized channel gain) as done by the standard discrete MDP method, the proposed algorithms use (3.34) to calculate $V^k(B,A)$ for each $B \in \mathcal{B}_\delta$ directly. Moreover, for the infinite case, by Lemma 3.3, the α-converged

approximate value function can be obtained within $\mathcal{O}(\log_\gamma \alpha)$ iterations. On the other hand, during online calculation, we retrieve $W_\delta^{k+1}(b, A)$ (or $W_\delta^*(b, A)$) from the look-up table and then use (3.34) to compute the energy allocation for the specific observation (b_k, h_k, A_k).

Moreover, the proposed algorithms calculate the energy allocation based on the continuous battery state and channel gain, and the obtained energy allocation is also continuous. Thus it provides higher precision for both offline calculation and online calculation than the conventional discrete MDP method, especially when the discretization step is large. Finally, as shown in Section 3.3, a better performance can be achieved by the proposed algorithm with a lower computational complexity compared with the conventional discrete MDP method.

3.4 Energy allocation with Imperfect Energy Prediction

Although energy harvesting is usually predictable, there may exist a non-negligible prediction error in practice. In this section, we treat the case of imperfect energy harvesting prediction where the prediction error is an independent random variable. We also consider a general payoff function $r(p, A)$, which is continuous, non-decreasing and concave with respect to p given $A \in \{0, 1\}$.

3.4.1 Model with Imperfect Energy Prediction

In this section, we assume that the energy harvesting process consists of a deterministic part e_k and a stochastic part ε_k, where ε_k is an independent random variable. The deterministic process e_k in practice is obtained from the prediction using historic observations, e.g., by using some prediction algorithm. In the extreme case that the prediction is not available, we can set $e_k = 0$ and treat the independent random variable $\varepsilon_k > 0$ as the harvested energy.

Incorporating the prediction error ε_k, the problem formulation is modified as follows:

$$b_{k+1} = \min\left\{b_{\max}, b_k + e_k + \varepsilon_k - p_k\right\}, \tag{3.49}$$

and

$$\mathcal{P}^* \triangleq \arg \max_{p_k(\cdot), k=1,2,\ldots,K} \left\{\mathbb{E}_{\boldsymbol{H},\boldsymbol{E},\boldsymbol{A}}\Big[\sum_{k=1}^{K} \gamma^{k-1} r(p_k(\Gamma_k), h_k)\Big]\right\}, \tag{3.50}$$

subject to the constraints in (3.1), (3.3), and (3.49), for $k = 1, 2, \ldots, K$, where $\boldsymbol{E} \triangleq [\varepsilon_1, \varepsilon_2, \ldots, \varepsilon_K]$. Accordingly, since ε_k is a random variable, the (approximate) value function update rules in (3.6)

and (3.12) are changed to

$$u^k(b_k, p_k, A_k) \triangleq \mathbb{E}_{\varepsilon_k, A_{k+1}|A_k}\left[v^{k+1}(\min\{b_{\max}, b_k + e_k + \varepsilon_k - p_k\}, A_{k+1})\right], \tag{3.51}$$

and

$$U^k(b_k, p_k, A_k) \triangleq \mathbb{E}_{\varepsilon_k, A_{k+1}|A_k}\left[W_\delta^{k+1}(\min\{b_{\max}, b_k + e_k + \varepsilon_k - p_k\}, A_{k+1})\right], \tag{3.52}$$

respectively.

Thus the update rules of the new approximate value function defined for the model with imperfect energy prediction is updated using (3.13), (3.14) and (3.52). Then we can still apply Algorithm 3.1 and Algorithm 3.2 to compute the energy allocation for finite- and infinite-horizon cases, respectively. Specifically, as compared to (3.6) and (3.12), the only difference in (3.51) and (3.52) is the expectation with respect to the prediction error ε_k, which preserves the concavity and monotonicity. Then, it is easy to verify that Proposition 3.2 and Proposition 3.3 still hold for the model with imperfect energy prediction. Also, since $r(p, A)$ is continuous, non-decreasing and concave with respect to p given A, the approximate value function for the general model is still concave by Theorem 3.1. Therefore, except for Theorem 3.2, all results derived for the prefect energy prediction are also valid for the general model with imperfect energy prediction.

However, note that, the optimal solution $p^*(h)$ in (3.34) is based on the facts that $U^k(b, p, A)$ is a piecewise linear function and $r(p, h) = \log(1+ph)$, which are no longer valid with the general payoff function and/or imperfect energy prediction. Then, in Algorithms 1 and 2, the steps marked by (*), which aim to solve the problem in (3.13), need to be modified accordingly. In particular, since the corresponding problem is still a convex optimization problem, we now can use some general convex solver to numerically solve (3.13).

3.4.2 Complexity and Performance

By analyzing the piecewise linear approximation method, Propositions 3.1 and 3.4 give the lower bound on the approximate value function and the upper bound on the approximation error, respectively, which are valid for both the models with the perfect and imperfect energy predictions. Also, for the infinite-horizon case, the convergence and the approximation error of Algorithm 3.2 are provided in (3.44) and Theorem 3.3 for the perfect energy prediction case, which also extends

to the model with the imperfect energy prediction. Thus the error in the energy allocation goes to zero as the approximation precision δ goes to zero, for both the finite- and infinite-horizon cases.

Moreover, the approximate value function is formed by the piecewise linear approximation and is concave with respect to the battery level. Thus, the problem in (3.13) is a convex optimization problem, which can be solved efficiently by the standard convex solver. Specifically, for the finite-horizon case, the energy allocations can be obtained in K iterations while for infinite-horizon case, the approximate value function converges within $\mathcal{O}(\log_\gamma \alpha)$ iterations. In both the finite- and infinite-horizon cases, $\mathcal{O}(1/\delta)$ convex optimization problems with single variable and single constraint are solved in each iteration. For the specific case that the energy is predicted perfectly and the payoff is the channel rate, the optimal solution to (3.13) can also be obtained in closed-form, as shown in (3.34). With the proposed algorithms, the continuous energy allocation is obtained by solving a continuous MDP model in a computationally efficient manner. As compared to the conventional discrete MDP method, the proposed algorithms do not involve exhaustive search.

Note that, based on the approximate value function in (3.13), (3.14) and (3.52), we have a mapping from the observation Γ_k to the energy allocation p_k, which is obtained by solving the optimization problem in (3.13) for each slot k. This mapping can be denoted as $\Pi(k):\ \Gamma \to p$. Using $\Pi(k)$, we denote the received expected payoff as

$$\bar{v}^k_{\Pi(k)}(b_k, A_k) \triangleq \mathbb{E}_{h_k}\Big[r(p_k(\Gamma_k), h_k) + \gamma \bar{u}^k(b_k, p_k(\Gamma_k), A_k)\Big|\ p_k(\Gamma) \in \Pi(k)\Big]\ , \tag{3.53}$$

where

$$\bar{u}^k(b_k, p_k, A_k) \triangleq \mathbb{E}_{\varepsilon_k, A_{k+1}|A_k}\left[\bar{v}^{k+1}_{\Pi(k)}(\min\{b_{\max}, b_k + e_k + \varepsilon_k - p_k\}, A_{k+1})\right] \tag{3.54}$$

and

$$\bar{v}^{K+1}_{\Pi(k)}(b, A) = v^{K+1}(b, A) = 0\ , \tag{3.55}$$

for all $b \in [0, b_{\max}]$ and $A \in \{0, 1\}$.

Proposition 3.8. *Suppose that $\Pi(k)$ is obtained by solving the continuous MDP problem with the approximate value function $W^k_\delta(b_k, A_k)$. We have*

$$\bar{v}^k_{\Pi(k)}(b, A) \geq W^k_\delta(b, A),\ \forall b \in [0, b_{\max}], \forall A \in \{0, 1\}\ , \tag{3.56}$$

for all $k \in [1, K]$, i.e., the performance of the obtained energy allocation is lower bounded by the approximate value function.

Proof. In the first iteration $k = K$, by (3.55) and (3.14), we know that $\bar{v}^{K+1}_{\Pi(k)}(b, A) \geq V^{K+1}(b, A) \geq W^{K+1}_{\delta}(b, A)$ for all $b \in [0, b_{\max}]$ and $A \in \{0, 1\}$. Since $\Pi(K)$ is obtained by solving (3.13), according to (3.53) we have $\bar{v}^{K}_{\Pi(K)}(b, A) \geq V^{K+1}(b, A) \geq W^{K}_{\delta}(b, A)$, where the first inequality follows since $\bar{v}^{K+1}_{\Pi(k)}(b, A) \geq W^{K+1}(b, A)$ for all $b \in [0, b_{\max}]$, $A \in \{0, 1\}$ and the second inequality follows since $V^{K+1}(b, A)$ is concave and non-decreasing. Using induction, the proposition holds. □

3.5 Simulation Results

We use the payoff function $r(p, h) = \log(1 + ph)$. We assume that the channel fading H_k is an i.i.d. random variable following the Rayleigh distribution with the parameter σ. We first assume that the harvested energy can be perfectly predicted. For the transmitter, we set the maximum transmission power as $p_{\max}/T_c = 6$ units per slot, the battery capacity as $b_{\max} = 15$ units, and the initial battery level as $b_0 = 2$ units. Further, we set the probability of the channel access suspension as $q = \hat{q} = 0.1$, the approximation precision δ of the approximating value function as 1 and 0.1, and the convergence error tolerance for the infinite-horizon case as $\alpha = 0.0001$.

We first evaluate the performance of the proposed algorithms. For comparison, we consider three simple energy allocation methods, the *greedy policy*, the *balanced policy*, and the standard discrete MDP method. The greedy policy tries to allocate as much energy as possible in each slot subject to the energy availability. On the other hand, the balanced policy tries to allocate a constant energy in each slot, e.g., the mean value of the harvested energy. Moreover, for the standard discrete MDP method, we discretize the battery level, the channel gain, and the transmission energy with the same precision factor δ, and then perform the dynamic programming algorithm and the value iteration algorithm on the discrete state space for the finite- and infinite-horizon cases, respectively.

For the finite-horizon case, we set $K = 30$, $\gamma = 1$, and $\sigma = 0.7, 0.8, 0.9, 1.0, 1.1, 1.2$. We randomly generate the prediction value e_k following a positive truncated-Gaussian distribution with the variance of 2. We consider two typical scenarios, an *energy-constrained scenario* with the mean of the harvested energy of 2, and a *power-constrained scenario* with the mean of the harvested energy of 4. In the energy-constrained scenario, the average harvested energy is much lower than the maximum transmission power and the energy schedule is mainly constrained by the energy availability. On the other hand, in the power-constrained scenario, the average harvested

energy approaches to the maximum transmission power and this constraint dominates the energy scheduling. For both scenarios, we compare the performance of the proposed algorithm with the standard discrete MDP method, the greedy policy and the balanced policy, averaged over 2×10^6 realizations in Fig. 3.6 and Fig. 3.7, respectively. Although we cannot obtain the optimal performance, we utilize the error bound given in (3.15) and (3.25) as an upper bound on the optimal performance. Also, the performance obtained by the standard discrete MDP method can serve as the lower bound. Moreover, the performance of the proposed algorithm with additional choices of approximation precision δ is shown in Fig. 3.8 for the energy-constrained scenario.

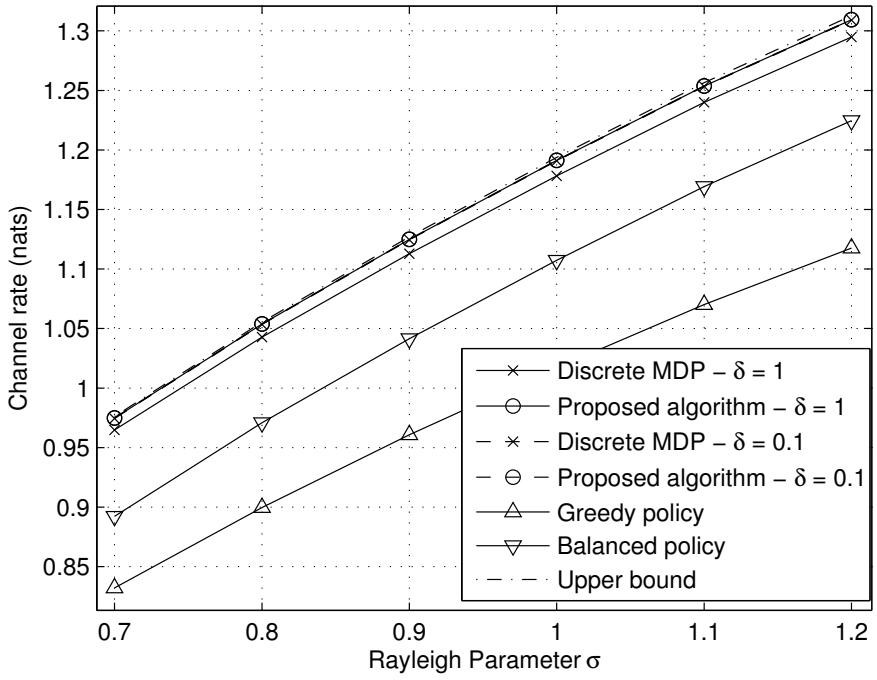

Figure 3.6: Performance comparisons in the energy-constrained scenario for the finite-horizon case.

It can be seen from Fig. 3.6 and Fig. 3.7 that for $\delta = 1$, the performance of the proposed algorithm tightly approaches the upper bound on the optimal performance in both scenarios while there is a gap between the proposed algorithm and the standard discrete MDP method. The main reason is that the discrete MDP method discretizes all continuous variables and causes some non-negligible error with the large discretization step. For $\delta = 0.1$, both the proposed algorithm and the standard discrete MDP method achieve the comparable performance, but their computational

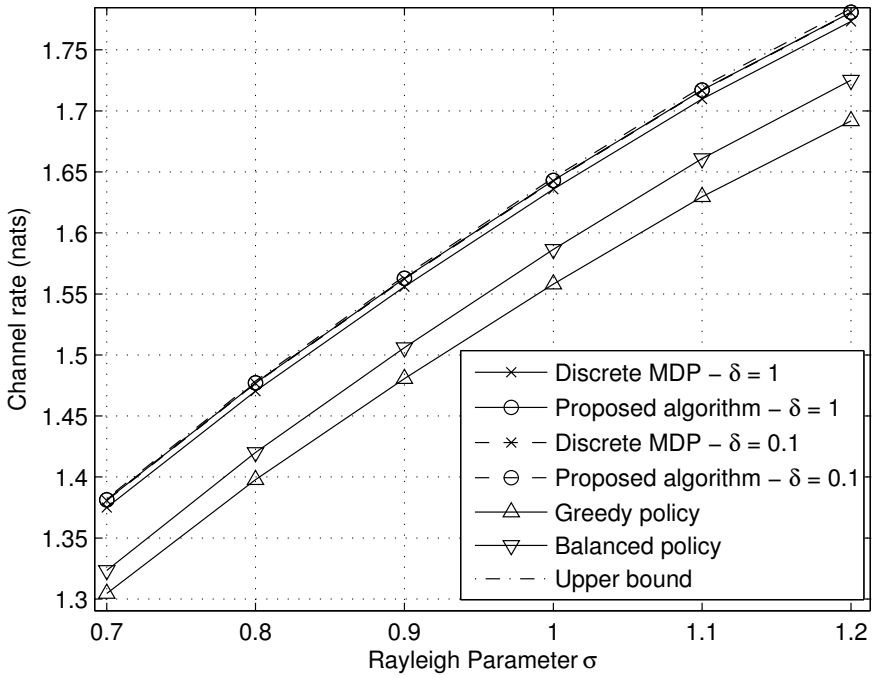

Figure 3.7: Performance comparisons in the power-constrained scenario for the finite-horizon case.

complexities are not comparable, e.g., the exhaustive search is involved in the latter. The greedy and balanced policies both have significantly inferior performances. Also, it is seen from Fig. 3.8 that the performance of the proposed algorithm improves as δ decreases, and as $\delta \to 0$ it approaches the optimal performance. Moreover, we note that the total rate increases as the Rayleigh parameter σ increases and the rate in the energy-constrained scenario is higher than that in the power-constrained scenario.

For the infinite-horizon case, we set $\gamma = 0.85$, $e_k = 3$, and $\sigma = 0.7, 0.8, 0.9, 1.0, 1.1, 1.2$. Similar to the finite-horizon case, we evaluate the performance for various energy allocation policies, averaged over 2×10^6 realizations. The performance comparisons for various energy allocation policies are shown in Fig. 3.9. Moreover, the convergence speeds of the proposed algorithm and the discrete MDP method (i.e., the value iteration algorithm [65]) are shown in Fig. 3.10 for $\sigma = 1$ and $\gamma = 0.8, 0.9$, which are also compared with the convergence speed bound.

Similar to the finite-horizon case, it is seen from Fig. 3.9 that the proposed algorithm has the best performance, tightly approaching the upper bound on the optimal performance. We note

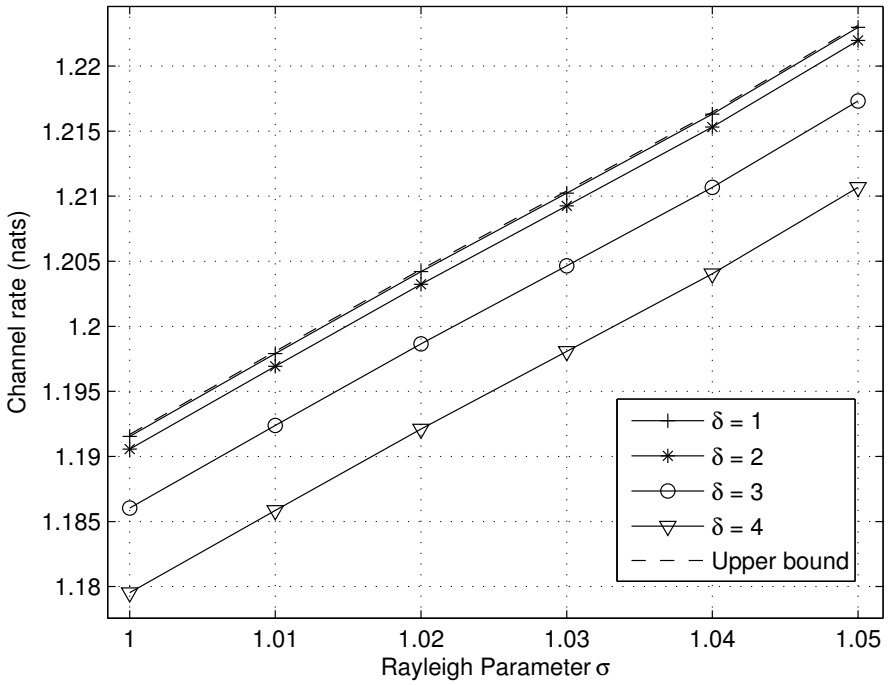

Figure 3.8: Performance under different approximation precisions in the energy-constrained scenario.

that the standard discrete MDP method with a discretization step of $\delta = 0.1$ performs worse than the proposed algorithm. Further, the approximation gap is slightly higher in the infinite case as compared to that in the finite case. Moreover, we see that the greedy approach has the worst performance. In addition, it is seen from Fig. 3.10 that the discount factor affects the convergence speed, as analyzed in Section 3.3. In the simulations for $\gamma = 0.8, 0.9$, the convergence speeds of the proposed algorithm are close to the convergence speed bounds (given in (3.47)), which converge within around 30 and 70 iterations for the different discount factors, respectively. Also, the conventional discrete MDP method and the proposed algorithm have the similar convergence speeds, while the proposed algorithm has lower complexity in each iteration.

We next evaluate the impact of the imperfect prediction error. We consider the finite-horizon case and set $K = 10$, $\gamma = 1$, $e_k = 3.5$, $\sigma = 1$, $q = 1 - \hat{q} = 0$, and $\delta = 0.1$. In this scenario, we only consider the impact of the imperfect prediction and we assume that the channel fading is known and the energy prediction error follows the discrete uniform distribution between $-v$ and v with

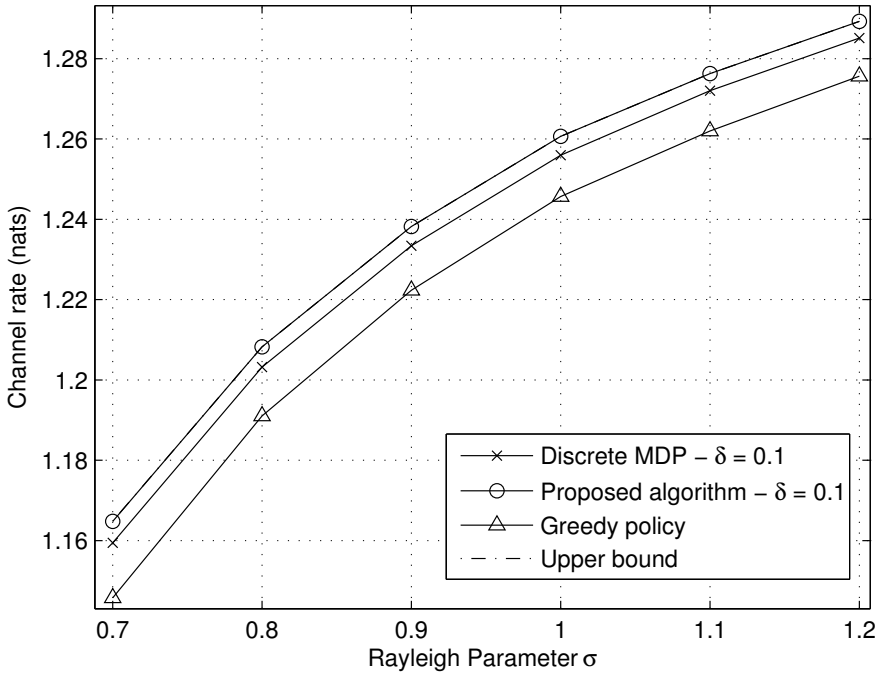

Figure 3.9: Performance comparisons for the infinite-horizon case.

the step of 0.1. The total payoff obtained by the proposed algorithm with causal information and the water-filling based algorithm in [69] with non-causal information is compared in Fig. 3.11, over different prediction error ranges $v = 0, 0.5, 1, 1.5, 2, 2.5$. It is seen from Fig. 3.11 that as v decreases, the performance gap of the two algorithms with and without non-causal information decreases and approaches zero.

3.6 Conclusions

We have considered the problem of optimal energy allocation for an access-controlled transmitter with energy harvesting capability, operating in time-slotted fashion with causal knowledge of the channel state and the energy harvesting state. The energy harvesting process is a sum of a deterministic non-causal estimate and a random causal prediction error. This problem is formulated as a Markov decision process with continuous state. To efficiently solve this problem for both the finite- and infinite-horizon cases, we have introduced the approximate value function and

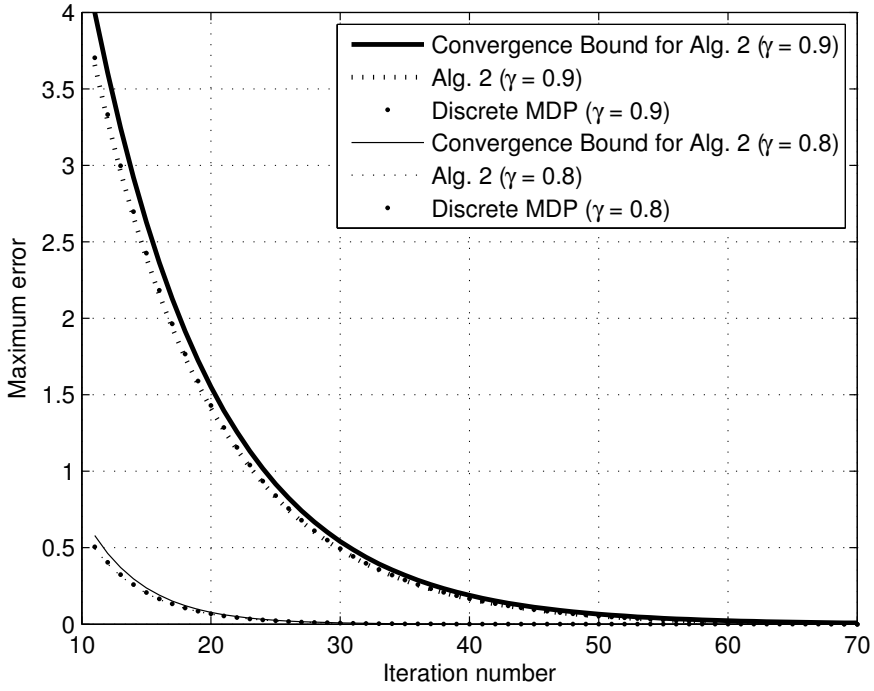

Figure 3.10: The convergence behavior of Algorithm 3.2 for $\sigma = 1, \delta = 0.1$.

developed efficient algorithms for obtaining the approximately optimal solutions. The proposed algorithms provide an approximately optimal continuous energy allocation, whose performance is better than that obtained by the standard discrete MDP method, in a computationally efficient manner. Simulation results demonstrate that the proposed algorithms can closely approach the optimal performance for both the finite- and infinite-horizon cases.

3.7 Appendices

3.7.1 Proof of Lemma 3.3

It is known that $\mathcal{T}_0$, which is the operator in the standard value iteration algorithm, is a γ-contraction [65]. Denoting $(b^*, A^*) \triangleq \arg ||\mathcal{T}_0\Big[V_1(b,A)\Big] - \mathcal{T}_0\Big[V_2(b,A)\Big]||_\infty$, for any (B_0, A_0) and $(B_0 + \delta, A_0)$ where $B_0, B_0 + \delta \in \mathcal{B}_\delta, A_0 \in \{0, 1\}$, we have that

$$\Big|\mathcal{T}_0\Big[V_1\Big](B_0, A_0) - \mathcal{T}_0\Big[V_2\Big](B_0, A_0)\Big| \leq \Big|\Big(\mathcal{T}_0\Big[V_1\Big] - \mathcal{T}_0\Big[V_2\Big]\Big)(b^*, A^*)\Big| \tag{3.57}$$

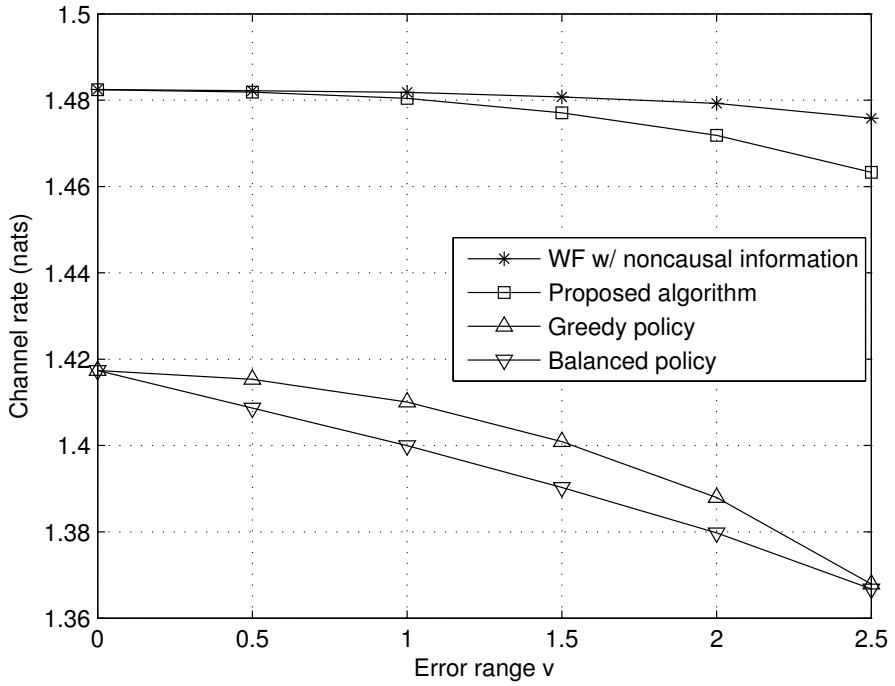

Figure 3.11: Performance comparisons for the finite-horizon case with different prediction error ranges.

and

$$\left|\mathcal{T}_0\Big[V_1\Big](B_0+\delta,A_0)-\mathcal{T}_0\Big[V_2\Big](B_0+\delta,A_0)\right| \quad \leq \left|\Big(\mathcal{T}_0\Big[V_1\Big]-\mathcal{T}_0\Big[V_2\Big]\Big)(b^*,A^*)\right| . \tag{3.58}$$

Note that, given a value function $V(b,A)$, $\mathcal{T}_\delta\Big[V\Big](b,A)$ is the piecewise linear function reconstructed from the sample set $\{\mathcal{T}_0\Big[V\Big](B,A) \mid B \in \mathcal{B}_\delta\}$, as in (3.14). Since $B_0, B_0+\delta \in \mathcal{B}_\delta$, then for any $b \in [B_0, B_0+\delta]$, we have

$$\begin{aligned}
&\left|\mathcal{T}_\delta\Big[V_1\Big](b,A)-\mathcal{T}_\delta\Big[V_2\Big](b,A)\right| \\
&\leq \max\left\{\left|\mathcal{T}_\delta\Big[V_1\Big](B_0,A)-\mathcal{T}_\delta\Big[V_2\Big](B_0,A)\right|, \left|\mathcal{T}_\delta\Big[V_1\Big](B_0+\delta,A)-\mathcal{T}_\delta\Big[V_2\Big](B_0+\delta,A)\right|\right\} \\
&= \max\left\{\left|\mathcal{T}_0\Big[V_1\Big](B_0,A)-\mathcal{T}_0\Big[V_2\Big](B_0,A)\right|, \left|\mathcal{T}_0\Big[V_1\Big](B_0+\delta,A)-\mathcal{T}_0\Big[V_2\Big](B_0+\delta,A)\right|\right\}
\end{aligned} \tag{3.59}$$

Since B_0 and A are arbitrarily chosen from $\mathcal{B}_\delta/\max\{\mathcal{B}_\delta\}$ and $\{0,1\}$, respectively, we have

$$\begin{aligned}
&||\mathcal{T}_\delta\Big[V_1(b,A)\Big]-\mathcal{T}_\delta\Big[V_2(b,A)\Big]|| \\
\leq&\max\Big\{\Big|\mathcal{T}_0\Big[V_1\Big](B_0,A_0)-\mathcal{T}_0\Big[V_2\Big](B_0,A_0)\Big|,\Big|\mathcal{T}_0\Big[V_1\Big](B_0+\delta,A_0)-\mathcal{T}_0\Big[V_2\Big](B_0+\delta,A_0)\Big|\Big\} &(3.60)\\
\leq&\Big|\Big(\mathcal{T}_0\Big[V_1\Big]-\mathcal{T}_0\Big[V_2\Big]\Big)(b^*,A^*)\Big| &(3.61)\\
=&||\mathcal{T}_\delta\Big[V_1(b,A)\Big]-\mathcal{T}_\delta\Big[V_2(b,A)\Big]||_\infty &(3.62)\\
\leq&\gamma||V_1(b,A)-V_2(b,A)||_\infty &(3.63)
\end{aligned}$$

where (3.60) follows from (3.59), (3.61) follows from (3.57)-(3.58), and (3.62) follows the definition of (b^*,A^*).

3.7.2 Proof of Theorem 3.3

Denote $\beta(b,A)\triangleq v^*(b,A)-\mathcal{T}_\delta\Big[v^*(b,A)\Big]$. By Lemma 3.3, we have

$$\begin{aligned}
&||W_\delta^{(i)}(b,A)-v^*(b,A)||_\infty \\
&=||W_\delta^{(i)}(b,A)+W_\delta^{(i+1)}(b,A)-W_\delta^{(i+1)}(b,A)-v^*(b,A)||_\infty \\
&\leq||W_\delta^{(i)}(b,A)-W_\delta^{(i+1)}(b,A)||_\infty+||W_\delta^{(i+1)}(b,A)-v^*(b,A)||_\infty \\
&=||\mathcal{T}_\delta\Big[W_\delta^{(i)}(b,A)\Big]-\mathcal{T}_\delta\Big[W_\delta^{(i-1)}(b,A)\Big]||_\infty+||\mathcal{T}_\delta\Big[W_\delta^{(i)}(b,A)\Big]-\mathcal{T}_\delta\Big[v^*(b,A)\Big]-\beta(b,A)||_\infty \\
&=||\mathcal{T}_\delta\Big[W_\delta^{(i)}(b,A)\Big]-\mathcal{T}_\delta\Big[W_\delta^{(i-1)}(b,A)\Big]||_\infty+||\mathcal{T}_\delta\Big[W_\delta^{(i)}(b,A)\Big]-\mathcal{T}_\delta\Big[v^*(b,A)\Big]||_\infty+||\beta(b,A)||_\infty \\
&\leq\gamma||W_\delta^{(i)}(b,A)-W_\delta^{(i-1)}(b,A)||_\infty+\gamma||W_\delta^{(i)}(b,A)+v^*(b,A)||_\infty+||\beta(b,A)||_\infty &(3.64)
\end{aligned}$$

where (3.64) follows the γ-contraction of the operator $\mathcal{T}_\delta$.

From (3.64), we have

$$\begin{aligned}
||W_\delta^{(i)}(b,A)-v^*(b,A)||_\infty&\leq\frac{\gamma||W_\delta^{(i)}(b,A)-W_\delta^{(i-1)}(b,A)||_\infty+||\beta(b,A)||_\infty}{1-\gamma} \\
&\leq\frac{\gamma\alpha+||\beta(b,A)||_\infty}{1-\gamma} &(3.65)
\end{aligned}$$

Also, since the only difference between $\mathcal{T}_\delta$ and $\mathcal{T}_0$ is the approximation process, then we have $\beta(b,A)=v^*(b,A)-\mathcal{T}_\delta\Big[v^*(b,A)\Big]=v^*(b,A)-\mathcal{L}\Big[\mathcal{T}_0\left[v^*(b,A)\right],\delta\Big]=v^*(b,A)-\mathcal{L}\Big[v^*(b,A),\delta\Big]$. Using

Proposition 3.4, we have

$$\begin{aligned} ||\beta(b,A)||_\infty &\leq ||2v^*(\delta,A) - v(0,A) - v^*(2\delta,A)||_\infty \\ &\leq ||v^*(\delta,A) - v^*(0,A)||_\infty \ . \end{aligned} \tag{3.66}$$

Therefore, (3.65) can be further written as

$$||W_\delta^{(i)}(b) - v^*(b)||_\infty \leq \frac{\gamma\alpha + ||2v^*(\delta,A) - v(0,A) - v^*(2\delta,A)||_\infty}{1-\gamma}. \tag{3.67}$$

Chapter 4

Energy-Bandwidth Allocation for Flat-Fading Point-to-Point Channels

In this chapter, we consider a multiuser system with multiple transmitters, each powered by a renewable energy source. Each transmitter communicates with its designated receivers and is constrained by the availability of the energy, the capacity of the battery, and the maximum (average) transmission power. Moreover, a frequency band is shared by all transmitters and we assume orthogonal channel access to avoid interference. We aim to obtain the optimal joint energy-bandwidth allocation over a fixed scheduling period based on the available information on the channel states and energy harvesting states at all transmitters, to maximize the weighted sum of the achievable rate.

Consider the special case of equal weights and each transmitter communicates with only one receiver. Then, without energy harvesting, TDMA is optimal for the maximum unweighted sum-rate, i.e., at any time the link with the highest rate takes all bandwidth. However, for energy harvesting transmitters, TDMA is no longer optimal. This is because the finite battery capacity leads to energy discharge and waste by some transmitters that are not scheduled to transmit in a time slot. Therefore, to make the best use of the harvested energy, multiple transmitters should split the frequency band and transmit in a same slot. In this chapter, we assume that the channel is flat fading and therefore each transmitter only needs to be allocated a portion of the total bandwidth.

We first consider the non-causal case, i.e., the energy harvesting and the channel fading can be

predicted for the scheduling period, and formulate a convex optimization problem with $\mathcal{O}(MK)$ variables and constraints, where M is the number of receivers and K is the number of scheduling time slots. Since the computational complexity of a generic convex solver becomes impractically high when the number of constraints is large [68], we will develop an iterative algorithm that alternates between energy allocation and bandwidth allocation. We will show that this algorithm converges to the optimal solution of the joint energy-bandwidth scheduling problem. For the special case that each transmitter only communicates with one receiver and all weights are equal, optimal algorithms to solve the energy and bandwidth allocation subproblems are also the optimal energy-bandwidth allocation algorithm that obtained a computational complexity of $\mathcal{O}(MK^2)$. We then consider the causal case, where the harvested energy and the channel gain can only be observed at the beginning of the corresponding time slot. We propose a suboptimal energy-bandwidth allocation algorithm that follows a similar structure of the noncausal optimal solution. Simulation results demonstrate that both the proposed non-causal and causal algorithms achieve substantial performance improvement over some heuristic scheduling policies. Moreover, in the next chapter, we will focus on the energy-bandwidth allocation in multiple broadcast channels and take the proportional fairness into account.

4.1 System Model and Problem Formulation

4.1.1 System Model

Consider a network consisting of N transmitters and M receivers sharing a total bandwidth of B Hz, where $N \leq M$ and each transmitter may communicate with multiple receivers. We assume a scheduling period of K time slots and no two transmitters can transmit in the same time slot and the same frequency band. Denote $a_m^k \in [0,1]$ as the normalized bandwidth allocation for link m in time slot k. We consider a flat and slow fading channel, where the channel gain is constant within the entire frequency band of B Hz and over the coherence time of T_c seconds, which is also the duration of a time slot. Assuming that each time slot consists of T time instants, we denote X_m^{ki} as the symbol sent to the receiver of link m at instant i in slot k. The corresponding received signal at receiver m is given by $Y_m^{ki} = X_m^{ki} h_m^k + Z_m^{ki}$, where h_m^k represents the complex channel gain for link m in slot k, and $Z_m^{ki} \sim \mathsf{CN}(0, 1/T)$ is the i.i.d. complex Gaussian noise (i.e., the power

spectral density of the noise is $1/T_c$). We denote $H_m^k \triangleq |h_m^k|^2$ and denote $p_m^k \triangleq \sum_{i=1}^{T} |X_m^{ki}|^2$ as the transmission energy consumption for link m in slot k (i.e., the sum of the symbols' energy in each slot). Without loss of generality, we normalize B to 1; then, a_m^k become the allocated bandwidth of link m in slot k. For link m, the upper bound of the achievable channel rate in slot k can be written as $a_m^k \log(1 + p_m^k H_m^k / a_m^k)$ [70]. Moreover, we denote $\mathcal{K} \triangleq \{1, 2, \ldots, K\}$ as the scheduling period, $\mathcal{N} \triangleq \{1, 2, \ldots, N\}$ as the set of transmitters, and $\mathcal{M} \triangleq \{1, 2, \ldots, M\}$ as the set of receivers. Further, we denote $\mathcal{M}_n \triangleq \{m \mid m \text{ is the receiver of transmitter } n, m \in \mathcal{M}\}$ as the set of receivers of transmitter n, where $\mathcal{M}_n \bigcap \mathcal{M}_{n'} = \phi$ for all $n \neq n' \in \mathcal{N}$.

Assume that each transmitter is equipped with an energy harvester and a buffer battery, as shown in Fig. 4.1. The energy harvester harvests energy from the surrounding environment. We denote E_n^k as the total energy harvested up to the end of slot k by transmitter n. Since in practice energy harvesting can be accurately predicted for a short period [71][66], we assume that the amount of the harvested energy in each slot is known. Moreover, the short-term prediction of the channel gain in slow fading channels is also possible [72]. Therefore, we assume that $\{H_m^k\}$ and $\{E_n^k\}$ are known non-causally before scheduling. Note that such non-causal assumption also leads to the performance upper bound of the system. We will relax this assumption and consider causal knowledge of the channels and energy harvesting in Section 4.4.

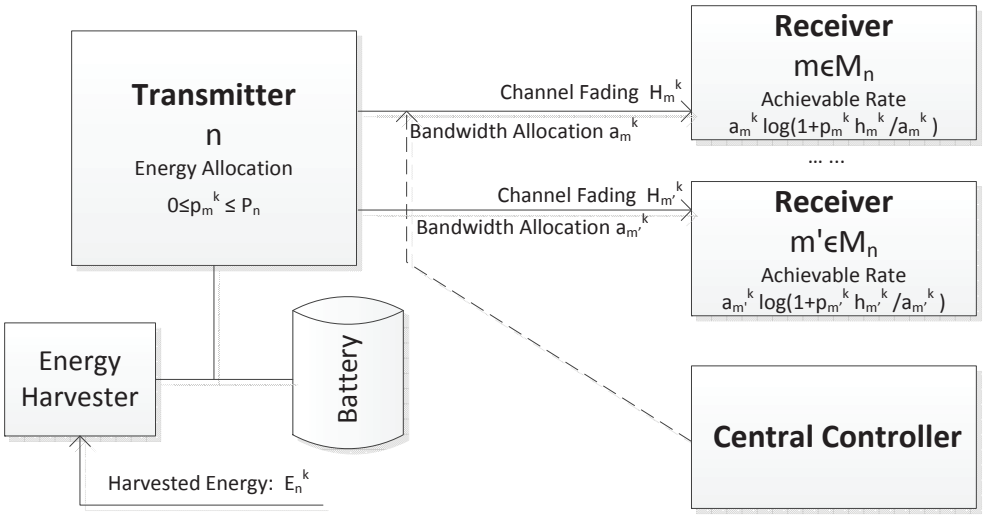

Figure 4.1: The system block diagram.

For transmitter n, assuming that the battery has a limited capacity $B_n^{\max}$ and is empty initially,

then the battery level at the end of slot k can be written as

$$B_n^k = B_n^{k-1} + \left(E_n^k - E_n^{k-1}\right) - \sum_{\kappa=1}^{k} \sum_{m \in \mathcal{M}_n} p_m^\kappa - \sum_{\kappa=1}^{k} D_n^\kappa, \tag{4.1}$$

where $D_n^k \geq 0$ represents the energy discharge (waste) for transmitter n in slot k. Moreover, B_n^k must satisfy $0 \leq B_n^k \leq B_n^{\max}$ for all $k \in \mathcal{K}$.

We assume that each transmitter n has a maximum per-slot transmission energy consumption, P_n, such that $\sum_{m \in \mathcal{M}_n} p_m^k \leq P_n$ for $k \in \mathcal{K}$. With the maximum transmission energy and the limited battery capacity, some of the harvested energy may not be able to be utilized, and is therefore wasted, i.e., D_n^k may necessarily be strictly positive in some slots. Then, the constraints on the battery level can be written as

$$0 \leq E_n^k - \sum_{\kappa=1}^{k} \sum_{m \in \mathcal{M}_n} p_m^\kappa - \sum_{\kappa=1}^{k} D_n^\kappa \leq B_n^{\max}. \tag{4.2}$$

Moreover, we denote $\mathcal{D} \triangleq \{\boldsymbol{D}_n \mid \boldsymbol{D}_n \triangleq [D_n^1, D_n^2, \ldots, D_n^K], n \in \mathcal{N}\}$ as the *discharge allocation*. Note that, we assume controllable energy discharge, i.e., the energy can be discharged and wasted anytime, even when the battery is not full.

Remark 4.1. *In the transmitter model, both the maximum transmission energy and the battery capacity are finite. If the harvested energy is ample, part of the energy has to be discharged even if the transmitter transmits at the maximum (available) transmission energy in each slot. That is, $D_n^{k*} > 0$ is due to the incoming energy being large enough that it cannot be used for transmission or storage.*

4.1.2 Problem Formulation

Define $0 \cdot \log(1 + \frac{x}{0}) \triangleq 0$. We use upper bounds of the achievable channel rate over a weighted sum of the M links and K slots as the performance metric, given by

$$C_{\mathcal{W}}(\mathcal{P}, \mathcal{A}) = \sum_{m \in \mathcal{M}} W_m \sum_{k \in \mathcal{K}} a_m^k \cdot \log(1 + \frac{p_m^k H_m^k}{a_m^k}),\ a_m^k \in [0,1], p_m^k \in [0, \infty)\ , \tag{4.3}$$

where $\mathcal{P} \triangleq \{\boldsymbol{p}_m \mid \boldsymbol{p}_m \triangleq [p_m^1, p_m^2, \ldots, p_m^K], m \in \mathcal{M}\}$ is the *energy allocation*, $\mathcal{A} \triangleq \{\boldsymbol{a}^k \mid \boldsymbol{a}^k \triangleq [a_1^k, a_2^k, \ldots, a_M^k], k \in \mathcal{K}\}$ is the *bandwidth allocation*, and $\mathcal{W} \triangleq \{W_m, m \in \mathcal{M}\}$ is the *weight set*. In particular, when $W_m = 1$ for all $m \in \mathcal{M}$, $C_{\mathcal{W}}(\mathcal{P}, \mathcal{A})$ becomes the throughput of the network.

Note that, both a_m^k and p_m^k can be zero in (4.3). However, if $a_m^k = 0$, the channel rate of link m in slot k is zero, even if the energy allocation $p_m^k > 0$, thus p_m^k is actually wasted. However, we still treat the pair $(a_m^k = 0, p_m^k > 0)$ as feasible as long as $\sum_{m\in\mathcal{M}_n} p_m^k \le P_n$.

We formulate the following energy-bandwidth allocation problem:

$$\max_{\mathcal{P},\mathcal{A},\mathcal{D}} C_{\mathcal{W}}(\mathcal{P},\mathcal{A}) \tag{4.4}$$

subject to

$$\begin{cases} 0 \le E_n^k - \sum_{\kappa=1}^{k}\sum_{m\in\mathcal{M}_n} p_m^\kappa - \sum_{\kappa=1}^{k} D_n^\kappa \le B_n^{\max} \\ \sum_{i=1}^{M} a_i^k = 1 \\ a_m^k \ge 0 \\ \sum_{m\in\mathcal{M}_n} p_m^k \le P_n \\ p_m^k \ge 0 \\ D_n^k \ge 0 \end{cases} \tag{4.5}$$

for all $k \in \mathcal{K}, m \in \mathcal{M}$ and $n \in \mathcal{N}$.

4.1.3 Optimal Energy Discharge Allocation

To efficiently solve the problem in (4.4)-(4.5), we consider a two-stage procedure. In the first stage, we obtain the optimal energy discharge allocation $\mathcal{D}^*$ such that

$$\max_{\mathcal{P},\mathcal{A},\mathcal{D}=\mathcal{D}^*} C_{\mathcal{W}}(\mathcal{P},\mathcal{A}) = \max_{\mathcal{P},\mathcal{A},\mathcal{D}} C_{\mathcal{W}}(\mathcal{P},\mathcal{A}) \tag{4.6}$$

with the constraints in (4.5). And in the second stage, we use $\mathcal{D}^*$ and define the energy expenditure for transmission as

$$\tilde{E}_n^k \triangleq E_n^k - \sum_{\kappa=1}^{k} D_n^{\kappa *} \ . \tag{4.7}$$

Then we solve the following problem:

$$\max_{\mathcal{P},\mathcal{A}} C_{\mathcal{W}}(\mathcal{P},\mathcal{A}) \tag{4.8}$$

subject to

$$\begin{cases} \tilde{E}_n^k - B_n^{\max} \le \sum_{\kappa=1}^{k}\sum_{m\in\mathcal{M}_n} p_m^\kappa \le \tilde{E}_n^k \\ \sum_{i=1}^{M} a_i^k = 1 \\ \sum_{m\in\mathcal{M}_n} p_m^k \le P_n \\ p_m^k \ge 0 \\ a_m^k \ge 0 \end{cases} \tag{4.9}$$

for all $n \in \mathcal{N}, m \in \mathcal{M}$ and $k \in \mathcal{K}$.

We consider the following greedy strategy to obtain the energy discharge allocation by assuming that each transmitter transmits at the maximum power in each slot, i.e.,

$$\begin{cases} D_n^k = \max\{B_n^{k-1} + E_n^k - E_n^{k-1} - \sum_{\kappa=1}^{k} \sum_{m\in\mathcal{M}_n} p_m^k - B_n^{\max}, 0\} \\ \sum_{m\in\mathcal{M}_n} p_m^k = \min\{P_n, B_n^{k-1} + E_n^k - E_n^{k-1}\} \end{cases}, \ k = 1, 2, \ldots, K \qquad (4.10)$$

for all $n \in \mathcal{N}$.

Note that, following (4.10), the total discharged energy is minimized and thus the amount of the energy used for transmission is maximized. Intuitively, this way the feasible domain becomes the largest, providing the best performance for transmission energy scheduling. Specifically, given a feasible bandwidth allocation $\mathcal{A}$, the achievable rate of each link is non-decreasing with respect to the transmission energy, and the battery of each transmitters operates independently. Therefore, following the same lines of the proof in [69], the optimality of (4.10) can be established. In particular, using any feasible energy discharge $\mathcal{D}$ corresponding to the minimal energy wastage, the optimal value of (4.8) is same, which is no less than the optimal value under any feasible energy discharge allocation with non-minimal energy wastage.

Lemma 4.1. *The discharge allocation given by* (4.10) *is the optimal* $\mathcal{D}^*$ *to the problem in* (4.4)-(4.5)*, i.e., it satisfies* (4.6)*, where the LHS of* (4.6) *is subject to the constraints in* (4.9) *and the RHS is subject to the constraints in* (4.5)*.*

Note that, $C_{\mathcal{W}}(\mathcal{P}, \mathcal{A})$ is continuous and jointly concave with respect to $a_m^k \in [0, 1]$ and $p_m^k \in [0, \infty)$ for $k \in \mathcal{K}, m \in \mathcal{M}$. Then, the problem in (4.8)-(4.9) is a convex optimization problem and can be solved by a generic convex solver, whose complexity becomes impractically high when the number of constraints is large [68], which in this case is $\mathcal{O}(MK)$. To reduce the computational complexity, we will develop an efficient algorithm in this paper, which exploits the structure of the optimal solution.

4.2 Iterative Algorithm and its Optimality

The problem in (4.8)-(4.9) is a convex optimization problem with linear constraints. When the objective function is differentiable in an open domain, the K.K.T. conditions are sufficient and

necessary for the optimal solution [68]. Note that, (4.3) is non-differentiable at $a_m^k = 0$. To use the K.K.T. conditions to characterize the optimality of the problem in (4.8)-(4.9), we consider the following approximation:

$$\mathsf{P}_{\mathcal{W}}(\epsilon): \quad \max_{\mathcal{P},\mathcal{A}} C_{\mathcal{W}}(\mathcal{P},\mathcal{A}) \tag{4.11}$$

subject to

$$\begin{cases} \tilde{E}_n^k - B_n^{\max} \leq \sum_{\kappa=1}^{k} \sum_{m\in\mathcal{M}_n} p_m^{\kappa} \leq \tilde{E}_n^k \\ \sum_{i=1}^{M} a_i^k = 1 \\ \sum_{m\in\mathcal{M}_n} p_m^k \leq P_n \\ p_m^k \geq 0 \\ a_m^k \geq \epsilon \end{cases} \tag{4.12}$$

for all $n \in \mathcal{N}, m \in \mathcal{M}, k \in \mathcal{K}$, where ϵ is a small positive number. In particular, $\mathsf{P}_{\mathcal{W}}(0)$ is the original problem in (4.8)-(4.9).

Lemma 4.2. *When $\epsilon \to 0^+$, the optimal value of $\mathsf{P}_{\mathcal{W}}(\epsilon)$ converges to the optimal value of the problem in* (4.8)-(4.9)*, i.e.,* $\lim_{\epsilon\to 0^+} \mathsf{P}_{\mathcal{W}}(\epsilon) = \mathsf{P}_{\mathcal{W}}(0)$.

Proof. Since the objective function $C_{\mathcal{W}}(\mathcal{P},\mathcal{A})$ is continuous with respect to $\mathcal{P}\times\mathcal{A} \in \{[0,\infty)\} \times \{[0,1]\}$ and the constraints in (4.12) are all linear, we have that the optimal solution of $\mathsf{P}_{\mathcal{W}}(\epsilon)$ is continuous with respect to ϵ, i.e., $\lim_{\epsilon\to 0^+} \arg \mathsf{P}_{\mathcal{W}}(\epsilon) = \arg \mathsf{P}_{\mathcal{W}}(0)$. Therefore, we have $\lim_{\epsilon\to 0^+} \mathsf{P}_{\mathcal{W}}(\epsilon) = \mathsf{P}_{\mathcal{W}}(0)$. □

By introducing the auxiliary variables $\{\lambda_n^k \geq 0\}$, $\{\mu_n^k \geq 0\}$, $\{\beta_m^k \geq 0\}$ and $\{\alpha^k\}$ and converting the constraints in (4.12) into the Lagrangian multiplier, we can define the Lagrangian function for

$\mathsf{P}_{\mathcal{W}}(\epsilon)$ as

$$\begin{aligned}\mathcal{L} \triangleq & \sum_{m=1}^{M} W_m \sum_{k=1}^{K} a_m^k \cdot \log(1+\frac{p_m^k H_m^k}{a_m^k}) \\ & - \sum_{n=1}^{N}\sum_{k=1}^{K}\Big(\sum_{m\in\mathcal{M}_n} p_m^k \sum_{\kappa=k}^{K}\lambda_n^\kappa - \lambda_n^k \tilde{E}_n^k\Big) \\ & + \sum_{n=1}^{N}\sum_{k=1}^{K}\Big(\sum_{m\in\mathcal{M}_n} p_m^k \sum_{\kappa=k}^{K}\mu_n^\kappa - \mu_n^k\big(\tilde{E}_n^k - B_n^{\max}\big)\Big) \\ & - \sum_{k=1}^{K}\alpha^k\big(\sum_{m=1}^{M} a_m^k - 1\big) \\ & + \sum_{k=1}^{K}\sum_{m=1}^{M}\beta_m^k(a_m^k-\epsilon)\ .\end{aligned}$$

Then, the following K.K.T. conditions, which are sufficient and necessary for the optimal solution to the convex optimization problem in (4.11)-(4.12), are obtained from the Lagrangian function:

$$\frac{H_m^k}{1+p_m^k H_m^k/a_m^k} = (v_n^k - u_n^k)/W_m,\ k\in\mathcal{K},\ n\in\mathcal{N},\ m\in\mathcal{M}_n \tag{4.13}$$

$$\log(1+\frac{p_m^k H_m^k}{a_m^k}) - \frac{p_m^k H_m^k}{a_m^k + p_m^k H_m^k} = (\alpha^k - \beta_n^k)/W_m,\ k\in\mathcal{K},\ n\in\mathcal{N},\ m\in\mathcal{M}_n \tag{4.14}$$

$$\lambda_n^k \cdot \big(\sum_{\kappa=1}^{k}\sum_{m\in\mathcal{M}_n} p_m^\kappa - \tilde{E}_n^k\big) = 0,\ k\in\mathcal{K},\ n\in\mathcal{N} \tag{4.15}$$

$$\mu_n^k \cdot \big(\sum_{\kappa=1}^{k}\sum_{m\in\mathcal{M}_n} p_m^\kappa - \tilde{E}_n^k + B_n^{\max}\big) = 0,\ k\in\mathcal{K},\ n\in\mathcal{N} \tag{4.16}$$

$$\alpha^k \cdot \big(\sum_{m=1}^{M} a_m^k - 1\big) = 0,\ k\in\mathcal{K} \tag{4.17}$$

$$\beta_m^k \cdot (a_m^k - \epsilon) = 0,\ k\in\mathcal{K},\ m\in\mathcal{M} \tag{4.18}$$

together with the constraints in (4.12), and $\lambda_n^k, \mu_n^k, \beta_m^k \geq 0$ for all $k\in\mathcal{K}$, $n\in\mathcal{N}$, and $m\in\mathcal{M}$, where in (4.13)

$$u_n^k \triangleq \sum_{\kappa=k}^{K}\mu_n^\kappa,\ v_n^k \triangleq \sum_{\kappa=k}^{K}\lambda_n^\kappa\ . \tag{4.19}$$

In this section, we will first decompose the energy-bandwidth allocation problem $\mathsf{P}_{\mathcal{W}}(\epsilon)$ in (4.11)-(4.12) into two subproblems, and then propose an iterative algorithm to solve $\mathsf{P}_{\mathcal{W}}(\epsilon)$. We will prove that the iterative algorithm converges to the optimal solution to the problem in (4.8)-(4.9).

4.2.1 Iterative Algorithm

To efficiently solve problem $\mathsf{P}_{\mathcal{W}}(\epsilon)$ in (4.11)-(4.12), we first decompose it into two groups of subproblems, corresponding to energy allocation and bandwidth allocation, respectively.

- Given the bandwidth allocation $\mathcal{A} = \{\boldsymbol{a}^k \mid k \in \mathcal{K}\}$, for each $n \in \mathcal{N}$, obtain the energy allocation $\boldsymbol{p}_m$ by solving the following subproblem:

$$\mathsf{EP}_n: \quad \max_{\boldsymbol{p}_m, m\in\mathcal{M}_n} \sum_{m\in\mathcal{M}_n} W_m \sum_{k=1}^{K} a_m^k \cdot \log(1+\frac{p_m^k H_m^k}{a_m^k}) \tag{4.20}$$

subject to

$$\begin{cases} \tilde{E}_n^k - B_n^{\max} \le \sum_{\kappa=1}^{k} \sum_{m\in\mathcal{M}_n} p_m^{\kappa} \le \tilde{E}_n^k \\ \sum_{m\in\mathcal{M}_n} p_m^k \le P_n \\ p_m^k \ge 0, m \in \mathcal{M}_n \end{cases}, \ k \in \mathcal{K}\ . \tag{4.21}$$

- Given the energy allocation $\mathcal{P} = \{\boldsymbol{p}_m \mid m \in \mathcal{M}\}$, for each $k \in \mathcal{K}$, obtain the bandwidth allocation $\boldsymbol{a}^k$ by solving the following subproblem:

$$\mathsf{BP}_k(\epsilon): \quad \max_{\boldsymbol{a}^k} \sum_{m=1}^{M} W_m \cdot a_m^k \cdot \log(1+\frac{p_m^k H_m^k}{a_m^k}) \tag{4.22}$$

subject to

$$\begin{cases} \sum_{i=1}^{M} a_i^k = 1 \\ a_m^k \ge \epsilon,\ m \in \mathcal{M} \end{cases}. \tag{4.23}$$

To obtain the optimal solution to the original problem in (4.8)-(4.9), we propose an iterative algorithm that alternatively solves EP_n for all $n \in \mathcal{N}$ and $\mathsf{BP}_k(\epsilon)$ for all $k \in \mathcal{K}$, with a diminishing ϵ over the iterations. To perform the algorithm, we initially set $a_m^k = 1/M, \forall m, k$, and solve EP_n to obtain the initial $\mathcal{P}$. In each iteration i, we first solve $\mathsf{BP}_k(\epsilon_0/i)$ to update $\boldsymbol{a}^k \in \mathcal{A}$ for all $k \in \mathcal{K}$, where ϵ_0 is a pre-specified positive value; with the updated $\mathcal{A}$, we then solve EP_n to update $\boldsymbol{p}_m \in \mathcal{P}$ for all $m \in \mathcal{M}$.

The proposed iterative algorithm is summarized in Algorithm 4.1 and its block diagram is shown in Fig. 4.2.

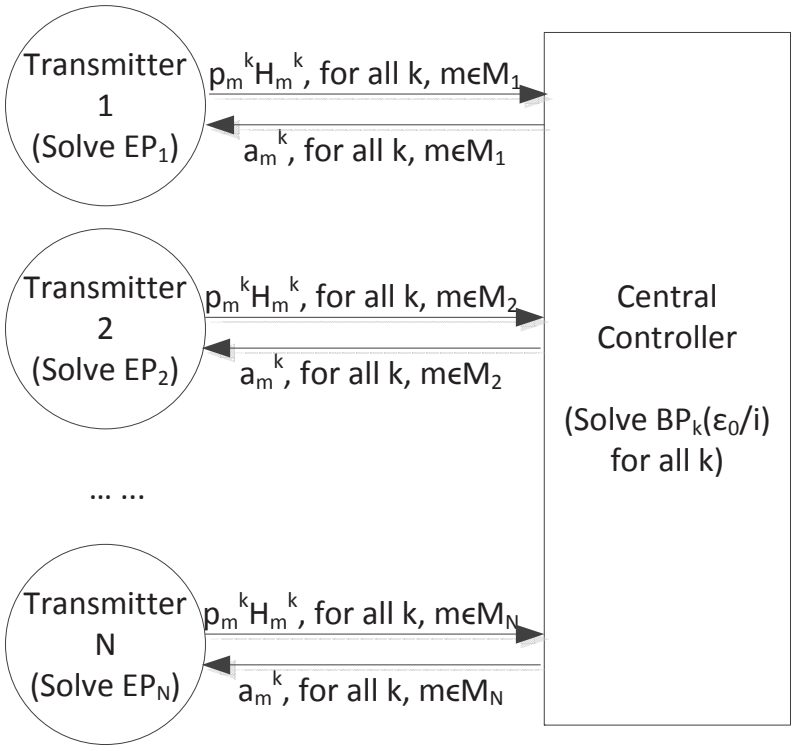

Figure 4.2: The block diagram of Algorithm 4.1.

Algorithm 4.1 - Iterative Energy-Bandwidth Allocation Algorithm

1: Initialization

$i = 0$, $\mathcal{A} = 1/M$, $V^{(0)} = 0$, choose any $\epsilon_0 > 0$,

Solve EP_n for all $n \in \mathcal{N}$ to generate the initial $\mathcal{P}$

Specify the maximum number of iterations I, the convergence tolerance $\delta > 0$

2: Energy-Bandwidth Allocation

REPEAT

$i \leftarrow i + 1$, $\epsilon \leftarrow \epsilon_0/i$

Solve $\mathsf{BP}_k(\epsilon)$ to update $\boldsymbol{a}^k \in \mathcal{A}$ for all $k \in \mathcal{K}$

Solve EP_n to update $\{\boldsymbol{p}_m \mid m \in \mathcal{M}_n\} \subset \mathcal{P}$ for all $n \in \mathcal{N}$

$V^{(i)} = C_{\mathcal{W}}(\mathcal{P}, \mathcal{A})$

UNTIL $|V^{(i)} - V^{(i-1)}| < \delta$ **OR** $i = I$

In the next subsection, we will show that Algorithm 4.1 converges and the pairwise optimal $\mathcal{A}$ and $\mathcal{P}$ can be obtained, which is also the optimal solution to the problem in (4.8)-(4.9).

We note that, $\mathcal{P}_{\mathcal{W}}(\epsilon)$ is a convex optimization problem with $O(MK)$ variables and constraints. The computational complexity of using the generic convex solver is non-linear with respect to the number of the variables and constraints, which may be impractically high when M and K become large. Using Algorithm 4.1, the optimal solution to $\mathcal{P}_{\mathcal{W}}(\epsilon)$ can be obtained by solving $\mathcal{O}(N + K)$ convex optimization subproblems which contains $\mathcal{O}(K|\mathcal{M}_n|)$ or $\mathcal{O}(M)$ variables and constraints. Therefore, the overall computational complexity can be significantly reduced with Algorithm 4.1 for large M and K.

4.2.2 Proof of Optimality

We first give the following proposition.

Proposition 4.1. *Given any bandwidth allocation $\{a_m^k > 0 \mid k \in \mathcal{K}\}, m \in \mathcal{M}$, the optimal energy allocation for the problem EP_n is unique. Also, given the energy allocation $\{p_m^k \mid m \in \mathcal{M}\}, k \in \mathcal{K}$ such that $\sum_{m=1}^{M} p_m^k > 0$, the corresponding optimal bandwidth allocation for the problem $\mathsf{BP}_k(\epsilon)$ is unique.*

Proof. This proposition can be obtained by verifying the strict concavity of $C_{\mathcal{W}}(\mathcal{P}, \mathcal{A})$ with respect to $\mathcal{P}$ given $\mathcal{A}$, and with respect to $\mathcal{A}$ given $\mathcal{P}$. □

Given a pair $(\mathcal{P}, \mathcal{A})$, if $\boldsymbol{p}_m \in \mathcal{P}$ is the optimal solution to EP_n for all $n \in \mathcal{N}$ given $\mathcal{A}$, and $\boldsymbol{a}^k \in \mathcal{A}$ is the optimal solution to $\mathsf{BP}_k(\epsilon)$ for all $k \in \mathcal{K}$ given $\mathcal{P}$, we say that $\mathcal{P}$ and $\mathcal{A}$ are pairwise optimal for $\mathsf{P}_{\mathcal{W}}(\epsilon)$. We also note that, for each subproblem, its K.K.T. conditions form a subset of those of $\mathsf{P}_{\mathcal{W}}(\epsilon)$ given the other primal variables, where any two subsets contain no common dual variable. Then, if the primal variables are pairwise optimal, the K.K.T. conditions in each corresponding subset are satisfied and hence all K.K.T. conditions of $\mathsf{P}_{\mathcal{W}}(\epsilon)$ are satisfied, i.e., the pairwise optimal solution is also the optimal energy-bandwidth allocation for $\mathsf{P}_{\mathcal{W}}(\epsilon)$.

Theorem 4.1. *The energy-bandwidth allocation $\{\mathcal{P}, \mathcal{A}\}$ is the optimal solution to $\mathsf{P}_{\mathcal{W}}(\epsilon)$ for any $\epsilon > 0$, if and only if, $\{\boldsymbol{p}_m, m \in \mathcal{M}_n\} \in \mathcal{P}$ is optimal to $\mathsf{P}_{\mathcal{W}}(\epsilon)$ given $\{\mathcal{P} \backslash \{\boldsymbol{p}_m, m \in \mathcal{M}_n\}, \mathcal{A}\}$ for all $n \in \mathcal{N}$, and $\boldsymbol{a}^k \in \mathcal{A}$ is optimal to $\mathsf{P}_{\mathcal{W}}(\epsilon)$ given $\{\mathcal{A} \backslash \boldsymbol{a}^k, \mathcal{P}\}$ for all $k \in \mathcal{K}$.*

We note that, for $\mathsf{BP}_k(\epsilon)$, when $\sum_{m=1}^{M} p_m^k = 0$, the objective value is zero for all feasible bandwidth allocations. Therefore, we can fix $a_m^k = 1/M$ as the optimal bandwidth allocation for this case in Algorithm 4.1. Then, by Proposition 4.1, we have that the optimal solution to each subproblem in Algorithm 4.1 is unique. The next theorem establishes the optimality of Algorithm 4.1. The proof is given in Appendix 4.7.1.

Theorem 4.2. *Algorithm 4.1 converges; and the converged solution $(\mathcal{P}, \mathcal{A})$ is the optimal solution to the problem in* (4.8)-(4.9).

Note that, the convergence is due to the expansion of the feasible domain by reducing ϵ resulting in the increasing objective value over iterations. The optimality can be proved by first verifying the pairwise optimality of the solution upon convergence and then showing it cannot be suboptimal.

4.3 Throughput Maximization for Multiple Point-to-Point Channels

In this section, we consider the special case that each transmitter can only communicate with one receiver and all links have the same weight, i.e., $\mathcal{M}_n = \{n\}$ and $W_m = 1$ for all $m \in \mathcal{M}$. The energy and bandwidth allocation subproblem can be rewritten as

$$\mathsf{EP}_n: \quad \max_{\boldsymbol{p}_n} \sum_{k=1}^{K} a_n^k \cdot \log(1 + \frac{p_n^k H_n^k}{a_n^k}) \tag{4.24}$$

subject to

$$\begin{cases} \tilde{E}_n^k - B_n^{\max} \le \sum_{\kappa=1}^{k} p_n^\kappa \le \tilde{E}_n^k \\ 0 \le p_n^k \le P_n \end{cases}, \ k \in \mathcal{K} \ , \tag{4.25}$$

and

$$\mathsf{BP}_k(\epsilon): \quad \max_{\boldsymbol{a}^k} \sum_{n=1}^{N} a_n^k \cdot \log(1 + \frac{p_n^k H_n^k}{a_n^k}) \tag{4.26}$$

subject to

$$\begin{cases} \sum_{i=1}^{N} a_i^k = 1 \\ a_n^k \ge \epsilon, \ n \in \mathcal{N} \end{cases}, \tag{4.27}$$

respectively.

4.3.1 Solving EP_n: Discounted Dynamic Water-Filling

Given $\boldsymbol{a}^k$, since EP_n is a subproblem of the problem in (4.11)-(4.12), its K.K.T. conditions form a subset of those of the original problem, given by (4.13), (4.15) and (4.16).

To develop an efficient algorithm, we first rewrite the K.K.T. condition in (4.13) as

$$p_n^k = a_n^k \cdot \Big(\frac{1}{v_n^k - u_n^k} - \frac{1}{H_n^k} \Big) \ . \tag{4.28}$$

Since the energy allocation must satisfy $0 \le p_n^k \le P_n$, (4.28) can be further written as

$$p_n^k = \min \Big\{ P_n, a_n^k \cdot \Big[\frac{1}{v_n^k - u_n^k} - \frac{1}{H_n^k} \Big]^+ \Big\} \ . \tag{4.29}$$

Comparing the K.K.T. conditions in (4.13) with (24) in [69], the only difference is the scaling factor a_n^k. Following the same analysis in [69], we have the following theorem.

Theorem 4.3. *Given any bandwidth allocation $\mathcal{A}$, a feasible energy allocation $\mathcal{P}$ is an optimal solution to* (4.8)-(4.9)*, if and only if it follows the discounted water-filling rule in* (4.29)*, where the water level $\frac{1}{v^k - u^k}$ may increase only at a battery depletion point (BDP) such that $B_n^k = 0$, and decrease only at a battery fully charged point (BFP) such that $B_n^k = B_n^{\max}$.*

Proof. Given any bandwidth allocation $\mathcal{A}$, we note that by the first KKT condition in (4.13) along with the constraints $0 \le p_n^k \le P_n$, the optimal energy allocation satisfies (4.28). Thus, the optimal energy level in slot k is determined by the dual variables v_n^k, u_n^k and the channel state H_n^k.

We note that, the KKT conditions in (4.15) and (4.16) constrain the changes of the water levels $\frac{1}{v_n^k - u_n^k}$. To satisfy these two conditions, λ^k may only be non-zeros at the BDPs, i.e., for k such

that $\tilde{E}_n^k - \sum_{t=1}^k p_n^t = B_n^k = 0$, and μ_n^k may only be non-zeros at the BFPs, i.e., for k such that $\tilde{E}_n^k - \sum_{t=1}^k p_n^t = B_n^k = B_n^{\max}$. Since the dual variables λ_n^k and μ_n^k are non-negative, u_n^k and v_n^k, which are defined in (4.19), are non-increasing over k. Specifically, since λ_n^k and μ_n^k cannot be both non-zero at the same time, the water level $\frac{1}{v_n^k - u_n^k}$ may only increase when v_n^k changes, i.e., λ_n^k is non-zero at the BDPs, or decrease when u_n^k changes, i.e., μ_n^k is non-zero at the BFPs. □

Theorem 4.3 gives the necessary and sufficient conditions for the optimal energy allocation given any bandwidth allocation. Given the set of BDP/BFPs corresponding to the optimal energy allocation, the optimal energy allocation and the corresponding the water level for the segment between two adjacent BDP/BFPs, (a, type of a) and (b, type of b), can be written as

$$p_n^k = \min\left(P_n\ ,\ a_n^k \cdot \big[w - \frac{1}{H_n^k}\big]^+\right)\ , \tag{4.30}$$

where w is the *water level of a segment* such that

$$\sum_{\kappa=a+1}^{b} p_n^\kappa = \min\left\{(b-a)P_n, \tilde{E}_n^b - \tilde{E}_n^a + \big(\mathbb{I}(a \text{ is BFP}) - \mathbb{I}(b \text{ is BFP})\big)B_n^{\max}\right\}\ , \tag{4.31}$$

with $\mathbb{I}(\mathcal{A})$ being an indicator function given by

$$\mathbb{I}(\mathcal{A}) \triangleq \begin{cases} 1, & \text{if } \mathcal{A} \text{ is true} \\ 0, & \text{otherwise} \end{cases}\ . \tag{4.32}$$

Specifically, (4.30)-(4.31) represent the water-filling operation in a segment between two optimal BDP/BFPs, as mentioned in Theorem 4.3. Also, (4.31) ensures that with the energy allocation the boundary points a and b are the desired BDP/BFPs.

For example, given the set of the BDP/BFPs, the relationship among the water level w^k, the energy allocation p^k, and the channel state H^k can be characterized as in Fig. 4.3. In particular, if the energy allocation shown in Fig. 4.3 is optimal for EP_n, the water level $w_n^k = 1/(v_n^k - u_n^k)$ can only increase at the BDPs, e.g., slot 2 , and decrease at the BFPs, e.g., slot 6, as well as the resulted energy allocation is feasible, i.e., the constraints in (4.12) are satisfied.

We will consider the "manually" generated set of BFP/BDPs which is called general BDP/BFPs set, where the BDP/BFPs are generated by constraining the battery be empty or fully-charged in some specific slots. In contrast to the optimal BDP/BFPs set, the energy allocation obtained by (4.30) based on a general BDP/BFPs set may not be feasible and/or optimal. Specifically, if the

obtained energy allocation satisfies the constraints in (4.12), we call the energy allocation *feasible*; if the obtained energy allocation only violates the battery capacity constraints in some time slots, i.e, $B_n^k \geq B_n^{\max}$ for some k, we call the energy allocation *semi-feasible*; otherwise, we call the energy allocation *infeasible*. Note that both semi-feasible and infeasible energy allocations are not feasible to the problem in EP_n.

For a specific case that, given a general BDP/BFPs set, by (4.30), the energy allocation is feasible and the corresponding water levels satisfy the optimality conditions in Theorem 4.3, this general BDP/BFPs set can be considered as the optimal BDP/BFPs set and the corresponding energy allocation is the optimal solution to EP_n. Therefore, in the following subsections, we want to compose such optimal BDP/BFPs set.

Denote a general BDP/BFPs set as $\mathcal{X} = \{(k, \text{type of } k) \mid k \text{ is a BDP or BFP}\}$ where each element in $\mathcal{X}$ is sorted by ascending order of k, e.g., a set that contains only the default BDPs is $\{(0, \text{BDP}), (K, \text{BDP})\}$. To obtain $\mathcal{X}^*$, starting from $\mathcal{X} = \{(0, \text{BDP})\}$, we can iteratively append the next optimal BDP or BFP to $\mathcal{X}$ until (K, BDP) is added, i.e., we consider the generated BDP/BFP set as $\mathcal{X}^*$. To identify if a specific time slot should be a BDP or BFP in $\mathcal{X}^*$, we recursively perform the following two operations on a segment between $(a, \text{type of } a)$ and $(b, \text{type of } b)$: *Forward Search* and *Backward Search*.

For the forward search operation, we find the largest $(k, \text{type of } k) \in \{(a+1, \text{BDP}), (a+2, \text{BDP}), \ldots, (b-1, \text{BDP}), (b, \text{type of } b)\}$ such that the energy allocation of the segment $[a+1, k]$, which is calculated by (4.30), is feasible or semi-feasible. If it is feasible, add (k, BDP) to $\mathcal{X}$ and continue the forward search for the segment between (k, BDP) and (K, BDP); if it is semi-feasible, we perform backward search for the segment between $(a, \text{type of } a)$ and (k, BDP).

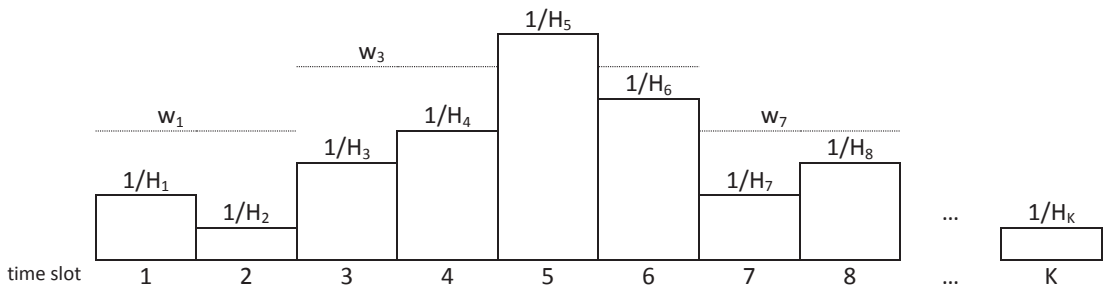

Figure 4.3: An example of a energy allocation and the corresponding water levels and BDPs/BFPs.

For the backward search operation, we find and eliminate the largest $B^{\max}$-violation point, i.e., the largest $k \in [a+1, b]$ such that $B^k > B^{\max}$. Specifically, we first obtain the energy allocation of the segment $[a+1, b]$ using (4.30) and find out the largest $B^{\max}$-violation point k. Then, setting k as a BFP, we obtain the energy allocation of the segment $[a+1, k]$ using (4.30) again. If the energy allocation is infeasible, we perform forward search on the segment between $(a, \text{type of } a)$ and (k, BFP); if the energy allocation is feasible, add (k, BFP) to $\mathcal{X}$ and perform forward search on the segment between (k, BFP) and (K, BDP); otherwise, we perform backward search on the segment between $(a, \text{type of } a)$ and (k, BFP).

The steps involved in these two operations are described below. We set the initial BDP/BFPs set as $\mathcal{X} = \{(0, \text{BDP})\}$ and apply the forward search operation on the segment between $(0, \text{BDP})$ and (K, BDP) to get the optimal set of BDPs and BFPs.

Algorithm 4.2 - Algorithm for finding optimal BDPs and BFPs

1: Algorithm: Run Forward Search on $\big((0, \text{BDP}), (K, \text{BDP})\big)$

2: Subroutine 1 - Forward Search $\big((a, \text{type of } a), (b, \text{type of } b)\big)$

If $a = K$, the search is complete.

For $(k_1,\ \text{type of } k_1) \in \{(a+1, \text{BDP}), \ldots, (b-1, \text{BDP}),\ (b, \text{type of } b)\}$

let $k =$ the largest $k_1 \in (a, b]$ such that the energy allocation from $a+1$ to k_1 calculated by (4.30) is feasible or semi-feasible

- if feasible, add (k, BDP) to $\mathcal{X}$
  and Forward Search $\big((k, \text{type of } k), (K, \text{BDP})\big)$
- if semi-feasible, Backward Search $\big((a, \text{type of } a), (k, \text{BDP})\big)$

3: Subroutine 2 - Backward Search $\big((a, \text{type of } a), (b, \text{type of } b)\big)$

Let $k =$ the largest $B^{\max}$-violation point in $(a, b]$

For the energy allocation calculated by (4.30) for segment $[a+1, k]$ where k is BFP

- if feasible, add (k, BFP) to $\mathcal{X}$
  and Forward Search $\big((k, \text{BFP}), (K, \text{BDP})\big)$
- if semi-feasible, Backward Search $\big((a, \text{type of } a), (k, \text{BFP})\big)$
- if infeasible, Forward Search $\big((a, \text{type of } a), (k, \text{BFP})\big)$

Algorithm 4.2 is a recursive algorithm, in which a BDP is added by the forward search while a BFP is added at the end of a consecutive recursion of the backward search. Specifically, readdressing the definition of the water level of a segment in (4.31), when a BDP is added, it is ensured that the

water level of the segment between the last BDP/BFP and the newly added BDP be lower than that of the segment between the newly added BDP and the next BDP/BFP that will be added in the subsequent recursion. Moreover, when a BFP is added, the opposite is ensured.

Note that, Algorithm 4.2 is implemented by recursively performing the forward search and the backward search, based on the water-filling operation. In the recursive process, the starting point a can only increase from 0 to K while the ending point b can only decrease from K to a for each starting point a. Since the complexity of the traditional water-filling algorithm is $\mathcal{O}(1)$, the complexity of Algorithm 4.2 can be further bounded by $\mathcal{O}(K^2)$.

Specifically, [69, Corollary 1] shows that for each BDP added by the forward search operation, the water level of the segment before the BDP is lower than that after the BDP; while [69, Proposition 2] shows that, for each BFP added by the backward search operation, the water level of the segment before the BFP is higher than that after the BFP. By Theorem 4.3, we know that such BDPs and BFPs added by the dynamic water-filling algorithm can satisfy the optimality conditions for the problem in EP_n, i.e., the water levels may only increase at BDPs and only decrease at BFPs. Thus, we arrive at the optimality.

Theorem 4.4. *By performing the dynamic water-filling algorithm, the resulted BDP/BFPs set is the optimal set of BDPs and BFPs for the problem in* EP_n*, i.e., we can get the optimal transmission schedule by using* (4.30) *to water-fill each segment between two adjacent points in the optimal BDP/BFP set with a constant water level.*

4.3.2 Solving $\mathsf{BP}_k(\epsilon)$: Bandwidth Fitting Algorithm

We first note that, when $p_n^k = 0$ and $a_n^k \geq \epsilon$, the channel rate achieved by transmitter n in slot k is zero. Therefore, in a slot k such that $\sum_{n=1}^N p_n^k = 0$, any feasible bandwidth allocation is optimal, achieving the maximum channel rate 0. However, in a slot k where $\sum_{n=1}^N p_n^k > 0$, in order to maximize the channel rate, the transmitter with zero energy allocation $p_n^k = 0$ must be allocated with the minimal bandwidth, i.e., $a_n^k = \epsilon$. We denote the energy allocation $\{p_n^k \mid \sum_{i=1}^N p_i^k > 0, n \in \mathcal{N}\}$ as the *non-zero energy allocation* and, in the remainder of this subsection, we will obtain the optimal bandwidth allocation given a non-zero energy allocation.

Since $\mathsf{BP}_k(\epsilon)$ is a subproblem of the problem given in (4.11)-(4.12), its K.K.T. conditions form a subset of those of the original problem, given by (4.14), (4.17) and (4.18).

Given a non-zero energy allocation, since we know that the transmitter with zero energy allocation should be allocated with the minimal bandwidth, we rewrite the K.K.T. condition related to the transmitters with the non-zero energy allocation in (4.14) as

$$-\log(\frac{a_n^k}{a_n^k+p_n^kH_n^k})-(1-\frac{a_n^k}{a_n^k+p_n^kH_n^k})=\alpha^k-\beta_n^k \tag{4.33}$$

for all $k\in\mathcal{K}$, and all n such that $p_n^k>0, n\in\mathcal{N}$.

Denoting $y(\alpha^k,\beta_n^k)$ as the solution to the following equation,

$$-\log(y(\alpha^k,\beta_n^k))-(1-y(\alpha^k,\beta_n^k))=\alpha^k-\beta_n^k, \tag{4.34}$$

from (4.33)-(4.34), we then have

$$a_n^k=p_n^kH_n^k\cdot z(\alpha^k,\beta_n^k)\ , \tag{4.35}$$

where

$$z(\alpha^k,\beta_n^k)\triangleq\frac{y(\alpha^k,\beta_n^k)}{1-y(\alpha^k,\beta_n^k)}\ , \tag{4.36}$$

and $0<y(\alpha^k,\beta_n^k)<1$.

By (4.18), we have that β_n^k must be zero when $a_n^k>\epsilon$. Then we divide $\{a_n^k, n\in\mathcal{N}\}$ into two sets: $\mathcal{T}^k\triangleq\{n\mid a_n^k>\epsilon, n\in\mathcal{N}\}$ and $\bar{\mathcal{T}}^k\triangleq\{n\mid a_n^k=\epsilon, n\in\mathcal{N}\}$. Then, (4.35) can be rewritten as

$$a_n^k=\begin{cases} p_n^kH_n^kz(\alpha^k,0), & \text{when } n\in\mathcal{T}^k, p_n^k>0\\ p_n^kH_n^kz(\alpha^k,\beta_n^k), & \text{when } n\in\bar{T}^k, p_n^k>0\end{cases}\ , \tag{4.37}$$

where $\beta_n^k\geq 0$ and

$$p_n^kH_n^kz(\alpha^k,\beta_n^k)=\epsilon,\ n\in\bar{\mathcal{T}}^k\ . \tag{4.38}$$

Also, we have

$$a_n^k=\epsilon\geq p_n^kH_n^kz(\alpha^k,\beta_n^k),\ \text{when } p_n^k=0\ . \tag{4.39}$$

Substituting (4.37) and (4.39) into the constraints $\sum_{n=1}^N a_n^k=1$, we further have

$$|\bar{\mathcal{T}}^k|\cdot\epsilon+\sum_{n\in\mathcal{T}^k}p_n^kH_n^kz(\alpha^k,0)=1\ . \tag{4.40}$$

Next, we characterize the optimality condition for the bandwidth allocation problem $\mathrm{BP}_k(\epsilon)$ given the non-zero energy allocation, as follows.

Theorem 4.5. *Given any energy allocation* $\{p_n^k \mid \sum_{i=1}^N p_i^k > 0, n \in \mathcal{N}\}$*, the bandwidth allocation* $\boldsymbol{a}^k$ *is the optimal to* $\mathsf{BP}(\epsilon)$*, if and only if, for every* $n \in \mathcal{T}^k$*, it satisfies*

$$a_n^k = (1 - |\bar{\mathcal{T}}^k| \cdot \epsilon) \frac{p_n^k H_n^k}{\sum_{i \in \mathcal{T}^k} p_i^k H_i^k}, \tag{4.41}$$

and for any $n \in \bar{\mathcal{T}}^k$*, it satisfies*

$$a_n^k = \epsilon \geq (1 - |\bar{\mathcal{T}}^k| \cdot \epsilon) \frac{p_n^k H_n^k}{\sum_{i \in \mathcal{T}^k} p_i^k H_i^k} \ , \tag{4.42}$$

for all $k \in \mathcal{K}$*.*

Proof. Rearranging (4.40), we have

$$z(\alpha^k, 0) = \frac{1 - |\bar{\mathcal{T}}^k| \cdot \epsilon}{\sum_{n \in \mathcal{T}^k} p_n^k H_n^k} \ . \tag{4.43}$$

Necessity: When $a_n^k \in \mathcal{T}^k$, we have $a_n^k > \epsilon$ and thus $\beta_n^k = 0$. Substituting (4.43) to (4.37), we have (4.41). When $a_n^k \in \bar{\mathcal{T}}^k$, we have $a_n^k = \epsilon$ and thus $\beta_n^k \geq 0$.

Note that, since $y(\alpha^k, \beta_n^k)$ is the solution to (4.34), which is an equation of the form $y - \log(y) = x$ for which y increases when x decreases for $y \in (0, 1)$, we see that $y(\alpha^k, \beta_n^k)$ increases as β_n^k increases. Then, we have $z(\alpha^k, \beta_n^k)$ increases as β_n^k increases given α^k, thus $z(\alpha^k, \beta_n^k) \geq z(\alpha^k, 0)$. Since $p_n^k H_n^k \geq 0$, we further have

$$p_n^k H_n^k z(\alpha^k, \beta_n^k) \geq p_n^k H_n^k z(\alpha^k, 0) \ . \tag{4.44}$$

Substituting (4.38) or (4.39), and (4.43) into the LHS and RHS of (4.44), respectively, we get (4.42).

Sufficiency: For the transmitters with zero energy allocation, it is easy to verify that the minimal bandwidth allocation is optimal. For other transmitters, since $a_n^k > 0$, by (4.35), we must have $0 < y(\alpha^k, \beta_n^k) < 1$ and thus $0 < z(\alpha^k, \beta_n^k) < \infty$. Note that, by (4.34), $y(\alpha^k, \beta_n^k) \in (0, 1)$ and $\alpha^k - \beta_n$ is one-to-one mapping. Therefore, for any a_n^k satisfying the sufficient conditions in Theorem 4.5, we can always find the corresponding dual variables α^k and β_n^k in (4.40) and (4.38), satisfying all the K.K.T. conditions. □

Intuitively, Theorem 4.5 states that the optimal bandwidth allocation should be proportional to the transmission "condition", i.e., $p_n^k H_n^k$. In particular, if the desired bandwidth allocation for transmitter n is less than the minimal requirement ϵ, a_n^k should be set as the minimal requirement

ϵ. Based on Theorem 4.5, we propose the following *iterative bandwidth fitting algorithm*. Initially, we set $\mathcal{T}^k = \{n \mid p_n^k > 0, n \in \mathcal{N}\}$ and $\bar{\mathcal{T}}^k = \mathcal{N} \setminus \mathcal{T}^k$. In each iteration, we calculate the bandwidth allocation a_n^k by (4.41) with the current $\mathcal{T}^k$ and $\bar{\mathcal{T}}^k$. We denote $\mathcal{V} = \{n \mid a_n^k \leq \epsilon, n \in \mathcal{T}^k\}$ as a "violation set", containing the elements in $\mathcal{T}^k$ that violate the definition of $\mathcal{T}^k \triangleq \{n \mid a_n^k > \epsilon, n \in \mathcal{N}\}$. Then, we move all $n \in \mathcal{V}$ from $\mathcal{T}^k$ to $\bar{\mathcal{T}}^k$. This iterative process ends when $\mathcal{V}$ is empty. Finally, with the obtained $\mathcal{T}^k$ and $\bar{\mathcal{T}}^k$, the optimal allocation can be calculated by (4.41)-(4.42).

The procedure of the algorithm is summarized as follows:

Algorithm 4.3 - Iterative Bandwidth Fitting Algorithm

1: Initialization

$\mathcal{T}^k = \{n \mid p_n^k > 0, n \in \mathcal{N}\}$, $\bar{\mathcal{T}}^k = \mathcal{N} \setminus \mathcal{T}^k$

2: Bandwidth Fitting

FOR $k \in \mathcal{K}$ such that $\sum_{n=1}^N p_n^k > 0$

REPEAT

Calculate a_n^k by (4.41) for all $n \in \mathcal{T}^k$

Set the violation set $\mathcal{V} = \{n \mid a_n^k \leq \epsilon, n \in \mathcal{T}^k\}$

Move all $n \in \mathcal{V}$ from $\mathcal{T}^k$ to $\bar{\mathcal{T}}^k$

UNTIL $\mathcal{V} = \{\ \}$

ENDFOR

2: Bandwidth Allocation

Obtain a_n^k with $\mathcal{T}^k$ and $\bar{\mathcal{T}}^k$ by (4.41)-(4.42) for all $n \in \mathcal{N}, k \in \mathcal{K}$ such that $\sum_{n=1}^N p_n^k > 0$

Note that, Algorithm 4.3 will terminate in at most N iterations since the elements transfer between $\mathcal{T}^k$ and $\bar{\mathcal{T}}^k$ is one-directional. Moreover, for all $k \in \mathcal{K}$ such that $\sum_{n=1}^N p_n^k > 0$, at the end of the last iteration, since $\mathcal{V}$ is empty, we have that the condition in (4.41) is satisfied by all $n \in \mathcal{T}^k$ and we have $a_n^k > \epsilon$ for all $n \in \mathcal{T}^k$. Also, for all other $n \in \bar{\mathcal{T}}^k$, obviously we have $a_n^k = \epsilon$. If (4.42) is also satisfied, we can further claim that with the obtained $\mathcal{T}^k$ and $\bar{\mathcal{T}}^k$, Algorithm 4.3 gives an optimal bandwidth allocation.

The next result shows that, at the end of each iteration (including the last iteration), with the obtained $\bar{\mathcal{T}}^k$, (4.42) is satisfied. The proof is given in Appendix 4.7.2.

Proposition 4.2. *For all $n \in \bar{\mathcal{T}}^k$, which is obtained by Algorithm 4.3 at the end of each iteration,* (4.42) *is satisfied for all $k \in \mathcal{K}$ such that $\sum_{n=1}^N p_n^k > 0$.*

With Proposition 4.2, we conclude that the bandwidth allocation obtained by Algorithm 4.3 is optimal. Moreover, since the number of iterations is bounded by N, the computational complexity of Algorithm 4.3 is $\mathcal{O}(N)$.

Remark 4.2. *In each iteration of Algorithm 4.1, N subproblems of EP_n and K subproblems of $\mathsf{BP}_k(\epsilon)$ need to be solved, using the discounted dynamic water-filling algorithm and the bandwidth fitting algorithm, whose computational complexities are $\mathcal{O}(K^2)$ and $\mathcal{O}(N)$, respectively. Thus the overall computational complexity of Algorithm 4.1 becomes $\mathcal{O}(NK^2)$, which is significantly lower than that of the generic convex tools.*

4.4 Suboptimal Algorithm with Causal Information

In Section 4.2, we proposed an iterative algorithm to obtain the optimal energy-bandwidth allocation with non-causal information of the channel gains and the harvested energy, whose performance can also serve as an upper bound on the achievable rate. In this section, we consider the case that the channel fading and energy harvesting are not predicable, i.e., their realizations can only be observed causally at the beginning of the corresponding slot. We will propose a heuristic algorithm to obtain the suboptimal energy-bandwidth allocation that follows the structure of the optimal solution. For simplicity, we still focus on the throughput maximization problem for point-to-point channels considered in Section 4.3.

We first give the structure of the optimal solution for the problem in (4.8)-(4.9).

Lemma 4.3. *If $(\mathcal{A}, \mathcal{P})$ is the optimal solution to the problem in* (4.8)-(4.9)*, then*

- $\{p_n^k \mid a_n^k > 0, n \in \mathcal{N}, k \in \mathcal{K}\}$ *satisfy*

$$p_n^k = \min\left\{P_n, a_n^k \cdot \left[w_n^k - \frac{1}{H_n^k}\right]^+ + \gamma_n^k\right\}, \tag{4.45}$$

  where γ_n^k is the energy adjuster and $w_n^k > 0$ may only increase/decrease at BDP/BFP;

- $\{a_n^k \mid \sum_{i=1}^N p_i^k > 0, n \in \mathcal{N}, k \in \mathcal{K}\}$ *satisfy*

$$a_n^k = \frac{p_n^k H_n^k}{\sum_{i \in \mathcal{N}} p_i^k H_i^k}\ . \tag{4.46}$$

Proof. Comparing (4.45) with the optimal energy allocation given in (4.29) by Theorem 4.3, the only difference is the term of energy adjuster γ_n^k. Note that, for the optimal energy allocation, given n, k, we have that $\gamma_n^k = 0$ if $p_n^k < P_n$ since the performance can be improved if p_n^k can be further increased by decreasing a positive γ_n^k. Therefore, we have that for the optimal energy allocation, (4.45) is equivalent to (4.29).

Given $\mathcal{P}$, we next show that the optimal $a_n^k = 0$ if and only if $p_n^k = 0$. Specifically, if $p_n^k = 0$, the rate of link n in slot k is constant zero for any $a_n^k \geq 0$. Since $\sum_{i=1}^N p_i^k > 0$ and $\sum_{n=1}^N a_n^k = 1$, if we reassign the non-zero bandwidth a_n^k of link n to any other links i such that $p_i^k > 0$ in slot k, the sum rate in slot k is increased. Therefore, we have $a_n^k = 0$ if $p_n^k = 0$. On the other hand, if $p_n^k > 0$, we have that the derivative of the objective function over a_n^k tends to infinity as $a_n^k \to 0^+$, which means that we can always move certain bandwidth from some other link to link n with $a_n^k = 0$ and $p_n^k > 0$, such that the rate loss of the other link is less than the rate gain of link n. Therefore, $a_n^k = 0$ is not optimal if $p_n^k > 0$. Hence, $a_n^k = 0$ if and only if $p_n^k = 0$. By eliminating the terms of $p_n^k = 0$ in the objective function, the optimal bandwidth allocation is positive and then Theorem 4.5 can be adapted for the case $\epsilon = 0$, i.e., (4.46) is obtained. □

Lemma 4.3 provides the structure of the optimal energy-bandwidth allocation, in which the water level w_n^k is the only parameter affected by the future channel fading and energy harvesting. Specifically, if the energy harvesting and channel gains are predictable, then the optimal w_n^k can be obtained, as in the proposed non-causal algorithm, where $\gamma_n^k = 0$ if $p_n^k < P_n$, and $\gamma_n^k \geq 0$ if $p_n^k = P_n$. In other words, in (4.45), γ_n^k does not affect the value of p_n^k when the optimal water level w_n^k is given. However, when the energy harvesting and channel fading processes are unpredictable, the optimal w_n^k is hard to obtain. Note that γ_n^k essentially acts as an adjusting factor to mitigate the energy waste caused by the non-optimality of w_n^k, i.e., if the suboptimal water level is lower than the optimal one and therefore causes the energy waste, we can try to utilize the wasted energy for transmission. Then, we use the potentially wasted energy as the adjuster, given by

$$\gamma_n^k = \max\left\{0, B_n^{k-1} + \Delta_n^k - \min\left\{P_n, a_n^k \cdot \left[w_n^k - \frac{1}{H_n^k}\right]^+\right\} - B_n^{\max}\right\} . \tag{4.47}$$

where $\Delta_n^k \triangleq E_n^k - E_n^{k-1}$ is the energy harvested energy in slot k. Specifically, γ_n^k becomes the actual energy wastage D_n^k if the water-filling fashion in (4.29) is followed using the water level w_n^k.

Based on Lemma 4.3, we design an *adaptive water-filling algorithm*, aiming to obtain a sub-

optimal energy-bandwidth allocation, which follows the structure of the optimal solution given in Lemma 4.3. With the proposed algorithm, except for the calculation of the water levels, all other optimality conditions are approached by the obtained energy-bandwidth allocation. Specifically, to avoid the use of the future information, the water levels are calculated by a heuristic method.

The proposed algorithm is an online algorithm. Initially, we set a water level w_n^0 for each transmitter $n \in \mathcal{N}$. At the beginning of slot k, we check the battery level of each transmitter. If the battery is empty or full, we decrease or increase the water level by a factor, e.g., $w_n^k = c \cdot w_n^{k-1}$(or w_n^{k-1}/c). Otherwise, we keep the water level unchanged. Then, based on the water level w_n^k, we calculate the energy allocation and bandwidth allocation $\{p_n^k, a_n^k \mid n \in \mathcal{N}\}$ by solving the equations (4.45), (4.46) and (4.47). In particular, substituting (4.47) into (4.45), there are two equations and two variables, which can be solved numerically.

Moreover, we propose the following choices of the initial water level w_n^0 and the factor c,

$$w_n^0 \approx N \cdot \mathbb{E}\left[E_n^k\right] + \mathbb{E}\left[\frac{1}{H_n^k}\right] , \tag{4.48}$$

and

$$c \approx 1 + P_n/w_n^0 \tag{4.49}$$

The algorithm is summarized as follows:

Algorithm 4.4 - Adaptive Water-Filling Algorithm (the superscript k is dropped)

1: Input

Current water level and battery level $\{w_n, B_n \mid n \in \mathcal{N}\}$

2: Output

Updated water level and battery level $\{w_n, B_n \mid n \in \mathcal{N}\}$

Energy-bandwidth allocation $\{p_n, a_n \mid n \in \mathcal{N}\}$

3: At the beginning of each slot

FOR $n \in \mathcal{N}$

IF $B_n = B_n^{\max}$ **THEN** $w_n \leftarrow w_n/c$

IF $B_n = 0$ **THEN** $w_n \leftarrow w_n \cdot c$

ENDFOR

Solve the equation group of (4.45), (4.46) and (4.47) to obtain $\{p_n, a_n \mid n \in \mathcal{N}\}$

$B_n \leftarrow \min\{P_n, B_n + \Delta_n - p_n\}$ for all $n \in \mathcal{N}$

4.5 Simulation Results

Suppose that there are $N = 4$ transmitters in the network and each communicates with one receiver, and we assume $W_n = 1$ for $n = 1, 2, 3, 4$. We set the scheduling period as $K = 40$ slots. For each transmitter n, we set the initial battery level $B_n^0 = 0$ and the maximum battery capacity $B_n^{\max} = 20$ units. Assume that the harvested energy follows a truncated Gaussian distribution with mean μ_E and variance of $\sigma^2 = 2$, and the fading channel parameter follows the standard complex Gaussian distribution, i.e., $h_n^k \sim \mathcal{CN}(0, 1)$, so that $H_n^k \sim \exp(1)$.

For comparison, we consider three scheduling strategies, namely, the *greedy policy*, the *TDMA greedy policy*, and the *equal bandwidth policy*. For the greedy policy, each transmitter tries to consume the harvested energy as much as possible in each slot, as calculated by (4.10). Then, the central controller allocates the bandwidth to each transmitter by using the iterative bandwidth fitting algorithm (i.e., Algorithm 4.3). For the TDMA greedy policy, each transmitter uses the maximum possible energy to transmit in each slot, and the central controller allocates the entire bandwidth to the transmitter with the maximum $p_n^k H_n^k$. For the equal bandwidth policy, the central controller allocates each transmitter equal bandwidth and then each transmitter uses the optimal energy allocation.

To evaluate the performance of different algorithms, we consider two scenarios, namely, the *energy-limited* scenario, where the maximum transmission power is $P_n = 10$ units per slot, and the *power-limited* scenario, where the maximum transmission power is $P_n = 5$ units per slot. Moreover, the convergence threshold in Algorithm 4.1 is set as $\delta = 10^{-3}$, and the initial water level and the parameter c in Algorithm 4.4 are set as $w_n^0 = 25$ and $c = 1.1$, respectively. We compare the achievable rates of different algorithms under different mean values μ_E of the harvested energy. In the energy-limited scenario, the transmitter has more freedom to schedule the harvested energy to be consumed in each slot because of the large maximum transmission power. One the other hand, in the power-limited scenario, the harvested energy would be consumed in the future slots since the maximum transmission power is reached more frequently. Furthermore, for both scenarios, when the energy harvesting parameter μ_E is small, it corresponds to the "energy-constrained" condition, where the scheduling is mainly constrained by the energy availability. And when μ_E is large, it corresponds to the "power-constrained" condition, where the scheduling is more constrained by the maximum transmission power.

Before we compare the performance of different algorithms, we first illustrate the convergence behavior of Algorithm 4.1 in Fig. 4.4 with $\mu_E = 4$. It is seen that Algorithm 4.1 converges (the relative error is less than 0.001) within 4 and 7 iterations for $P_n = 5$ and $P_n = 10$, respectively. Next, we set $\mu_E = 4$ and $P_n = 10$ and give the 20-slot snapshots (slot 20 - slot 40) of the obtained energy-bandwidth allocation in Fig. 4.5, Fig. 4.6 and Fig. 4.7. Specifically, Fig. 4.5 and Fig. 4.6 illustrate the relationship among the water level w_n^k, transmission energy p_n^k and the battery level B_n^k obtained by Algorithm 4.1 and Algorithm 4.4, respectively, showing that although both algorithms follow the water-filling structure with the dynamic water levels, their water levels vary according to different rules, based on the dynamic of the battery. Moreover, the optimal bandwidth allocation a_n^k obtained by Algorithm 4.1 is illustrated in Fig. 4.7, and we can see that most of the time the channel is shared by multiple transmitters to maximize the sum-rate.

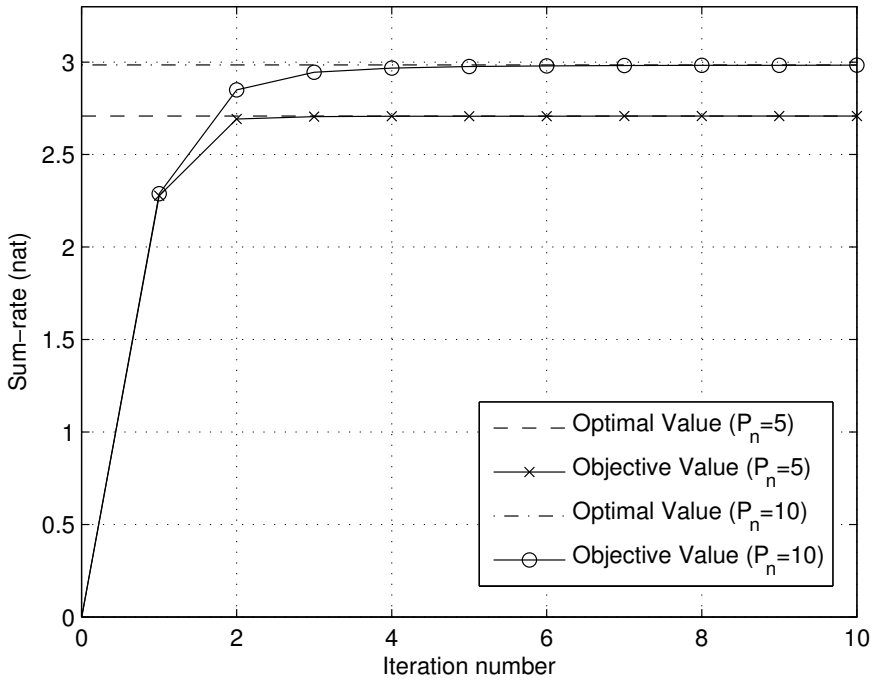

Figure 4.4: The convergence of Algorithm 4.1 for $\mu_E = 4$.

We then run the simulation 1000 times to obtain the rates given by various scheduling strategies, as well as by the optimal schedule solved by a general convex solver, shown in Fig. 4.8 and Fig. 4.9, for the energy-limited scenario and the power-limited scenario, respectively. It is seen from

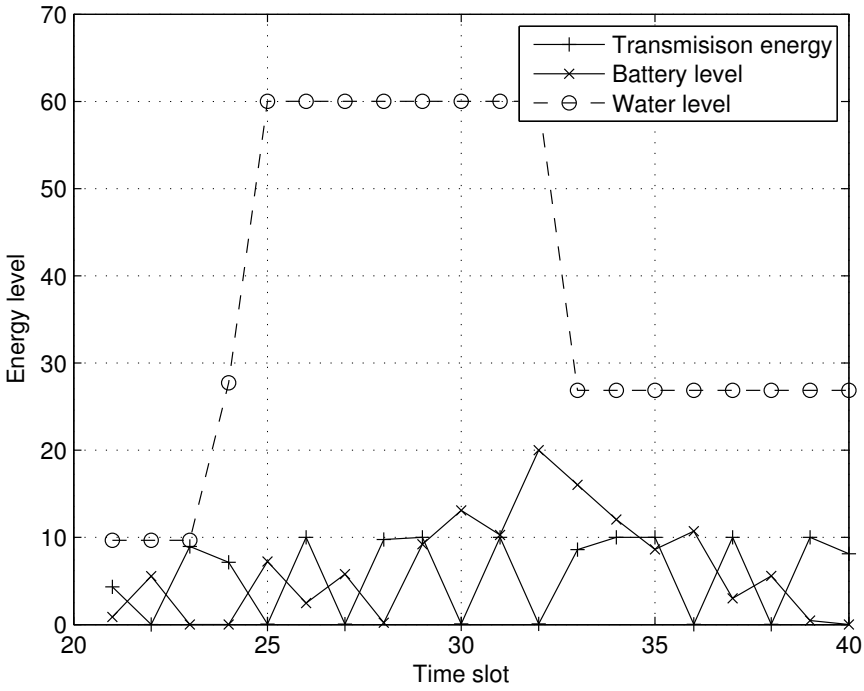

Figure 4.5: 20-slot snapshot of the optimal energy allocation obtained by Algorithm 4.1 for a particular transmitter ($\mu_E = 4, P_n = 10$).

that for both scenarios the proposed non-causal iterative algorithm (Algorithm 4.1) achieves the same performance as that corresponding to the optimal energy-bandwidth allocation solved by the generic convex solver, corroborating the optimality of Algorithm 4.1 as stated by Theorem 2. Also, the proposed causal algorithm (Algorithm 4.4) performs worse than the optimal policy but still better than the other heuristic policies. Moreover, for all policies, the performance is improved as the mean of the harvested energy increases.

From Fig. 4.8, for the energy-limited scenario, the performance gap between the TDMA greedy policy and the optimal solution increases as the mean of the harvested energy increases. It is because when the mean of the harvested energy is high, due to the maximum transmission power and battery capacity constraints, the single-user transmission of TDMA results in significant energy waste by the non-transmitting transmitters in each slot.

On the other hand, from Fig. 4.9, for the power-limited scenario, the performance gap between the optimal solution and some of the suboptimal algorithms (Algorithm 4.4 and the greedy policy)

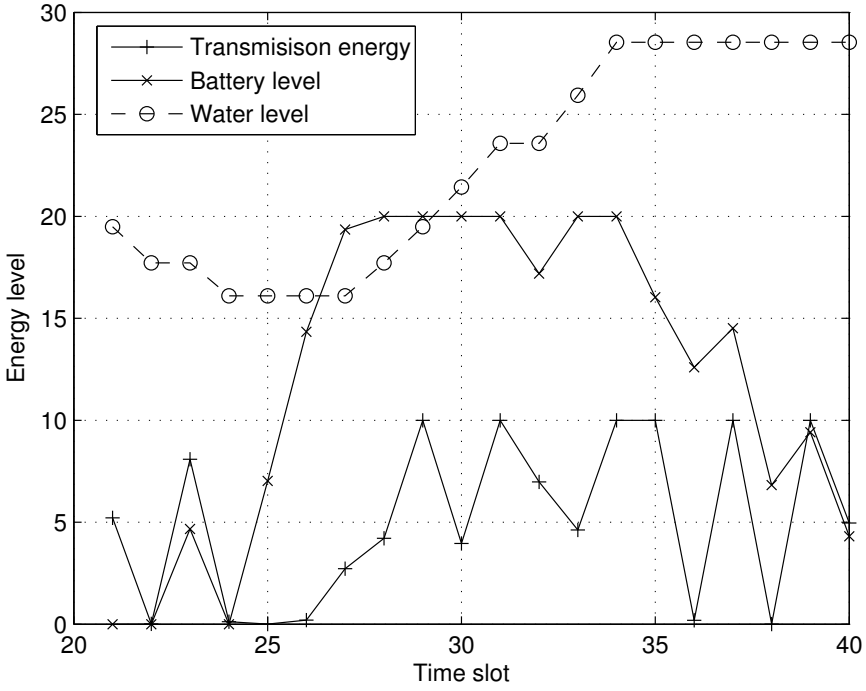

Figure 4.6: 20-slot snapshot of the energy allocation obtained by Algorithm 4.4 for a particular transmitter ($\mu_E = 4, P_n = 10$).

decreases as the mean of the harvested energy increases. It is because when the harvested energy is ample, the optimal energy allocation achieves the maximum transmission power more frequently and approaches the greedy policy. Also, in the power-limited scenario, the TDMA greedy policy performs significantly worse than other algorithms since the low maximum transmission power results in a lot of energy waste in the absence of any channel sharing.

Moreover, as expected, the performance in the energy-limited scenario is better than that in the power-limited energy for all policies. This is because the lower maximum transmission power restricts the flexibility of the energy scheduling and causes waste of energy due to the limited battery capacity.

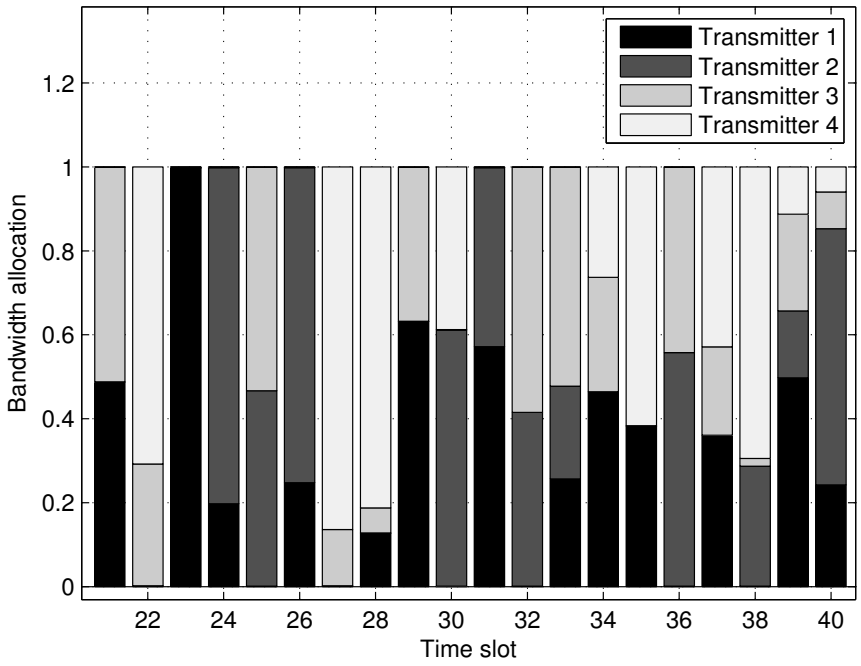

Figure 4.7: 20-slot snapshot of the optimal bandwidth allocation by Algorithm 4.1 ($\mu_E = 4, P_n = 10$).

4.6 Conclusions

In this paper, we have considered the joint energy-bandwidth allocation problem for multiple energy harvesting transmitters over K time slots. This problem is formulated as a convex optimization problem with $\mathcal{O}(MK)$ variables and constrains, where M is the number of the receivers and K is number of the slots in a scheduling period, which is hard to solve with a generic convex tool. We have proposed an energy-bandwidth allocation algorithm that iterates between solving the energy allocation subproblem and the bandwidth allocation subproblem, and the convergence and the optimality of the iterative algorithm have been shown. When each transmitter communicates with one receiver and the sum-rate is unweighted, the discounted dynamic water-filling algorithm and the bandwidth fitting algorithm are proposed to optimally solve the energy and bandwidth allocation subproblems, respectively. Moreover, a heuristic algorithm is also proposed to obtain the suboptimal energy-bandwidth allocation causally and efficiently, by following the structure of

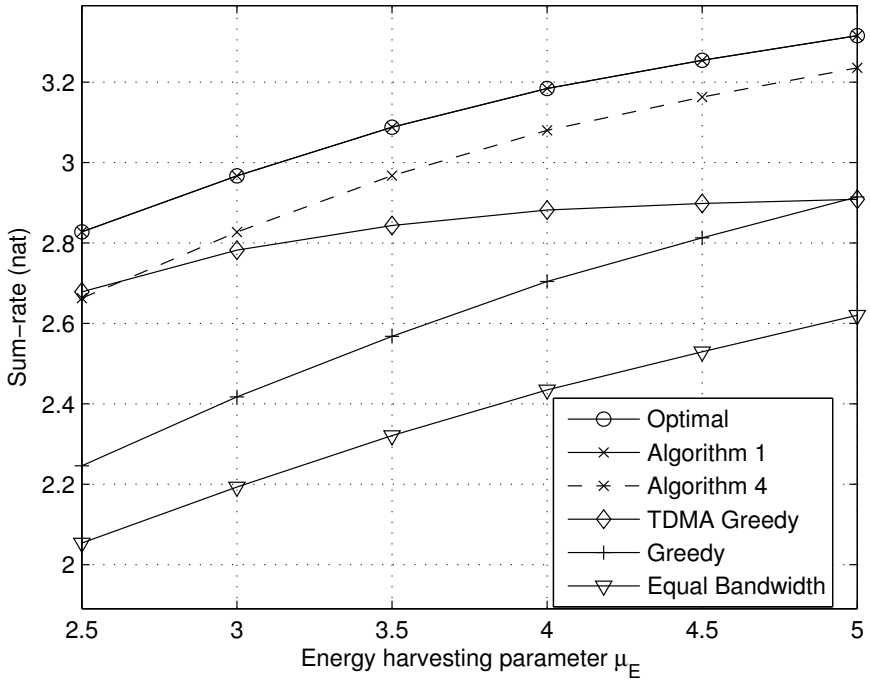

Figure 4.8: Performance comparisons in the energy-limited scenario ($P_n = 10$, $B_n^{\max} = 20$).

the optimal energy-bandwidth solution. In a companion paper, we will consider multiple broadcast channels under the joint energy-bandwidth allocation framework and develop efficient algorithms for solving the two subproblems under both orthogonal and non-orthogonal access.

4.7 Appendices

4.7.1 Proof of Theorem 4.2

We note that, the feasible domain of $\mathsf{BP}_k(\epsilon_0/i)$ expands with iterations while the feasible domain of EP_n remains unchanged. Since we successively solve the maximization problems EP_n and $\mathsf{BP}_k(\epsilon_0/i)$ in iteration i, we have that the objective value is non-decreasing over the iterations. On the other hand, the objective function is upper bounded by $C_{\mathcal{W}}(\mathcal{P}, \mathcal{A}) \leq \sum_{m=1}^{M} \sum_{k=1}^{K} \log(1 + P_m H_m^k)$ therefore the algorithm converges. Since the feasible domain of $\mathsf{P}_{\mathcal{W}}(\epsilon)$ is a closed set for $\epsilon \geq 0$, at the converged point V, we can find the corresponding $\mathcal{P}_0$ and $\mathcal{A}_0$ which are pairwise optimal for $\mathsf{P}_{\mathcal{W}}(\epsilon)$ otherwise $V = C_{\mathcal{W}}(\mathcal{P}_0, \mathcal{A}_0)$ can be increased by performing another iteration. Specifically, if

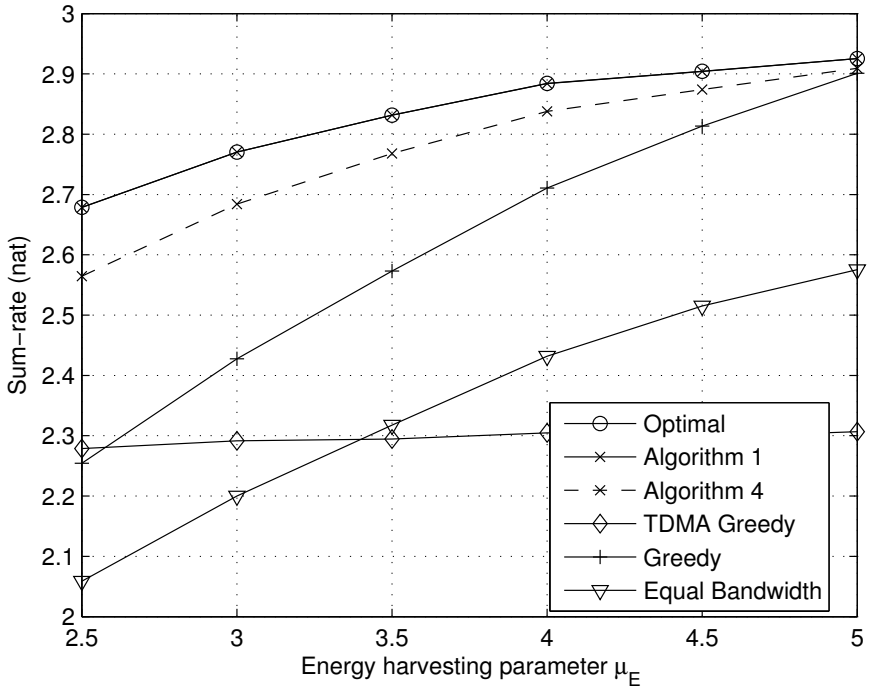

Figure 4.9: Performance comparisons in the power-limited scenario ($P_n = 5$, $B_n^{\max} = 20$).

V is reached within finite iterations m', $\mathcal{P}_0$ and $\mathcal{A}_0$ are pairwise optimal for $\mathsf{P}_{\mathcal{W}}(\epsilon_0/i')$; otherwise, $\mathcal{P}_0$ and $\mathcal{A}_0$ are pairwise optimal for $\mathsf{P}_{\mathcal{W}}(0)$.

We first consider the case that V is reached within finite iterations i'. Since V is reached within finite iterations i', we have that $\mathcal{P}_0$ and $\mathcal{A}_0$ are pairwise optimal for both $\mathsf{P}_{\mathcal{W}}(\epsilon_0/i')$ and $\mathsf{P}_{\mathcal{W}}(\epsilon_0/(i'-1))$. Then, by Theorem 4.1, $(\mathcal{P}_0, \mathcal{A}_0)$ is the optimal solution to $\mathsf{P}_{\mathcal{W}}(\epsilon_0/i')$ and $\mathsf{P}_{\mathcal{W}}(\epsilon_0/(i'-1))$. Note that, since the feasible domain of $\mathsf{P}_{\mathcal{W}}(\epsilon_0/i')$ is expanded from that of $\mathsf{P}_{\mathcal{W}}(\epsilon_0/(i'-1))$ by decreasing ϵ, $(\mathcal{P}_0, \mathcal{A}_0)$ is not on the boundary of $a_n^k \geq \epsilon_0/i'$, i.e., the equality of $a_m^k \geq \epsilon_0/i'$ does not hold. Therefore, continually expanding the feasible domain of $\mathsf{P}_{\mathcal{W}}(\epsilon)$ by decreasing ϵ from ϵ_0/i' to 0, $(\mathcal{P}_0, \mathcal{A}_0)$ remains at a local optimal point and thus also a global optimal point according to the domain's convexity.

We then consider the case that V can only be approached with infinite iterations. For this case, we have that $\mathcal{P}_0$ and $\mathcal{A}_0$ are pairwise optimal for $\mathsf{P}_{\mathcal{W}}(0)$. However, we note that, even so, $(\mathcal{P}_0, \mathcal{A}_0)$ is not necessarily optimal solution to $\mathsf{P}_{\mathcal{W}}(0)$ when $a_m^k = 0$ for some $m \in \mathcal{M}$ and $k \in \mathcal{K}$. To show the optimality of $(\mathcal{P}_0, \mathcal{A}_0)$, we use the proof by contradiction. Suppose that $\mathcal{P}_0$ and

$\mathcal{A}_0$ are pairwise optimal for $\mathsf{P}_{\mathcal{W}}(0)$ but $(\mathcal{P}_0, \mathcal{A}_0)$ is not an optimal solution to $\mathsf{P}_{\mathcal{W}}(0)$. Denote $\mathcal{Z} \triangleq \{(m,k) \mid a_m^k = 0, a_m^k \in \mathcal{A}_0, p_m^k \in \mathcal{P}_0\}$ as the set of the links with zero bandwidth allocation. Since $\mathcal{P}_0$ and $\mathcal{A}_0$ are pairwise optimal for $\mathsf{P}_{\mathcal{W}}(0)$, we have that all K.K.T. conditions hold except for the links $(n,k) \in \mathcal{Z}$, i.e., excluding the links in $\mathcal{Z}$, $(\mathcal{P}_0, \mathcal{A}_0)$ is optimal for $\mathsf{P}_{\mathcal{W}}(0)$ by Theorem 4.1 (excluding the links in $\mathcal{Z}$, the problem $\mathsf{P}_{\mathcal{W}}(0)$ is equivalent to $\mathsf{P}_{\mathcal{W}}(\epsilon')$ where ϵ' is the remaining smallest bandwidth allocation). However, since we also have that $(\mathcal{P}_0, \mathcal{A}_0)$ is not optimal for $\mathsf{P}_{\mathcal{W}}(0)$, then we know that $\{a_m^k = 0, p_m^k = 0 \mid (m,k) \in \mathcal{Z}\}$ is suboptimal, i.e., we can always reassign an arbitrary small bandwidth from some non-zero bandwidth link to a zero bandwidth link and then perform EP_n to achieve a new objective value which is higher than V. Obviously, due to the increase of the objective value, the energy allocation of the link with the newly assigned bandwidth must increase from zero to a positive value after solving EP_n with the new bandwidth allocation. Specifically, for a link $(m,k) \in \mathcal{Z}$, if reassigning an arbitrary small bandwidth can result in the corresponding p_m^k increased form zero to a positive value, we must have $H_m^k > v_n^k - u_n^k$ such that $m \in \mathcal{M}_n$ by Theorem 4.3, i.e., according to the water-filling solution, $v_n^k - u_n^k$ increases after solving EP_n with the new $a_m^k > 0$ while the new p_m^k determined by (4.29) must be positive.

However, in each specific iteration, we have $a_m^k > 0$ and the optimal solution to EP_n satisfies $H_m^k \leq v_n^k - u_n^k$ such that $m \in \mathcal{M}_n$ when $p_m^k = 0$, by (4.29). Note that, the objective function is continuous and the problem is a convex optimization problem. Then, following the algorithm, when a_m^k converges to zero, we also have $H_m^k \leq v_n^k - u_n^k$ when $p_m^k = 0$, which is contradiction to the above suboptimal assumption. Therefore, the converged objective value must be the optimal value for problem $\mathsf{P}_{\mathcal{W}}(0)$.

4.7.2 Proof of Proposition 4.2

Note that, initially, $\bar{\mathcal{T}}^k$ contains the elements such that $p_n^k = 0$ and, obviously, (4.42) is satisfied. Following the procedure of Algorithm 4.3, at the end of each iteration, new elements are added to $\bar{\mathcal{T}}^k$. Therefore, we need to show that, for any $n \in \bar{\mathcal{T}}^k$, (a) (4.42) is satisfied for n in the iteration when n is added to $\bar{\mathcal{T}}^k$; (b) (4.42) is still satisfied for n in the next iterations.

We first show that, at the end of each iteration, $n_0 \in \mathcal{V}$, which is newly added to $\bar{\mathcal{T}}^k$, satisfies (4.42) after this move. At the beginning of the iteration, we have the sets $\mathcal{T}^k$ and $\bar{\mathcal{T}}^k$. Following Algorithm 4.3, we recalculate a_n^k by (4.41) for all $n \in \mathcal{T}^k$ and all $k \in \mathcal{K}$. After this recalculation, if

$\mathcal{V}$ is non-empty, i.e., there exists $n_0 \in \mathcal{V}$ such that $a^k_{n_0} \leq \epsilon$, we will move n_0 from $\mathcal{T}^k$ to $\bar{\mathcal{T}}^k$ at the end of the iteration. Also, we have

$$\epsilon \geq a^k_{n_0} = p^k_{n_0} H^k_{n_0} \frac{1 - |\bar{\mathcal{T}}^k| \cdot \epsilon}{\sum_{i \in \mathcal{T}^k} p^k_i H^k_i} \tag{4.50}$$

$$= p^k_{n_0} H^k_{n_0} \frac{1 - |\bar{\mathcal{T}}^k| \cdot \epsilon - a^k_{n_0}}{\sum_{i \in \mathcal{T}^k} p^k_i H^k_i - p^k_{n_0} H^k_{n_0}} \tag{4.51}$$

$$\geq p^k_{n_0} H^k_{n_0} \frac{1 - |\bar{\mathcal{T}}^k| \cdot \epsilon - \epsilon}{\sum_{i \in \mathcal{T}^k} p^k_i H^k_i - p^k_{n_0} H^k_{n_0}} \tag{4.52}$$

$$= p^k_{n_0} H^k_{n_0} \frac{1 - |\bar{\mathcal{T}}^k \cup n_0| \cdot \epsilon}{\sum_{i \in \mathcal{T}^k / n_0} p^k_i H^k_i}, \tag{4.53}$$

where (4.51) follows since $a^k_{n_0} = p^k_{n_0} H^k_{n_0} \frac{1-|\bar{\mathcal{T}}^k| \cdot \epsilon}{\sum_{i \in \mathcal{T}^k} p^k_i H^k_i}$ and $a^k_{n_0} = p^k_{n_0} H^k_{n_0} \frac{a^k_{n_0}}{p^k_{n_0} H^k_{n_0}}$ and we know that if $c = (a+b)/(x+y)$ and $c = b/y$, then $c = a/x = b/y = (a+b)/(x+y)$. (4.52) follows since $a^k_{n_0} \leq \epsilon$.

Rearranging (4.53), we have $\epsilon \geq (1 - |\bar{\mathcal{T}}^k \cup n_0| \cdot \epsilon) \frac{p^k_{n_0} H^k_{n_0}}{\sum_{i \in \mathcal{T}^k / n_0} p^k_i H^k_i}$ where $n_0 \in \bar{\mathcal{T}}^k \cup n_0$, $\bar{\mathcal{T}}^k \leftarrow \bar{\mathcal{T}}^k \cup n_0$ and $\mathcal{T}^k \leftarrow \mathcal{T}^k / n_0$ are the new sets generated at the end of the iteration, respectively. Hence, n_0, which is newly added to $\bar{\mathcal{T}}^k$, satisfies (4.42).

We next show that, n_0 will also satisfy (4.42) in subsequent iterations. By (4.50)-(4.53), we also have

$$\frac{1 - |\bar{\mathcal{T}}^k| \cdot \epsilon}{\sum_{i \in \mathcal{T}} p^k_i H^k_i} \geq \frac{1 - |\bar{\mathcal{T}}^k \cup n_0| \cdot \epsilon}{\sum_{i \in \mathcal{T}^k / n_0} p^k_i H^k_i} \ , \tag{4.54}$$

i.e., the value of $\frac{1-|\bar{\mathcal{T}}^k| \cdot \epsilon}{\sum_{i \in \mathcal{T}} p^k_i H^k_i}$ decreases over the iterations, and so is the value of $p^k_{n0} H^k_{n0} \frac{1-|\bar{\mathcal{T}}^k| \cdot \epsilon}{\sum_{i \in \mathcal{T}} p^k_i H^k_i}$. Moreover, by (4.50), we have that $\epsilon \geq p^k_{n_0} H^k_{n_0} \frac{1-|\bar{\mathcal{T}}^k| \cdot \epsilon}{\sum_{i \in \mathcal{T}} p^k_i H^k_i}$ in the current iteration. Therefore, in the subsequent iterations, (4.42) remains satisfied for n_0.

Chapter 5

Energy-Bandwidth Allocation for Flat-Fading Broadcast Channels

In the last chapter, for a network with multiple orthogonal broadcast channels and energy harvesting transmitters, we proposed an iterative algorithm for computing the optimal energy-bandwidth allocation to maximize the weighted throughput. For the special case that each transmitter only communicates with one receiver and all weights are equal, the algorithms for efficiently solving the energy and bandwidth allocation subproblems are also proposed. In this chapter, we develop algorithms for solving the two subproblems for the general case of multiple broadcast channels. Moreover, for a single (non-orthogonal) broadcast channel with energy harvesting transmitter, the optimal energy scheduling over static and two-user fading channels was discussed in [73] and [74], respectively. In this chapter, we treat the energy-bandwidth allocation problem for multiple broadcast channels, including both orthogonal and non-orthogonal broadcast. Taking the proportional fairness into account, [75] discussed the convergence of the general proportionally-fair scheduling without energy harvesting. For energy harvesting transmitters with unbounded battery capacity, heuristic algorithms have been proposed in [52] to find the time-power allocations under the proportional fairness. The proportionally-fair energy-bandwidth allocation in multiple orthogonal broadcast channels is also treated in this chapter.

In particular, we consider a network with multiple transmitters, each powered by the renewable energy source. We assume that the transmitters are assigned orthogonal frequency bands to avoid

interfering from each other. In orthogonal broadcast, the frequency band assigned to the transmitter is further split for the transmission to each designated receiver orthogonally (i.e., no interference); on the other hand, in non-orthogonal broadcast, the transmissions to all designated receivers take place on the same frequency band assigned to the transmitter. For the special case where all links have equal weights, with orthogonal or non-orthogonal broadcast, we show that each transmitter should only use the strongest channel in each slot, i.e., multiple broadcast channels reduce to multiple point-to-point channels, and thus we can directly use the algorithms in Chapter 4 to obtain the optimal energy-bandwidth allocation. For the general weighted case, we develop algorithms for solving the two subproblems, i.e., energy allocation and bandwidth allocation, for both orthogonal and non-orthogonal broadcast. We also reveal that the gain by non-orthogonal broadcast over orthogonal broadcast is limited with energy harvesting transmitters.

Moreover, we formulate a proportionally-fair (PF) throughput maximization problem with orthogonal broadcast. In point-to-point channels without energy harvesting, in slot k, the optimal PF scheduler schedules the link with $\max_m R_m^k/A_m^k$, where R_m^k is the rate achievable by link m in slot k and A_m^k is the average rate of link m up to slot k. The average rate is computed over a time window as a moving average: $R_m^{k+1} = (1-\alpha)A_m^k + \alpha R_m^k$ if link m is scheduled in slot k, and $A_m^{k+1} = (1-\alpha)A_m^k$ otherwise [75]. However, in the presence of energy harvesting, using a single link is not optimal and thus scheduling multiple links in a slot and splitting the bandwidth is essential. To efficiently solve the PF throughput maximization problem, we convert it to a weighted throughput maximization problem with proper weights. The algorithm to obtain such weights is also proposed.

5.1 Multiple Orthogonal Broadcast Channels

Consider a network consisting of N transmitters and M receivers where transmitter $n \in \mathcal{N}$ communicates with receivers in the set $\mathcal{M}_n$ ($\bigcup_n \mathcal{M}_n = \mathcal{M}$, and $\mathcal{M}_n \bigcap \mathcal{M}_{n'} = \Phi$ for $n \neq n'$) in an orthogonal broadcast channel. Our goal is to schedule the transmission in K slots $\mathcal{K} \triangleq \{1, 2, \ldots, K\}$ to maximize the weighted sum-rate by proper energy and bandwidth allocation (i.e., the problem in (4.4)-(4.5)). Specifically, in Chapter 4, we first gave the optimal energy discharge schedule in (4.10) and then proposed an iterative algorithm (Algorithm 4.1) to obtain the optimal energy allocation

$\mathcal{P} \triangleq \{p_m^k, \forall m \in \mathcal{M}, k \in \mathcal{K}\}$ and the bandwidth allocation $\mathcal{A} \triangleq \{a_m^k, \forall m \in \mathcal{M}, k \in \mathcal{K}\}$.

Recall the general energy-bandwidth allocation problem $\mathsf{P}_{\mathcal{W}}(\epsilon)$ for multiple orthogonal broadcast channels formulated in (4.11)-(4.12):

$$\mathsf{P}_{\mathcal{W}}(\epsilon): \quad \max_{\mathcal{P},\mathcal{A}} C_{\mathcal{W}}(\mathcal{P},\mathcal{A}) \tag{5.1}$$

subject to

$$\begin{cases} \tilde{E}_n^k - B_n^{\max} \le \sum_{\kappa=1}^{k} \sum_{m\in\mathcal{M}_n} p_m^\kappa \le \tilde{E}_n^k \\ \sum_{m=1}^{M} a_m^k = 1 \\ \sum_{m\in\mathcal{M}_n} p_m^k \le P_n \\ p_m^k \ge 0 \\ a_m^k \ge \epsilon \end{cases} \tag{5.2}$$

for all $n \in \mathcal{N}, m \in \mathcal{M}, k \in \mathcal{K}$, where

$$C_{\mathcal{W}}(\mathcal{P},\mathcal{A}) = \sum_{m\in\mathcal{M}} W_m \sum_{k\in\mathcal{K}} a_m^k \log(1 + \frac{p_m^k H_m^k}{a_m^k}),\ a_m^k \in [0,1], p_m^k \in [0,\infty), \tag{5.3}$$

$\mathcal{W} \triangleq \{W_m, \forall m \in \mathcal{M}\}$ is the set of weights, ϵ is the required minimal bandwidth allocation, $\tilde{E}_n^k$ is the effective harvested energy after optimally discharging the surplus energy in (4.10), and $B_n^{\max}$ is the battery capacity of transmitter n.

Introducing the non-negative dual variables λ_n^k, μ_n^k, α^k, β_m^k and ξ_n^k for all $n \in \mathcal{N}, m \in \mathcal{M}$ and $k \in \mathcal{K}$, we denote

$$\begin{aligned} \mathcal{M}(\mathcal{P},\mathcal{A}) \triangleq & -\sum_{n,k} \lambda_n^k \left(\sum_{\kappa=1}^{k} \sum_{m\in\mathcal{M}_n} p_m^\kappa - \tilde{E}_n^k \right) + \sum_{n,k} \mu_n^k \left(\sum_{\kappa=1}^{k} \sum_{m\in\mathcal{M}_n} p_m^\kappa - \tilde{E}_n^k + B_n^{\max} \right) \\ & - \sum_k \alpha^k (\sum_m a_m^k - 1) + \sum_{m,k} \beta_m^k (a_m^k - \epsilon) - \sum_{n,k} \xi_n^k (\sum_{m\in\mathcal{M}_n} p_m^k - P_n) \\ = & -\sum_{n,k} \left(\sum_{m\in\mathcal{M}_n} p_m^k \sum_{\kappa=k}^{K} \lambda_n^\kappa - \lambda_n^k \tilde{E}_n^k \right) + \sum_{n,k} \left(\sum_{m\in\mathcal{M}_n} p_m^k \sum_{\kappa=k}^{K} \mu_n^\kappa - \mu_n^k \left(\tilde{E}_n^k - B_n^{\max} \right) \right) \\ & - \sum_k \alpha^k (\sum_m a_m^k - 1) + \sum_{m,k} \beta_m^k (a_m^k - \epsilon) - \sum_{n,k} \xi_n^k (\sum_{m\in\mathcal{M}_n} p_m^k - P_n)\ , \end{aligned} \tag{5.4}$$

as the Lagrangian multipliers. Then, the Lagrangian functions for $\mathsf{P}_{\mathcal{W}}(\epsilon)$ can be defined as

$$\mathcal{L}_O \triangleq C_{\mathcal{W}}(\mathcal{P},\mathcal{A}) + \mathcal{M}(\mathcal{P},\mathcal{A})\ . \tag{5.5}$$

5.1.1 Maximizing Network Throughput

For the special case that all links have equal weights, e.g., $\mathcal{W} = \{W_m = 1, m \in \mathcal{M}\}$, the following result states that each transmitter should only use its strongest channel.

Theorem 5.1. *The problem $P_{\{1\}}(0)$ in multiple orthogonal broadcast channels is equivalent to the energy-bandwidth allocation problem in point-to-point channels formulated as*

$$\max_{\mathcal{P},\mathcal{A}} \sum_{n\in\mathcal{N},k\in\mathcal{K}} a^k_{m^k_n} \log\left(1+\frac{p^k_{m^k_n} H^k_{m^k_n}}{a^k_{m^k_n}}\right) \tag{5.6}$$

subject to the constraints in (5.2)*, where $m^k_n \triangleq \arg\max_{m\in\mathcal{M}_n}\{H^k_m\}$ for each $k \in \mathcal{K}$. Thus the optimal energy-bandwidth allocation can be efficiently solved by the algorithms in Chapter 4.*

Proof. The first-order condition is necessary for optimality, which can be written as

$$\frac{H^k_m}{1+p^k_m H^k_m/a^k_m} = \frac{v^k_n - u^k_n + \xi^k_n}{W_m},\ m \in \mathcal{M}_n\ , \tag{5.7}$$

with
$$u^k_n \triangleq \sum_{\kappa=k}^{K} \mu^\kappa_n\ ,$$

$$v^k_n \triangleq \sum_{\kappa=k}^{K} \lambda^\kappa_n. \tag{5.8}$$

By setting $W_m = 1$, we then have

$$p^k_m = a^k_m \left[\frac{1}{v^k_n - u^k_n + \xi^k_n} - \frac{1}{H^k_m}\right]^+\ . \tag{5.9}$$

When $\sum_{m\in\mathcal{M}} p^k_m > 0$ and $\epsilon = 0$, the optimal bandwidth allocation is given as [53]

$$a^k_m = \frac{p^k_m H^k_m}{\sum_{j\in\mathcal{M}} p^k_j H^k_j},\ m \in \mathcal{M}\ . \tag{5.10}$$

Then, for any transmitter n such that $\sum_{m\in\mathcal{M}_n} p^k_m > 0$ and denoting $\Delta \triangleq \sum_{m\in\mathcal{M}_n} a^k_m$, we further have

$$a^k_m = \frac{p^k_m H^k_m \Delta}{\sum_{j\in\mathcal{M}_n} p^k_j H^k_j},\ m \in \mathcal{M}_n \subseteq \mathcal{M}\ . \tag{5.11}$$

Substituting (5.11) into (5.9), we then have

$$p^k_m = \frac{p^k_m H^k_m}{\sum_{j\in\mathcal{M}} p^k_j H^k_j}\left[\frac{1}{v^k_n - u^k_n + \xi^k_n} - \frac{1}{H^k_m}\right]^+ \Delta,\ m \in \mathcal{M}_n\ . \tag{5.12}$$

Replacing p_j^k in (5.12) by (5.9), we have

$$p_m^k = p_m^k \frac{\left[\frac{1}{v_n^k - u_n^k + \xi_n^k} - \frac{1}{H_m^k}\right]^+ H_m^k \Delta}{a_m^k \left[\frac{1}{v_n^k - u_n^k + \xi_n^k} - \frac{1}{H_m^k}\right]^+ H_m^k + \sum_{j \in \mathcal{M}_n, j \neq m} a_j^k \left[\frac{1}{v_n^k - u_n^k + \xi_n^k} - \frac{1}{H_j^k}\right]^+ H_j^k} \ . \tag{5.13}$$

When $p_m^k > 0$, $\left[\frac{1}{v_n^k - u_n^k + \xi_n^k} - \frac{1}{H_m^k}\right]^+ > 0$ and (5.13) can be further written as

$$1 = \frac{\Delta}{a_m^k + \left(\sum_{j \in \mathcal{M}_n, j \neq m} a_j^k \left[\frac{1}{v_n^k - u_n^k + \xi_n^k} - \frac{1}{H_j^k}\right]^+ H_j^k\right) / \left(\left[\frac{1}{v_n^k - u_n^k + \xi_n^k} - \frac{1}{H_m^k}\right]^+ H_m^k\right)} \ , \tag{5.14}$$

$$\Rightarrow \quad \Delta = a_m^k + \sum_{j \in \mathcal{M}_n, j \neq m} a_j^k \left(\frac{\left[1/(v_n^k - u_n^k + \xi_n^k) - 1/H_j^k\right]^+}{[1/(v_n^k - u_n^k + \xi_n^k) - 1/H_m^k]^+} \frac{H_j^k}{H_m^k} \right) \ . \tag{5.15}$$

Moreover, according to the definition of Δ, we also have

$$a_m^k + \sum_{j \in \mathcal{M}_n, j \neq m} a_j^k \cdot 1 = \Delta \ . \tag{5.16}$$

Denoting $m_n^k \triangleq \max_{m \in \mathcal{M}_n} \left\{H_m^k\right\}$, by (5.9) and (5.11), we have $p_{m_n^k}^k > 0$ when $\sum_{m \in \mathcal{M}_n} p_m^k > 0$. Note that, since

$$\frac{\left[1/(v_n^k - u_n^k + \xi_n^k) - 1/H_j^k\right]^+}{\left[1/(v_n^k - u_n^k + \xi_n^k) - 1/H_{m_n^k}^k\right]^+} \cdot \frac{H_j^k}{H_{m_n^k}^k} \leq 1 \tag{5.17}$$

for all $j \in \{m \in \mathcal{M}_n \mid m \neq m_n^k\}$, we must have $a_j^k = 0$ for all $j \in \{m \in \mathcal{M}_n \mid m \neq m_n^k\}$ so that (5.15) and (5.16) are both satisfied.

Therefore, when $\sum_{m \in \mathcal{M}_n} p_m^k > 0$, we must have $p_{m_n^k}^k > 0$ and $p_j^k = 0$ for $\{\forall j \in \mathcal{M}_n \mid j \neq m_n^k\}$. On the other hand, when $\sum_{m \in \mathcal{M}_n} p_m^k = 0$, we have $p_m^k = 0$ for all $m \in \mathcal{M}_n$ given n and k thus the achievable rate is zero no matter which channel is selected. □

5.1.2 Optimal Algorithms for Solving Subproblems

For the general weighted sum-rate problem, the iterative algorithm developed in Chapter 4 decomposes $\mathsf{P}_{\mathcal{W}}(\epsilon)$ as follows.

- Given the bandwidth allocation $\mathcal{A}_n \triangleq \{a_m^k, \forall m \in \mathcal{M}_n, k \in \mathcal{K}\}$, for each $n \in \mathcal{N}$, obtain the energy allocation $\boldsymbol{p}_m \triangleq [p_m^1, p_m^2, \ldots, p_m^K]$ by solving the following subproblem:

$$\mathsf{EP}_n(\mathcal{A}_n, \mathcal{W}): \quad \max_{\boldsymbol{p}_m, m \in \mathcal{M}_n} \sum_{m \in \mathcal{M}_n} W_m \sum_{k=1}^{K} a_m^k \log(1 + \frac{p_m^k H_m^k}{a_m^k}) \tag{5.18}$$

subject to

$$\begin{cases} \tilde{E}_n^k - B_n^{\max} \le \sum_{\kappa=1}^{k} \sum_{m\in\mathcal{M}_n} p_m^\kappa \le \tilde{E}_n^k \\ \sum_{m\in\mathcal{M}_n} p_m^k \le P_n \\ p_m^k \ge 0,\ m \in \mathcal{M}_n \end{cases}, \ k \in \mathcal{K}\ . \tag{5.19}$$

- Given the energy allocation $\mathcal{P}_k \triangleq \{p_m^k, \forall m \in \mathcal{M}\}$, for each $k \in \mathcal{K}$, obtain the bandwidth allocation $\boldsymbol{a}^k \triangleq [a_1^k, a_2^k, \ldots, a_M^k]$ by solving the following subproblem:

$$\mathsf{BP}_k(\mathcal{P}_k, \epsilon, \mathcal{W}): \quad \max_{\boldsymbol{a}^k} \sum_{m=1}^{M} W_m a_m^k \log(1 + \frac{p_m^k H_m^k}{a_m^k}) \tag{5.20}$$

subject to

$$\begin{cases} \sum_{i=1}^{M} a_i^k = 1 \\ a_m^k \ge \epsilon,\ m \in \mathcal{M} \end{cases}. \tag{5.21}$$

In Chapter 4, algorithms for solving the above two subproblems are obtained for the special case of point-to-point channels and equal weights. We now develop algorithms for the general case.

5.1.2.1 Solving the Bandwidth Allocation Subproblem

Based on the Lagrangian function defined in (5.5), the first-order condition and the complementary slackness of the bandwidth allocation problem can be written as

$$\log(1 + \frac{p_m^k H_m^k}{a_m^k}) - \frac{p_m^k H_m^k}{a_m^k + p_m^k H_m^k} = \frac{(\alpha^k - \beta_m^k)}{W_m}\ , \tag{5.22}$$

$$\alpha^k(\sum_m a_m^k - 1) = 0, \tag{5.23}$$

$$\beta_m^k(a_m^k - \epsilon) = 0, \tag{5.24}$$

which along with the constraints in (5.21) constitute the K.K.T. conditions of $\mathsf{BP}_k(\mathcal{P}_k, \epsilon, \mathcal{W})$. Since $\mathsf{BP}_k(\mathcal{P}_k, \epsilon, \mathcal{W})$ is a convex optimization problem with linear constraints, its K.K.T. conditions are sufficient and necessary for optimality when $\epsilon > 0$ [68].

Denote $x_m^k = X_m(\alpha^k, \beta_m)$ as the solution to

$$x_m^k - \log(x_m^k) = (\alpha^k - \beta_m^k)/W_m + 1\ , 0 < x_m < 1. \tag{5.25}$$

Note that, for $x \in (0,1)$, $x - \log(x) \in (1, \infty)$. Then, $x_m^k \in (0,1)$ exists when $\alpha^k - \beta_m^k \ge 0$ and the bandwidth allocation given by

$$a_m^k = p_m^k H_m^k \frac{X_m(\alpha^k, \beta_m^k)}{1 - X_m(\alpha^k, \beta_m^k)},\ (0 < X_m(\alpha^k, \beta_m^k) < 1) \tag{5.26}$$

for $p_m^k > 0$ satisfies the first-order condition in (5.22).

When $p_m^k = 0$, we have $\alpha^k = \beta_m^k \geq 0$ by (5.22). If $\alpha^k = \beta_m^k > 0$, we have $a_m^k = \epsilon$ by (5.24). Otherwise, we can set $a_m^k = \epsilon$ and the K.K.T. conditions still hold. Thus the minimal bandwidth should be assigned to the receiver with zero transmission energy.

We note that, if there exists an m such that $p_m^k > 0$, the left-hand-side of (5.22) is greater than 0 and thus $\alpha^k > 0$. Then, by (5.23), $\sum_m a_m^k = 1$ must hold. Assigning the minimal bandwidth to the receiver with zero transmission energy and substituting (5.26), we further have

$$\sum_{m \in \mathcal{Z}_0^c} p_m^k H_m^k \frac{X_m(\alpha^k, \beta_m)}{1 - X_m(\alpha, \beta_m)} + |\mathcal{Z}_0|\epsilon = 1 \ , \tag{5.27}$$

where $\mathcal{Z}_0 \triangleq \{m \mid p_m^k = 0\} = \{m \mid p_m^k = 0, a_m^k = \epsilon\}$ and $\mathcal{Z}_0^c$ is the complementary set of $\mathcal{Z}_0$. Moreover, by (5.24), we know that $\beta_m^k = 0$ when $a_m^k > \epsilon$. Then, (5.27) can be further written as

$$\sum_{m \in \mathcal{Z}_1^c \cap \mathcal{Z}_0^c} p_m^k H_m^k \frac{X_m(\alpha^k, 0)}{1 - X_m(\alpha^k, 0)} + |\mathcal{Z}_1|\epsilon = 1 - |\mathcal{Z}_0|\epsilon \ , \tag{5.28}$$

where $\mathcal{Z}_1 \triangleq \{m \mid p_m^k > 0, \beta_m^k > 0\}$.

Note that, for any $m \in \mathcal{Z}_1$, we have

$$a_m^k = p_m^k H_m^k \frac{X_m(\alpha^k, \beta_m^k)}{1 - X_m(\alpha^k, \beta_m^k)} = \epsilon, \ (\beta_m^k > 0) \ . \tag{5.29}$$

According to (5.25), since $X_m(\alpha, \beta)$ is decreasing with respect to α and increasing with respect to $\beta \geq 0$ when $X_m(\alpha, 0) \in (0, 1)$, then so does $\frac{X_m(\alpha,\beta)}{1 - X_m(\alpha,\beta)}$. Hence, we further have

$$p_m^k H_m^k \frac{X_m(\alpha^k, 0)}{1 - X_m(\alpha^k, 0)} \leq p_m^k H_m^k \frac{X_m(\alpha^k, \beta_m^k)}{1 - X_m^k(\alpha^k, \beta_m^k)} = \epsilon, \ m \in \mathcal{Z}_1 \ . \tag{5.30}$$

Therefore, (5.28) can be written as

$$\sum_{m \in \mathcal{Z}_0^c} \max\left\{\epsilon, p_m^k H_m^k \frac{X_m(\alpha^k, 0)}{1 - X_m(\alpha^k, 0)}\right\} = 1 - |\mathcal{Z}_0|\epsilon \ . \tag{5.31}$$

Theorem 5.2. *Suppose that α^k is the solution to* (5.31)*. Then, the optimal bandwidth allocation for $\mathsf{BP}_k(\mathcal{P}_k, \epsilon, \mathcal{W})$ is given by*

$$a_m^k = \begin{cases} \epsilon, & \text{if } p_m^k = 0 \\ \max\left\{\epsilon, p_m^k H_m^k \frac{X_m(\alpha^k, 0)}{1 - X_m(\alpha^k, 0)}\right\}, & \text{if } p_m^k > 0 \end{cases} \ . \tag{5.32}$$

Proof. The first term in (5.32) follows since the minimal bandwidth should be allocated to the receiver with zero transmission energy. Also, by (5.30) and (5.26) we have the second term in (5.32). Moreover, when α^k satisfies (5.31), all K.K.T. conditions of the bandwidth allocation problem are satisfied therefore the optimal bandwidth allocation is obtained. □

Denote

$$G(\alpha) \triangleq \sum_{m\in\mathcal{Z}_0^c} \max\left\{\epsilon, p_m^k H_m^k \frac{X_m(\alpha^k,0)}{1-X_m(\alpha^k,0)}\right\} . \tag{5.33}$$

We note that $X_m(\alpha^k,0) \in (0,1)$ is continuous and decreasing with respect to α^k, then so does $\frac{X_m(\alpha^k,0)}{1-X_m(\alpha^k,0)}$. Since $p_m^k H_m^k$ is constant, we have that $G(\alpha^k) \in (0,+\infty)$ is also continuous and decreasing with respect to α^k. Then, we may use the bisection method [76] to find out α^k such that $G(\alpha^k) = 1 - |\mathcal{Z}_0|\epsilon$ and the optimal bandwidth allocation can be obtained by (5.32).

The procedure for solving the bandwidth allocation is summarized as follows.

Algorithm 5.1 - Solving bandwidth allocation subproblem $\mathsf{BP}_k(\mathcal{P}_k, \epsilon, \mathcal{W})$

1: Initialization

Specify initial $\alpha_u > \alpha_l > 0$ ($G(\alpha_u) < 1 - |\mathcal{Z}_0|\epsilon < G(\alpha_l)$) and error tolerance $\delta > 0$

2: **REPEAT**

$\alpha \leftarrow (\alpha_u + \alpha_l)/2$

FOR all $m \in \mathcal{M}$

Calculate $X_m(\alpha, 0)$ by solving (5.25) with $\beta = 0$

ENDFOR

Evaluate $G(\alpha)$ using $\{X_m(\alpha,0), m \in \mathcal{M}\}$

IF $|G(\alpha) - 1 + |\mathcal{Z}_0|| < \delta$ **THEN** Goto step 3 **ENDIF**

IF $G(\alpha) > 1 - |\mathcal{Z}_0|\epsilon$ **THEN** $\alpha_l \leftarrow \alpha$ **ELSE** $\alpha_h \leftarrow \alpha$ **ENDIF**

3: **FOR** all $m \in \mathcal{M}$

Calculate a_m^k by (5.32)

ENDFOR

Since we need to solve for $X_m(\alpha, 0)$ from (5.25) repeatedly, we can pre-compute the solutions to $y = x - \log(x),\ x \in (0,1)$ and store them in a look-up table. Then the overall complexity of Algorithm 5.1 is $\mathcal{O}(M)$ for solving $\mathsf{BP}_k(\mathcal{P}_k, \epsilon, \mathcal{W})$.

Remark 5.1. *In Chapter 4, we focused on the special case of equal weights, where the optimal bandwidth allocation can be directly obtained by the iterative bandwidth fitting algorithm (Algo-*

rithm 4.3) without solving the dual variable α^k and calculating the intermediate variable $X_m(\alpha^k, 0)$. However, for the general weighted case, we need to solve the equation group consisting of (5.25) *for all $m \in \mathcal{M}$ and* (5.31) *to obtain the dual variable α^k and then calculate the optimal bandwidth allocation given by* (5.32).

5.1.2.2 Solving the Energy Allocation Subproblem

$\mathsf{EP}_n(\mathcal{A}_n, \mathcal{W})$ is a convex optimization problem with linear constraints thus its K.K.T. conditions are necessary and sufficient for optimality [68]. Using the Lagrangian function defined in (5.5), in addition to the first-order condition and the feasibility constraints, the complementary slackness can be written as

$$\lambda^k(\sum_{\kappa=1}^{k}\sum_{m\in\mathcal{M}_n} p_m^\kappa - E^k) = 0, \tag{5.34}$$

$$\mu_n^k(\sum_{\kappa=1}^{k}\sum_{m\in\mathcal{M}_n} p_m^\kappa - E^k + B^{\max}) = 0, \tag{5.35}$$

$$\xi_n^k(\sum_{m\in\mathcal{M}_n} p_m^k - P_n) = 0 \tag{5.36}$$

constituting the K.K.T. conditions.

Taking the derivative of (5.4) on p_m^k and using the first-order condition, we have

$$p_m^k = a_m^k \left[\frac{W_m}{v_n^k - u_n^k + \xi_n^k} - \frac{1}{H_m^k}\right]^+ . \tag{5.37}$$

By (5.36), when $\sum_{m\in\mathcal{M}_n} p_m^k = P_n$, we have $\xi_n^k \geq 0$ and otherwise $\xi_n^k = 0$. Then, we have

$$p_m^k = a_m^k \left[\frac{W_m}{v_n^k - u_n^k} - \frac{1}{H_m^k}\right]^+ \tag{5.38}$$

when $\sum_{m\in\mathcal{M}_n} a_m^k \left[\frac{W_m}{v_n^k - u_n^k} - \frac{1}{H_m^k}\right]^+ < P_n$. Otherwise, since the constraint requires $\sum_{m\in\mathcal{M}_n} p_m^k \leq P_n$, given v_n^k and u_n^k, we can determine $\bar{\xi}_n^k \geq 0$ such that

$$\sum_{m\in\mathcal{M}_n} a_m^k \left[\frac{W_m}{v_n^k - u_n^k} - \frac{1}{H_m^k}\right]^+ \geq \sum_{m\in\mathcal{M}_n} a_m^k \left[\frac{W_m}{v_n^k - u_n^k + \bar{\xi}_n^k} - \frac{1}{H_m^k}\right]^+ = P_n . \tag{5.39}$$

Then we can treat

$$\bar{P}_m^k \triangleq a_m^k \left[\frac{W_m}{v_n^k - u_n^k + \bar{\xi}_n^k} - \frac{1}{H_m^k}\right]^+ \tag{5.40}$$

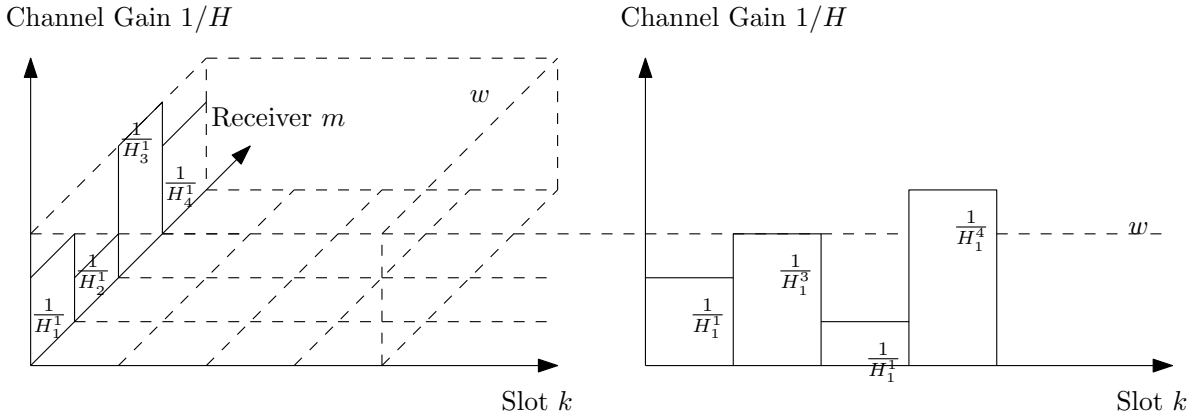

Figure 5.1: Two-dimensional water-filling. The "water" (energy) is filled over both the receiver-axis (left) and time-axis (right) with the same water level w as interpreted in (5.41)-(5.42).

as the maximum transmission energy for each receiver and thus the optimal energy allocation is

$$p_m^k = \min\left\{\bar{P}_m^k, a_m^k\left[W_m w_n^k - \frac{1}{H_m^k}\right]^+\right\}, \tag{5.41}$$

where $w_n^k \triangleq 1/(v_n^k - u_n^k)$.

We note that, p_m^k in (5.41) is a function of w_n^k. Then, using the same analysis in Chapter 4, we have the following proposition:

Proposition 5.1. *Given any bandwidth allocation $\mathcal{A}_n$, p_m^k is the optimal energy allocation for $\mathsf{EP}_n(\mathcal{A}_n, \mathcal{W})$, if and only if, the feasible allocation p_m^k follows the generalized two-dimensional water-filling formula in* (5.41)*, where the water level w_n^k may only increase at BDP such that $B_n^k = 0$ and only decrease at BFP such that $B_n^k = B_n^{\max}$.*

We note that, in the orthogonal broadcast channel, each transmitter communicates with multiple receivers and the transmitted energy is drawn from the same battery. Then, according to (5.41), the water (energy) is not only filled along the time axis but also along the receiver index axis, as shown in Fig. 5.1. In other words, given two adjacent BDP/BFPs (a, the type of a) and (b, the type of b) where $a \leq b$, the energy allocation p_m^k can be calculated by (5.41) with the same water level $w_n^k = w^{ab}$ for all receiver $m \in \mathcal{M}_n$ and slot $k \in [a+1, b]$. Then, the water level w^{ab} should be determined by

$$\sum_{k=a+1}^{b}\sum_{m=1}^{M} p_m^k(w^{ab}) = E^b - E^a + \left(\mathbb{I}(a \text{ is BFP}) - \mathbb{I}(a \text{ is BDP})\right) B_n^{\max} \tag{5.42}$$

where $\mathbb{I}(\cdot)$ is an indicator function and $p_m^k(w^{ab})$ is calculated by (5.41) with $w_n^k = w^{ab}$ for $k \in [a+1, b]$.

In [69], a single-user dynamic water-filling algorithm is proposed to find the BDP/BFP set by recursively performing the "forward search" and "backward search" operations with conventional water-filling. Since here the increase/decrease of the water level also occurs at BDP/BFPs, replacing the conventional water-filling used in [69] by the two-dimensional water-filling in (5.41)-(5.42), we can obtain the BDP/BFP set for optimal energy allocation in multiple orthogonal broadcast channels. We name this algorithm as the *two-dimensional dynamic water-filling algorithm*. Moreover, after obtaining the optimal BDP/BFP set, the optimal energy allocation can be further calculated by (5.41)-(5.42).

Remark 5.2. *We note that, with equal weights, by Theorem 5.1, the energy-bandwidth allocation problem for multiple orthogonal broadcast channels is equivalent to that for multiple point-to-point channels treated in Chapter 4. Although the general algorithms developed in this section can obtain the optimal energy-bandwidth allocation for the equal weight case, solving the problem by using Theorem 5.1 along with the algorithms in Chapter 4 has a lower computational complexity. Specifically, for the general case, the energy allocation subproblem* $\mathsf{EP}_n(\mathcal{A}_n, \mathcal{W})$ *contains* $\mathcal{O}(|\mathcal{M}_n|K)$ *variables and the bandwidth allocation subproblem* $\mathsf{BP}_k(\mathcal{P}_k, \epsilon, \mathcal{W})$ *contains* $\mathcal{O}(M)$ *variables, whereas the corresponding subproblems in Chapter 4 contain only* $\mathcal{O}(K)$ *and* $\mathcal{O}(N)$ *variables, respectively. Also, the iterative bandwidth fitting algorithm in Chapter 4 does not require the calculation of the dual variable* α^k *and the intermediate variables* $X_m(\alpha^k, 0)$*, providing better computational efficiency.*

5.2 Multiple Non-Orthogonal Broadcast Channels

5.2.1 Problem Formulation

We consider a system with multiple non-orthogonal broadcast channels, where each transmitter communicates with all its receivers on the same (assigned) frequency band at the same time. Denoting X_{mki} as the symbol sent for receiver m at instant i in slot k, the signal received at receiver m is $Y_{mki} = h_{mk}X_{mki} + \left(h_{mk}\sum_{m_0 \neq m} X_{m_0ki} + Z_{mki}\right)$, where h_{mk} represents the complex channel gain for receiver m in slot k and $Z_{mki} \sim \mathsf{CN}(0,1)$ is the i.i.d. complex Gaussian noise. We note that, $\sum_{m_0 \neq m} X_{m_0ki}$ represents the interference and is treated as noise by receiver m.

Moreover, we denote the channel gain and the energy consumption in each slot k as $H_m^k \triangleq |h_{mk}|^2$ and $p_m^k \triangleq \frac{1}{T_c}\sum_i |X_{mki}|^2$, respectively.

We denote $\tilde{a}_n^k$ as the amount of bandwidth used by transmitter n. Then, we use the upper bound of the achievable rate over a weighted sum of the M receivers and K slots as the performance metric, given by [70]

$$\tilde{C}_{\mathcal{W}}(\mathcal{P},\tilde{\mathcal{A}}) \triangleq \sum_{n\in\mathcal{N}}\sum_{k\in\mathcal{K}} \tilde{a}_n^k \sum_{m\in\mathcal{M}_n} W_m \log\left(1+\frac{p_m^k H_m^k/\tilde{a}_n^k}{\sum_{m_0 \mid H_m^k<H_{m_0}^k} p_{m_0}^k H_m^k/\tilde{a}_n^k+1}\right) , \tag{5.43}$$

where $\tilde{\mathcal{A}} \triangleq \{\tilde{a}_n^k, \forall n\in\mathcal{N}, k\in\mathcal{K}\}$. Note that, the rate in each slot is achieved by decoding the messages in the order of the channel quality [77], i.e., we decode the message from a weaker channel prior to that from a stronger channel. Moreover, we assume no two channels have the same gain in the same slot.

We define the energy-bandwidth allocation problem in multiple non-orthogonal broadcast channels as follows:

$$\tilde{\mathsf{P}}_{\mathcal{W}}(\epsilon): \quad \max_{\mathcal{P},\tilde{\mathcal{A}}} \tilde{C}_{\mathcal{W}}(\mathcal{P},\tilde{\mathcal{A}}) \tag{5.44}$$

subject to (5.2), where $\sum_{m\in\mathcal{M}} a_m^k = 1$ and $a_m^k \geq \epsilon$ is replaced by $\sum_n \tilde{a}_n^k = 1$ and $\tilde{a}_n^k \geq \epsilon$, respectively.

We note that, the above problem is non-convex due to the non-convexity of the objective function. To obtain the energy-bandwidth allocation, we first define $\tilde{p}_n^k \triangleq \sum_{m\in\mathcal{M}_n} p_m^k$ for all $n\in\mathcal{N}$ and rewrite (5.44) as

$$\max_{\tilde{p}_n^k,\tilde{a}_n^k}\left\{\sum_n\sum_k \max_{\sum_{m\in\mathcal{M}_n} p_m^k=\tilde{p}_n^k}\left\{\tilde{a}_n^k \sum_{m\in\mathcal{M}_n} W_m\log\left(1+\frac{p_m^k H_m^k/\tilde{a}_n^k}{\sum_{m_0 \mid H_m^k<H_{m_0}^k} p_{m_0}^k H_m^k/\tilde{a}_n^k+1}\right)\right\}\right\} . \tag{5.45}$$

Denoting

$$F_n^k(p) \triangleq \max_{\pi_m:\sum_{m\in\mathcal{M}_n}\pi_m=1,\pi_m\geq 0} \sum_{m\in\mathcal{M}_n} W_m\log\left(1+\frac{\pi_m p H_m^k}{\left(\sum_{m_0 \mid H_m<H_{m_0}}\pi_m\right)pH_m^k+1}\right) , \tag{5.46}$$

we further write (5.45) as

$$\max_{\mathcal{P},\tilde{\mathcal{A}}} \tilde{C}_{\mathcal{W}}(\mathcal{P},\tilde{\mathcal{A}}) = \max_{\tilde{p}_n^k,\tilde{a}_n^k} \sum_n\sum_k \tilde{a}_n^k F_n^k(\tilde{p}_n^k/\tilde{a}_n^k) , \tag{5.47}$$

where $\tilde{\mathcal{P}} \triangleq \{\tilde{p}_n^k, \forall n\in\mathcal{N}, k\in\mathcal{K}\}$ is the total energy allocation.

To solve $\tilde{\mathsf{P}}_{\mathcal{W}}(\epsilon)$, we first solve (5.47) to obtain the optimal bandwidth allocation $\tilde{\mathcal{A}}$ and the optimal total energy allocation $\tilde{\mathcal{P}}$. Then, given the total energy allocation $\tilde{\mathcal{P}}$, we further optimally split the total energy for each receiver by solving (5.46).

The optimal solution to (5.46) is given in [73], which is summarized in the following Lemma:

Lemma 5.1. *For any (n,k), we have a set of energy cut-off lines $\{L_m^k, \forall m \in \mathcal{M}_n\}$ sorting in ascending order such that $L_a^k \leq L_b^k$ if $H_a^k > H_b^k$ for all $a,b \in \mathcal{M}_n$. For any $a \in \mathcal{M}_n$, the optimal energy splitting is*

$$p_a^k = \begin{cases} L_b^k - L_a^k, & \text{if } L_b^k < \tilde{p}_n^k \\ \tilde{p}_n^k - L_b^k, & \text{if } L_a^k \leq \tilde{p}_n^k \leq L_b^k \\ 0 & \text{if } \tilde{p}_n^k < L_a^k \end{cases}, \tag{5.48}$$

where $L_a^k \leq L_b^k$ are two adjacent cut-off lines.

The procedure for computing $\{L_m^k, \forall m \in \mathcal{M}_n\}$ is also given in [73].

5.2.2 Solving the Problem in (5.47)

The convexity of $F_n^k(p)$ has been shown in [73], given by the following lemma:

Lemma 5.2. *$F_n^k(p)$ is strictly concave with respect to p, whose first-order derivative is continuous.*

Then, the problem in (5.47) is still an energy-bandwidth allocation problem with the rate function defined in (5.46), which is increasing and jointly concave with respect to the total energy and bandwidth allocations. Note that the problem in (5.47) and the problem in (4.8)-(4.9) have the same feasible domain and the corresponding optimal energy allocations both follow the water-filling formula (will be shown later in this section). Then, it is easy to verify that the optimal energy discharge given by (4.10) and the iterative algorithm (Algorithm 4.1) can also give the optimal solution to the problem in (5.47).

Hence we focus on the energy and bandwidth allocation subproblems as follows:

- Energy allocation subproblem: Denote $\tilde{\mathcal{A}}_n \triangleq \{\tilde{a}_n^k, k \in \mathcal{K}\}$,

$$\tilde{\mathsf{EP}}_n(\tilde{\mathcal{A}}_n, \mathcal{W}): \quad \max_{\tilde{p}_n^k} \sum_n \sum_k \tilde{a}_n^k F_n^k(\tilde{p}_n^k/\tilde{a}_n^k), \tag{5.49}$$

$$\text{subject to } \begin{cases} \tilde{E}_n^k - B_n^{\max} \leq \sum_{\kappa=1}^k \tilde{p}_n^\kappa \leq \tilde{E}_n^k \\ 0 \leq \tilde{p}_n^k \leq P_n \end{cases}, \ k \in \mathcal{K}. \tag{5.50}$$

- Bandwidth allocation subproblem: Denote $\tilde{\mathcal{P}}_k \triangleq \{\tilde{p}_n^k, n \in \mathcal{N}\}$,

$$\tilde{\mathsf{BP}}_k(\tilde{\mathcal{P}}_k, \epsilon, \mathcal{W}): \quad \max_{\tilde{a}_n^k} \sum_n \sum_k \tilde{a}_n^k F_n^k(\tilde{p}_n^k/\tilde{a}_n^k) \ , \tag{5.51}$$

subject to

$$\text{subject to } \begin{cases} \sum_{n=1}^N \tilde{a}_n^k \leq 1 \\ \tilde{a}_n^k \geq \epsilon \end{cases} , \ n \in \mathcal{N}. \tag{5.52}$$

Using the Lagrangian multiplier defined in (5.4), we first write the Lagrangian function for the problem in (5.47) as

$$\mathcal{L}_N \triangleq \sum_n \sum_k \tilde{a}_n^k F_n^k(\tilde{p}_n^k/\tilde{a}_n^k) + \mathcal{M}(\tilde{\mathcal{P}}, \tilde{\mathcal{A}}) \ . \tag{5.53}$$

5.2.2.1 Solving the Energy Allocation Subproblem

Since $\tilde{\mathsf{EP}}_n(\tilde{\mathcal{A}}_n, \mathcal{W})$ is a convex optimization problem with linear constraints, its K.K.T. conditions are sufficient and necessary for optimality when $\epsilon > 0$ [68]. With $\mathcal{L}_N$ defined in (5.53), we can write the first-order condition for the non-orthogonal broadcast channel as

$$\partial\left(\tilde{a}_n^k F_n^k(\tilde{p}_n^k/\tilde{a}_n^k)\right)/\partial \tilde{p}_n^k \triangleq (F_n^k)'(\tilde{p}_n^k/\tilde{a}_n^k) = v_n^k - u_n^k \tag{5.54}$$

where v_n^k and u_n^k are defined in (5.8), and $(F_n^k)'(p)$ denotes the first-order derivative of $F_n^k(p)$. For all $p \geq 0$, we further derive the derivative of $F_n^k(p)$ in closed-form:

Proposition 5.2. *For any $p \geq 0$, the derivative of $F_n^k(p)$ is*

$$(F_n^k)'(p) = \max_{m \in \mathcal{M}_n} \left\{ \frac{W_m}{p + 1/H_m^k} \right\} \ . \tag{5.55}$$

The proof of Proposition 5.2 is provided in Appendix 5.6.1.

Moreover, we note that $(F_n^k)'(\tilde{p}_n^k/\tilde{a}_n^k)$ is strictly decreasing with respect to $\tilde{p}_n^k$ due to the strict concavity of $F_n^k(p)$. Then using (5.54) and Proposition 5.2, $\tilde{p}_n^k$ can be uniquely determined as follows

$$\tilde{p}_n^k = \tilde{a}_n^k \left((F_n^k)'\right)^{-1}(1/w_n^k) \tag{5.56}$$

$$= \min\left\{ P_n, \tilde{a}_n^k \max_{m \in \mathcal{M}_n} \left\{ \left[W_m w_n^k - \frac{1}{H_m^k} \right]^+ \right\} \right\} \tag{5.57}$$

where $w_n^k = 1/(v_n^k - u_n^k)$ and $(\cdot)^{-1}$ denotes the inverse function.

We note that, since $\mathsf{P}_{\mathcal{W}}(\epsilon)$ and $\tilde{\mathsf{P}}_{\mathcal{W}}(\epsilon)$ have the same Lagrangian multipliers, by analyzing the K.K.T. conditions and using Proposition 5.2, it is easy to verify that the changes of w_n^k still follows Proposition 5.1, i.e., it may only increase/decrease at the BDP/BFP. Then, we treat (5.57) as a water-filling formula and the water level is determined by

$$\sum_{k=a+1}^{b} \tilde{p}_n^k(w^{ab}) = E^b - E^a + \left(\mathbb{I}(a \text{ is BFP}) - \mathbb{I}(a \text{ is BDP})\right) B_n^{\max} \tag{5.58}$$

where $\tilde{p}_n^k(w^{ab})$ is calculated by (5.57) with $w_n^k = w^{ab}$ for $k \in [a+1, b]$.

As for the energy allocation problem in multiple orthogonal broadcast channels, since here the water level change also occurs at BDP/BFPs, we can use the water-filling in (5.57)-(5.58) to replace the conventional water-filling operation in [69, Algorithm 5.2], and then the BDP/BFP set can be obtained. After obtaining the BDP/BFP set, using (5.57)-(5.58), we obtain the optimal total energy allocation.

5.2.2.2 Solving the Bandwidth Allocation Subproblem

When $\sum_{n\in\mathcal{N}} \tilde{p}_n^k = 0$, the sum-rate in slot k is zero. Thus, in this subsection we focus on the case $\sum_{n\in\mathcal{N}} \tilde{p}_n^k > 0$.

Since $\tilde{\mathsf{BP}}_k(\tilde{\mathcal{P}}_k, \epsilon, \mathcal{W})$ is a convex optimization problem with linear constraints, its K.K.T. conditions are sufficient and necessary for optimality when $\epsilon > 0$ [68]. The first-order condition can be written as

$$\frac{\partial\left(\tilde{a}_n^k F_n^k(\tilde{p}_n^k/\tilde{a}_n^k)\right)}{\partial \tilde{a}_n^k} = F_n^k(\tilde{p}_n^k/\tilde{a}_n^k) - (F_n^k)'(\tilde{p}_n^k/\tilde{a}_n^k)\tilde{p}_n^k/\tilde{a}_n^k = \alpha^k \ , \ n \in \mathcal{N}, k \in \mathcal{K} \ , \tag{5.59}$$

where the value of $F_n^k(\tilde{p}_n^k/\tilde{a}_n^k)$ can be calculated using the algorithm in [73]. Taking the constraints in (5.52) into account, $\tilde{a}_n^k$ must satisfy

$$\sum_{n=1}^{N} \max\{\tilde{a}_n^k, \epsilon\} = 1, \ k \in \mathcal{K} \ . \tag{5.60}$$

We note that, for each $k \in \mathcal{K}$, we have $N+1$ equations [(5.59) for all $n \in \mathcal{N}$ and (5.60)] and $N+1$ variables [$\tilde{a}_n^k$ for all $n \in \mathcal{N}$ and α^k]. Therefore, all the variables $\tilde{a}_n^k$ can be uniquely determined by solving the equation group given $k \in \mathcal{K}$.

Since $F_n^k(p)$ is concave by Lemma 5.2, $aF_n^k(p/a)$ is jointly concave with respect to p and a. Then, $\partial\left(aF_n^k(p/a)\right)/\partial a$ is non-increasing with respect to a given p. Also, the left-hand-side of (5.60) is

non-decreasing with respect to a. Therefore, given α^k, we can use the bisection method to find the corresponding $\tilde{a}_n^k(\alpha^k)$ in (5.59). Finally we can use the bisection method again to determine the proper α^k such that (5.60) is satisfied. The procedure for computing the bandwidth allocation is summarized as follows.

Algorithm 5.2 - Solving bandwidth allocation subproblem $\tilde{\mathsf{BP}}_k(\mathcal{P}_k, \epsilon, \mathcal{W})$

1: Initialization
Specify initial $\alpha_u^k > \alpha_l^k > 0$ such that $\sum_{n=1}^N \max\{\tilde{a}_n^k(\alpha_u^k), \epsilon\} < 1 < \sum_{n=1}^N \max\{\tilde{a}_n^k(\alpha_l^k), \epsilon\}$
Specify error tolerance $\delta > 0$
2: **REPEAT**
$\alpha \leftarrow (\alpha_u^k + \alpha_l^k)/2$
FOR all $n \in \mathcal{N}$
(*) Solve (5.59) to obtain $\tilde{a}_n^k(\alpha)$ using the bisection method
ENDFOR
IF $|\sum_{n=1}^N \max\{\tilde{a}_n^k(\alpha^k), \epsilon\} - 1| < \delta$ **THEN** Goto step 4 **ENDIF**
IF $\sum_{n=1}^N \max\{\tilde{a}_n^k(\alpha^k), \epsilon\} > 1$ **THEN** $\alpha_l^k \leftarrow \alpha$ **ELSE** $\alpha_h^k \leftarrow \alpha$ **ENDIF**
3: **FOR** all $n \in \mathcal{N}$
Calculate $\tilde{a}_n^k$ by (5.32)
ENDFOR

The complexity of Algorithm 5.2 is $\mathcal{O}(N)$.

Remark 5.3. *Comparing Algorithm 5.2 with Algorithm 5.1, the main difference lies in the step marked by "*", where the corresponding bandwidth allocations a_m^k and $\tilde{a}_n^k$ are calculated by solving the same equation [i.e.,* (5.25)*] in Algorithm 5.1 and multiple different equations [i.e.,* (5.59) *with different $F_n^k(\tilde{p}_n^k/\tilde{a}_n^k)$ for all $n \in \mathcal{N}$] in Algorithm 5.2.*

5.2.3 Special Case: Equal Weights

When $W_m = 1$ for all $m \in \mathcal{M}$, by Proposition 5.2, we have

$$(F_n^k)'(p) = \max_{m \in \mathcal{M}_n} \left\{ \frac{1}{p + 1/H_m^k} \right\} , \tag{5.61}$$

for all $p \geq 0$. Since, given any $a, b \in \mathcal{M}_n$ such that $H_a > H_b > 0$, we have $1/(p + 1/H_a) > 1/(p + 1/H_b)$ for all $p \geq 0$, then we have

$$(F_n^k)'(p) = \max_{m \in \mathcal{M}_n} \left\{ \frac{1}{p + 1/H_m^k} \right\} = \frac{1}{p + 1/\max_{m \in \mathcal{M}_n}\{H_m^k\}} \ . \tag{5.62}$$

Therefore, by (5.46), we must have

$$F_n^k(p) = \log(1 + pH_{m_n^k}^k) \tag{5.63}$$

where $m_n^k \triangleq \arg\max_{m \in \mathcal{M}_n}\{H_m^k\}$, i.e., each transmitter uses only the strongest channel to transmit in each slot. Then, we have the following corollary.

Corollary 5.1. *Theorem 5.1 also holds for the network with multiple non-orthogonal broadcast channels. Moreover, with equal weights, networks with multiple orthogonal and non-orthogonal broadcast channels achieve the same maximum throughput.*

Remark 5.4. *When the weights are equal, by Corollary 5.1, the energy-bandwidth allocation for multiple orthogonal broadcast channels is equivalent to that for multiple point-to-point channels treated in Chapter 4. Comparing to the algorithms in Chapter 4, the general algorithms in this section involve solving subproblems with more variables and constraints and the additional calculations of $F_n^k(p)$ and α. Thus we should use Corollary 5.1 along with the algorithms in Chapter 4 to solve the energy allocation problem when the weights are equal.*

5.2.4 Achievable Rate Regions

Denoting $C_{O,m}(\mathcal{P}, \mathcal{A})$ and $C_{N,m}(\mathcal{P}, \mathcal{A})$ as the sum-rate of receiver m achieved by the energy-bandwidth allocation $(\mathcal{P}, \mathcal{A})$ in K slots for multiple orthogonal and non-orthogonal broadcast channels, respectively. Then, the rate region can be defined as $\mathcal{R}_{(\cdot)} \triangleq \{(r_1, r_2, \ldots, r_M) \mid 0 \leq r_m \leq C_{(\cdot),m}(\mathcal{P}, \mathcal{A}),\ \mathcal{P}, \mathcal{A} \text{ are feasible}\}$, where $(r_1, r_2, \ldots, r_M)$ is the sum-rate vector for all receivers.

Lemma 5.3. *The rate region $\mathcal{R}_O$ is convex for the network with multiple orthogonal broadcast channels.*

Proof. Consider two sum-rate vectors $R^1, R^2 \in \mathcal{R}_O$ and the corresponding energy-bandwidth allocation as $(\mathcal{P}^1, \mathcal{A}^1)$ and $(\mathcal{P}^2, \mathcal{A}^2)$. Then, given any $\theta \in (0, 1)$ and $\bar{\theta} = 1 - \theta$, consider $R^3 = \theta R^1 + \bar{\theta} R^2$,

where $R^i \triangleq (r_1^i, r_2^i, \ldots, r_M^i)$. We note that, $C_{O,m}(\mathcal{P}, \mathcal{A})$ is sum of a series of log functions which are concave with respect to p_m^k and a_m^k. Then, for $m \in \mathcal{M}$, we have

$$r_m^3 = \theta r_m^1 + \bar{\theta} r_m^2 \tag{5.64}$$

$$\leq \theta C_{O,m}(\mathcal{P}^1, \mathcal{A}^1) + \bar{\theta} C_{O,m}(\mathcal{P}^2, \mathcal{A}^2) \tag{5.65}$$

$$\leq C_{O,m}(\theta \mathcal{P}^1 + \bar{\theta}\mathcal{P}^2, \theta \mathcal{A}^1 + \bar{\theta}\mathcal{A}^2) \tag{5.66}$$

where $\mathcal{P}^3 \triangleq \theta \mathcal{P}^1 + \bar{\theta}\mathcal{P}^2$ and $\mathcal{A}^3 \triangleq \theta \mathcal{A}^1 + \bar{\theta}\mathcal{A}^2$. Note that, since $\mathsf{P}_{\mathcal{W}}(\epsilon)$ is a convex optimization problem and its feasible domain is also convex, $(\mathcal{P}^3, \mathcal{A}^3)$ is a feasible energy-bandwidth allocation. Then, by definition we have $R^3 \in \mathcal{R}_O$ and thus $\mathcal{R}_O$ is a convex set. □

Moreover, for the network with multiple non-orthogonal broadcast channels, we define a convex region

$$\bar{\mathcal{R}}_N \triangleq \left\{ (r_1, r_2, \ldots, r_M) : r_m \leq \tilde{\mathsf{P}}_{\{W_m=1, W_i=0, \forall i \neq m\}}(0), \sum_m r_m \leq \tilde{\mathsf{P}}_{\{W_m=1, \forall m\}}(0) \right\} . \tag{5.67}$$

Note that for $\mathcal{W} = \{W_m = 1, W_i = 0, \forall i \neq m\}$, $\tilde{\mathsf{P}}_{\mathcal{W}}(0)$ and $\mathsf{P}_{\mathcal{W}}(0)$ maximize the sum-rate for the single receiver m and the two problems are the same. Then we have

$$\tilde{\mathsf{P}}_{\{W_m=1, W_i=0, \forall i \neq m\}}(0) = \mathsf{P}_{\{W_m=1, W_i=0, \forall i \neq m\}}(0) = \max_{\mathcal{P}, \mathcal{A} \text{ are feasible}} C_{(\cdot),m}(\mathcal{P}, \mathcal{A}),\ m \in \mathcal{M} . \tag{5.68}$$

For $W_m = 1, m \in \mathcal{M}$, by Theorem 5.1 and Corollary 5.1, $\tilde{\mathsf{P}}_{\{W_m=1, \forall m\}}(0)$ and $\mathsf{P}_{\{W_m=1, \forall m\}}(0)$ have the same solution, which can be denoted as $(\mathcal{P}^*, \mathcal{A}^*)$. For any $(r_1, r_2, \ldots, r_M) \in \mathcal{R}_N$, by definition, we have $r_m \leq \max_{\mathcal{P}, \mathcal{A} \text{ are feasible}} C_{N,m}(\mathcal{P}, \mathcal{A})$ and $\sum_m r_m \leq \sum_m C_{N,m}(\mathcal{P}^*, \mathcal{A}^*)$. Then, we have $\mathcal{R}_N \subseteq \bar{\mathcal{R}}_N$ and the sum-rate vectors $(C_{(\cdot),1}(\mathcal{P}^*, \mathcal{A}^*), C_{(\cdot),2}(\mathcal{P}^*, \mathcal{A}^*), \ldots, C_{(\cdot),M}(\mathcal{P}^*, \mathcal{A}^*))$ and $(\ldots, 0, \mathsf{P}_{\{W_m=1, W_i=0, \forall i \neq m\}}(0), 0, \ldots)$ for all $m \in \mathcal{M}$ can be achieved with both orthogonal and non-orthogonal broadcast.

We give an example for the network with one transmitter and two receivers. According to the above analysis, $\mathcal{R}_O$ and $\bar{\mathcal{R}}_N$ have three common points on the boundary as shown in Fig. 5.2: $(R_1, 0)$ for $\{W_{11} = 1, W_{12} = 0\}$, $(0, R_2)$ for $\{W_{11} = 0, W_{12} = 1\}$, and (R_1^*, R_2^*) for $\{W_{11} = W_{12} = 0.5\}$. Due to the concavity of $\mathcal{R}_O$ and $\bar{\mathcal{R}}_N$, the maximum improvement (Euclidean distance between boundary of $\mathcal{R}_O$ and $\bar{\mathcal{R}}_N$) of using the non-orthogonal broadcast channel is bounded by

$$\Delta = \max \left\{ \frac{(R_2 - R_2^*)(R_1^* + R_2^* - R_2)}{\sqrt{(R_2 - R_2^*)^2 + R_1^{*2}}}, \frac{(R_1 - R_1^*)(R_2^* + R_1^* - R_1)}{\sqrt{(R_1 - R_1^*)^2 + R_2^{*2}}} \right\} . \tag{5.69}$$

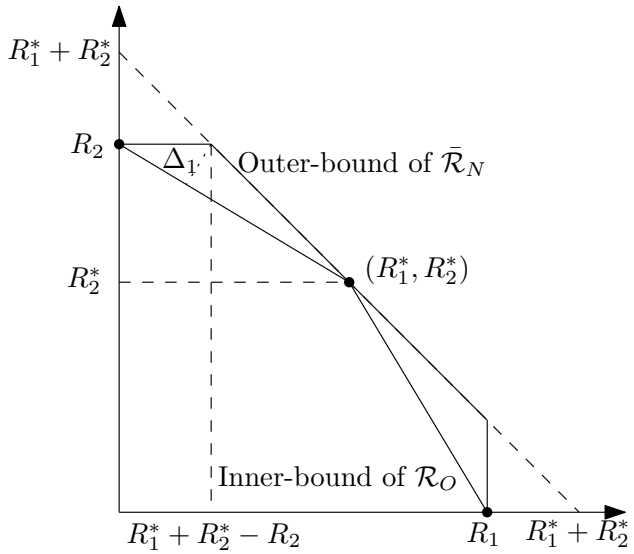

Figure 5.2: Rate regions of orthogonal and non-orthogonal broadcast channels.

5.3 Achieving Proportional Fairness in Orthogonal Broadcast Channels

In this section, we formulate a proportionally-fair (PF) throughput maximization problem for the network with multiple orthogonal broadcast channels, and show that it can be converted to a weighted throughput maximization problem with some proper weights.

5.3.1 PF Throughput Maximization

We consider the following utility function

$$U(\mathcal{P}, \mathcal{A}) \triangleq \sum_{m \in \mathcal{M}} \log \left(\sum_{k \in \mathcal{K}} a_m^k \log(1 + \frac{p_m^k H_m^k}{a_m^k}) \right) \tag{5.70}$$

Then, the PF throughput maximization problem is formulated as

$$\mathsf{F}_\epsilon : \quad \max_{\mathcal{P}, \mathcal{A}} U(\mathcal{P}, \mathcal{A}) \tag{5.71}$$

subject to the constraints in (5.2), whose solution is known to result in proportional fairness [52][75]. Without loss of generality, we assume $\tilde{E}_n^K > 0$ for all $n \in \mathcal{N}$ and thus each transmitter achieves a non-zero sum-rate to make the PF throughput lower bounded.

We next convert F_ϵ into a weighted throughput problem $\mathsf{P}_{\mathcal{W}}(\epsilon)$. Specifically, given $\mathcal{W}$, we denote $R_m(\mathcal{W})$ as the sum-rate achieved for receiver m by the optimal solution to $\mathsf{P}_{\mathcal{W}}(\epsilon)$; we also denote $\bar{R}_m$ as the sum-rate achieved for receiver m by the optimal solution to F_ϵ. We note that, since the rate region $\mathcal{R}_O$ is convex, $R_m(\mathcal{W})$, which is the tangent point of a hyperplane (defined by $\mathcal{W}$) to $\mathcal{R}_O$, is continuous in $\mathcal{W}$.

Theorem 5.3. *Given $\mathcal{W}$, the optimal solution to $\mathsf{P}_{\mathcal{W}}(\epsilon)$ is also optimal to F_ϵ, if and only if, there exists $\theta > 0$ such that $W_m R_m(\mathcal{W}) = \theta$ for all $m \in \mathcal{M}$, where $R_m(\mathcal{W})$ is the sum-rate achieved for receiver m by the optimal solution to $\mathsf{P}_{\mathcal{W}}(\epsilon)$.*

Proof. We note that $\mathsf{P}_{\mathcal{W}}(\epsilon)$ and F_ϵ have the same decision variables and the same constraints and they can use the same Lagrangian multiplier as defined in (5.4). Then, the Lagrangian functions for $\mathsf{P}_{\mathcal{W}}(\epsilon)$ and F_ϵ can be defined as (5.5) and

$$\mathcal{L}_F \triangleq \sum_{m\in\mathcal{M}} \log\left(\sum_{k\in\mathcal{K}} a_m^k \log(1+\frac{p_m^k H_m^k}{a_m^k})\right) + \mathcal{M}(\mathcal{P},\mathcal{A}), \tag{5.72}$$

respectively. Taking the first-order derivatives with respect to p_m^k, we have

$$\frac{\partial \mathcal{L}_P}{\partial p_m^k} = W_m \frac{\partial\left(a_m^k \log(1+\frac{p_m^k H_m^k}{a_m^k})\right)}{\partial p_m^k} + \frac{\partial \mathcal{M}}{\partial p_m^k}\ , \tag{5.73}$$

$$\frac{\partial \mathcal{L}_F}{\partial p_m^k} = \frac{1}{\bar{R}_m} \frac{\partial\left(a_m^k \log(1+\frac{p_m^k H_m^k}{a_m^k})\right)}{\partial p_m^k} + \frac{\partial \mathcal{M}}{\partial p_m^k}\ ; \tag{5.74}$$

also, we can obtain the derivative with respect to a_m^k in the same form as above. Note that, for $\mathsf{P}_{\mathcal{W}}(\epsilon)$ and F_ϵ, their K.K.T. conditions are sufficient and necessary for optimality when $\epsilon > 0$. Also, since $\bar{R}_m$ is the sum-rate achieved for receiver m by the optimal solution to F_ϵ and $R_m(\mathcal{W})$ is the sum-rate achieved by the optimal solution to $\mathsf{P}_{\mathcal{W}}(\epsilon)$, when $W_m = 1/R_m(\mathcal{W})$ for all $m \in \mathcal{M}$, the solution satisfies the K.K.T. conditions of F_ϵ also satisfies those of $\mathsf{P}_{\mathcal{W}}(\epsilon)$, and vice versa. Therefore, $\mathsf{P}_{\mathcal{W}}(\epsilon)$ and F_ϵ have the same optimal solution. Moreover, we note that scaling W_m by a positive factor θ does not affect the optimality of $\mathsf{P}_{\mathcal{W}}(\epsilon)$ and thus the above equivalence condition can be further relaxed to $W_m = \theta/R_m(\mathcal{W})$ where $\theta > 0$. Furthermore, since the objective functions of the two problems are both continuous, we can further extend the result to the case of $\epsilon = 0$. □

We call $\mathcal{W}$ the *PF weights* if $\mathsf{P}_{\mathcal{W}}(\epsilon)$ and F_ϵ have the same optimal solution.

5.3.2 Obtaining the PF Weights

To obtain the PF weights, we first define an optimization problem:

$$\min_{(\frac{1}{W_1},\frac{1}{W_2},\ldots,\frac{1}{W_M})\in\mathcal{R}_O} \max_{\mathcal{P},\mathcal{A}} \left\{ \sum_m W_m \left(\sum_k a_m^k \log(1+\frac{p_m^k H_m^k}{a_m^k}) - 1/W_m \right) \right\} \tag{5.75}$$

subject to

$$\begin{cases} \sum_k a_m^k \log(1+\frac{p_m^k H_m^k}{a_m^k}) \geq 1/W_m, \quad n\in\mathcal{N}, m\in\mathcal{M}_n \\ \text{Constraints in (5.2)} \end{cases} . \tag{5.76}$$

We note that, since $1/W_m$ is drawn from the rate region $\mathcal{R}_O$, the optimal value of (5.75) is zero, and $\sum_k a_m^k \log(1+\frac{p_m^k H_m^k}{a_m^k}) - 1/W_m = 0$. By Theorem 5.3, the PF weights is also the optimal solution to (5.75). Then, denoting $\bar{W}_m \triangleq W_m + \lambda_m$ where $\lambda_m \geq 0$ is the dual variable, we convert the inner maximization problem in (5.75) to its dual problem and (5.75) can be further written as

$$\min_{(\frac{1}{W_1},\frac{1}{W_2},\ldots,\frac{1}{W_M})\in\mathcal{R}_O, \bar{W}_m\geq W_m} \max_{\mathcal{P},\mathcal{A} \text{ subject to (5.2)}} \left\{ \sum_m \bar{W}_m \left(\sum_k a_m^k \log(1+\frac{p_m^k H_m^k}{a_m^k}) - 1/W_m \right) \right\} . \tag{5.77}$$

Note that the inner problem of (5.77) is equivalent to the weighted throughput optimization problem $\mathsf{P}_{\bar{\mathcal{W}}}(\epsilon)$ with an additional constant term $\sum_m \bar{W}_m/W_m$, where $\bar{\mathcal{W}} = \{\bar{W}_m, m\in\mathcal{M}\}$. Thus, when $W_m = \bar{W}_m = 1/R_m(\mathcal{W})$, the problem in (5.77) is optimally solved (the optimal value is zero, which is same as the problem in (5.75)) and by Theorem 5.3 the optimal PF weights are obtained. Then, we can write the subgradient for the outer minimization problem in (5.77) as [68]

$$g_{\bar{W}_m} = R_m(\bar{\mathcal{W}}) - 1/W_m \ , \tag{5.78}$$

$$g_{W_m} = \bar{W}_m/W_m^2 > 0 \ . \tag{5.79}$$

Since the subgradient of W_m is positive, the optimal $1/W_m$ is on the positive boundary of $\mathcal{R}_O$. Note that $(R_1(\bar{\mathcal{W}}), R_2(\bar{\mathcal{W}}), \ldots, R_M(\bar{\mathcal{W}}))$ is on the positive boundary of $\mathcal{R}_O$ and changes continuously as $\bar{W}$ changes. Then, the following update rule

$$\begin{cases} W_m \leftarrow \min\left\{\bar{W}_m, \left[W_m - \delta\cdot(R_m(\bar{\mathcal{W}}) - 1/W_m)\right]^+\right\} \\ \bar{W}_m \leftarrow \max\left\{W_m, \left[\bar{W}_m - \delta\cdot g_{\bar{W}_m}\right]^+\right\} \end{cases} , \tag{5.80}$$

enforces that W_m always moves closer to the point on the positive boundary of $\mathcal{R}_O$ and $\bar{W}_m$ is updated by the subgradient. Specifically, if we fix W_m (or $\bar{W}_m$) and update $\bar{W}_m$ (or W_m) only

using the second (first) term in (5.80), W_m (or $\bar{W}_m$) can converge and the optimal $\bar{W}_m$ (or W_m) can be obtained for the fixed W_m (or $\bar{W}_m$).

To find the PF weights, we need to obtain the optimal solution to (5.77) such that $W_m = \bar{W}_m$. Specifically, we choose the same initial condition and step size for W_m and $\bar{W}_m$, and simultaneously update W_m and $\bar{W}_m$ in each iteration. Then, W_m and $\bar{W}_m$ remain the same in each iteration and the update rule becomes

$$W_m^{(i+1)} = \bar{W}_m^{(i+1)} \leftarrow \left[\bar{W}_m^{(i)} - \delta(i) \cdot g_{\bar{W}_m}^{(i)}\right]^+ , \tag{5.81}$$

where the step size $\delta(i)$ satisfies $\lim_{i\to\infty} \delta(i) = 0$ and $\sum_{i=1}^{+\infty} \delta(i) = +\infty$, e.g., $\delta(i) = 1/i$. In particular, if $W_m^{(i+1)}$ can converge, the problem in (5.77) is optimally solved and finally we have $\bar{W}_m = W_m$ for all $m \in \mathcal{M}$, i.e., $R_m(\mathcal{W}) = 1/W_m$. By Theorem 5.3, $\mathcal{W}$ are the PF weights.

The procedure for computing the PF energy-bandwidth allocation is summarized as follows.

Algorithm 5.3 - PF energy-bandwidth allocating algorithm

1: Initialization

$i = 0$

Specify the initial fairness weights $\mathcal{W}^{(0)}$, convergence threshold δ_0, maximum iteration number I

2: Obtaining the PF weight

REPEAT

$i \leftarrow i + 1$

Solve $\mathsf{P}_{\mathcal{W}^{(i-1)}}(\epsilon)$ to obtain $(\mathcal{P}^{(i)}, \mathcal{A}^{(i)})$

Update $\mathcal{W}^{(i)}$ by (5.81)

UNTIL $\sum_m |R_m(\mathcal{W}^{(i)}) - 1/W_m^{(i)}| \le \delta_0$ **OR** $i = I$

3: Choose the energy-bandwidth Allocation

$(\mathcal{P}^{(i)}, \mathcal{A}^{(i)})$ is the obtained energy-bandwidth allocation

Note that, the convergence of the proposed algorithm is highly dependent on the selection of the initial value, i.e., $\mathcal{W}^{(0)}$. Specifically, we can set

$$\frac{1}{W_m^{(0)}} \approx \mathbb{E}_{\{\tilde{E}_n^k, H_n^k\}}\left[\bar{R}_m(K)\right] , \tag{5.82}$$

as the initial PF weights, where $\bar{R}_m(K)$ denotes the sum-rate achieved by the solution to F_ϵ given the realizations $\{\tilde{E}_n^k, H_n^k, n \in \mathcal{N}, k \in \mathcal{K}\}$ in the scheduling period K, and the simulation results in Section 5.4 demonstrate that the optimal performance is approached closely in a few iterations.

5.4 Simulation Results

We first focus on a single transmitter and compare the achievable rate regions for orthogonal and non-orthogonal two-user broadcast channels, i.e, $N = 1$ and $M = 2$. For the transmitter, we set the initial battery level $B_n^k = 0$, the battery capacity $B_n^{\max} = 20$ units, and we do not apply the maximum power constraint. We generate the realizations of the harvested energy and channel gains following the truncated Gaussian distribution $\mathcal{N}(10, 2)$ and the Rayleigh distribution with the parameter 2, respectively. Moreover, we consider two scheduling period, $K = 1$ slot and $K = 10$ slots, and show the sum-rate improvement by the non-orthogonal broadcast over the orthogonal broadcast in Fig. 5.3 and Fig. 5.4, respectively. Specifically, we note that when $K = 10$ the improvement is quite marginal. Moreover, in Fig. 5.4, two curves share three common points corresponding to the sum-rate achieved by the solution to $\mathcal{P}_0(W_1, W_2)$ for $(W_1, W_2) = (1, 0), (0.5, 0.5)$ and $(0, 1)$, respectively. Also, when $W_1 = W_2 = 0.5$, the sum-rates are maximized for both the orthogonal and non-orthogonal broadcast, which are same.

5.4.1 Weighted Sum-Rate Maximization

We then consider a network with multiple broadcast channels where there are $N = 3$ transmitters and each communicates with 2 receivers, i.e., $\mathcal{M}_1 = \{1, 2\}, \mathcal{M}_2 = \{3, 4\}, \mathcal{M}_3 = \{5, 6\}$. We set the scheduling period as $K = 20$ slots. For each transmitter n, we set the initial battery level $B_n^0 = 0$ and the battery capacity $B_n^{\max} = 20$ units. We assume that the harvested energy follows a truncated Gaussian distribution with mean μ_n and variance of 2. We also assume a Rayleigh fading channel with the parameter σ_m.

For comparison, we consider two simple scheduling strategies, namely, the *greedy energy policy* and the *equal bandwidth policy*. For the greedy energy policy, each transmitter first tries to use up the available energy in each slot. Then, given the available energy for each transmitter, we solve the energy-bandwidth allocation problem slot by slot, i.e., $\mathsf{P}_{\mathcal{W}}(0)$ for $K = 1$, to calculate the energy and bandwidth allocated for each receiver. For the equal bandwidth policy, we first assign the bandwidth for each transmitter equally. Then, given the assigned bandwidth for each transmitter, we solve an energy-bandwidth allocation problem transmitter by transmitter, i.e., $\mathsf{P}_{\mathcal{W}}(0)$ for $N = 1$, to calculate the energy and bandwidth (for orthogonal broadcast channel only) allocated for each

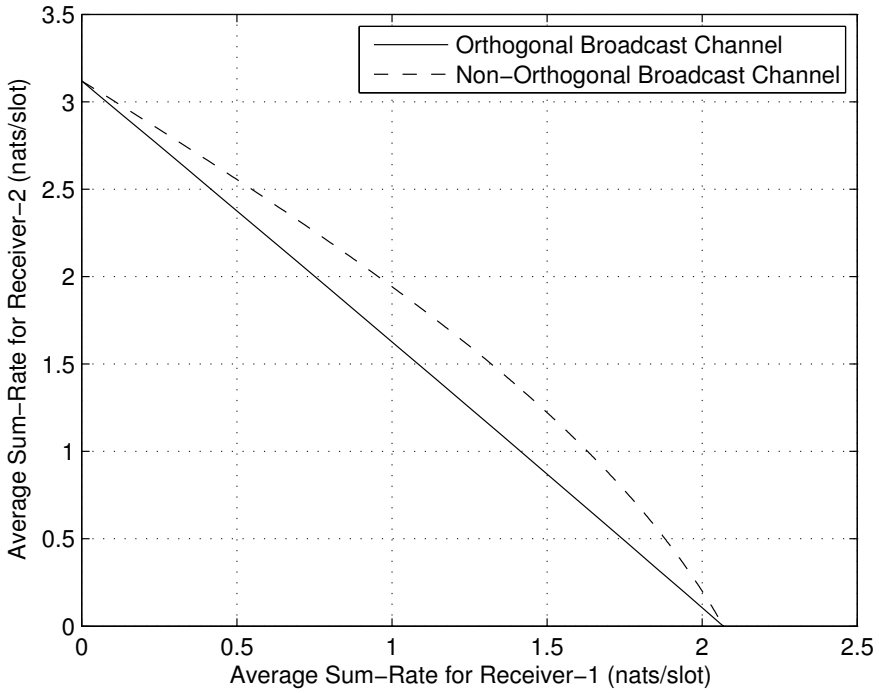

Figure 5.3: Achievable sum-rate regions of two-user orthogonal/non-orthogonal broadcast channels ($K = 1$).

receiver.

To compare the performance of the different algorithms and policies, we evaluate the (weighted) sum-rate for the multiple orthogonal broadcast channels (O-BCs) and non-orthogonal broadcast channels (NO-BCs), respectively. We use $\mathcal{W}_1 = \{W_m = 1/6\}$ and $\mathcal{W}_2 = \{W_m = (2(n-1)+m)/21\}$ for the unweighted and weighted sum-rate cases, respectively, and set the channel fading parameter $\sigma_m = 2$. Moreover, we assume the power unconstrained case where the energy harvesting rate is $\mu_n = 6, 7, 8, 9, 10, 11$ units per slot and a power constrained case where the maximum power constraint is $P_n = 10$ and the energy harvesting rate is $\mu_n = 1, 2, 3, 4, 5, 6$ units per slot. We run the simulation 500 times to obtain the performance for the different algorithm and policies, as shown in Figs. 5.5, 5.6, and 5.7 for the power unconstrained case with $\mathcal{W}_1$, the power unconstrained case with $\mathcal{W}_2$, and the power constrained case with $\mathcal{W}_2$, respectively.

As shown in Fig. 5.5, the maximum throughput in NO-BC is the same as that in O-BC under the optimal energy-bandwidth allocation and the greedy energy policy. This is because in both O-

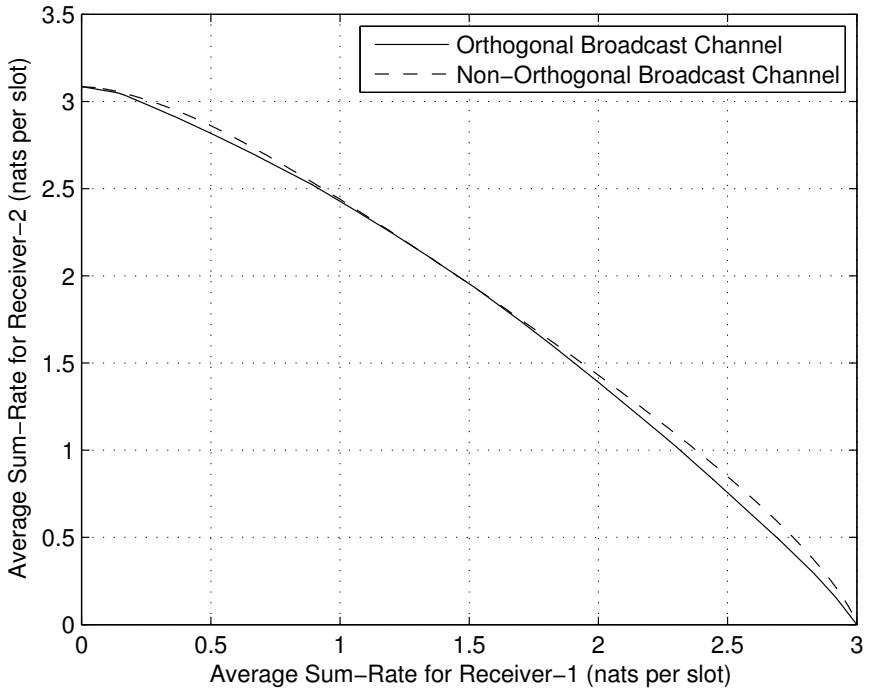

Figure 5.4: Achievable sum-rate regions of two-user orthogonal/non-orthogonal broadcast channels ($K = 10$).

BC and NO-BC, the optimized bandwidth allocation requires that each transmitter only transmit to the receiver with the strongest channel in each slot when the weights are equal (e.g., $\mathcal{W}_1$), as stated in Theorem 5.1 and Corollary 5.1. For the equal bandwidth policy, O-BC performs worse than NO-BC since the NO-BC makes better use of the allocated bandwidth by optimally treating the interference. When we use the unequal weights $\mathcal{W}_2$, it is seen in Figs. 5.6 and 5.7 that we may get better performance by using NO-BC instead of O-BC under all policies. However, for the optimal energy-bandwidth allocation, such improvement is quite marginal. Moreover, when the maximum power is constrained, it is seen in Fig. 5.7 that the gap between the performances of the optimal energy-bandwidth allocation and the greedy energy policy decreases as the energy harvesting rates increases.

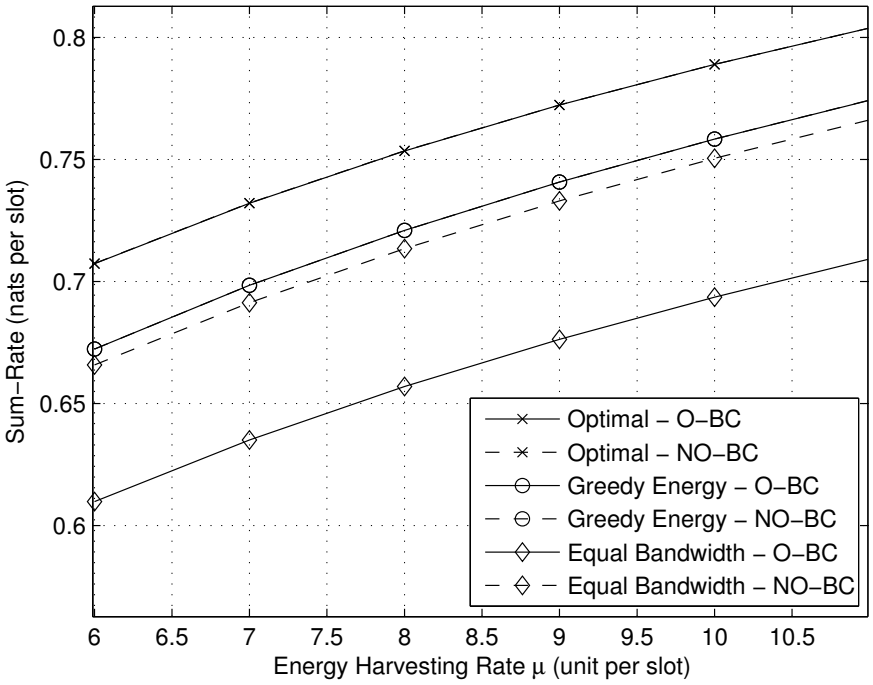

Figure 5.5: Sum-rate comparisons for different policies without the maximum power ($\mathcal{W}_1$).

5.4.2 PF Throughput Maximization

We next evaluate the PF throughput performance in the network with multiple orthogonal broadcast channels. For comparison, we consider three scheduling strategies, namely, the *greedy policy*, the *traditional PF policy*, and the *approximate PF policy*. For the greedy policy, the transmitter evenly splits the maximum available energy for the transmission to each receiver in each slot, i.e., $p_m^k = B_n^k/|\mathcal{M}_n|$, and the equal bandwidth is also allocated, i.e., $a_m^k = 1/M$. For the traditional PF policy, the transmitter tries to use the maximum available energy in each slot and one transmission link is chosen to use the entire bandwidth as follows:

$$\arg\max_m \left\{ \log(1 + p_m^k H_m^k)/\tilde{R}_m^k \right\}, \tag{5.83}$$

where we denote $\tilde{R}_m^k$ as the average sum-rate before slot k [75]. For the approximate PF policy, we use the approximate PF weights given in (5.82) and then solve a weighted sum-rate maximization problem.

To evaluate the performance of the different algorithm and policies, we consider two scenarios,

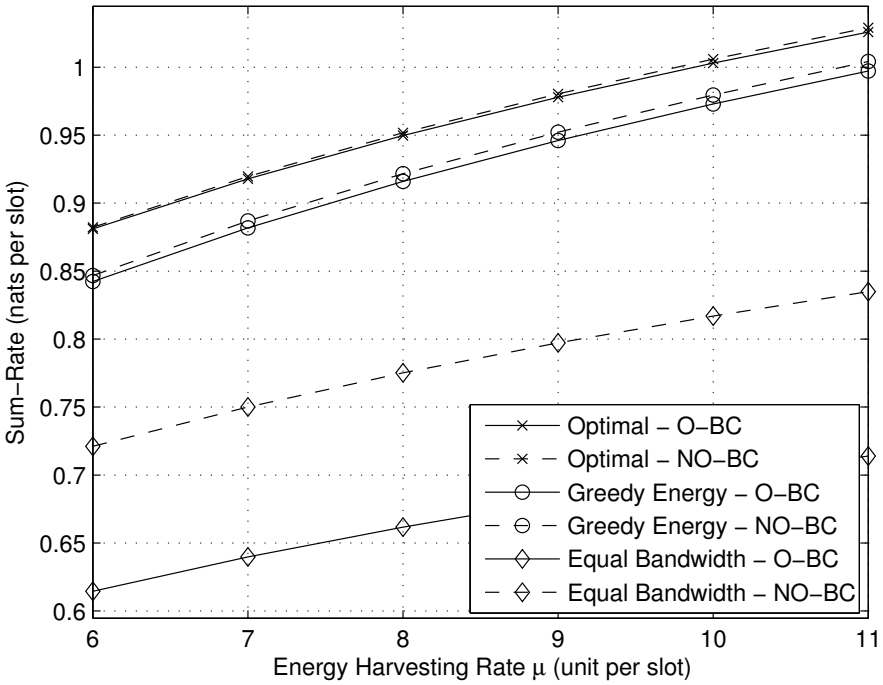

Figure 5.6: Weighted sum-rate comparisons for different policies without the maximum power ($\mathcal{W}_2$).

namely, the *varying EH scenario*, where the different transmitters have different means of the energy harvesting such that $\mu_1 + 2 = \mu_2 + 1 = \mu_3$ and the channel fading parameter is $\sigma = 2$ for all transmitters, and *varying channel scenario*, where the different transmitters have different channel fading parameters such that $\sigma_{1(\cdot)} + 0.5 = \sigma_{2(\cdot)}$ and the mean of the energy harvesting is $\mu = 2$ for all transmitters. In both the scenarios, the maximum power is unconstrained and we compare the performance of Algorithm 5.3 and the other three polices with the optimal PF throughput obtained using the generic convex solver. Specifically, in the varying EH scenario and the varying channel scenario, we assume $\mu_1 = 1, 2, 3, 4, 5, 6$ units per slot and $\sigma_{1(\cdot)} = 1, 1.2, 1.4, 1.6, 1.8, 2$, respectively. We run the simulation 500 times to obtain the performance for the different algorithm and policies, as well as the optimal schedule solved by a general convex solver, as shown in Fig. 5.8 and Fig. 5.9 for the varying EH scenario and the varying channel scenario, respectively.

From Fig. 5.8 and Fig. 5.9, it is seen that for both scenarios Algorithm 5.3 achieves the same performance as that achieved by the optimal energy-bandwidth allocation solved by the generic convex solver, which is better than the other policies, as excepted. Specifically, the performance

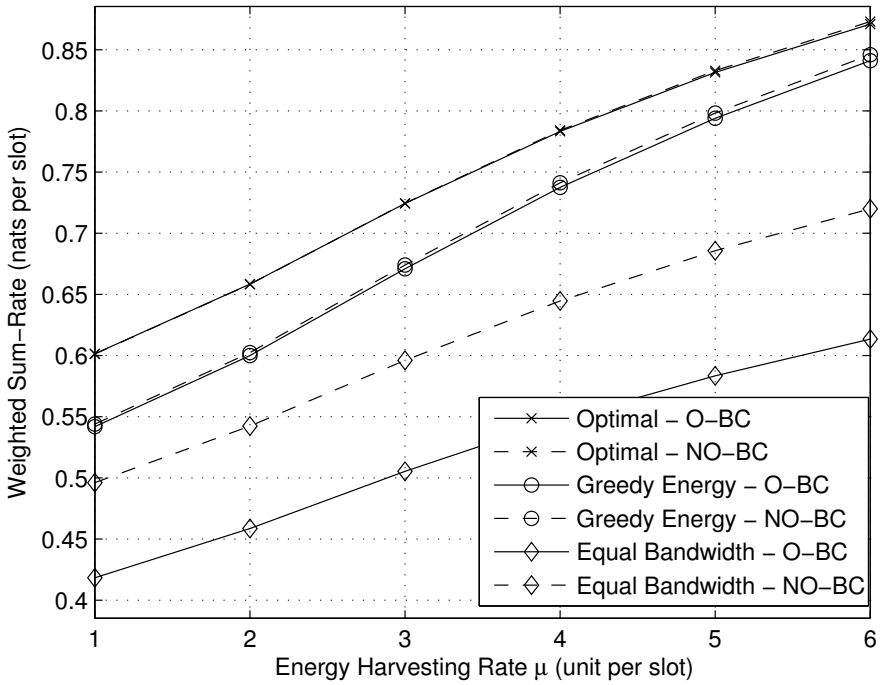

Figure 5.7: Weighted sum-rate comparisons for different policies with the maximum power ($\mathcal{W}_2$, $P_n = 10$).

of the approximate PF policy is close to the optimal performance and better than that of the traditional PF and greedy policies. It is because the energy harvesting and channel fading processes are stationary and erodic and the sum-rate achieved by the optimal energy-bandwidth allocation is close to the PF weights parameter. Also, the traditional PF policy is optimal for the transmitters without using the renewable energy source. However, due to the energy harvesting process with the finite battery capacity, the potential energy overflow necessitates the bandwidth share to maximize the proportionally-fair throughput. Therefore, the traditional PF policy gives the suboptimal performance for the transmitters powered by the renewable energy source. Moreover, the greedy policy, which does not take the energy and the fairness factors into account, provides the worst performance among the simulated algorithm/polices.

We also evaluate the convergence speed of Algorithm 5.3 with different initial weights $\mathcal{W}$, i.e., the approximate PF weights and equal weights, as shown in Fig. 5.10 for $K = 20$. It is seen that, the convergence speed with the initial approximate PF weights is faster than that with the initial

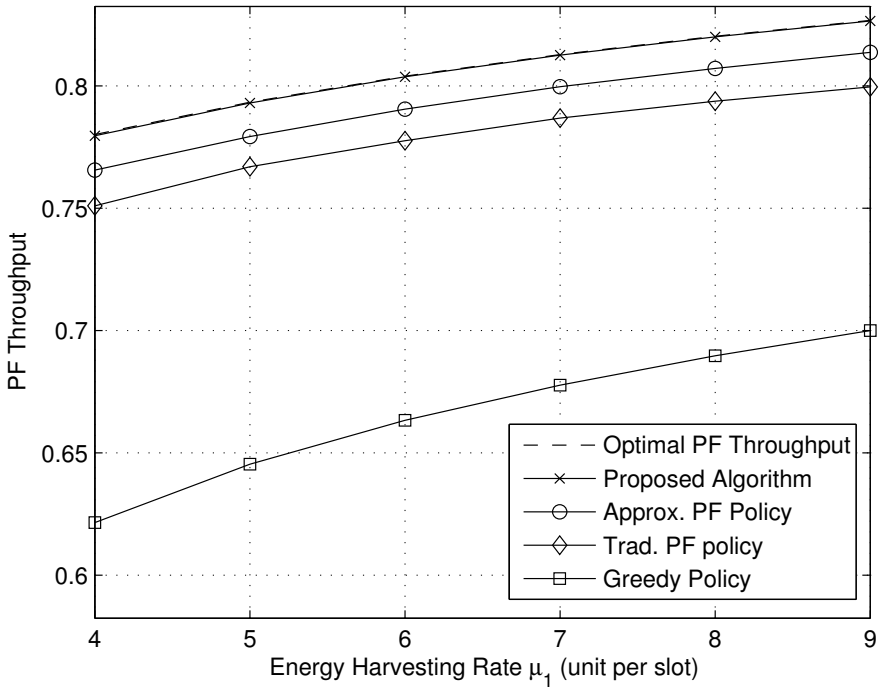

Figure 5.8: Performance comparisons in the varying EH scenario.

equal weights, approaching to the optimal performance after around 10 iterations.

5.5 Conclusions

We have treated the energy-bandwidth allocation problem for a network consisting of multiple energy harvesting transmitters, each broadcasting to multiple receivers, to maximize the weighted throughput and the proportionally fair throughput. Based on the general iterative algorithm developed in Chapter 4 that alternatively solves the energy and bandwidth allocation subproblems, we have developed optimal algorithms for solving the two subproblems for both orthogonal and non-orthogonal broadcast. Moreover, for orthogonal broadcast, we have shown that the PF throughput maximization problem can be converted to the weighted throughput maximization problem with proper weights. Simulation results demonstrate that the proposed algorithms offer significant performance improvement over various suboptimal allocation schemes. Moreover, it is seen that with energy-harvesting transmitters, non-orthogonal broadcast offers limited gain over orthogonal

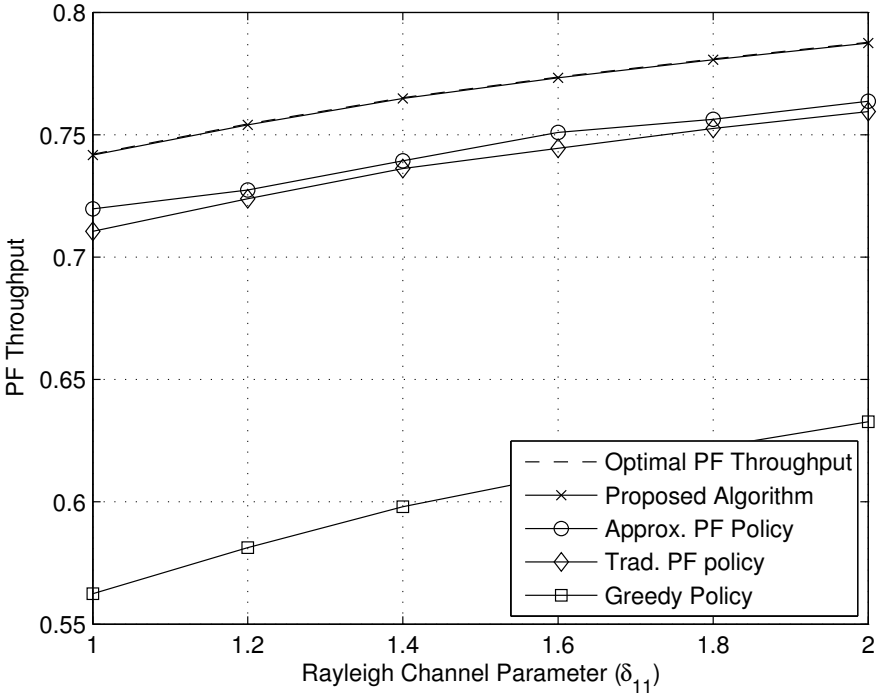

Figure 5.9: Performance comparisons in the varying channel scenario.

broadcast.

5.6 Appendix

5.6.1 Proof of Proposition 5.2

By Lemma 5.1, we have

$$(F_n^k)'(p) = \partial \left(\sum_{m \in \mathcal{M}_n} W_m \log(1 + \frac{p_m^k(p) H_m^k}{H_m^k \sum_{m_0 \mid H_m^k < H_{m_0}^k} p_{m_0}^k(p) + 1}) \right) / \partial p \tag{5.84}$$

$$= \partial \left(W_a \log(1 + \frac{(p - L_a^k) H_a^k}{L_a^k H_a^k + 1}) \right) / \partial p \tag{5.85}$$

$$= \frac{W_a}{p + 1/H_a^k} \ , \ p \in [L_a^k, L_b^k] \tag{5.86}$$

where (5.85) follows because (5.48) indicates that, for any $a \in \mathcal{M}_n$, $p_a^k(p)$ is constant when $p < L_a^k$ or $p > L_b^k$.

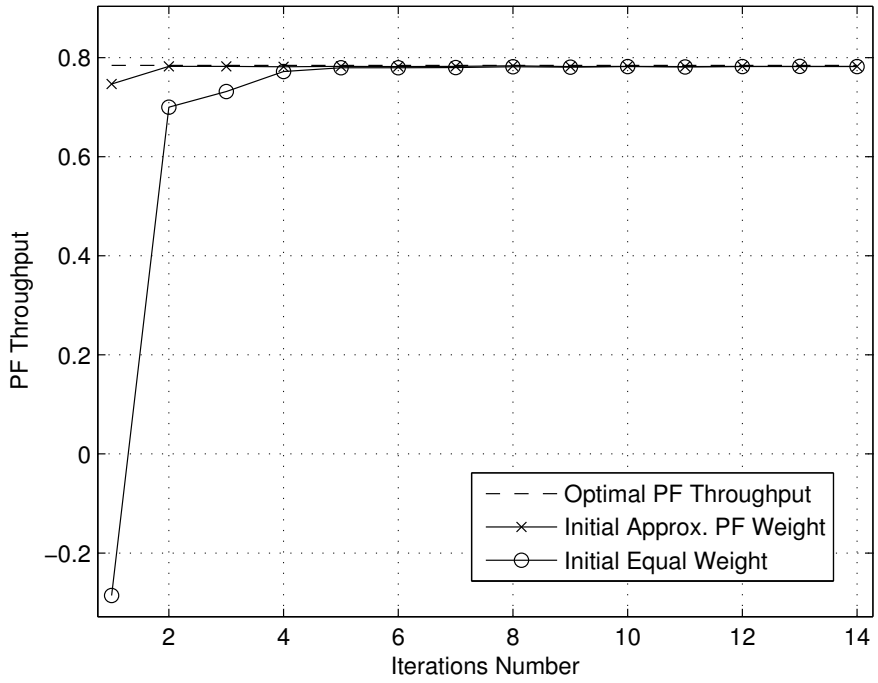

Figure 5.10: Convergence behavior of Algorithm 5.3.

Hence $(F_n^k)'(p)$ is a piecewise function composed by the segments in the form of $f_m^k(p) \triangleq W_m/(p_m^k + 1/H_m^k)$. By Lemma 5.2, $(F_n^k)'(p)$ is continuous. Thus, for any two adjacent different cutoff lines $L_a^k < L_b^k$, L_a^k is the intersection of the two curves $f_a^k(p) = W_a/(p + 1/H_a^k)$ and $f_b^k(p) = W_b/(p + 1/H_b^k)$.

Denoting the intersection of $f_a^k(p)$ and $f_b^k(p)$ as I_{ab}^k (i.e., $p = I_{ab}$ such that $f_a^k(I_{ab}^k) = f_b^k(I_{ab}^k)$), we then have

$$L_a^k = I_{ab}^k \triangleq \frac{H_b^k W_b - H_a^k W_a}{H_b^k H_a^k (W_a - W_b)} \ . \tag{5.87}$$

Specifically, for any $a, b \in \mathcal{M}_n$, I_{ab}^k is unique if it exists. Then, we can write

$$F_n^k(\tilde{p}) = \int_0^{\tilde{p}} (F_n^k)'(p)dp \tag{5.88}$$

$$= \max_{\{I_{ab}^k < I_{bc}^k < \ldots < \tilde{p} \mid a,b,c,\ldots \in \mathcal{M}_n\}} \left\{ \sum_{ab} \int_{I_{ab}^k}^{\min\{I_{bc}^k, \tilde{p}\}} f_a^k(p)dp \right\} \ , \tag{5.89}$$

where (5.89) follows since $(F_n^k)'(p)$ is a piecewise function with the segments of $f_m^k(p)$ and I_{ab}^k is the intersection of $f_a^k(p)$ and $f_b^k(p)$.

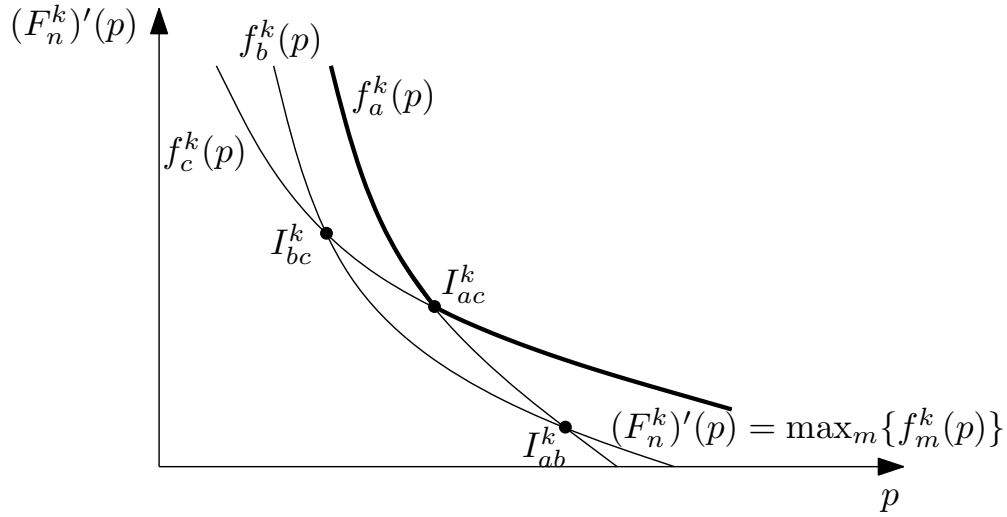

Figure 5.11: The derivative of $F_n^k(p)$.

Then, as shown in Fig. 5.11, we can obtain a set of I_{ab}^k and it is easy to verify that the optimal solution to the problem in (5.89) forms the derivative of $F_n^k(p)$ as

$$(F_n^k)'(p) = \max_{m \in \mathcal{M}_n} \left\{ \frac{W_m}{p + 1/H_m^k} \right\} . \tag{5.90}$$

Chapter 6

Energy-Subchannel Allocation for Multiuser Networks in Frequency-Selective Fading Channels

In this chapter, we focus on the energy-subchannel allocation in frequency-selective fading channels. Specifically, we consider a network with multiple transmitters, each powered by a renewable energy source and equipped with a finite-capacity battery. We assume a frequency-selective fading channel and split the frequency band into multiple flat fading subchannels with equal bandwidth. To avoid interference, no two transmitters can transmit in the same subchannel and the same time slot.

We first assume that the harvested energy and channel gain can be predicated for a scheduling period and formulate an energy-subchannel allocation problem to maximize the sum-rate in a scheduling period, which is a mixed integer optimization problem where the energy allocation is continuous and the subchannel allocation is binary. We first decompose the problem into distributed price-based energy-subchannel allocation problems for each transmitter, and a subgradient algorithm is used to update the price of each subchannel. To solve the price-based energy-subchannel allocation problem, we derive a controlled water-filling mechanism which is used in each recursion of the dynamic water-filling algorithm proposed in [69]. Specifically, the controlled water-filling incorporates the channel price and gain by setting a price-related water-filling stage higher than the channel-related water-filling stage (the inverse of the channel gain) in the conventional water-

filling such that the subchannel is used only when the water level is higher than the price-related water-filling stage. Moreover, we show that the proposed energy-subchannel allocation algorithm is asymptotically optimal when the bandwidth of each subchannel goes to zero.

Moreover, we also propose a causal algorithm without the predictions of the energy harvesting and channel fading processes, using a Q-learning approach [78]. At the beginning of each slot, the transmitter independently decides the amount of the energy used in the current slot based on the current battery level and then the energy-subchannel allocation is calculated given the allocated energy of each transmitter.

6.1 System Model and Problem Formulations

6.1.1 System Model

We consider a network consisting of N transmitter-receiver pairs, where each transmitter is powered by a renewable energy source and sends data to its respective receiver. The frequency band of B Hz is divided into M equal-bandwidth subchannels and each subchannel is flat-fading. Denote $\beta \triangleq B/M$ Hz as the bandwidth of each subchannel. To avoid interference, each subchannel can be used by only one transmitter in each time slot. Let $a_{nm}^k \in \{0,1\}$ be the subchannel allocation indicator, where $a_{nm}^k = 1$ indicates that transmitter n transmits on subchannel m in slot k, and $a_{nm}^k = 0$ otherwise. We assume that each subchannel gain is constant over a coherence time of T_c seconds, which is also the duration of the slot, and each slot consists of $T = \beta T_c$ time instants (i.e., β samples are transmitted per second). Denoting X_{nm}^{ki} as the symbol sent by transmitter n at instant i in slot k and subchannel m, the received signal (by receiver n at instant i in slot k and subchannel m) is given by $Y_{nm}^{ki} = X_{nm}^{ki} h_{nm}^k + Z_{nm}^{ki}$, where h_{nm}^k denotes the complex channel gain of subchannel m between the n-th transmitter-receiver pair and $Z_{nm}^{ki} \sim \mathsf{CN}(0, \frac{\beta}{T})$ is the i.i.d. complex Gaussian noise. (The power spectral density of the noise is $1/T_c$ so that the noise power is β/T_c which is the total variance of β noise samples (per second). Therefore, the variance of each noise sample is $1/T_c = \beta/T$.) Denote $H_{nm}^k \triangleq |h_{nm}^k|^2$ and denote $p_{nm}^k \triangleq \sum_{i=1}^{T} |X_{nm}^{ki}|^2$ as the transmission energy consumption in a slot. Then the capacity of the above discrete-time channel is given by $\log(1 + \frac{H_{nm}^k p_{nm}^k / T}{\beta/T}) = \log(1 + p_{nm}^k H_{nm}^k/\beta)$ nats per channel use [70]. Since each slot of T_c seconds contains $T = T_c\beta$ channel uses, the upper-bound of the achievable rate is then $\beta \log(1 + p_{nm}^k H_{nm}^k/\beta)$

nats per second per subchannel. Moreover, we denote $\mathcal{P} \triangleq \{p_{nm}^k, n \in \mathcal{N}, m \in \mathcal{M}, k \in \mathcal{K}\}$ and $\mathcal{A} \triangleq \{a_{nm}^k, n \in \mathcal{N}, m \in \mathcal{M}, k \in \mathcal{K} \mid a_{nm}^k \in \{0,1\}\}$ as the energy allocation and subchannel allocation, respectively, where $\mathcal{N} \triangleq \{1, 2, \ldots, N\}$ is the set of transmitters, $\mathcal{M} \triangleq \{1, 2, \ldots, M\}$ is the set of subchannels, and $\mathcal{K} \triangleq \{1, 2, \ldots, K\}$ is the set of time slots in a scheduling period.

Each transmitter is powered by the energy harvested from the surrounding environment and buffered by a finite-capacity battery. We first assume that the amount of the harvested energy in each slot can be perfectly predicted for the scheduling period [71][66] and denote E_n^k as the total energy harvested up to the end of slot k by transmitter n; we also assume that the gain H_{nm}^k of each subchannel is predictable [72]. Thus $\{E_n^k, H_{nm}^k, n \in \mathcal{N}, m \in \mathcal{M}, k \in \mathcal{K}\}$ is known at the beginning of each scheduling period. In Section 6.3, we will relax the non-causal assumption on E_n^k and H_{nm}^k and develop a causal energy-subchannel allocation algorithm.

Assuming that the battery has a finite capacity $B_n^{\max}$ and is empty initially, the battery level at transmitter n at the end of slot k can be written as

$$B_n^k = \min\left\{B_n^{\max}, B_n^{k-1} + \left(E_n^k - E_n^{k-1}\right) - \sum_{m\in\mathcal{M}} p_{nm}^k\right\}, \tag{6.1}$$

where $B_n^k \geq 0$ for all $n \in \mathcal{N}$ and $k \in \mathcal{K}$. Moreover, each subchannel m is allocated to at most one transmitter in each slot k, i.e., $\sum_{n\in\mathcal{N}} a_{nm}^k \leq 1$ for all $k \in \mathcal{K}, m \in \mathcal{M}$.

6.1.2 Problem Formulation

For each transmitter n, we use the upper-bound of the achievable sum-rate over K slots as the performance metric, given by

$$C_n(\mathcal{P}_n, \mathcal{A}_n) \triangleq \sum_{k\in\mathcal{K}} \sum_{m\in\mathcal{M}} \beta a_{nm}^k \log(1 + p_{nm}^k H_{nm}^k/\beta) \ , \tag{6.2}$$

where $\mathcal{P}_n \triangleq \{p_{nm}^k, m \in \mathcal{M}, k \in \mathcal{K}\} \subseteq \mathcal{P}$ and $\mathcal{A}_n \triangleq \{a_{nm}^k, m \in \mathcal{M}, k \in \mathcal{K}\} \subseteq \mathcal{A}$. We note that, although (6.2) may not be achievable by practical codes and modulations, it is a commonly used metric for evaluating the communication system performance [41][42].

We formulate the energy-subchannel allocation problem as follows:

$$\max_{\mathcal{P},\mathcal{A}} \sum_{n\in\mathcal{N}} C_n(\mathcal{P}_n, \mathcal{A}_n) \ , \tag{6.3}$$

subject to

$$\begin{cases} E_n^k - B_n^{\max} \leq \sum_{\kappa=1}^{k} \sum_{m\in\mathcal{M}} p_{nm}^{\kappa} \leq E_n^k & n \in \mathcal{N}, k \in \mathcal{K} \\ \sum_{n\in\mathcal{N}} a_{nm}^k \leq 1 & m \in \mathcal{M}, k \in \mathcal{K} \\ p_{nm}^k \geq 0 & n \in \mathcal{N}, m \in \mathcal{M}, k \in \mathcal{K} \\ a_{nm}^k \in \{0,1\} & n \in \mathcal{N}, m \in \mathcal{M}, k \in \mathcal{K} \end{cases}, \tag{6.4}$$

where the first constraint in (6.4) is the non-recursive form of (6.1).

Note that, the problem in (6.3)-(6.4) is a mixed integer programming problem where the subchannel allocation $\mathcal{A}$ is a set of binary variables and the energy allocation $\mathcal{P}$ is a set of non-negative real variables. Even though it is convex for fixed $\mathcal{A}$, obtaining the jointly optimal energy-subchannel allocation needs an exhaustive search over all N^M possible subchannel allocations. Our objective is to develop a low-complexity suboptimal algorithm for solving (6.3)-(6.4) with provable performance guarantee and asymptotic optimality. By removing the second constraint in (6.4) and adding it to the objective function with the use of Lagrangian multipliers, we define the Lagrangian function as

$$\begin{aligned} \mathcal{L}(\mathcal{P},\mathcal{A},\Lambda) &\triangleq \sum_{n\in\mathcal{N}} C_n(\mathcal{P}_n,\mathcal{A}_n) - \sum_{k\in\mathcal{K}}\sum_{m\in\mathcal{M}} \lambda_m^k \left(\sum_{n\in\mathcal{N}} a_{nm}^k - 1\right) \\ &= \sum_{k\in\mathcal{K}}\sum_{n\in\mathcal{N}}\sum_{m\in\mathcal{M}} a_{nm}^k \beta \left[\log(1 + p_{nm}^k H_{nm}^k/\beta) - \lambda_m^k/\beta\right] + \sum_{k\in\mathcal{K}}\sum_{m\in\mathcal{M}} \lambda_m^k \ , \end{aligned} \tag{6.5}$$

where $\Lambda \triangleq \{\lambda_m^k \geq 0, m \in \mathcal{M}, k \in \mathcal{K}\}$ is the set of the dual variables. Then, the dual of the original problem in (6.3)-(6.4) can be written as

$$\inf_{\Lambda\,:\,\lambda_m^k \geq 0} \left\{ \max_{\mathcal{P},\mathcal{A}} \mathcal{L}(\mathcal{P},\mathcal{A},\Lambda) \right\} \ , \tag{6.6}$$

where the inner maximization problem has the following constraints

$$\begin{cases} E_n^k - B_n^{\max} \leq \sum_{\kappa=1}^{k} \sum_{m\in\mathcal{M}} p_{nm}^{\kappa} \leq E_n^k & n \in \mathcal{N}, k \in \mathcal{K} \\ p_{nm}^k \geq 0 & n \in \mathcal{N}, m \in \mathcal{M}, k \in \mathcal{K} \\ a_{nm}^k \in \{0,1\} & n \in \mathcal{N}, m \in \mathcal{M}, k \in \mathcal{K} \end{cases} . \tag{6.7}$$

The next theorem indicates that the strong duality holds for the original problem in (6.3)-(6.4) when the subchannels bandwidth $\beta \to 0$. Note that, this result and its proof are similar to those in [58].

Theorem 6.1. *When $M \to \infty$, and $B = o(M)$, the gap between the primal problem in* (6.3)-(6.4) *and its dual problem in* (6.6)-(6.7) *goes to zero.*

Proof. When $M \to \infty$, and $B = o(M)$, the bandwidth $\beta = B/M$ of each subchannel becomes infinitesimal. We first consider the case when the channel is flat-fading, i.e., $H_{nm}^k = H_n^k, \forall m \in \mathcal{M}$. Then, the location of the allocated subchannel on the frequency band does not affect the achievable rate and thus the energy-subchannel allocation problem is equivalent to an energy-bandwidth allocation problem such that the frequency band is split to all transmitters in fractions, which is given by

$$\max_{\alpha_n^k, p_n^k} \sum_{n\in\mathcal{N}} \sum_{k\in\mathcal{K}} \alpha_n^k \log(1 + p_n^k H_n^k/\alpha_n^k) \tag{6.8}$$

subject to

$$\begin{cases} E_n^k - B_n^{\max} \le \sum_{\kappa=1}^k p_n^\kappa \le E_n^k & n \in \mathcal{N}, k \in \mathcal{K} \\ p_n^k \ge 0 & n \in \mathcal{N}, k \in \mathcal{K} \\ 0 \le \sum_{n\in\mathcal{N}} \alpha_n^k \le B & k \in \mathcal{K} \\ \alpha_n^k \ge 0 & n \in \mathcal{N}, k \in \mathcal{K} \end{cases}, \tag{6.9}$$

where α_n^k and p_n^k are the bandwidth and energy allocated to transmitter n in slot k, respectively. Defining $0 \cdot \log(1 + p/0) \triangleq \lim_{a\to 0^+} a \cdot \log(1 + p/a) = 0$, the energy-bandwidth allocation problem in (6.8)-(6.9) is a convex optimization problem with linear constraints, whose strong duality holds, i.e., the portion of the bandwidth is utilized when the corresponding dual variable is positive.

Now consider the frequency-selective channel with total bandwidth $B = o(M)$. When $M \to \infty$, the total frequency band is divided into a set of infinitesimal frequency bands. By continuity, the channel gains within each band approaches a constant value as the subdivision becomes finer and finer. Note that, every achievability with splitting frequency among different users in each subdivision can be transformed into assigning different frequency subchannels (or frequency point) to different transmitters as $M \to \infty$ and vice versa. Thus, the two problems are equivalent when $M \to \infty$ and the strong duality holds. □

Denoting

$$U_{n,\Lambda}(\mathcal{P}_n, \mathcal{A}_n) \triangleq \sum_{k\in\mathcal{K}} \sum_{m\in\mathcal{M}} \beta a_{nm}^k \left[\log(1 + p_{nm}^k H_{nm}^k/\beta) - \lambda_m^k/\beta\right], \tag{6.10}$$

we decompose the inner maximization problem in (6.6) into N subproblems, each associated with a transmitter n, given by

$$\max_{\mathcal{P}_n, \mathcal{A}_n} U_{n,\Lambda}(\mathcal{P}_n, \mathcal{A}_n) \tag{6.11}$$

subject to

$$\begin{cases} E_n^k - B_n^{\max} \le \sum_{\kappa=1}^{k} \sum_{m\in\mathcal{M}} p_{nm}^{\kappa} \le E_n^k & k \in \mathcal{K} \\ p_{nm}^k \ge 0 & m \in \mathcal{M}, k \in \mathcal{K} \\ a_{nm}^k \in \{0,1\} & m \in \mathcal{M}, k \in \mathcal{K} \end{cases} . \tag{6.12}$$

Since $\mathcal{L}(\mathcal{P},\mathcal{A},\Lambda) = \sum_{n\in\mathcal{N}} U_{n,\Lambda}(\mathcal{P}_n,\mathcal{A}_n) + \sum_{m\in\mathcal{M},k\in\mathcal{K}} \lambda_m^k$, and there is no constraint that interrelates different values of n, the inner optimization of (6.6) can be solved by independently solving the problems in (6.11)-(6.12) for all $n \in \mathcal{N}$. Moreover, in the utility function (6.10), the dual variable λ_m^k can be interpreted as the price of using the subchannel. To maximize $U_{n,\Lambda}(\mathcal{P}_n,\mathcal{A}_n)$, if the potential achievable sum-rate of choosing the subchannel, $\beta\log(1+p_{nm}^k H_{nm}^k/\beta)$, is less than the cost λ_m^k/β, the transmitter would not use the subchannel.

We now consider the outer optimization in (6.6). Given $\Lambda^{(i-1)}$ and denoting

$$(\mathcal{P}^{(i)},\mathcal{A}^{(i)}) \triangleq \arg\max_{\mathcal{P},\mathcal{A}} \mathcal{L}(\mathcal{P},\mathcal{A},\Lambda^{(i-1)}) \tag{6.13}$$

subject to the constraints in (6.7), the subgradient of λ_m^k is $g_{\lambda_m^k}^{(i)} \triangleq \sum_{n\in\mathcal{N}} {a_{nm}^k}^{(i)} - 1$ and the price can be adjusted according to

$${\lambda_m^k}^{(i)} = \left[{\lambda_m^k}^{(i-1)} + \delta(i)\cdot g_{\lambda_m^k}^{(i)}\right]^+ \tag{6.14}$$

until $\mathcal{L}(\mathcal{P}^{(i)},\mathcal{A}^{(i)},\Lambda^{(i-1)})$ converges. Note that, using a non-summable diminishing step size $\delta(i)$ such that $\lim_{i\to\infty}\delta(i) = 0$ and $\lim_{i\to\infty}\sum_i \delta(i) = \infty$, e.g., $\delta(i) = 1/i$, the subgradient method in (6.13)-(6.14) can obtain the optimal solution to the dual problem in (6.6)-(6.7) when $i \to \infty$ (if (6.13) can be optimally solved) [68]. However, with finite number of subgradient updates, the dual problem may not be optimally solved. As a result, the obtained solution may not be feasible to the primal problem in (6.3)-(6.4). Therefore, a final adjustment is needed.

The procedure for solving the energy-subchannel allocation problem in (6.3)-(6.4) is summarized as follows.

Algorithm 6.1 - Energy-subchannel allocation

1: Initialization

Specify the maximum number of iterations I

Specify the initial price $\Lambda^{(0)} \triangleq \{\lambda_m^{k\,(0)}, m \in \mathcal{M}, k \in \mathcal{K}\}$

$i \leftarrow 0$

2: **REPEAT** [Solving the dual problem in (6.6)-(6.7)]

$i \leftarrow i + 1$

Update $(\mathcal{P}^{(i)}, \mathcal{A}^{(i)})$ by solving the problem in (6.13) given $\Lambda^{(i-1)}$, which is equivalent to solving the problem in (6.11)-(6.12) for all $n \in \mathcal{N}$ (Algorithm 6.2, Section 6.2.1)

FOR all $m \in \mathcal{M}, k \in \mathcal{K}$

Update $\lambda_m^{k\,(i)}$ using (6.14)

ENDFOR

UNTIL $i > I$ **OR** the optimal value of (6.13) converges

3: Record the solution to the dual problem

$(\tilde{\mathcal{P}}, \tilde{\mathcal{A}}) \leftarrow (\mathcal{P}^{(i)}, \mathcal{A}^{(i)})$

Obtain a feasible solution to the primal problem in (6.3)-(6.4) based on $(\tilde{\mathcal{P}}, \tilde{\mathcal{A}})$ (Section 6.2.3)

We note that the problem in (6.11)-(6.12) is still a mixed integer program, and will be treated in the next section.

6.2 Solving the Price-Based Energy-Subchannel Allocation Problem

In this section, we focus on solving the price-based energy-subchannel allocation problem in (6.11)-(6.12). We note that, given any feasible subchannel allocation $\mathcal{A}_n$, the problem in (6.11)-(6.12) is a convex optimization problem over $\mathcal{P}_n$ with the linear constraints. Thus its K.K.T. conditions are sufficient and necessary for optimality [68]. Using the similar analysis as in [69, Theorem 2], we can conclude that given $\mathcal{A}_n$ the optimal $\mathcal{P}_n$ has a water-filling form, given by

$$p_{nm}^k = a_{nm}^k \beta \left[\frac{1}{w_n^k} - \frac{1}{H_{nm}^k} \right]^+ . \tag{6.15}$$

Moreover, the water level $1/w_n^k$ may increase only in the slot when the battery is depleted, i.e., battery depletion point (BDP) $B_n^k = 0$, and may decrease only in the slot when the battery is fully-charged, i.e., battery fully-charged point (BFP) $B_n^k = B_n^{\max}$.

6.2.1 Proposed Algorithm

To solve the problem in (6.11)-(6.12), based on the above condition, we propose an algorithm to find a set of BDP/BFPs $\mathcal{X}_n$ such that, for each adjacent pair $(a,b) \subseteq \mathcal{X}_n$, when the dual of the following problem

$$\max_{a_{nm}^k, p_{nm}^k} \sum_{k=a+1}^{b} \sum_{m\in\mathcal{M}} \beta a_{nm}^k \left[\log(1+p_{nm}^k H_{nm}^k/\beta) - \lambda_m^k/\beta\right] \tag{6.16}$$

subject to

$$\begin{cases} \sum_{k=a+1}^{b} \sum_{m\in\mathcal{M}} p_{nm}^k \le \mathbb{U}_n(a,b) & \\ p_{nm}^k \ge 0 & k\in[a+1,b], m\in\mathcal{M} \\ a_{nm}^k \in \{0,1\} & k\in[a+1,b], m\in\mathcal{M} \end{cases}, \tag{6.17}$$

where

$$\mathbb{U}_n(a,b) \triangleq B_n^a + \left(E_n^b - E_n^a\right) - B_n^b = E_n^b - E_n^a + \big(\mathbb{I}(a \text{ is BFP}) - \mathbb{I}(b \text{ is BFP})\big) B_n^{\max}$$

is optimally solved, 1) the obtained energy allocation follows the water-filling rule in (6.15), where the water level $1/w_n^k$ may only increase/decrease at BDP/BFPs, respectively; and 2) the energy allocation is feasible, i.e., for any adjacent pair $(a,b) \subseteq \mathcal{X}_n$, $B_n^a = 0/B_n^{\max}$ if a is a BDP/BFP and $0 \le B_n^k \le B_n^{\max}$ for all $k \in [a+1,b]$.

6.2.1.1 Forward/Backward Search

In [69], for a single-user energy-harvesting transmitter, an algorithm is proposed to find the BDP/BFP set by recursively performing the forward/backward search. Here we adopt the same procedure to search for the BDP/BFP sets, where the *Forward Search* and *Backward Search* operations are performed on a segment between two adjacent BDP/BFPs, e.g., $[a, \text{type of } a]$ and $[b, \text{type of } b]$, recursively. Specifically, we start the algorithm by performing the Forward Search on $[0, \text{BDP}]$ and $[K, \text{BDP}]$ with the initial BDP/BFP set $\mathcal{X}_n = \{[0, \text{BDP}]\}$. New BDP/BFPs are appended to $\mathcal{X}_n$ as the algorithm proceeds. The algorithm is listed as follows.

Algorithm 6.2 - Procedure for solving (6.11)-(6.12)

INPUT: Channel price Λ

OUTPUT: Energy-subchannel allocation $(\mathcal{P}_n, \mathcal{A}_n)$

ALGORITHM: Run Forward Search on $\big([0, \text{BDP}], [K, \text{BDP}]\big)$

1: Subroutine 1 - Forward Search $\big([a, \text{type of } a], [b, \text{type of } b]\big)$

If $a = K$, the search is complete.

FOR $[k_1,\ \text{type of } k_1] \in \{[a+1, \text{BDP}], \ldots, [b-1, \text{BDP}],\ [b, \text{type of } b]\}$

(*) Solve the dual of the problem in (6.16)-(6.17) with $(a \leftarrow a+1, b \leftarrow k_1)$ using (6.27), (6.28) and (6.34)

ENDFOR

Let $k =$ the largest $k_1 \in [a+1, b]$ such that the obtained energy allocation contains no negative battery level, i.e., $B_n^k \geq 0$ for all $k \in [a+1, k_1]$

- if contains no over-charged battery level, i.e., $B_n^k \leq B_n^{\max}$ for all $k \in [a+1, k_1]$, record the obtained (p_{nm}^k, a_{nm}^k), add $(k, \text{type of } k)$ to $\mathcal{X}_n$, Forward Search $\big([k, \text{type of } k], [K, \text{BDP}]\big)$
- otherwise, let $c =$ the largest slot with the over-charged battery level, Backward Search $\big([a, \text{type of } a], [k, \text{BDP}], c\big)$

2: Subroutine 2 - Backward Search $\big([a, \text{type of } a], [b, \text{type of } b], k\big)$

(*) Set k as BFP and obtain the allocation by solving the dual of the problem in (6.16)-(6.17) with $(a \leftarrow a+1, b \leftarrow k)$ using (6.27), (6.28) and (6.34)

- if feasible, record the obtained (p_{nm}^k, a_{nm}^k), add $[k, \text{BFP}]$ to $\mathcal{X}_n$, Forward Search $\big([k, \text{BFP}], [K, \text{BDP}]\big)$
- if contains over-charged battery level only, set the largest one as c, Backward Search $\big([a, \text{type of } a], [k, \text{BFP}], c\big)$
- if contains negative battery level, Forward Search $\big([a, \text{type of } a], [k, \text{BFP}]\big)$

Note that, the original version of Algorithm 6.2 is proposed in [69] for single-user energy allocation to maximize the sum-rate. There since the problem is convex with linear constraints, it was shown that the algorithm obtains a set of BDP/BFPs along with the optimal energy allocation, where the energy allocation has the water-filling form and the water level may only increase/decrease at BDP/BFPs, respectively.

In this chapter, the step marked by $(*)$ in Algorithm 6.2 solves the dual of the problem in (6.16)-(6.17), whose optimal solution follows a controlled water-filling structure (c.f. Proposition 6.1) and the water level is non-decreasing as the available energy $\mathbb{U}_n(a, b)$ increases. Since the

problem in (6.16)-(6.17) is non-convex, its strong duality cannot be guaranteed. Thus, due to the duality gap, the equality may not hold for the first constraint in (6.17) even if its dual problem is optimally solved. Denote the energy residual as

$$R_n(a,b) \triangleq \mathbb{U}_n(a,b) - \sum_{k=a+1}^{b} \sum_{m\in\mathcal{M}} p_{nm}^k \ , \tag{6.18}$$

where (p_{nm}^k, a_{nm}^k) is the energy-subchannel allocation obtained by solving the dual of the problem in (6.16)-(6.17). If $R_n(a,b) = 0$, slot b is a BDP/BFP. On the other hand, if $R_n(a,b) > 0$, slot b is a pseudo BDP/BFP. (For pseudo BDP/BFP, we treat the energy residual as "used", e.g., the energy residual is reallocated in Section 6.2.3.)

Using a similar analysis as in [69, Section III.D], we can also verify the following property of Algorithm 6.2.

Lemma 6.1. *Algorithm 6.2 obtains a set of pseudo BDP/BFPs $\mathcal{X}_n$ along with the feasible energy-subchannel allocation. Moreover, the obtained energy-subchannel for any adjacent pair $(a,b) \subseteq \mathcal{X}_n$ has the water-filling form in* (6.15)*, where the water level may only increase/decrease at pseudo BDP/BFP, respectively.*

However, if the duality gap exists for the problem in (6.16)-(6.17), the obtained energy-subchannel allocation is suboptimal for its primal problem. In Section 6.2.2, it is shown that the gap between the output of Algorithm 6.2 and the optimal solution to the problem in (6.11)-(6.12) is at most $K\beta$ (c.f. Theorem 6.2).

Next we show that the optimal solution to the dual of the problem in (6.16)-(6.17) has a *controlled water-filling* form.

6.2.1.2 Controlled Water-Filling

Introducing the dual variable $w_n^{ab} \geq 0$ and defining the Lagrangian function

$$\mathcal{L}_n^{ab}(w_n^{ab}, \mathcal{P}_n, \mathcal{A}_n) \triangleq \sum_{k=a+1}^{b} \sum_{m\in\mathcal{M}} a_{nm}^k \beta \left[\log(1 + \frac{p_{nm}^k H_{nm}^k}{\beta}) - \frac{\lambda_m^k}{\beta}\right] - w_n^{ab} \left(\sum_{k=a+1}^{b} \sum_{m\in\mathcal{M}} p_{nm}^k - \mathbb{U}_n(a,b)\right) \ , \tag{6.19}$$

the dual of the problem in (6.16)-(6.17) can be written as

$$\inf_{w_n^{ab}\geq 0} \left\{ \max_{p_{nm}^k \geq 0, a_{nm}^k \in \{0,1\}} \mathcal{L}_n^{ab}(w_n^{ab}, \mathcal{P}, \mathcal{A}) \right\} \ . \tag{6.20}$$

Given a_{nm}^k, the inner maximization problem in (6.20) is convex with linear constraints. Thus the first-order condition together with the constraint $p_{nm}^k \geq 0$ is sufficient for the optimality of p_{nm}^k [68]. Then we have

$$p_{nm}^k = \beta a_{nm}^k \left[\frac{1}{w_n^{ab}} - \frac{1}{H_{nm}^k}\right]^+ , \tag{6.21}$$

where the dual variable $1/w_n^{ab}$ can be considered as the *water level* and is constant between adjacent pair $(a,b) \subseteq \mathcal{X}_n$. Substituting (6.21) into (6.20), the dual problem can be written as

$$\min_{w_n^{ab}\geq 0} \max_{a_{nm}^k \in \{0,1\}} \sum_{k=a+1}^{b} \sum_{m\in\mathcal{M}} \beta a_{nm}^k \left(\left[\log(\frac{H_{nm}^k}{w_n^{ab}})\right]^+ - \left[1 - \frac{w_n^{ab}}{H_{nm}^k}\right]^+ - \frac{\lambda_m^k}{\beta} \right) + w_n^{ab}\mathbb{U}_n(a,b). \tag{6.22}$$

Then, the optimal subchannel allocation is given by

$$\begin{aligned}
a_{nm}^k &= \mathbb{I}\left(\left[\log(\frac{H_{nm}^k}{w_n^{ab}})\right]^+ - \left[1 - \frac{w_n^{ab}}{H_{nm}^k}\right]^+ - \frac{\lambda_m^k}{\beta} > 0 \right) && (6.23)\\
&= \mathbb{I}\left(\log\frac{H_{nm}^k}{w_n^{ab}} - (1 - \frac{w_n^{ab}}{H_{nm}^k}) - \frac{\lambda_m^k}{\beta} > 0 \right) \mathbb{I}\left(w_n^{ab} \leq H_{nm}^k \right) && (6.24)\\
&= \mathbb{I}\left(\log\frac{1/w_n^{ab}}{1/H_{nm}^k} - \log\frac{e^{(1-\frac{w_n^{ab}}{H_{nm}^k})+\frac{\lambda_m^k}{\beta}}/H_{nm}^k}{1/H_{nm}^k} > 0 \right) \mathbb{I}\left(w_n^{ab} \leq H_{nm}^k \right) && (6.25)\\
&= \mathbb{I}\left(\frac{1}{w_n^{ab}} - \frac{1}{H_{nm}^k/e^{(1-\frac{w_n^{ab}}{H_{nm}^k})+\frac{\lambda_m^k}{\beta}}} > 0 \right) \mathbb{I}\left(\frac{1}{w_n^{ab}} \geq \frac{1}{H_{nm}^k} \right) && (6.26)\\
&= \mathbb{I}\left(\frac{1}{w_n^{ab}} - \frac{1}{\tilde{H}_{nm}^k(w_n^{ab})} > 0 \right) \mathbb{I}\left(\frac{1}{w_n^{ab}} \geq \frac{1}{H_{nm}^k} \right) , && (6.27)
\end{aligned}$$

where

$$\tilde{H}_{nm}^k(w) \triangleq H_{nm}^k/e^{(1-\frac{w}{H_{nm}^k})+\frac{\lambda_m^k}{\beta}} .$$

Hence the optimal solution to the inner problem of (6.20) is given by the following *controlled water-filling* rule, as illustrated in Fig. 6.1,

$$p_{nm}^k = \beta \left(\frac{1}{w_n^{ab}} - \frac{1}{H_{nm}^k} \right)^+ \mathbb{I}\left(\frac{1}{w_n^{ab}} - \frac{1}{\tilde{H}_{nm}^k(w_n^{ab})} > 0 \right) , \tag{6.28}$$

where w_n^{ab} is the optimal dual variable for the problem in (6.20).

To calculate the optimal dual variable w_n^{ab}, we first substitute (6.23) into (6.22) and the problem in (6.22) can be rewritten as

$$\min_{w_n^{ab}\geq 0} F(w_n^{ab}) , \tag{6.29}$$

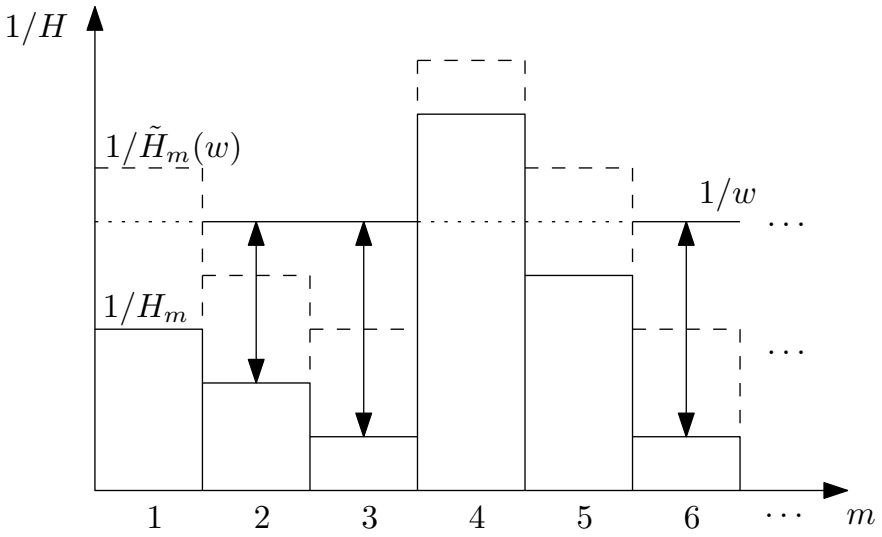

Figure 6.1: The controlled water-filling. For subchannels $2, 3$ and 6, the amount of the allocated energy is represented by the distance between $1/w$ and $1/H_m$. No energy is allocated to subchannels 1 and 5 due to the control of $1/\tilde{H}_m(w)$, and subchannel 4 due to the deep fading $1/H_m$.

where

$$F(w) \triangleq \sum_{k=a+1}^{b} \sum_{m\in\mathcal{M}} \beta \left(\left[\log(\frac{H_{nm}^k}{w}) \right]^+ - \left[1 - \frac{w}{H_{nm}^k} \right]^+ - \frac{\lambda_m^k}{\beta} \right)^+ + w\mathbb{U}_n(a,b) \ . \tag{6.30}$$

It is easy to verify that $F(w)$ is continuous and differentiable except at some points w_0 such that $\left[\log(\frac{H_{nm}^k}{w_0})\right]^+ - \left[1 - \frac{w_0}{H_{nm}^k}\right]^+ - \frac{\lambda_m^k}{\beta} = 0$. That is, the non-differentiable point satisfies $w = \tilde{H}_{nm}^k(w) \leq H_{nm}^k$. Specifically, at the differentiable point, the derivative of $F(w)$ can be written as

$$\begin{aligned} F'(w) &= -\sum_{k=a+1}^{b} \sum_{m\in\mathcal{M}} \beta \left(\frac{1}{w} - \frac{1}{H_{nm}^k} \right)^+ \mathbb{I}\left(\left[\log(\frac{H_{nm}^k}{w}) \right]^+ - \left[1 - \frac{w}{H_{nm}^k} \right]^+ - \frac{\lambda_m^k}{\beta} > 0 \right) + \mathbb{U}_n(a,b) \\ &= -\sum_{k=a+1}^{b} \sum_{m\in\mathcal{M}} \beta \left(\frac{1}{w} - \frac{1}{H_{nm}^k} \right)^+ \mathbb{I}\left(\frac{1}{w} - \frac{1}{\tilde{H}_{nm}^k(w)} > 0 \right) + \mathbb{U}_n(a,b) \ . \end{aligned} \tag{6.31}$$

And at the non-differentiable point, we have

$$\begin{cases} F'(w^+) = -\sum_{k=a+1}^{b} \sum_{m\in\mathcal{M}} \beta \left(\frac{1}{w} - \frac{1}{H_{nm}^k} \right)^+ \mathbb{I}\left(\frac{1}{w} - \frac{1}{\tilde{H}_{nm}^k(w)} > 0 \right) + \mathbb{U}_n(a,b) \\ F'(w^-) = -\sum_{k=a+1}^{b} \sum_{m\in\mathcal{M}} \beta \left(\frac{1}{w} - \frac{1}{H_{nm}^k} \right)^+ \mathbb{I}\left(\frac{1}{w} - \frac{1}{\tilde{H}_{nm}^k(w)} \geq 0 \right) + \mathbb{U}_n(a,b) \end{cases} . \tag{6.32}$$

Note that, since the Lagrangian duality function $F(w)$ is convex with respect to w [68], $F'(w^+)$ is non-decreasing with respect to w for all $w \geq 0$. Since $F'(w^-) \leq F'(w^+)$ for all $w \geq 0$, when we

use

$$\tilde{w} = \min \arg_w \{F'(w^+) \geq 0, w \geq 0\} \tag{6.33}$$

we always have $F'(\tilde{w}^-) \leq 0 \leq F'(\tilde{w}^+)$ and $\tilde{w}$ is the optimal dual variable for the problem in (6.20). In particular, when $\tilde{w}$ is a differentiable point, we have $F'(\tilde{w}^+) = F'(\tilde{w}^-) = 0$.

Moreover, by (6.28) and (6.32), (6.33) can be further written as

$$\tilde{w} = \min \arg_w \left\{ \mathbb{U}_n(a,b) - \sum_{k=a+1}^{b} \sum_{m \in \mathcal{M}} p_{nm}^k \geq 0 \right\} \tag{6.34}$$

$$= \min \arg_w \left\{ R_n(a,b) \geq 0 \right\} \tag{6.35}$$

where $R_n(a,b)$ is the energy residual defined in (6.18).

Since the dual problem in (6.20) is solved optimally, from the Lagrangian function $\mathcal{L}_n^{ab}(w_n^{ab}, \mathcal{P}_n, \mathcal{A}_n)$ in (6.19), it follows that $w_n^{ab} R_n(a,b)$ is the duality gap between the primal problem in (6.16)-(6.17) and the dual in (6.20) [68], where $R_n(a,b)$ is given in (6.18) and $w_n^{ab} = \tilde{w}$. In case that $R_n(a,b) = 0$, i.e., we can find a water level w such that the equality in (6.34) holds, then we have strong duality thus the energy-subchannel allocation obtained by solving the dual problem in (6.20) is optimal for the problem in (6.16)-(6.17).

Proposition 6.1. *The optimal solution to the dual problem in* (6.20) *follows the controlled water-filling in* (6.27), (6.28) *and* (6.34). *When the energy residual* $R_n(a,b) = 0$, *the strong duality holds and the obtained energy-subchannel allocation is optimal for the problem in* (6.16)-(6.17).

Remark 6.1. *Note that,* (6.27) *is not the unique optimal subchannel allocation. For example,* $a_{nm}^k = \mathbb{I}(1/w_n^{ab} - 1/\tilde{H}_{nm}^k(w) \geq 0)\mathbb{I}\left(w_n^{ab} \leq H_{nm}^k\right)$ *is also optimal for the inner maximization problem of* (6.20). *Specifically, given the optimal dual variable* $\tilde{w}$, *if there exists a unique* (m,k) *such that* $\tilde{H}_{nm}^k(\tilde{w}) = \tilde{w}$, *then* $a_{nm}^k = 0$ *and* 1 *are both optimal for the inner maximization problem in* (6.20). *When we take* $a_{nm}^k = 0$, *by* (6.34), *we always have* $\sum_{k=a+1}^{b} \sum_{m \in \mathcal{M}} p_{nm}^k \leq \mathbb{U}_n(a,b)$, *i.e., the obtained energy-subchannel allocation is feasible to the primal problem in* (6.16)-(6.17). *On the other hand, if we take* $a_{nm}^k = 1$, *the energy allocation may become infeasible since* $F'(\tilde{w})$ *is non-differentiable at* $\tilde{w}$ *and* $F'(\tilde{w}^-) = \mathbb{U}_n(a,b) - \sum_{k=a+1}^{b} \sum_{m \in \mathcal{M}} p_{nm}^k \leq 0$. *In case that we have multiple* (m,k) *such that* $\tilde{H}_{nm}^k(\tilde{w}) = \tilde{w}$, *to reduce the duality gap, we can modify* a_{nm}^k *from* 0 *to* 1 *for such* (m,k) *one by one until the energy allocation becomes infeasible. Obviously, these changes do not affect the optimality for the dual problem in* (6.20) *but the duality gap reduces as* $R_n(a,b)$ *decreases.*

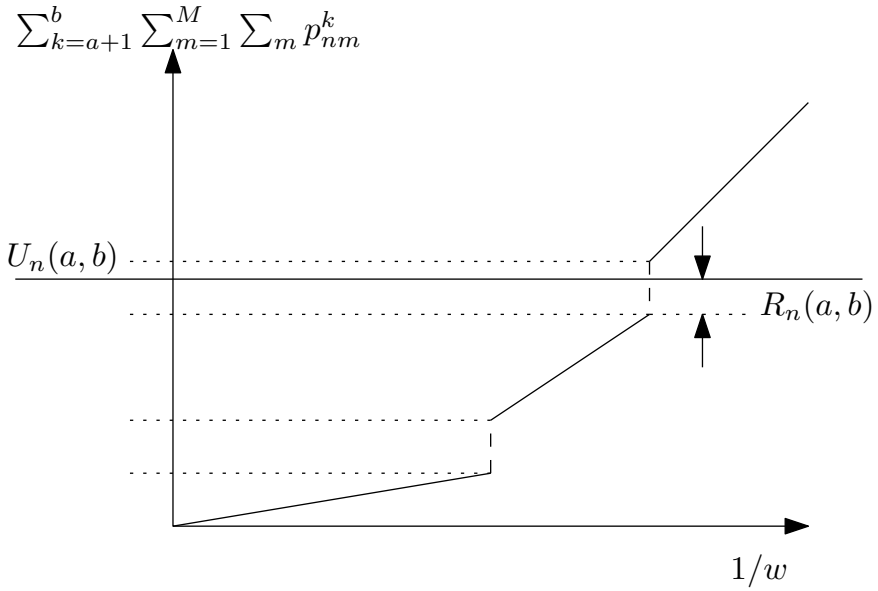

Figure 6.2: The relationship between the water level $1/w_n^{ab}$ and energy consumption $\sum_{k=a+1}^{b}\sum_{m} p_{nm}^{k}$ using controlled water-filling. When $\mathbb{U}_n(a,b)$ is between the marked two dotted-lines, $R_n(a,b)$ is the distance between $\mathbb{U}_n(a,b)$ and the lower dotted-line; otherwise, $R_n(a,b)=0$.

6.2.2 Performance Analysis

6.2.2.1 Duality Gap of the Problem in (6.16)-(6.17)

Recall that $w_n^{ab}R_n(a,b)$ is the duality gap between the primal problem in (6.16)-(6.17) and the dual problem in (6.20). To bound this gap, we first sketch the energy consumption $\sum_{k=a+1}^{b}\sum_{m\in\mathcal{M}} p_{nm}^{k}$ calculated by the controlled water-filling in (6.28) as a function of the water level $1/w$, shown in Fig. 6.2, which is not continuous. Note that, for a value of $\mathbb{U}_n(a,b)$ on the continuous segment of the curve, the corresponding water level $1/w$ is such that $R_n(a,b)=0$. Then, by Proposition 6.1, the strong duality holds for the problem in (6.16)-(6.17). On the other hand, for a value of $\mathbb{U}_n(a,b)$ in the discontinuous gap, the amount of unutilized energy $R_n(a,b)>0$ and the duality gap is $w_n^{ab}R_n(a,b)$.

Proposition 6.2. *The duality gap between the primal problem in* (6.16)-(6.17) *and the dual problem*

in (6.20) *is bounded by*

$$w_n^{ab} R_n(a,b) \leq \beta \max_{m\in\mathcal{M}, k\in[a+1,b]} \left\{1 - G(\lambda_m^k)\right\} \tag{6.36}$$

$$\leq \beta \tag{6.37}$$

where w_n^{ab} *is the optimal dual variable and* $G(\lambda)$ *is the root of* $x - \log x - 1 = \lambda/\beta$ *for* $0 \leq x \leq 1$. *Specifically,* $G(\lambda)$ *is a continuous and decreasing function, and* $G(0) = 1$.

Proof. By (6.31)-(6.32), for any $w \geq 0$, we have

$$F'(w^+) - F'(w^-) = \sum_{k=a+1}^{b} \sum_{m\in\mathcal{M}} \beta \left(\frac{1}{w} - \frac{1}{H_{nm}^k}\right)^+ \mathbb{I}\left(\frac{1}{w} - \frac{1}{\tilde{H}_{nm}^k(w)} = 0\right) . \tag{6.38}$$

When $\tilde{w}$ is the optimal dual variable for the problem in (6.20), by (6.18), $F'(\tilde{w}^+)$ is the energy residual after using the energy-subchannel allocation obtained by (6.28) and we also have $F'(\tilde{w}^-) \leq 0 \leq F'(\tilde{w}^+)$. Note that, as discussed in Remark 1, the energy residual may be further reduced by modifying some a_{nm}^k from 0 to 1 without affecting the optimality of the problem in (6.20) and the feasibility of the problem in (6.16)-(6.17). Thus $R_n(a,b)$ is bounded by

$$R_n(a,b) \leq F'(\tilde{w}^+) \tag{6.39}$$

$$\leq F'(\tilde{w}^+) - F'(\tilde{w}^-) \tag{6.40}$$

$$= \sum_{k=a+1}^{b} \sum_{m\in\mathcal{M}} \beta \left(\frac{1}{\tilde{w}} - \frac{1}{H_{nm}^k}\right)^+ \mathbb{I}\left(\frac{1}{\tilde{w}} - \frac{1}{\tilde{H}_{nm}^k(\tilde{w})} = 0\right) . \tag{6.41}$$

We next show that, after the procedure in Remark 1, (6.41) can be tightened as

$$R_n(a,b) \leq \beta \max_{m\in\mathcal{M}, k\in[a+1,b]} \left\{ \frac{1}{\tilde{H}_{nm}^k(\tilde{w})} - \frac{1}{H_{nm}^k} \mid \tilde{w} = \tilde{H}_{nm}^k(\tilde{w}) \leq H_{nm}^k \right\} . \tag{6.42}$$

Specifically, if there exists unique (m,k) such that $\tilde{H}_{nm}^k(\tilde{w}) = \tilde{w}$, then (6.42) holds trivially. If there are multiple (m,k) such that $\tilde{H}_{nm}^k(\tilde{w}) = \tilde{w}$, after the procedure in Remark 1, there must exist a subchannel that when this subchannel is used the energy residual becomes negative (i.e., the energy allocation becomes infeasible). Then, by contradiction, if (6.42) does not hold, for any (m,k) such that $\tilde{H}_{nm}^k(\tilde{w}) = \tilde{w}$ and $a_{nm}^k = 0$, using the subchannel m in slot k can always lead positive energy

residual, i.e.,

$$R_n(a,b) - \beta \left(\frac{1}{\tilde{H}^k_{nm}(\tilde{w})} - \frac{1}{H^k_{nm}} \right)^+ \tag{6.43}$$

$$> R_n(a,b) - \beta \max_{m\in\mathcal{M}, k\in[a+1,b]} \left\{ \frac{1}{\tilde{H}^k_{nm}(\tilde{w})} - \frac{1}{H^k_{nm}} \mid \tilde{w} = \tilde{H}^k_{nm}(\tilde{w}) \le H^k_{nm} \right\} \tag{6.44}$$

$$> 0 \ . \tag{6.45}$$

We next bound the duality gap $w^{ab}_n R_n(a,b)$. Note that, by (6.41), if there does not exist (n,k) such that $\tilde{H}^k_{nm}(w^{ab}_n) = w^{ab}_n$, we have $R_n(a,b) = 0$. Otherwise, by (6.42), we have

$$w^{ab}_n R_n(a,b) \le \max_{k\in[a+1,b], m\in\mathcal{M}} \left\{ w^{ab}_n \beta \left(\frac{1}{w^{ab}_n} - \frac{1}{H^k_{nm}} \right) \mid w^{ab}_n = \tilde{H}^k_{nm}(w^{ab}_n) \le H^k_{nm}, \right\} \tag{6.46}$$

$$\le \beta \max_{k\in[a+1,b], m\in\mathcal{M}} \left\{ 1 - \frac{w^{ab}_n}{H^k_{nm}} \mid w^{ab}_n = \tilde{H}^k_{nm}(w^{ab}_n) \le H^k_{nm} \right\} \tag{6.47}$$

$$\le \beta \ . \tag{6.48}$$

Moreover, we solve the following equation:

$$\tilde{H}^k_{nm}(w) \triangleq H^k_{nm} / e^{(1-\frac{w}{H^k_{nm}}) + \frac{\lambda^k_m}{\beta}} = w \tag{6.49}$$

$$\Longrightarrow \frac{w}{H^k_{nm}} - \log \frac{w}{H^k_{nm}} = 1 + \frac{\lambda^k_m}{\beta} \ . \tag{6.50}$$

Denoting $G(\lambda)$ as the root of $x - \log(x) = 1 + \lambda/\beta$, it is easy to verify that, when $0 \le x \le 1$, $G(\lambda)$ is a continuous decreasing function where $G(0) = 1$. Then, substituting $G(\lambda)$ into (6.47), we have (6.36). □

6.2.2.2 Performance Bound for Algorithm 6.2

Note that, Proposition 6.2 gives the bound on the duality gap between the primal problem in (6.16)-(6.17) and its dual problem in (6.20) for any adjacent BDP/BFPs; and Algorithm 6.2 solves such dual problems in (6.20) for all adjacent pairs $(a,b) \subseteq \mathcal{X}_n$. The next result bounds the gap between the output of Algorithm 6.2 and the optimal solution to the problem in (6.11)-(6.12).

Theorem 6.2. *Suppose that $(\tilde{\mathcal{P}}_n, \tilde{\mathcal{A}}_n)$ is the solution obtained by Algorithm 6.2 and $(\mathcal{P}^*_n, \mathcal{A}^*_n)$ is the optimal solution to the problem in* (6.11)-(6.12)*. The performance gap is bounded by*

$$U_{n,\Lambda}(\mathcal{P}^*_n, \mathcal{A}^*_n) - U_{n,\Lambda}(\tilde{\mathcal{P}}_n, \tilde{\mathcal{A}}_n) \le \sum_{(a,b)\subseteq\mathcal{X}_n} w^{ab}_n R_n(a,b) \tag{6.51}$$

$$\le K\beta \ , \tag{6.52}$$

where $\mathcal{X}_n$ is the (pseudo) BDP/BFP set obtained by Algorithm 6.2, $1/w_n^{ab}$ is the corresponding water level for any adjacent pair $(a,b) \subseteq \mathcal{X}_n$.

Proof. Introducing the dual variables $\Gamma_n \triangleq \{\gamma_n^k \geq 0, k \in \mathcal{K}\}$ and $\Theta_n \triangleq \{\theta_n^k \geq 0, k \in \mathcal{K}\}$, we define the Lagrangian function for the problem in (6.11)-(6.12) as

$$\begin{aligned}&\mathcal{L}_{n,\Lambda}(\Gamma_n, \Theta_n, \mathcal{P}_n, \mathcal{A}_n)\\ &\triangleq U_{n,\Lambda}(\mathcal{P}_n, \mathcal{A}_n) + \sum_{k\in\mathcal{K}} \gamma_n^k \left(E_n^k - \sum_{\kappa=1}^{k} \sum_{m\in\mathcal{M}} p_{nm}^{\kappa} \right) - \sum_{k\in\mathcal{K}} \theta_n^k \left(E_n^k - \sum_{\kappa=1}^{k} \sum_{m\in\mathcal{M}} p_{nm}^{\kappa} - B_n^{\max} \right) . \quad (6.53)\end{aligned}$$

Then, the dual problem of (6.11)-(6.12) is

$$\inf_{\Gamma_n,\Theta_n \,:\, \gamma_n^k\geq 0, \theta_n^k \geq 0} \left\{ \max_{\mathcal{A}_n,\mathcal{P}_n \,:\, a_{nm}^k \in \{0,1\}, p_{nm}^k \geq 0} \mathcal{L}_{n,\Lambda}(\Gamma_n, \Theta_n, \mathcal{P}_n, \mathcal{A}_n) \right\}. \quad (6.54)$$

Since the first-order condition is sufficient for the optimality of the inner maximization problem of (6.54) given $\mathcal{A}_n$, the optimal energy allocation is

$$p_{nm}^k = a_{nm}^k \beta \left[\frac{1}{w_n^k} - \frac{1}{H_{nm}^k} \right]^+ , \quad (6.55)$$

where the water level $1/w_n^k$ is determined by

$$w_n^k \triangleq \sum_{\kappa=k}^{K} (\gamma_n^{\kappa} - \theta_n^{\kappa}) . \quad (6.56)$$

For all adjacent pair $(a,b) \subseteq \mathcal{X}_n$, we denote $\tilde{w}_n^k \triangleq w_n^{ab}$ for all $k \in [a+1, b]$. Then, for $k = 1, 2, \ldots, K-1$, we calculate $\tilde{\theta}_n^k \geq 0$ and $\tilde{\gamma}_n^k \geq 0$ based on $\tilde{w}_n^k$ and $\tilde{w}_n^{k+1}$ by the following rules: when $\tilde{w}_n^k > \tilde{w}_n^{k+1}$, we set $\tilde{\gamma}_n^k = \tilde{w}_n^k - \tilde{w}_n^{k+1}$ and $\tilde{\theta}_n^k = 0$; when $\tilde{w}_n^k < \tilde{w}_n^{k+1}$, we set $\tilde{\gamma}_n^k = 0$ and $\tilde{\theta}_n^k = \tilde{w}_n^{k+1} - \tilde{w}_n^k$; when $\tilde{w}_n^k = \tilde{w}_n^{k+1}$, we set $\tilde{\theta}_n^k = \tilde{\gamma}_n^k = 0$. Moreover, for $k = K$, we set $\tilde{\gamma}_n^K = \tilde{w}_n^K$ and $\tilde{\theta}_n^K = 0$. Note that, by Lemma 6.1, the water level $1/\tilde{w}_n^k$ may only increase/decrease at (pseudo) BDP/BFPs, respectively. Then, we have $\tilde{\gamma}_n^k > 0$ only if k is a (pseudo) BDP and $\tilde{\theta}_m^k > 0$ only if k is a (pseudo) BFP, and $\tilde{\gamma}_n^k = 0$ and $\tilde{\theta}_m^k = 0$ otherwise.

Denoting $\tilde{\Gamma}_n \triangleq \{\tilde{\gamma}_n^k, k \in \mathcal{K}\}$ and $\tilde{\Theta}_n \triangleq \{\tilde{\theta}_n^k, k \in \mathcal{K}\}$, by the weak duality, we always have

$$\begin{aligned}U_{n,\Lambda}(\mathcal{P}_n^*, \mathcal{A}_n^*) - U_{n,\Lambda}(\tilde{\mathcal{P}}_n, \tilde{\mathcal{A}}_n) &\leq \min_{\gamma_n^k\geq 0, \theta_n^k \geq 0} \max_{a_{nm}^k \in \{0,1\}, p_{nm}^k \geq 0} \mathcal{L}_{n,\Lambda}(\Gamma_n, \Theta_n, \mathcal{P}_n, \mathcal{A}_n) - U_{\Lambda}(\tilde{\mathcal{P}}_n, \tilde{\mathcal{A}}_n)\\ &\leq \max_{a_{nm}^k \in \{0,1\}, p_{nm}^k \geq 0} \mathcal{L}_{n,\Lambda}(\tilde{\Gamma}_n, \tilde{\Theta}_n, \mathcal{P}_n, \mathcal{A}_n) - U_{n,\Lambda}(\tilde{\mathcal{P}}_n, \tilde{\mathcal{A}}_n) . \quad (6.57)\end{aligned}$$

By removing the terms with $\tilde{\gamma}_n^k = 0$ and/or $\tilde{\theta}_n^k = 0$ in (6.53), we have

$$\begin{aligned}
&\max_{a_{nm}^k \in \{0,1\}, p_{nm}^k \geq 0} \mathcal{L}_{n,\Lambda}(\tilde{\Gamma}_n, \tilde{\Theta}_n, \mathcal{P}_n, \mathcal{A}_n) \\
&= \max_{a_{nm}^k \in \{0,1\}, p_{nm}^k \geq 0} \{U_{n,\Lambda}(\mathcal{P}_n, \mathcal{A}_n) \\
&\quad + \sum_{k \in \mathcal{X}_n \text{ is BDP}} \tilde{\gamma}_n^k \left(E_n^k - \sum_{\kappa=1}^{k} \sum_{m \in \mathcal{M}} p_{nm}^\kappa \right) - \sum_{k \in \mathcal{X}_n \text{ is BFP}} \tilde{\theta}_n^k \left(E_n^k - \sum_{\kappa=1}^{k} \sum_{m \in \mathcal{M}} p_{nm}^\kappa - B_n^{\max} \right) \Bigg\} .
\end{aligned} \tag{6.58}$$

Note that, since $E_n^0 = 0$ and $B_n^0 = 0$ (i.e., $k = 0$ is a BDP), for any (pseudo) BDP/BFP $k \in \mathcal{X}_n$, we have

$$\begin{aligned}
&E_n^k - \sum_{\kappa=1}^{k} \sum_{m \in \mathcal{M}} p_{nm}^\kappa \\
&= \left(E_n^k - E_n^0 - \sum_{\kappa=1}^{k} \sum_{m \in \mathcal{M}} p_{nm}^\kappa + \mathbb{I}(0 \text{ is BFP}) B_n^{\max} - \mathbb{I}(k \text{ is BFP}) B_n^{\max} \right) + \mathbb{I}(k \text{ is BFP}) B_n^{\max} \\
&= \sum_{(a,b) \subseteq \mathcal{X}_n, b \leq k} \left(E_n^b - E_n^a + \mathbb{I}(a \text{ is BFP}) B_n^{\max} - \mathbb{I}(b \text{ is BFP}) B_n^{\max} - \sum_{\kappa=a+1}^{b} \sum_{m \in \mathcal{M}} p_{nm}^\kappa \right) + \mathbb{I}(k \text{ is BFP}) B_n^{\max} \\
&= \sum_{(a,b) \subseteq \mathcal{X}_n, b \leq k} \left(\mathbb{U}_n(a,b) - \sum_{\kappa=a+1}^{b} \sum_{m \in \mathcal{M}} p_{nm}^\kappa \right) + \mathbb{I}(k \text{ is BFP}) B_n^{\max} .
\end{aligned} \tag{6.59}$$

Substituting (6.59) into (6.58), we further have

$$\begin{aligned}
&\max_{a_{nm}^k\in\{0,1\},p_{nm}^k\geq 0} \mathcal{L}_{n,\Lambda}(\tilde{\Gamma}_n,\tilde{\Theta}_n,\mathcal{P}_n,\mathcal{A}_n)\\
&=\max_{a_{nm}^k\in\{0,1\},p_{nm}^k\geq 0}\left\{U_{n,\Lambda}(\mathcal{P}_n,\mathcal{A}_n)+\sum_{k\in\mathcal{X}_n \text{ is BDP}}\tilde{\gamma}_n^k\sum_{(a,b)\subseteq\mathcal{X}_n,b\leq k}\left(\mathbb{U}_n(a,b)-\sum_{\kappa=a+1}^{b}\sum_{m\in\mathcal{M}}p_{nm}^{\kappa}\right)\right.\\
&\quad\left.-\sum_{k\in\mathcal{X}_n \text{ is BFP}}\tilde{\theta}_n^k\left(\sum_{(a,b)\subseteq\mathcal{X}_n,b\leq k}\left(\mathbb{U}_n(a,b)-\sum_{\kappa=a+1}^{b}\sum_{m\in\mathcal{M}}p_{nm}^{\kappa}\right)+B_n^{\max}-B_n^{\max}\right)\right\}\\
&=\max_{a_{nm}^k\in\{0,1\},p_{nm}^k\geq 0}\left\{U_{n,\Lambda}(\mathcal{P}_n,\mathcal{A}_n)+\sum_{(a,b)\subseteq\mathcal{X}_n}\left(\mathbb{U}_n(a,b)-\sum_{\kappa=a+1}^{b}\sum_{m\in\mathcal{M}}p_{nm}^{\kappa}\right)\sum_{\kappa=a+1}^{K}\left(\tilde{\gamma}_n^{\kappa}-\tilde{\theta}_n^{\kappa}\right)\right\}
\end{aligned}\tag{6.60}$$

$$\begin{aligned}
&=\sum_{(a,b)\subseteq\mathcal{X}_n}\max_{a_{nm}^k\in\{0,1\},p_{nm}^k\geq 0}\left\{\sum_{k=a+1}^{b}\sum_{m\in\mathcal{M}}\beta a_{nm}^k\left[\log(1+\frac{p_{nm}^k H_{nm}^k}{\beta})-\frac{\lambda_m^k}{\beta}\right]\right.\\
&\quad\left.+\left(\mathbb{U}_n(a,b)-\sum_{k=a+1}^{b}\sum_{m\in\mathcal{M}}p_{nm}^k\right)w_n^{ab}\right\}\\
&=U_{n,\Lambda}(\tilde{\mathcal{P}}_n,\tilde{\mathcal{A}}_n)+\sum_{(a,b)\subseteq\mathcal{X}_n}\left(\mathbb{U}_n(a,b)-\sum_{k=a+1}^{b}\sum_{m\in\mathcal{M}}\tilde{p}_{nm}^k\right)w_n^{ab} \qquad (6.61)\\
&=U_{n,\Lambda}(\tilde{\mathcal{P}}_n,\tilde{\mathcal{A}}_n)+\sum_{(a,b)\subseteq\mathcal{X}_n}R_n(a,b)w_n^{ab}\ , \qquad (6.62)
\end{aligned}$$

where (6.60) follows since $\gamma_m^k=0$ if k is not a (pseudo) BDP and $\theta_m^k=0$ if k is not a (pseudo) BFP, and (6.61) follows since $(\tilde{\mathcal{P}}_n,\tilde{\mathcal{A}}_n)$ is obtained by solving the dual problem in (6.20) for all adjacent pairs $(a,b)\subseteq\mathcal{X}_n$ where w_n^{ab} is corresponding optimal dual variable. Then, using (6.57), (6.51) follows. Moreover, by Proposition 6.2, we further have

$$U_{n,\Lambda}(\mathcal{P}_n^*,\mathcal{A}_n^*)-U_{n,\Lambda}(\tilde{\mathcal{P}}_n,\tilde{\mathcal{A}}_n)\leq\sum_{(a,b)\subseteq\mathcal{X}_n}\beta\leq K\beta\ . \tag{6.63}$$

□

Note that, if the strong duality of the problem in (6.16)-(6.17) holds, the energy-subchannel allocation obtained by solving the dual problem is also optimal for the primal problem, and by Proposition 6.1 we have $R_n(a,b)=0$. Then, when the strong duality of the problem in (6.16)-(6.17) holds for all adjacent pairs $(a,b)\subseteq\mathcal{X}_n$, we have $R_n(a,b)=0$ for all adjacent pair $(a,b)\subseteq\mathcal{X}_n$, and by Theorem 6.2 we further have the following corollary.

Corollary 6.1. *Let $\mathcal{X}_n$ be the BDP/BFP set obtained by Algorithm 6.2. If the strong duality of the problem in* (6.16)-(6.17) *holds for all adjacent pairs $(a, b) \subseteq \mathcal{X}_n$, the energy-subchannel allocation obtained by Algorithm 6.2 is optimal for the problem in* (6.11)-(6.12).

Moreover, if we let $M \to \infty$ and $B = o(B)$, then $\beta \to 0$ and by Theorem 6.2, the gap to optimality diminishes.

Corollary 6.2. *The energy-subchannel allocation obtained by Algorithm 6.2 is asymptotically optimal for the problem in* (6.11)-(6.12) *when $M \to \infty$ and $B = o(M)$.*

If the price-based energy-subchannel allocation problem in (6.11)-(6.12) can be solved optimally, then the dual problem in (6.6)-(6.7) is solved optimally by Algorithm 6.1. By Theorem 6.1, when $M \to \infty$ and $B = o(M)$, we have the strong duality for the original problem in (6.3)-(6.4). And thus the obtained primal solution is optimal to the original problem.

Corollary 6.3. *When $M \to \infty$ and $B = o(M)$, the energy-subchannel allocation obtained by Algorithm 6.1 is asymptotically optimal for the original problem in* (6.3)-(6.4).

6.2.3 Final Energy-Subchannel Allocation Adjustment

In general, Algorithm 6.2 is suboptimal for solving the problem in (6.11)-(6.12). Thus the optimality of the dual problem in (6.6)-(6.7) may not be achieved even with an infinite number of subgradient updates, and the obtained subchannel allocation in step 2 of Algorithm 6.1 may be infeasible, i.e., a subchannel may be allocated to more than one transmitter. To recover the feasibility of the obtained subchannel allocation, for any (m, k) such that $\sum_{n\in\mathcal{N}} \tilde{a}_{nm}^k > 1$, we will only retain the strongest transmitter, i.e., for the strongest transmitter $n_0 \triangleq \arg\max_n \left\{p_{nm}^k H_{nm}^k\right\}$, we keep $\tilde{a}_{n_0 m}^k = 1$, and for other transmitters, we update $\tilde{a}_{nm}^k \leftarrow 0$, $R_n(a, b) \leftarrow R_n(a, b) + \tilde{p}_{nm}^k$ and then set $\tilde{p}_{nm}^k \leftarrow 0$. Note that, although in theory the feasibility is a potential issue of the proposed algorithm, simulations show that Algorithm 6.1 yields feasible solution most of the time.

Recall that as well as the above feasibility recovery of the subchannel allocation, the positive energy residual $R_n(a, b)$ is introduced by the weak duality of the problem in (6.16)-(6.17) that may be zero. Note that, the objective function in (6.3) is non-decreasing with respect to p_{nm}^k. We next focus on the segment between slots a and b such that $R_n(a, b)$ is larger than a positive threshold (namely *target segment*), and reallocate the energy residual to improve the performance.

Specifically, for each target segment $(a, b) \subseteq \mathcal{X}_n$, the energy surplus can be written as for $k \in [a+1, b]$:

$$R_n^k \triangleq \mathbb{I}(a \text{ is BFP}) B_n^{\max} + E_n^k - E_n^a - \sum_{\kappa=a+1}^{k} \sum_{m \in \mathcal{M}} \tilde{p}_{nm}^{\kappa} \ , \tag{6.64}$$

which contains the energy residual that can be reallocated in the current slot, i.e., the reallocatable energy, and the energy reserved for future use according to the energy allocation $\tilde{p}_{nm}^k$. In particular, we have $R_n(a, b) = R_n^b - \mathbb{I}(b \text{ is BFP}) B_b^{\max}$.

Note that, when we reallocate E_0 to subchannel m_0 in slot k_0, i.e., $p_{nm_0}^{k_0} \leftarrow p_{nm_0}^{k_0} + E_0$, by (6.64), R_n^k is decreased by E_0 for all $k \in [k_0, b]$. Since the energy surplus cannot be negative, the reallocatable energy accumulated by slot k can be written as

$$\bar{E}_n^k \triangleq \min_{\kappa \in [k,b]} \{R_n^{\kappa}, R_n^b - \mathbb{I}(b \text{ is BFP}) B_b^{\max}\} \ , \tag{6.65}$$

i.e., given $\tilde{p}_{nm}^k$ we cannot reallocate more than a total of $\bar{E}_n^k$ to the slots before k otherwise the energy surplus becomes negative for some slot after k and/or b is no longer a BFP. Then, the increment of the reallocatable energy in adjacent slots, i.e., $\bar{E}_n^k - \bar{E}_n^{k-1}$, is the energy residual newly introduced in slot k and, we can reallocate the increment to the allocated channels evenly for immediate use:

$$r_{nm}^k = \begin{cases} (\bar{E}_n^k - \bar{E}_n^{k-1}) / \sum_{m' \in \mathcal{M}} a_{nm'}^k & \text{if } a_{nm}^k = 1 \\ 0 & \text{if } a_{nm}^k = 0 \end{cases} \tag{6.66}$$

and

$$\tilde{p}_{nm}^k \leftarrow \tilde{p}_{nm}^k + r_{nm}^k \tag{6.67}$$

for all $k \in [a+1, b]$ such that $\bar{E}_n^k - \bar{E}_n^{k-1} > 0$ and $m \in \mathcal{M}$. Specifically, using the reallocation in (6.66), we have $\sum_{k=a+1}^{b} \sum_{m \in \mathcal{M}} r_{nm}^k = R_n(a, b)$.

6.3 Causal Energy-Subchannel Allocation

So far we have assumed that both the harvested energy and the channel states for future K time slots are known in advance for energy-subchannel allocation. In this section, we consider a causal scheduling mechanism where we assume each transmitter can only observe the current battery level and channel gains at the beginning of each slot. In our proposed causal scheme, at the beginning of each slot, each transmitter determines its *total transmission energy* based on the battery level,

and then the energy-subchannel allocation for the current slot is calculated by solving a one-shot energy-subchannel allocation problem. We will make use of the statistics of the energy harvesting and channel fading processes in computing the total transmission energy policy.

Denoting $\pi_n(b)$ as the decision policy for the total transmission energy (i.e., at any slot, given the battery level b, transmitter n spends $\pi_n(b)$ transmission energy in this slot), we formulate the following problem to maximize the sum of discounted expected utilities $J^k(\boldsymbol{\pi}(\boldsymbol{B}^{k-1}))$ by choosing a proper total transmission energy policy:

$$\max_{\pi_n(b)\,:\,0\le\pi_n(b)\le b} \mathbb{E}_{\{\boldsymbol{H}^k,\tilde{\boldsymbol{E}}^k,k=1,2,\ldots\}}\left[\sum_k \eta^{k-1} J^k(\boldsymbol{\pi}(\boldsymbol{B}^{k-1}))\right] , \tag{6.68}$$

where $\boldsymbol{B}^{k-1} \triangleq [B_1^{k-1}, B_2^{k-1}, \ldots, B_N^{k-1}]$ is the vector of the battery levels at the beginning of slot k, $\boldsymbol{H}^k \triangleq [H_{11}^k, H_{12}^k, \ldots, H_{NM}^k]$ and $\tilde{\boldsymbol{E}}^k \triangleq [\tilde{E}_1^k, \tilde{E}_2^k, \ldots, \tilde{E}_N^k]$ are the vectors of the channel gains and harvested energy in slot k, respectively, $\boldsymbol{\pi}(\boldsymbol{B}^{k-1}) \triangleq [\pi_1(B_1^{k-1}), \pi_2(B_2^{k-1}) \ldots, \pi_N(B_N^{k-1})]$ is the vector of the total transmission energy, $\eta \in [0, 1)$ is the discount factor, and the battery level is updated by

$$B_n^k = \min\{B_n^{\max}, B_n^{k-1} + \tilde{E}_n^k - \pi_n(B_n^{k-1})\} . \tag{6.69}$$

Specifically, in (6.68), we define the utility function as the maximum sum-rate in slot k given the total transmission energy $\boldsymbol{\pi}(\boldsymbol{B}^{k-1})$, i.e.,

$$J^k(\boldsymbol{\pi}(\boldsymbol{B}^{k-1})) \triangleq \max_{a_{nm}^k, p_{nm}^k} \left\{\sum_n \sum_m \beta a_{nm}^k \log(1 + p_{nm}^k H_{nm}^k/\beta)\right\} , \tag{6.70}$$

subject to

$$\begin{cases} \sum_m p_{nm}^k \le \pi_n(B_n^{k-1}) & n \in \mathcal{N} \\ \sum_n a_{nm}^k \le 1 & m \in \mathcal{M} \\ p_{nm}^k \ge 0 & n \in \mathcal{N}, m \in \mathcal{M} \\ a_{nm}^k \in \{0, 1\} & n \in \mathcal{N}, m \in \mathcal{M} \end{cases} . \tag{6.71}$$

Note that, the one-shot energy-allocation problem in (6.70)-(6.71) is a special case of the problem in (6.3)-(6.4) where $K = 1$ and $E_n^1 = \pi_n(B_n^{k-1})$, and thus it can be solved by Algorithm 6.1. Moreover, when $K = 1$, in Algorithm 6.1, the solution to the price-based energy-bandwidth allocation in (6.11)-(6.12) is given in closed-form, i.e., (a_{nm}^k, p_{nm}^k) are given by (6.27)-(6.28), respectively, where the water level $1/w_n^k$ is determined by $w_n^k = \min \arg_w \left\{\pi_n(B_n^{k-1}) - \sum_{m\in\mathcal{M}} p_{nm}^k \ge 0\right\}$.

The problem in (6.68) is an infinite-horizon Markov decision process (MDP) consisting of N independent Markov chains. Since each transmitter can only observe its own battery level, the utility has to be viewed as a stochastic function by each transmitter, where the randomness is introduced by the other transmitters' battery levels, channel gains, and total transmission energy policies. For each transmitter, since the statistic of the stochastic utility function is hard to characterize, we use the Q-learning technique [78] to obtain the total transmission energy policy. In general, Q-learning is a useful numerical method to solve an MDP problem with stochastic utility function [78][79].

We first define the Q-function $Q_n(b,p)$, which represents the expected utility if transmitter n chooses the total transmission energy p when its battery level is b. Then, in each iteration i, the Q-function can be updated as follows [78]:

$$Q_n(B_n^{i-1},P_n^i) \leftarrow Q_n(B_n^{i-1},P_n^i)+\alpha^i\left[J^i(\boldsymbol{\pi}(\boldsymbol{B}^{i-1}))+\eta \max_{0\le p\le B_n^i} Q_n(B_n^i,p)-Q_n(B_n^{i-1},P_n^i)\right] , \quad (6.72)$$

where $\alpha^i \in [0,1]$ is the learning rate, $\eta \in [0,1)$ is the discount factor, and

$$P_n^i \leftarrow \pi_n(B_n^{i-1}) = \begin{cases} \arg\max_{0\le p\le B_n^{i-1}} Q_n(B_n^{i-1},p) & \text{with probability of } 1-\epsilon \\ \text{random } p\in[0,B_n^{i-1}] & \text{with probability of } \epsilon \end{cases} . \quad (6.73)$$

is the total transmission energy for transmitter n. Note that both B_n^i and P_n^i are discretized and therefore (6.72) amounts to updating an element in a two-dimensional lookup table in each iteration. Under certain conditions, $Q_n(b,p)$ converges to the expected utility corresponding to the optimal $\pi_n(b)$ in (6.68), with probability 1 [78]. Specifically, the lookup tables $\{Q_n(b,p), n\in\mathcal{N}\}$ are computed offline, using the realizations of the energy harvesting and channel fading processes $\tilde{\boldsymbol{E}}^k$ and $\boldsymbol{H}^k$. For the online energy-subchannel allocation, at the beginning of slot k, given the battery level B_n^{k-1}, the total transmission energy is given by

$$\pi_n(B_n^{k-1}) = \arg \max_{0\le p\le B_n^{k-1}} Q_n(B_n^{k-1},p) , \quad (6.74)$$

for all $n\in\mathcal{N}$.

The procedure for computing $\{Q_n(b,p), n\in\mathcal{N}\}$ is summarized as follows.

Algorithm 6.3 - Computing the total transmission energy policy by Q-learning

1: Initialization: Randomly generate the non-negative Q-function such that $Q_n(b,p) = 0$ for $p > b$ for all $n \in \mathcal{N}$, specify $\epsilon > 0, \alpha > 0$, $0 < \eta < 1$, and $I > 0$

2 $i \leftarrow 0$

REPEAT

Calculate $\boldsymbol{\pi}(\boldsymbol{B}^{i-1})$ using (6.73)

Calculate $J^i(\boldsymbol{\pi}(\boldsymbol{B}^{i-1})$ by solving the problem in (6.70)-(6.71)

Update $\boldsymbol{B}^i$ using (6.69)

Update $Q_n(B_n^{i-1}, P_n^i)$ using (6.72) for all $n \in \mathcal{N}$

IF $Q_n(b,p)$ converges **OR** $i = I$

Obtain the policy $\pi_n(b) \leftarrow \arg\max_{0 \le p \le b} Q_n(b,p)$ and stop

ELSE

$i \leftarrow i + 1$

ENDIF

6.4 Simulation Results

Suppose that there are $N = 4$ transmitters in the network and the scheduling period is $K = 20$ slots. We assume that the total bandwidth is $B = 2$ MHz and divide the channel into $M = 16$ subchannels. For each transmitter n, we set the initial battery level as $B_n^0 = 0$ and the battery capacity as $B_n^{\max} = 6$ units. Assume that the harvested energy in each slot follows a truncated Gaussian distribution with mean μ and variance 1.5 and the channel is frequency-selective Rayleigh fading, where the delay spread is $\sigma_\tau = 1\ \mu s$, the number of the paths is $3\lfloor \sigma_\tau B \rfloor = 6$, the power of the j-th path is $\sigma_j^2 = \sigma_h^2 \exp(-\frac{j}{\sigma_\tau B})$, and σ_h^2 is chosen to normalize the path loss to $\sum_{j=1}^{6} \sigma_j^2/\beta = \sigma$, where σ^2 is the channel parameter. Moreover, in Algorithm 6.3, we set the discount factor $\eta = 0.9$, the Q-learning exploration probability $\epsilon = 0.1$, the learning factor $\alpha = 0.2$, the discretization step for the battery level, energy, and the decision policy is 0.3, and the maximum iteration number is $I = 2 \times 10^5$ iterations.

For comparison, we consider two greedy scheduling strategies, namely, the *energy greedy policy* (with the optimized subchannel) and the *energy-subchannel greedy policy*. For the energy greedy policy, each transmitter tries to use up its available energy in each slot, i.e., $\sum_m p_{nm}^k = B_n^k$.

Then, given the available energy, we calculate the energy-subchannel allocation by solving the problem in (6.3)-(6.4) for $K = 1$ using Algorithm 6.1. For the energy-subchannel greedy policy, the subchannel is always allocated to the transmitter with the best channel gain, i.e., $a_{nm}^k = \mathbb{I}(n = \arg\max_n\{H_{nm}^k, \forall n \in \mathcal{N}\})$, and each transmitter tries to use up its available energy in each slot, i.e., $\sum_m p_{nm}^k = B_n^k$. Then, given the subchannel allocation, we always split the available energy to each allocated subchannel evenly. Moreover, since Algorithm 6.1 solves the dual of the problem in (6.3)-(6.4), the Lagrangian duality function is an upper-bound on the performance of the optimal energy-subchannel allocation $(\mathcal{P}_n^*, \mathcal{A}_n^*)$, i.e.,

$$\sum_{n\in\mathcal{N}} C_n(\mathcal{P}_n^*, \mathcal{A}_n^*) \leq \max_{\mathcal{P},\mathcal{A} \text{ satisfies (6.7)}} \mathcal{L}(\mathcal{P}, \mathcal{A}, \Lambda_0) \tag{6.75}$$

$$= \max_{\mathcal{P}_n,\mathcal{A}_n \text{ satisfy (6.12) for } n\in\mathcal{N}} \left\{ \sum_{n\in\mathcal{N}} U_{n,\Lambda_0}(\mathcal{P}_n, \mathcal{A}_n) + \sum_{k\in\mathcal{K}} \sum_{m\in\mathcal{M}} \lambda_m^k \right\} \tag{6.76}$$

where Λ_0 the channel price obtained by Algorithm 6.1. Since Algorithm 6.2 solves the price-based energy-allocation problem in (6.11)-(6.12), by Theorem 6.2, (6.76) can be further bounded by

$$\sum_{n\in\mathcal{N}} C_n(\mathcal{P}_n^*, \mathcal{A}_n^*) \leq \sum_{n\in\mathcal{N}} \left(U_{n,\Lambda_0}(\tilde{\mathcal{P}}_n, \tilde{\mathcal{A}}_n) + \sum_{(a,b)\subseteq\mathcal{X}_n} R_n(a,b) \right) + \sum_{k\in\mathcal{K}} \sum_{m\in\mathcal{M}} \lambda_m^k \tag{6.77}$$

$$\leq \mathcal{L}(\tilde{\mathcal{P}}, \tilde{\mathcal{A}}, \Lambda_0) + \sum_{n\in\mathcal{N},(a,b)\subseteq\mathcal{X}_n} R_n(a,b) \tag{6.78}$$

where $(\tilde{\mathcal{P}}, \tilde{\mathcal{A}})$ is the energy-subchannel allocation obtained by Algorithm 6.2 and $\mathcal{X}_n$ is the corresponding (pseudo) BDP/BFP set. We use (6.78) as an upper-bound on the sum-rate of the optimal energy-subchannel allocation.

To evaluate the performance of the different algorithms/policies, we consider two scenarios, *energy-harvesting varying scenario* (EH scenario), where we fix the channel parameter $\sigma^2 = 1$ and simulate for various means of the harvested energy $\mu = 1.6, 1.8, 2.0, 2.2, 2.4, 2.6$, and *channel-fading varying scenario* (CF scenario), where we fix the mean of the harvested energy $\mu = 2$ and simulate for various channel parameters $\sigma^2 = 0.7, 0.8, 0.9, 1.0, 1.1, 1.2$. For each scenario, we run the simulation 500 times to compare the performances of the proposed non-causal algorithm (Algorithm 6.1) with and without the energy residual reuse, respectively, the causal algorithm (Algorithm 6.3), the energy greedy policy, and the energy-subchannel greedy policy, along with the upper-bound on the optimal performance given in (6.78), as shown in Figs. 6.3 and 6.4 for EH and CF scenarios, respectively.

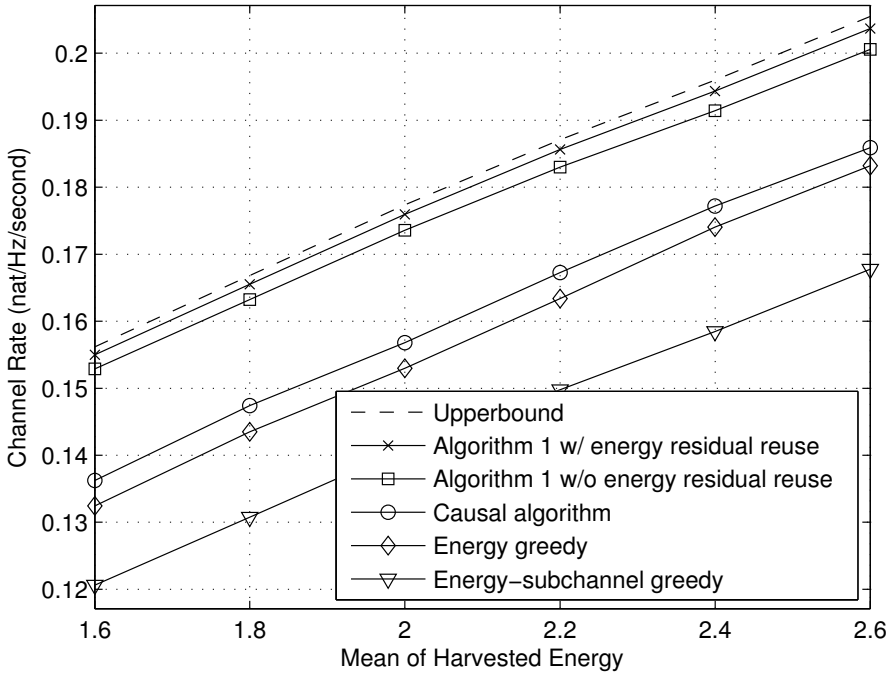

Figure 6.3: Performance comparisons for various energy harvesting mean parameter μ (EH scenario).

It is seen from Figs. 6.3 and 6.4 that the proposed non-causal algorithm with energy residual reuse achieves the best performance, which is close to the upper-bound on the optimal performance and slightly better than the non-causal algorithm without energy residual reuse. For the causal algorithm, since the energy-subchannel allocation is calculated without using the predictions of the harvested energy and subchannel gains in the future slots, it performs worse as compared to the proposed non-causal algorithm, as expected. Although both the causal algorithm and energy greedy policy optimize the subchannel allocation given the total energy spending in each slot, the causal algorithm performs better because it learns the relationship between the total energy expenditure and the sum-rate from the past slots and then uses it to decide the energy spending in the current slot. Moreover, the energy-subchannel greedy policy performs the worst among the simulated algorithms/policies. For both scenarios and algorithms/policies, the performance improves as the mean of the energy harvesting or the channel parameter increases.

Next, we set $\sigma^2 = 1$, $\mu = 2$, and the initial $\lambda_m^k = 0$ to examine the convergence of Algorithm

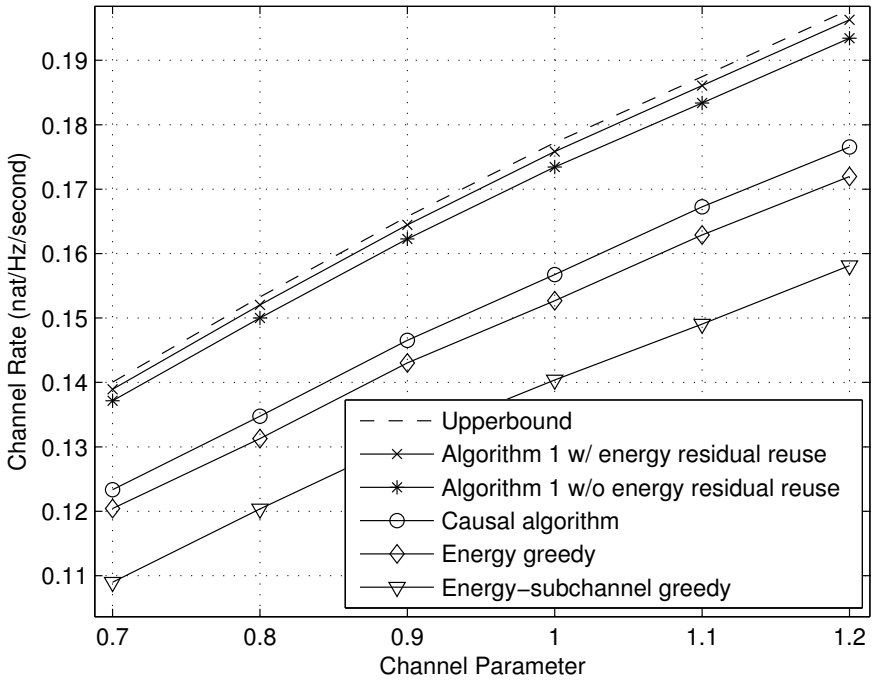

Figure 6.4: Performance comparisons for various channel parameter σ^2 (CF scenario).

6.1. We compare the upper-bound on the optimal performance and the sum-rate achieved by the obtained feasible energy-subchannel allocation with and without the reuse of the energy residual, respectively, over the iterations. It can be seen from Fig. 6.5 that the upper-bound on the optimal performance decreases and the sum-rate increases with iterations, respectively. The three curves converge after around 30 iterations and finally leave a small gap due to the weak duality of the problem in (6.3)-(6.4) and the suboptimality of Algorithm 6.2. We note that, after utilizing the energy residual, the performance of Algorithm 6.1 improves and the gap to the upper-bound on the optimal performance decreases. Specifically, this gap represents the maximum rate loss of the proposed non-causal algorithm compared with the optimal solution. Moreover, in Fig. 6.6, we show the number of the occurrences that a subchannel is allocated to more than one transmitter (which is called conflict) for the allocation obtained by Algorithm 6.1 over the iterations. It is seen that the number of the conflicts decreases in general and finally drops to 0 after 27 iterations.

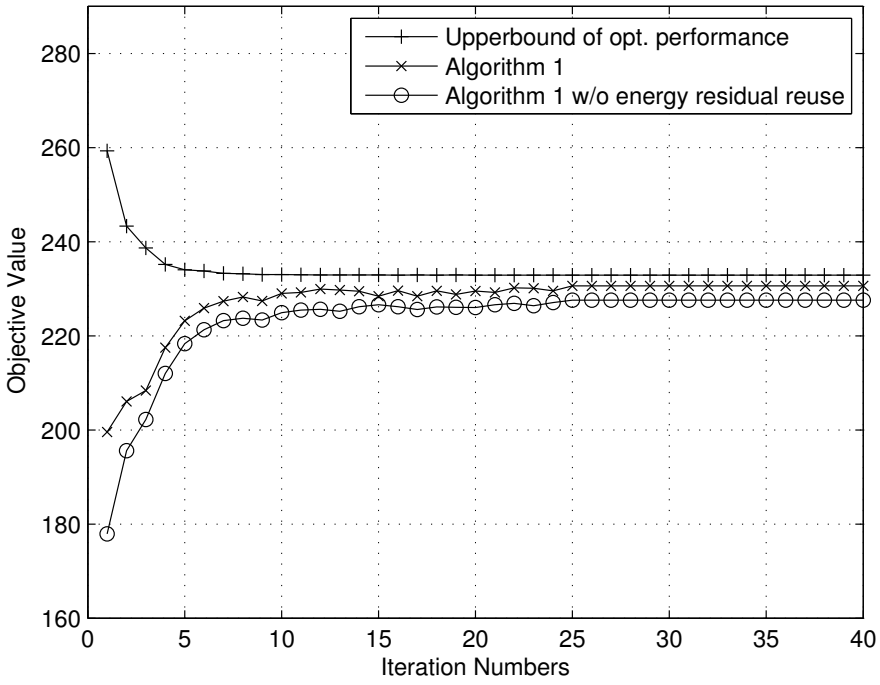

Figure 6.5: The convergence of Algorithm 6.1 over iterations.

6.5 Conclusions

We have considered the energy-subchannel scheduling problem for multiple energy harvesting transmitters in frequency-selective fading channels. Assuming that the harvested energy and channel gains can be predicted for the scheduling period, we have developed an algorithm to obtain the energy-subchannel allocation for the scheduling period for each transmitter. Although the joint energy-subchannel scheduling problem is a mixed integer program and non-convex, it is shown that the proposed algorithm is asymptotically optimal when the bandwidth of each subchannel goes to zero. A causal algorithm is also proposed based on the Q-learning method that makes use of the statistics of the energy harvesting and channel fading processes. Simulation results demonstrate that the proposed non-causal algorithm performs closely to the upper-bound on the optimal performance and the proposed causal algorithm outperforms several heuristic allocation policies.

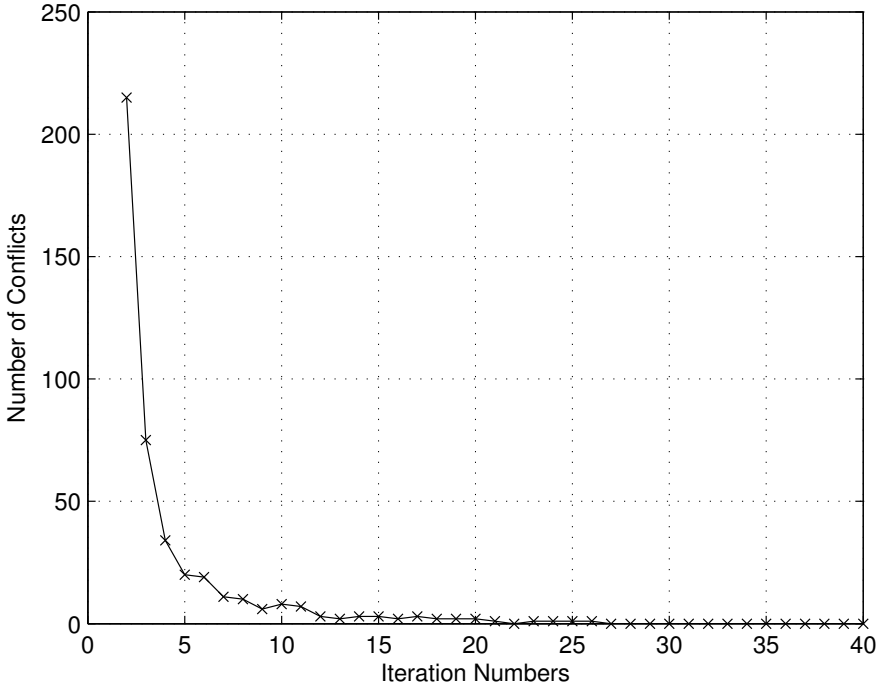

Figure 6.6: The number of subchannel conflicts over iterations.

Chapter 7

Conclusions

Motivated by the rapid developments of energy harvesting technologies and the increasing demands for wireless communication systems, we focused on the energy harvesting communications and studied the resource allocation problems to make the best use of the limited resources. In this thesis, we proposed resource allocation algorithms for the following energy harvesting communication systems:

- energy allocation for the energy harvesting communication tags (EnHANTs);
- energy allocation for single energy harvesting transmitter;
- jointly energy-bandwidth allocation for energy harvesting networks in multiple flat-fading point-to-point channels;
- jointly energy-bandwidth allocation for energy harvesting networks in multiple flat-fading broadcasting channels;
- jointly energy-subchannel allocation for energy harvesting networks in frequency-selective fading channels.

By proposing the resource allocation algorithms, we aim to make the energy harvesting communication system operate in an efficient way, making the best use of the limited resource and providing the reliable and quality communication service.

Bibliography

[1] S. Sudevalayam and P. Kulkarni, "Energy harvesting sensor nodes: survey and implications," *IEEE Commun. Surveys Tuts.*, vol. 13, no. 3, pp. 443–461, Sep. 2011.

[2] J. A. Paradiso and T. Starner, "Energy scavenging for mobile and wireless electronics," *IEEE Trans. Pervasive Computing*, vol. 4, pp. 18–27, Jan. 2005.

[3] C. Han and et al, "Green radio: radio techniques to enable energy-efficient wireless networks," *IEEE Commun. Mag.*, vol. 49, no. 6, pp. 46–54, Jun. 2011.

[4] Y. Chen, S. Zhang, S. Xu, and G. Li, "Fundamental trade-offs on green wireless networks," *IEEE Commun. Mag.*, vol. 49, no. 6, pp. 30–37, Jun. 2011.

[5] A. Bianzino, C. Chaudet, D. Rossi, and J. Rougier, "A survey of green networking research," *IEEE Commun. Surveys Tuts.*, vol. 14, no. 1, pp. 3–20, Jan. 2012.

[6] H. Bogucka and A. Conti, "Degrees of freedom for energy savings in practical adaptive wireless systems," *IEEE Commun. Mag.*, vol. 49, no. 6, pp. 38–45, Jun. 2011.

[7] Y. Wu and et al, "Green transmission technologies for balancing the energy efficiency and spectrum efficiency trade-off," *IEEE Commun. Mag.*, vol. 52, no. 11, pp. 112–120, Nov. 2014.

[8] D. Gunduz, K. Stamatiou, M. Michelusi, and M. Zorzi, "Designing intelligent energy harvesting communication systems," *IEEE Commun. Mag.*, vol. 52, no. 1, pp. 210–216, Jan. 2014.

[9] M. Ismail and W. Zhuang, "Green radio communications in a heterogeneous wireless medium," *IEEE Wireless Commun. Mag.*, vol. 21, no. 3, pp. 128–135, Jun. 2014.

[10] L. Guan and A. Zhu, "Green communications: digital predistortion for wideband RF power amplifiers," *IEEE Microw. Mag.*, vol. 15, no. 7, pp. 84–99, Nov. 2014.

[11] J. Wu, "Green wireless communications: from concept to reality," *IEEE Wireless Commun. Mag.*, vol. 19, no. 4, pp. 4–5, Aug. 2012.

[12] Z. Zheng, X. Zhang, L. Cai, R. Zhang, and X. Shen, "Sustainable communication and networking in two-tier green cellular networks," *IEEE Trans. Wireless Commun.*, vol. 21, no. 4, pp. 47–53, Aug. 2014.

[13] A. Conti, M. Win, and M. Chiani, "Slow adaptive M-QAM with diversity in fast fading and shadowing," vol. 55, no. 5, pp. 895–905, May 2007.

[14] Z. Hasan, H. Boostanimehr, and V. Bhargava, "Green cellular networks: a survey, some research issues and challenges," *IEEE Commun. Surveys Tuts.*, vol. 13, no. 4, pp. 524–540, Nov. 2011.

[15] R. Prasad, S. Devasenapathy, V. Rao, and J. Vazifehdan, "Reincarnation in the ambiance: devices and networks with energy harvesting," *IEEE Commun. Surveys Tuts.*, vol. 16, no. 1, pp. 195–213, Sep. 2014.

[16] I. Krikidis, S. Timotheou, S. Nikolaou, G. Zheng, D. Ng, and R. Schober, "Simultaneous wireless information and power transfer in modern communication systems," *IEEE Commun. Mag.*, vol. 52, no. 11, pp. 104–110, Nov. 2014.

[17] S. Chen, P. Sinha, N. Shroff, and C. Joo, "Finite-horizon energy allocation and routing scheme in rechargeable sensor networks," in *Proc. IEEE INFOCOM 11'*, Apr. 2011, pp. 2273–2281.

[18] G. Yang, B. Stark, S. Hollis, and S. Burrow, "Challenges for energy harvesting systems under intermittent excitation," *IEEE J. Emerg. Sel. Topics Circuits Syst.*, vol. 4, no. 3, pp. 364–374, Sep. 2014.

[19] M. Gorlatova, P. Kinget, I. Kymissis, D. Rubenstein, X. Wang, and G. Zussman, "Energy harvesting active networked tags (EnHANTs) for ubiquitous object networking," in *Proc. ACM MobiCom 09'*, Sep. 2009, pp. 18–25.

[20] ——, "Energy harvesting active networked tags (EnHANTs) for ubiquitous object networking," *IEEE Wireless Commun. Mag.*, vol. 17, no. 6, pp. 18–25, Dec. 2010.

[21] O. Ozel and S. Ulukus, "Achieving AWGN capacity under stochastic energy harvesting," *IEEE Trans. Inf. Theory*, vol. 58, no. 10, pp. 6471–6483, Oct. 2012.

[22] R. Rajesh, V. Sharma, and P. Viswanath, "Capacity of Gaussian channels with energy harvesting and processing cost," *IEEE Trans. Inf. Theory*, vol. 60, no. 5, pp. 2563–2575, May 2014.

[23] Y. Dong and A. Ozgur, "Approximate capacity of energy harvesting communication with finite battery," in *Proc. IEEE ISIT 14'*, Jun. 2014, pp. 801–805.

[24] O. Ozel, K. Tutuncuoglu, S. Ulukus, and A. Yener, "Capacity of the discrete memoryless energy harvesting channel with side information," in *Proc. IEEE ISIT 14'*, Jun. 2014, pp. 796–800.

[25] A. Nasir, X. Zhou, S. Durrani, and R. Kenedy, "Relaying protocols for wireless energy harvesting and information processing," *IEEE Trans. Wireless Commun.*, vol. 12, no. 7, pp. 3622–3636, Jul. 2013.

[26] L. Lin, N. Shroff, and R. Srikant, "Asymptotically optimal energy-aware routing for multihop wireless networks with renewable energy sources," *IEEE/ACM Trans. Netw.*, vol. 15, no. 5, pp. 1021–1034, Oct. 2007.

[27] Y. Wu and W. Liu, "Routing protocol based on genetic algorithm for energy harvesting-wireless sensor networks," *IET Wireless Sensor Syst.*, vol. 3, no. 2, pp. 112–118, Jun. 2013.

[28] S. Sarkar, M. Khouzani, and K. Kar, "Optimal routing and scheduling in multihop wireless renewable energy networks," *IEEE Trans. Autom. Control*, vol. 58, no. 7, pp. 1792–1798, Jul. 2013.

[29] G. Martinez, S. Li, and C. Zhou, "Wastage-aware routing in energy-harvesting wireless sensor networks," *IEEE Sensors J.*, vol. 14, no. 9, pp. 2967–2974, Sep. 2014.

[30] H. Dhillon, Y. Li, P. Nuggehalli, Z. Pi, and J. Andrews, "Fundamentals of heterogeneous cellular networks with energy harvesting," *IEEE Trans. Wireless Commun.*, vol. 13, no. 5, pp. 2782–2797, May 2014.

[31] M. Zheng, P. Pawelczak, S. Stanczak, and H. Yu, "Planning of cellular networks enhanced by energy harvesting," vol. 17, no. 6, pp. 1092–1095, Jun. 2013.

[32] L. Liu, R. Zhang, and K. Chua, "Wireless information transfer with opportunistic energy harvesting," *IEEE Trans. Wireless Commun.*, vol. 12, no. 1, pp. 288–300, Jan. 2013.

[33] S. Kim and et al, "Ambient RF energy-harvesting technologies for self-sustainable standalone wireless sensor platforms," *Proc. IEEE*, vol. 102, no. 11, pp. 1649–1666, Nov. 2014.

[34] V. Chawla and S. H. Dong, "An overview of passive RFID," *IEEE Commun. Mag.*, vol. 45, no. 9, pp. 11–17, Sep. 2007.

[35] A. Janek, C. Steger, R. Weiss, J. Preishuber-Pfluegl, and M. Pistauer, "Lifetime extension of semi-passive UHF RFID tags using special power management techniques and energy harvesting devices," in *Proc. IEEE AFRICON 07'*, Sep. 2007, pp. 1–7.

[36] F. Iannello, O. Simeone, and U. Spagnolini, "Energy management policies for passive RFID sensors with RF-energy harvesting," in *Proc. IEEE ICC 10'*, May 2010, pp. 1–6.

[37] K. Yang and X. Wang, "Battery-aware adaptive modulation based on large-scale MDP," *IEEE Trans. Wireless Commun.*, vol. 7, no. 1, pp. 72–77, Jan. 2008.

[38] ——, "Battery-aware adaptive modulation with QoS constraints," *IEEE Trans. Commun.*, vol. 54, no. 10, pp. 1797–1805, Oct. 2006.

[39] V. Sharma, U. Mukherji, V. Joseph, and S. Gupta, "Optimal energy management policies for energy harvesting sensor nodes," *IEEE Trans. Wireless Commun.*, vol. 9, no. 4, pp. 1326–1336, Apr. 2010.

[40] K. Tutuncuoglu and A. Yener, "Optimum transmission policies for battery limited energy harvesting nodes," *IEEE Trans. Commun.*, vol. 11, no. 3, pp. 1180–1189, Mar. 2012.

[41] C. Ho and R. Zhang, "Optimal energy allocation for wireless communications with energy harvesting constraints," *IEEE Trans. Signal Process.*, vol. 60, no. 9, pp. 4808–4818, Sep. 2012.

[42] O. Ozel, K. Tutuncuoglu, J. Yang, S. Ulukus, and A. Yener, "Transmission with energy harvesting nodes in fading wireless channels: optimal policies," *IEEE J. Sel. Areas Commun.*, vol. 29, no. 8, pp. 1732–1743, Sep. 2011.

[43] Z. Wang, V. Aggarwal, and X. Wang, "Renewable energy scheduling for fading channels with maximum power constraint," in *Proc. IEEE Allerton 13'*, Oct. 2013, pp. 1394–1400.

[44] Q. Bai, R. Amjad, and J. Nossek, "Average throughput maximization for energy harvesting transmitters with causal energy arrival information," in *Proc. IEEE WCNC 13'*, Apr. 2013, pp. 4232–4237.

[45] P. Blasco, D. Gunduz, and M. Dohler, "A learning theoretic approach to energy harvesting communication system optimization," *IEEE Trans. Wireless Commun.*, vol. 12, no. 4, pp. 1872–1882, Apr. 2013.

[46] J. Yang and S. Ulukus, "Optimal packet scheduling in a multiple access channel with energy harvesting transmitters," *J. Commun. Netw.*, vol. 14, no. 2, pp. 140–150, Apr. 2012.

[47] K. Tutuncuoglu and A. Yener, "Sum-rate optimal power policies for energy harvesting transmitters in an interference channel," *J. Commun. Netw.*, vol. 14, no. 2, pp. 151–161, Apr. 2012.

[48] O. Ozel, Y. Jing, and S. Ulukus, "Optimal broadcast scheduling for an energy harvesting rechargeable transmitter with a finite capacity battery," *IEEE Trans. Wireless Commun.*, vol. 11, no. 8, pp. 2193–2203, Jun. 2012.

[49] L. Huang and M. Neely, "Utility optimal scheduling in energy-harvesting networks," *IEEE/ACM Trans. Netw.*, vol. 21, no. 4, pp. 1117–1130, Aug. 2013.

[50] B. Gurakan, O. Ozel, J. Yang, and S. Ulukus, "Energy cooperation in energy harvesting communications," *IEEE Trans. Commun.*, vol. 61, no. 12, pp. 4884–4898, Nov. 2013.

[51] K. Tutuncuoglu and A. Yener, "Cooperative energy harvesting communications with relaying and energy sharing," in *Proc. IEEE ITW 13'*, Sep. 2013, pp. 1–5.

[52] N. Tekbiyik, T. Girici, E. Uysal-Biyikoglu, and K. Leblebicioglu, "Proportional fair resource allocation on an energy harvesting downlink," *IEEE Trans. Wireless Commun.*, vol. 12, no. 4, pp. 1699–1711, Apr. 2013.

[53] Z. Wang, V. Aggarwal, and X. Wang, "Optimal energy-bandwidth allocation for energy harvesting interference networks," in *Proc. IEEE ISIT 14'*, Jul. 2014, pp. 1166–1170.

[54] K. Kim, Y. Han, and S. Kim, "Joint subcarrier and power allocation in uplink OFDMA systems," *IEEE Commun. Lett.*, vol. 9, no. 6, pp. 526–528, Jun. 2005.

[55] H. Zhu and J. Wang, "Chunk-based resource allocation in OFDMA systems - Part II: Joint chunk, power and bit allocation," *IEEE Trans. Commun.*, vol. 60, no. 2, pp. 499–509, Dec. 2011.

[56] A. Abrardo, M. Belleschi, P. Detti, and M. Moretti, "Message passing resource allocation for the uplink of multi-carrier multi-format systems," *IEEE Trans. Wireless Commun.*, vol. 11, no. 1, pp. 1536–1276, Jan. 2012.

[57] K. Yang, N. Prasad, and X. Wang, "A message-passing approach to distributed resource allocation in uplink DFT-Spread-OFDMA systems," *IEEE Trans. Commun.*, vol. 59, no. 4, pp. 1099–1113, Apr. 2011.

[58] W. Yu and R. Liu, "Dual methods for nonconvex spectrum optimization of multicarrier systems," *IEEE Trans. Commun.*, vol. 54, no. 7, pp. 1310–1322, Jul. 2006.

[59] L. Yang and G. B. Giannakis, "Battery-aware adaptive modulation with QoS constraints," *IEEE Signal Process. Mag.*, vol. 21, no. 6, pp. 26–54, Nov. 2004.

[60] D. L. Donoho, "Compressed sensing," *IEEE Trans. Inf. Theory*, vol. 52, no. 4, pp. 1289–1306, Apr. 2006.

[61] M. A. Davenport, P. T. Boufounos, M. B. Wakin, and R. G. Baraniuk, "Signal processing with compressive measurements," IEEE J. Select. Topics Sig. Process., vol. 4, no. 2, pp. 445–460, Apr. 2010.

[62] C. Carbonelli and U. Mengali, "M-PPM noncoherent receivers for uwb applications," *IEEE Trans. Wireless Commun.*, vol. 5, no. 8, pp. 2285–2294, Aug. 2006.

[63] C. Hu, R. Khanna, J. Nejedlo, , K. Hu, H. Liu, and P. Chiang, "A 90 nm-CMOS, 500 Mbps, 3-5 Ghz fully-integrated IR-UWB transceiver with multipath equalization using pulse injection-locking for receiver phase synchronization," *IEEE J. Solid-State Circuits*, vol. 46, no. 5, pp. 1076–1088, May 2011.

[64] A. Seyedi and B. Sikdar, "Performance modeling of transmission schedulers for sensor networks capable of energy harvesting," in *Proc. IEEE ICC 10'*, May 2010, pp. 1–5.

[65] M. Puterman, *Markov Decision Processes: Discrete Stochastic Dynamic Programming.* New York: John Wiley & Sons, 1994.

[66] J. Piorno, C. Bergonzini, K. Atienza, and T. Rosing, "Prediction and management in energy harvested wireless sensor nodes," in *Proc. VITAE 09'*, May 2009, pp. 6–10.

[67] J. Lu, S. Liu, Q. Wu, and Q. Qiu, "Accurate modeling and prediction of energy availability in energy harvesting real-time embedded systems," in *Proc. Green Computing Conf. 10'*, Aug. 2010, pp. 469–476.

[68] S. Boyd and L. Vandenberghe, *Convex Optimization.* Cambridge: Cambridge University Press, 2009.

[69] Z. Wang, V. Aggarwal, and X. Wang, "Iterative dynamic water-filling for fading multiple-access channels with energy harvesting," *available at arXiv 1401.2376*, Aug. 2013.

[70] T. Cover and J. Thomas, *Elements of Information Theory.* New York: Wiley, 1991.

[71] M. Gorlatova, A. Wallwater, and G. Zussman, "Networking low-power energy harvesting devices: measurements and algorithms," *IEEE Trans. Mobile Comput.*, vol. 12, no. 9, pp. 1853–1233, Sep. 2013.

[72] A. Duel-Hallen, "Fading channel prediction for mobile radio adaptive transmission systems," *Proc. IEEE*, vol. 95, no. 12, pp. 2299–2313, Dec. 2007.

[73] J. Yang, O. Ozel, and S. Ulukus, "Broadcasting with an energy harvesting rechargeable transmitter," *IEEE Trans. Wireless Commun.*, vol. 11, no. 2, pp. 571–583, Feb. 2012.

[74] ——, "Optimal scheduling over fading broadcast channels with an energy harvesting transmitter," in *Proc. IEEE CAMSAP 11'*, Dec. 2011, pp. 193–196.

[75] H. Kushner and P. Whiting, "Convergence of proportional-fair sharing algorithms under general conditions," *IEEE Trans. Wireless Commun.*, vol. 3, no. 4, pp. 1250–1259, Jul. 2004.

[76] R. Burden and J. Faires, *Numerical Analysis.* Boston: PWS-KENT, 1989.

[77] D. Tse and P. Viswanath, *Fundamentals of Wireless Communication.* Cambridge: Cambridge University Press, 2005.

[78] R. Sutton and A. Barto, *Reinforcement Learning: An Introduction.* Cambridge, MA: MIT Press, 1988.

[79] L. Buoniu and B. S. R. Babuka, "Multi-agent reinforcement learning: an overview," *Innovations in Multi-Agent Systems and Applications*, vol. 310, no. 1, pp. 183–221, 2010.